Universiteit Leiden
The Netherlands

The design and synthesis of novel heterodinuclear complexes combining a DNA-cleaving agent and a DNA-targeting moiety

Hoog, P. de

Citation
Hoog, P. de. (2008, February 28). *The design and synthesis of novel heterodinuclear complexes combining a DNA-cleaving agent and a DNA-targeting moiety*. Retrieved from https://hdl.handle.net/1887/12619

Version:	Corrected Publisher's Version
License:	Licence agreement concerning inclusion of doctoral thesis in the Institutional Repository of the University of Leiden
Downloaded from:	https://hdl.handle.net/1887/12619

Note: To cite this publication please use the final published version (if applicable).

The design and synthesis of novel heterodinuclear complexes combining a DNA-cleaving agent and a DNA-targeting moiety

The search for novel anticancer agents

Proefschrift

ter verkrijging van de graad van Doctor aan de Universiteit Leiden, op gezag van de Rector Magnificus prof. mr. P.F. van der Heijden, volgens besluit van het College voor Promoties te verdedigen op donderdag 28 februari 2008 klokke 16.15 uur

door

Paul de Hoog

geboren te Sliedrecht, Nederland in 1979

Samenstelling promotiecommissie

Promotor:	Prof. Dr. Jan Reedijk
Co-promotor:	Dr. Patrick Gamez
Referent:	Prof. Dr. G.A. van der Marel
Overige Leden:	Prof. Dr. B. Meunier (Palumed, Toulouse) Dr. M. Pitié (LCC, Toulouse) Prof. Dr. J. Brouwer

This work was possible thanks to the financial support of the Chemical Research Council of the Netherlands through the CERC3 program.

What gets us into trouble is not what we do not know,
it is what we know for sure that just is not so.

Mark Twain (1835-1910)

Aan mijn ouders, Debbie en Jesse

Contents

List of abbreviations		6
List of complexes used in this thesis		8
Chapter 1	General introduction	11
Chapter 2	Influence of the copper coordination geometry on the DNA cleavage activity of Clip-Phen complexes studied by DFT.	47
Chapter 3	A New Approach for the Preparation of Efficient DNA Cleaving Agents: Ditopic Copper-Platinum Complexes Based on 3-Clip-Phen and Cisplatin.	63
Chapter 4	DNA Cleavage and binding selectivity of a heterodinuclear Pt-Cu(3-Clip-Phen) complex.	81
Chapter 5	Platinated copper(3-Clip-Phen) complexes as effective DNA-cleaving and cytotoxic agents.	103
Chapter 6	Change of the bridge linking a platinum moiety and the DNA-cleaving agent Cu(3-Clip-Phen).	117
Chapter 7	Triazine as a building block for the generation of multifunctional heteronuclear platinum/copper complexes.	131
Chapter 8	Exploring the DNA-cleaving abilities of novel heteronuclear ruthenium-copper complexes.	147
Chapter 9	Summary, general discussions and perspectives	165
Samenvatting		172
Curriculum Vitae		175
List of publications		176
Acknowledgements		178

List of abbreviations

5-MF	5-methylfuranone
A	Adenine
Å	Ångstrom
A498	Renal cancer cell line
A549	Lung cancer cell line
ATP	Adenosine TriPhosphate
B	Becke
Bipy	Bipyridine
Boc	tert-butyl acetate
Boc_2O	Di-tert-butyl dicarbonate
C	Cytosine
COSY	Correlation Spectroscopy
CTP	Cytidine TriPhosphate
DCM	DiChloroMethane
DFT	Density Functional Theory
DIPEA	DiIsoPropylEthylAmine
DMF	DimMethylFormamide
DMSO	DiMethyl SulfOxide
DNA	DeoxyriboNucleic Acid
DPPZ	DiPyrido[3,2-a:2¢,3¢-c]PhenaZine
DSB	Double-Strand Breaks
EDTA	EthyleneDiamine Tetraacetic Acid
EPR	Enhanced Permeability and Retention
ESI	Electrospray Ionization
EVSA-T	Breast cancer cell line
FCS	Fetal Calf Serum
Fmoc	(9H-fluoren-9-yl)methylcarbamate
Fmoc-Osu	N-(9-Fluorenylmethoxycarbonyloxy)succinimide
G	Guanine
GC	Gas Chromatography
GSH	Glutathione
GTP	Guanosine TriPhosphate
H226	Non-small cell lung cancer cell line
HCT-15	Colorectal cancer cell line
HeLa	Cervical cancer cell line
HEPES	4-(2-HydroxyEthyl)-1-PiperazineEthaneSulfonic acid
HMG	High-Mobility Group
HPLC	High Performance Liquid Chromatography
Hs683	Glioblastomas cell line
IGROV	Ovarian cancer cell line
LoVo	Colorectal cancer cell line
M19 MEL	Melanoma cell line
MCF7	Breast cancer cell line
MEM	Minimal Essential Medium
MeOH	Methanol
MPA	MercaptoPropionic Acid

MS	Mass Spectroscopy
MTT	3-(4,5-dimethylthiazol)-2-yl)-2,5-diphenyl-2H-tetrazolium bromide
NER	Nucleotide Excision Repair
NMR	Nuclear Magnetic Resonance
OD	Optical Density
ODN	Oligonucleotide
P	Perdew
PAGE	PolyAcrylamide Gel Electrophoresis
PBS	Phosphate Buffered Saline
PCC	Pyridinium ChloridotrioxidoChromate
Phen	Phenanthroline
Py	2-Pyridyl
QZ4P	Quadruple ζ with four polarization functions
RNA	RiboNucleic Acid
RPMI	Roswell Park Memorial Institute medium
RT	Room Temperature
SPE	Single-Point Energies
SRB	SulfoRhodamine B
SSB	Single-Strand Breaks
STO	Slater Type Orbital
T	Thymine
Taq	Thermus Aquaticus
TBE	Tris-Borate-Edta
Terpy	Terpyridine
TFA	TriFluoroAcetic acid
THF	TetraHydroFuran
TMS	TetraMethylSilane
Tris	2-Amino-2-(hydroxymethyl)propane-1,3-diol
TTP	Thymidine TriPhosphate
TZ2P	Triple ζ with two polarization functions
U2-OS	human osteosarcoma cell line
U-373MG	Glioblastomas cell line
UV	UltraViolet
Vis	Visible
WIDR	Colon cancer cell line
ZORA	Zeroth-Order Regular Approximation

List of complexes used in this thesis

DFT calculated complexes

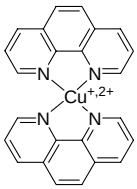

1^{dft}

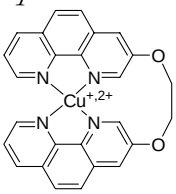

2^{dft}

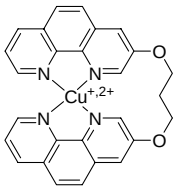

3^{dft}

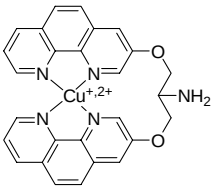

4^{dft}

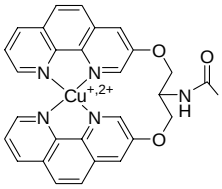

5^{dft}

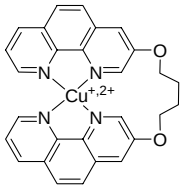

6^{dft}

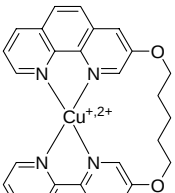

7^{dft}

Chapter 2 The complexes have been prepared by Pitié et al. *Eur. J. Inorg. Chem.* **2003**, 528

The prepared Complexes

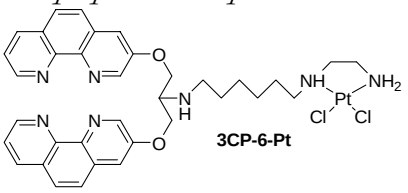

3CP-6-Pt

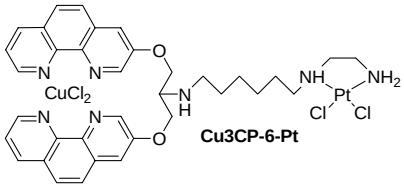

Cu3CP-6-Pt

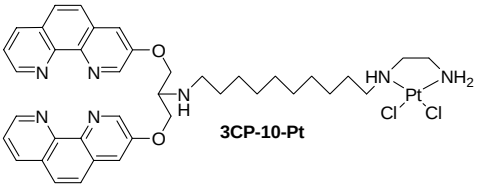

3CP-10-Pt

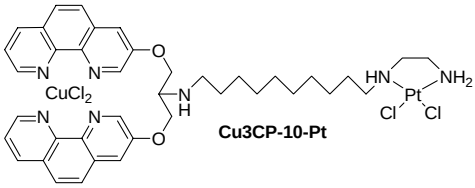

Cu3CP-10-Pt

Chapter 3

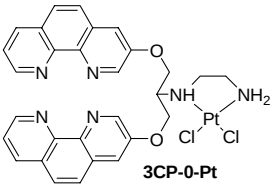

3CP-0-Pt

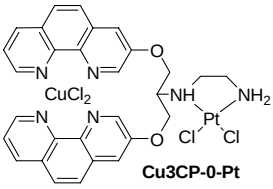

Cu3CP-0-Pt

Chapter 4

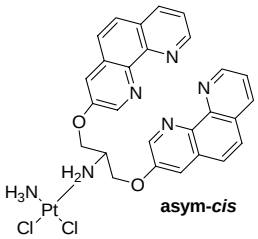

asym-*cis*

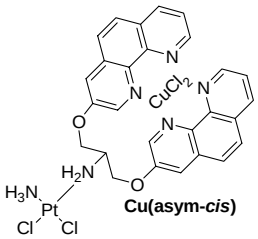

Cu(asym-*cis*)

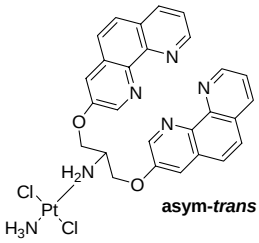

asym-*trans*

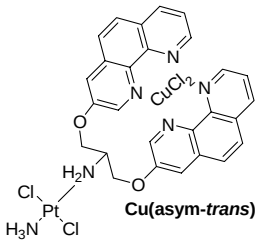

Cu(asym-*trans*)

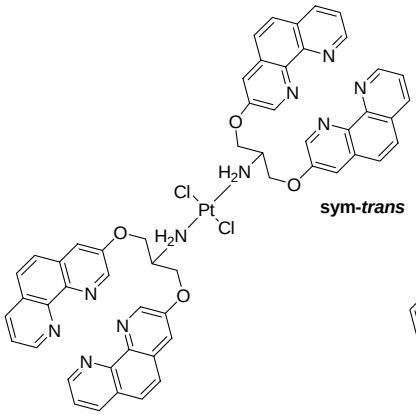

sym-*trans*

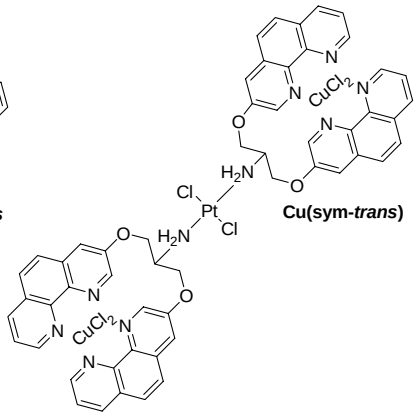

Cu(sym-*trans*)

Chapter 5

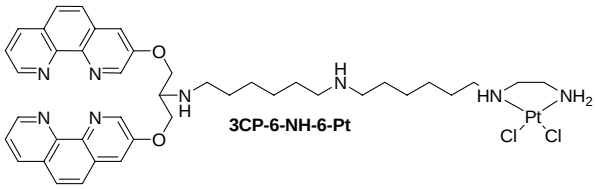

3CP-6-NH-6-Pt

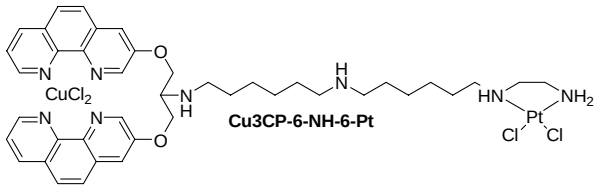

Cu3CP-6-NH-6-Pt

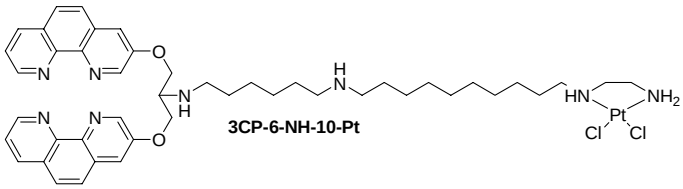

3CP-6-NH-10-Pt

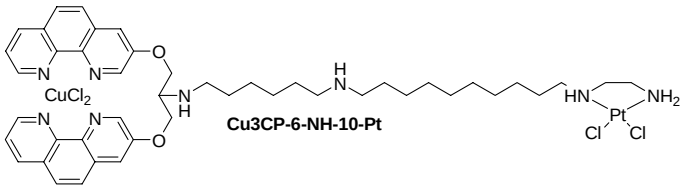

Cu3CP-6-NH-10-Pt

Chapter 6

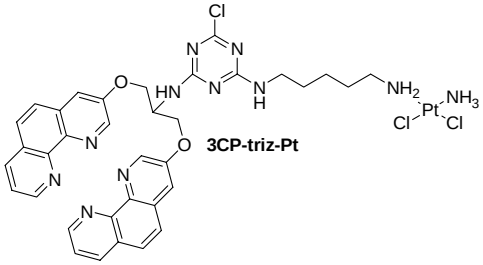

3CP-triz-Pt

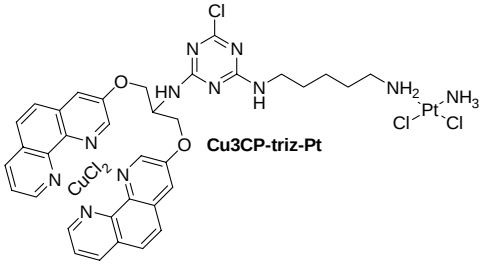

Cu3CP-triz-Pt

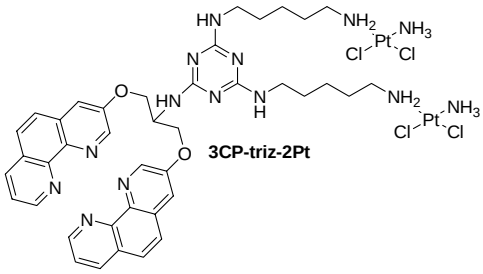

3CP-triz-2Pt

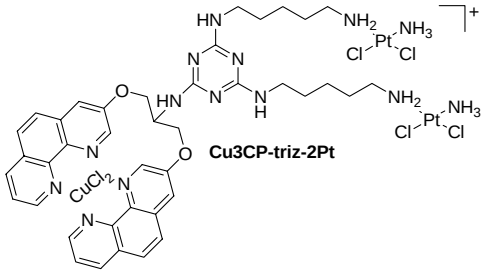

Cu3CP-triz-2Pt

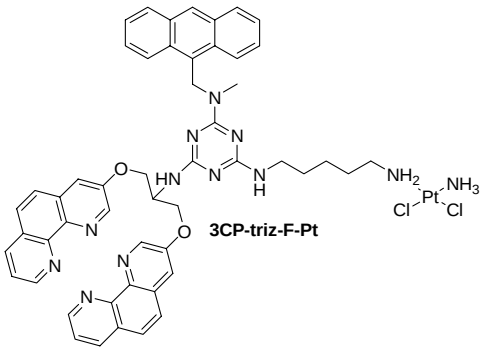

3CP-triz-F-Pt

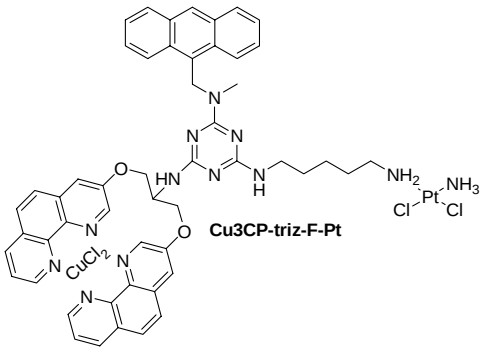

Cu3CP-triz-F-Pt

Chapter 7

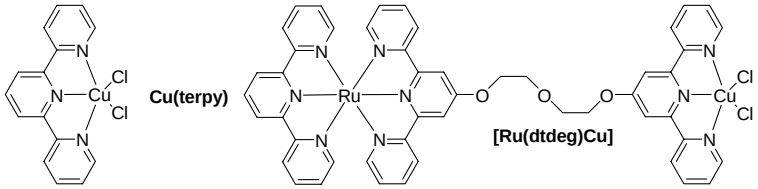

Cu(terpy)

[Ru(dtdeg)Cu]

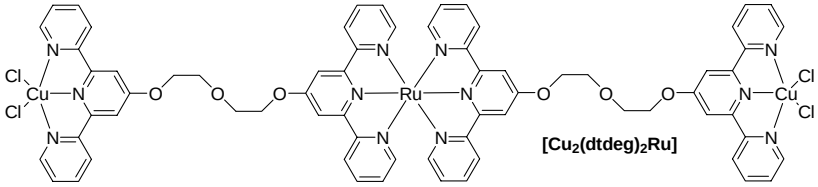

[Cu_2(dtdeg)$_2$Ru]

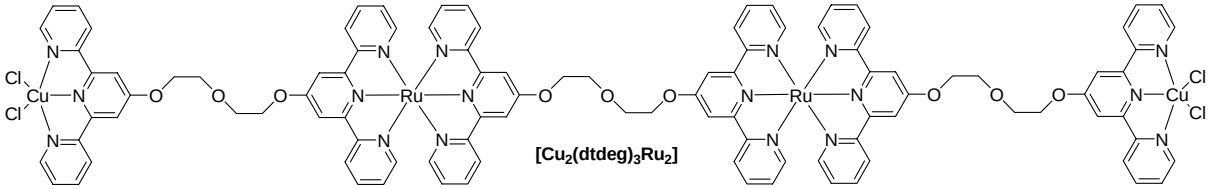

[Cu_2(dtdeg)$_3$$Ru_2$]

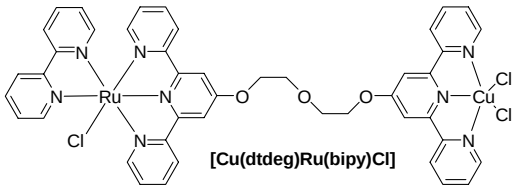

[Cu(dtdeg)Ru(bipy)Cl]

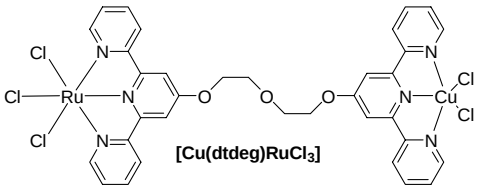

[Cu(dtdeg)$RuCl_3$]

Chapter 8

Chapter 1

General introduction

1.1 Fighting cancer

Cancer is a leading cause of death worldwide. In 2005 it accounted for approximately 13% of all deaths.[1] Cancer is a generic term for a group of over 100 diseases that exhibit some common characteristics, namely the uncontrolled growth of cells, and which can affect and damage adjacent normal tissues.[2] It may also spread through the body and reach other organs, a process referred to as metastasis. Lung, breast, colorectal and prostate cancers are the most frequently occurring and cause the majority of deaths.

Abnormalities in genes responsible for cell growth and repair can cause cancer. The changes in the genes are often the result of the influence of external agents, such as tobacco smoke, radiation, chemicals or infections by viruses like for example Hepatitis B. The cancer develops from a single cell. The transformation from a normal cell into a tumor cell is a multistage process. This development can be initiated by external agents or inherited genetic factors.[1] Ageing also increases the incidence dramatically, possibly as a result of less efficient cellular repair mechanisms.

Several approaches are employed to treat cancer, such as surgery, chemotherapy, radiation therapy, monoclonal antibody therapy or combinations of these therapies. The choice of treatment depends on the nature of the tumor, the stage of the disease and the general state of the patient. Decades of research have improved the therapies, so that substantial cure rates can nowadays be achieved for several cancer types. Testicular cancer, with a cure rate approaching 100%, is a prime example of this scientific progress. This cancer is treated with a combination of anti-tumor drugs that interact with DNA,[3] namely etopside, cisplatin (Figure 1.1) and bleomycin.[4, 5]

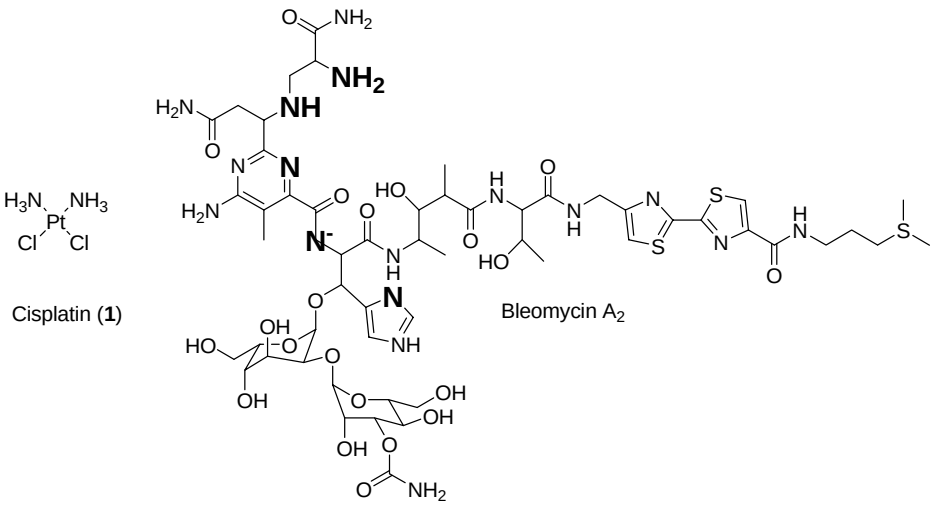

Figure 1.1 Structural formulae of the antitumor drugs cisplatin (**1**) and bleomycin A_2, whose metal-binding domain has been highlighted in bold.

1.2 Discovery of cisplatin

The chemical structure of *cis*-diamminedichloridoplatinum(II), generally referred to as cisplatin, was already described in 1844,[6] but its anti-proliferate activity was discovered by Rosenberg *et al.* in 1965.[7] Actually, the influence of an electric field on the growth and division of *E.coli* bacteria was investigated and a filamentous growth was observed which is a phenomenon that normally occurs when the DNA replication is blocked. It was found that not the electric field, but the products formed by electro-chemical reactions of the platinum electrodes used during the experiment were responsible for the cell division arrest. These products were identified as *cis*- and *trans*-$Pt(NH_3)_2Cl_2$ and *cis*- and *trans*-$Pt(NH_3)_2Cl_4$, but only the *cis*-complexes showed antibacterial activities. Subsequently, the anti-tumor activity of cisplatin was revealed in 1969[8], and in 1978 the FDA approved this drug for clinical use. Nowadays, cisplatin is widely used in cancer chemotherapy against a variety of solid tumors, and is especially effective against testicular, ovarian, head an neck and small-cell lung cancers.[9, 10]

1.3 Mechanism of action of cisplatin

Cisplatin is administrated intravenously to the body. In the bloodstream, the chloride ion concentration is approximately 100 mM; therefore, cisplatin remains a neutral molecule. After reaching its target, cisplatin is taken up in the cell. The precise mechanism of cellular uptake still remains under debate. Cisplatin uptake does not have a pH optimum, nor is inhibited by structural analogues, which suggest that it enters the cell by passive diffusion.[11, 12] Nevertheless, more and more evidences about alternative pathways involving active transport are reported.[13-15] Recent studies have demonstrated that transporters controlling the intracellular copper homeostasis are also involved in the regulation of the influx and efflux of Pt-based antitumor agents.[16-18]

Within the cell the chloride concentration is lower which facilitates the hydrolysis of cisplatin, yielding the monoaqua $[Pt(NH_3)_2Cl(H_2O)]^+$ and the diaqua $[Pt(NH_3)_2(H_2O)_2]^{2+}$ species.[19-22] These complexes are far more reactive in comparison with the neutral species, because the water ligand is a better leaving group than the chloride anion. Inside the cell many potential binding sites are present including RNA, thiol-containing molecules, proteins, membrane phospholipids[23] and DNA.[11] The primary target could be identified by the filamentous growth observed by Rosenberg *et al.*, a phenomenon characteristic of DNA damaging agents like UV-radiation and ionization radiation.[24] Moreover, the numbers of platinum atoms binding to proteins, RNA and DNA in HeLa cells were determined.[25] The ratio of platinum to each macromolecule was calculated. The results showed that; one out of 30000 to 300000 proteins molecules, and one out of 10 to 1000 RNA molecules hold one platinum

molecule and that every DNA macromolecule contained nine platinum atoms.[25] Furthermore, a clear correlation is usually found between the Pt-DNA adduct levels and the sensitivity of the cells to the drug.[26, 27] This strong evidence was the basis of intensive scientific research devoted to the investigation of the interactions between cisplatin and DNA.

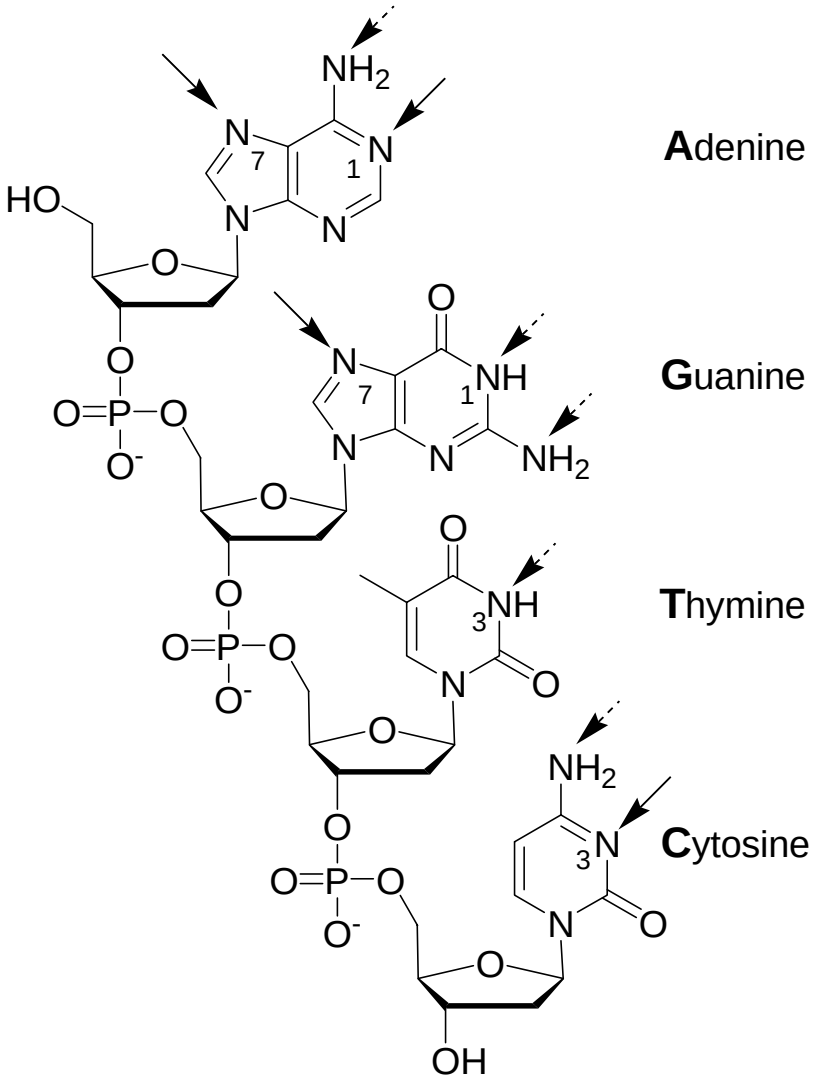

Figure 1.2 Potential binding sites of cisplatin in double stranded DNA. Dashed arrows represent binding sites after loss of a H^+.

The four nucleobases, i.e. adenine (A), guanine (G), cytosine (C), and thymine (T) offer eleven potential binding sites in total (Figure 1.2), because platinum is a soft metal and therefore coordinates preferentially to the nitrogen atoms of the nucleobases. However, at physiological conditions the binding sites indicated by a dashed arrow cannot coordinate platinum because they are protonated. The N3 of purines are sterically hindered by the deoxyribose unit and can therefore not coordinate platinum. The N1 atom of adenine and the N3 atom of cytosine are involved in hydrogen bonding, so platinum cannot bind in double-stranded DNA. The N7 atoms of adenine and guanine can coordinate platinum, though a strong preference is observed for

guanine.[28, 29] The difference in reactivity can be explained by the strong hydrogen bond between the hydrogen of the amine ligand of cisplatin and the oxo group at the C6 position of guanine, and by a stronger electronic interaction between platinum and the guanine.[30-32] Cisplatin forms initially monofunctional adducts with DNA that further react to produce a variety of bifunctional products (Figure 1.3). Mainly the 1,2-d(GG) intrastrand adduct is formed in about 60-65 % of the cases, but the 1,2-d(AG) intrastrand (20-25 %), 1,3-d(GG) intrastrand (6 %) and the 1,2-d(GG) interstrand (1,5%) adducts were also found.[33-35] It is not known yet, which adduct is primarily responsible for the cytotoxicity. Although, it is believed that the former is primarily responsible for the anti-tumor activity of the drug, because it is the predominant adduct and because *trans*-$Pt(NH_3)_2Cl_2$, which an inactive compound, is not able to form this adduct. *Trans*-$Pt(NH_3)_2Cl_2$ does not show any cytotoxicity, because it produces mainly 1,3-intrastrand and interstrand adducts.[36] This is supported by the finding that the nucleotide excision repair (NER) is more effective on 1,3-intrastrand adducts than 1,2-intrastrand adducts.[37]

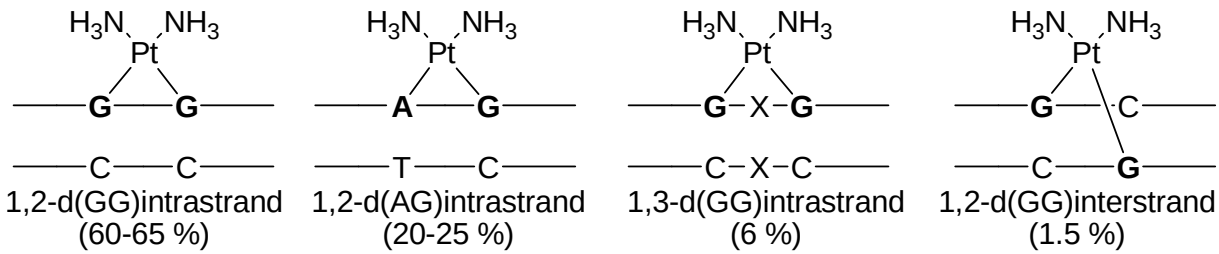

Figure 1.3 The four different platinum-DNA adducts found and their abundance.

The changes in the local conformation of DNA induced by the 1,2-intrastrand adduct have been investigated in detail by NMR spectroscopy[38-40] and X-ray crystallography[41, 42] (Figure 1.4). The 3D structures revealed that the binding of cisplatin to two neighboring guanines induces moderately small, but important local distortions in the DNA duplex. Thus, the DNA is bended towards the major groove by 40-80° (NMR and X-ray structures show variations in bending depending on the used sequence of the oligonucleotide).[43] Furthermore, the helix is partially unwinded, which opens up the minor groove. The 1,3-intrastrand Pt-DNA adduct causes a 27-33° bending towards the major groove.[44, 45] The interstrand adducts bend the DNA towards the minor groove by 20-40°, but a remarkable degree of unwinding is observed in this case, namely 80°.[46-48]

Figure 1.4 Structure of the 1,2-d(GG) intrastrand DNA-cisplatin adduct, as determined by X-ray diffraction.[42]

1.4 The effect of the DNA damage induced by cisplatin

The structural change of DNA has an inevitable biological effect, and this is believed to be the decisive factor regarding the anti-tumor properties of cisplatin. The presence of the Pt-DNA adducts has several consequences on the interaction of proteins with DNA and the ability of the duplex to function as a template for the replication and transcription.[49] The recognition of Pt-adducts is the initiation of a downstream of signaling pathways. Ultimately, the cellular responses may lead to programmed cell death (apoptosis), or necrosis,[50, 51] but they may also lead to the repair of the DNA. Two types of proteins can be distinguished: (i) the proteins that can selectively recognize the distortion of the DNA (ii) and the proteins which are involved in the packaging, or DNA-dependent functions which inevitably encounter the Pt-DNA adducts.

A well-studied example of the first class of proteins is the family of high-mobility domain proteins (HMG). The HMG proteins are involved in the regulation of nuclear functions including transcription, replication, recombination, and general chromatin remodeling.[52] Interestingly, the HMG proteins are able to selectively recognize the 1,2-d(GG) and 1,2-d(AG) intrastrand, but not the 1,3-d(GG) intrastrand adducts.[53] The crystal structure of the binding product of the 1,2-d(GG) intrastrand crosslink in an oligonucleotide by the HMG1 domain A is shown in Figure 1.5.[54] The function of the HMG domain is still unclear. It was found that an increase of the HMG protein level sensitizes breast cancer to cisplatin;[55] on the contrary, some cisplatin-resistant cell lines show that the HMGB1 is over expressed.[56] Other proteins that can recognize the cisplatin DNA damage sites have been recently reviewed.[49, 57, 58]

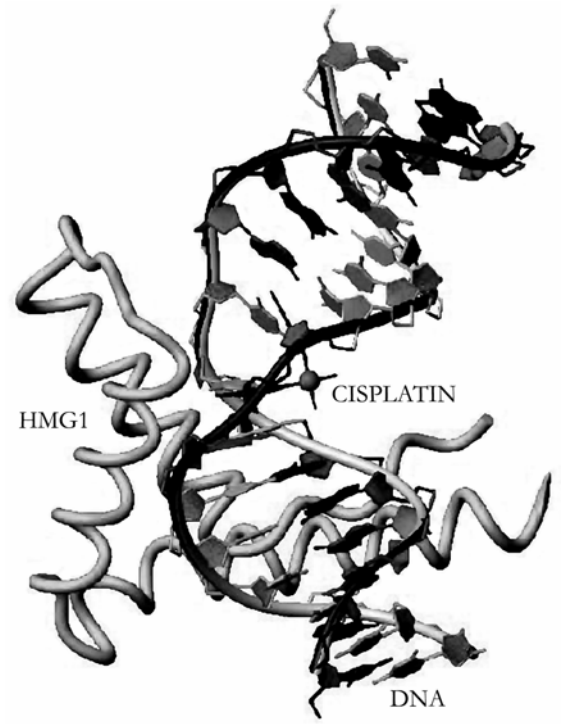

Figure 1.5 Structure of the HMG1 domain A bound to the 1,2-d(GG) intrastrand Pt-DNA adduct.[54]

The human polymerases α and β inevitably encounter the cisplatin-DNA adduct and are believed to contribute to the cytotoxicity of cisplatin.[59] However, some human polymerases are able to bypass the cisplatin-DNA adducts and incorporate the wrong base pairs, a process called translesion synthesis.[60] This process has a critical role at the mutagenic properties of cisplatin, because it can carry out DNA synthesis with lesions present.[61] Closely related to the mutagenicity of cisplatin is the evolution of resistance of some cancer cell lines against the drug.[62, 63]

1.5 Limitations of cisplatin

Despite the unparalleled success of cisplatin, the drug has several drawbacks. Serious side effects may appear during cisplatin treatment, such as nausea, vomiting, ototoxicity, neuropathy, myelosupression and the dose-limiting factor nephrotoxicity.[32, 64, 65] Several protective and rescue agents are usually added to the chemotherapy to reduce these side effects. For example, nephrotoxicity is reduced by intravenous hydration and diuresis.[66] Intrinsic and acquired resistance is a major drawback in chemotherapy, and cisplatin is no exception.[67-70] The mechanisms of resistance vary significantly between the different tumors types. Furthermore, numerous mechanisms of resistance act simultaneously in a cancer cell type,[69] which is a topical challenge for the scientific community.

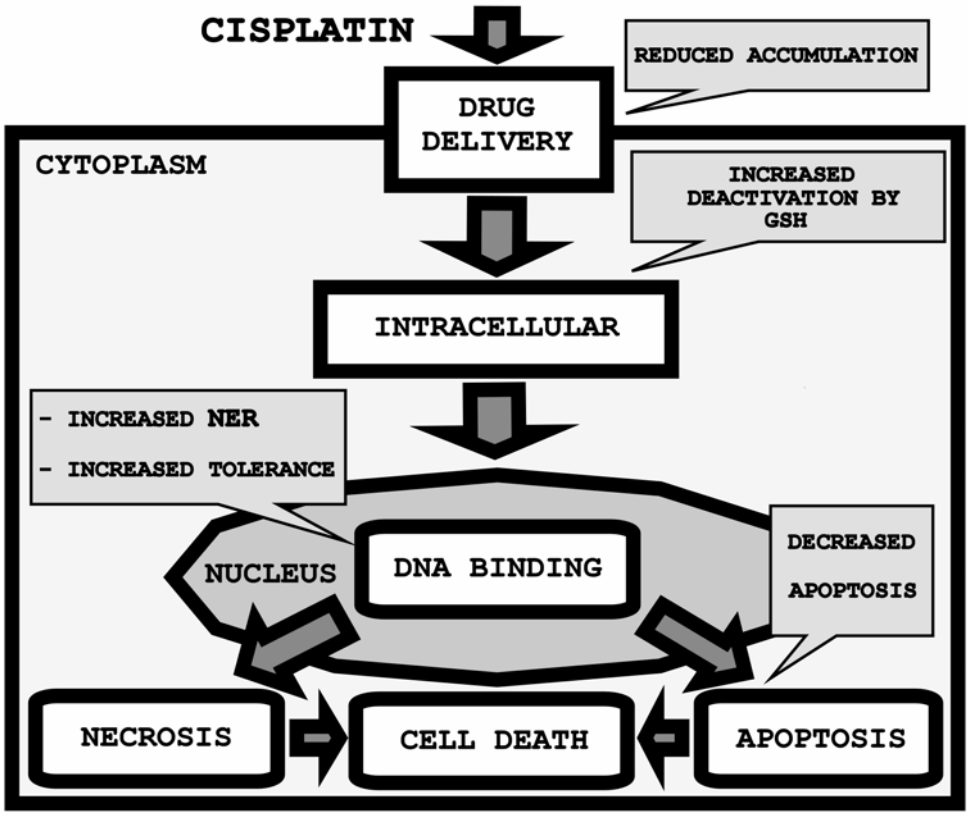

Figure 1.6 Main mechanism of cisplatin resistance in the cell. Two mechanisms of resistance act before binding to DNA, *i.e.* reduced accumulation and increased deactivation by glutathione (GSH). After binding of cisplatin to DNA three mechanisms of resistance can occur, namely increase NER activity, increased tolerance and decreased apoptosis.

Cisplatin resistance can either prevent the drug to reach its target or block the cellular response, leading to apoptosis or necrosis (Figure 1.6). In order to bind to DNA, cisplatin first has to enter the cell. Decreased uptake or increased efflux of cisplatin results in lower amounts of the drug inside the cell. In vitro models have shown that acquired resistance of cisplatin can lead to a decrease in accumulation of the drug by a factor of two to four.[71] Once inside the cell, cisplatin can bind to intracellular thiols, like glutathione and metallothionein.[72] Especially glutathione (0.5 – 10 mM) is present in high concentrations in the cytosol.[73] Increased concentrations of intracellular thiols are evidently established as a mechanism of resistance in cisplatin resistant tumor cells.[69, 71]

After entering the nucleus and binding to DNA, two types of resistance to cisplatin may be observed, or will be developed. The cisplatin damage can be recognized and repaired by the nucleotide excision repair (NER). Increased NER activity appears to be a major mechanism of resistance. The 1,2-intrastrand and the 1,2-interstrand cisplatin-DNA adducts are found to be repaired more efficiently in some cisplatin resistant cell lines.[51, 74] The other mechanism of resistance is a general problem encountered in chemotherapy. The presence of gaps in replicated DNA can be lethal. Therefore, the post-replication process is needed to repair them. However,

this repair system is also capable to synthesize DNA along the cisplatin-induced lesions. In some cisplatin resistant cell lines, an increased ability to bypass cisplatin adducts is observed; this phenomenon is often referred to as "increased tolerance".[75]

The recognition of the cisplatin-DNA adducts by proteins can ultimately lead to apoptosis of the cancer cells. However, it is common that the proteins of the apoptotic pathway may malfunction.[76] Therefore, the malfunctioning apoptotic route is believed to be a process generating cisplatin resistance.[77] Much research studies have been focusing on the design of novel platinum-containing drugs that are able to overcome these cisplatin problems.

1.6 New approaches in platinum drug design

Literally, several thousands of platinum compounds have been synthesized during the search of improved drugs.[78, 79] From these molecules, only about 35 complexes have entered the clinical trials.[80, 81] Nowadays, besides cisplatin, three platinum-based drugs are clinically used (Figure 1.7) on a global scale, whereas a few others are only used in certain countries.

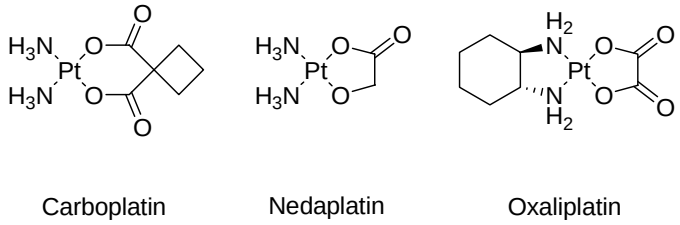

Figure 1.7 Structural formulae of the new platinum drugs used in the clinic.

The majority of the active platinum complexes has the following general formula *cis*-[Pt(Am)$_2$X$_2$], where Am is an inert amine and X a leaving group (labile ligand). *Cis*-diammine-1,1-cyclobutane-dicarboxylatoplatinum(II) (Carboplatin) (Figure 1.7) is no exception, and therefore its mechanism of action is similar to the one of cisplatin. However, Carboplatin is less reactive than cisplatin.[82] Carboplatin is approved for its worldwide usage since 1986. The rate of aquation of the leaving group of carboplatin, i.e. the cyclobutanedicarboxylate ligand, is almost twice lower due to the chelating effect. As a result, compared to cisplatin, Carboplatin causes less severe side effects, although a higher dose is needed.[83] For this reason, Carboplatin is used to treat ovarian cancer patients who often suffer from critical side effects.[84] Carboplatin is a typical example of a second generation platinum drug, because the nature of the leaving groups has been optimized to reduce the side effects. Another example is *cis*-diammine(glycolato)platinum(II) (Nedaplatin) (Figure 1.7), which is approved in Japan for example for clinical use since 1995.[85] Both Nedaplatin and Carboplatin are cross-resistant to cisplatin, which indicates that their mechanisms of action are similar. In the third generation platinum drugs, the NH_3 ligands are replaced by primary or secondary amines. A good example is (*1R,2R*-diaminocyclohexane)oxalatoplatinum(II)

(Oxaliplatin) (Figure 1.7)[86], which is used in the clinic worldwide for the treatment of colorectal cancer.[87] Interestingly, the higher lipophilicity of the cyclohexanediamine ligand ensures a better uptake in cancer cells compared to cisplatin, and the formation of its DNA adduct is distinct.[58, 88] Therefore, Oxaliplatin has a different spectrum of activity compared to cisplatin, and it is able to circumvent cisplatin resistance.[89, 90] However, the structure of its DNA adduct (1,2-d(GG) intrastrand), as determined from the structure of an oligonucleotide adduct, is quite similar.[88]

Cisplatin is administered intravenously, which often is very uncomfortable for the patient. Therefore, Pt(IV) complexes have been developed to be administered orally, and thus improve the quality of life of the patient. The best example of this class of compounds is satraplatin (Figure 1.8). This promising drug is currently in phase-III clinical trials and is active against a number of tumors including cisplatin resistant cell lines.[91] The mechanism of action is believed to involve the intra- and extra-cellular reduction of the Pt(IV) complex prior to its reaction with DNA.

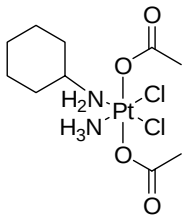

Satraplatin

Figure 1.8 Structural formula of Satraplatin.

A major cause of cisplatin resistance is the detoxification by intracellular thiols. In order to reduce the possibility of reaction of platinum with glutathione, sterically crowded platinum complexes have been designed and prepared.[92] These complexes also are supposed to be less active in hydrolysis. The complex ZD0473 (Figure 1.9) has entered Phase-II clinical trials.[83] It shows activity against several cancer cell lines, including some cisplatin resistant ones.[93]

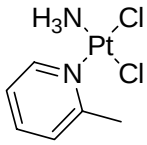

ZD0473

Figure 1.9 Structural formula of the sterically hindered complex ZD0473.

Because *cis*-Pt(NH_3)Cl_2 shows anti-tumor activity, while *trans*-Pt(NH_3)Cl_2 shows not, it has been generally believed that *trans*-compounds are incapable of inducing anti-proliferate activity. However, by changing the amines to more bulky groups (Figure 1.10), a series of trans complexes have been synthesized that show good cytotoxicities and also different cellular distributions compared to cisplatin.[94, 95] Thus, *trans*-Pt(pyridine)$_2$$Cl_2$ shows cytotoxicity against

cisplatin-resistant cell lines.[96, 97] Fascinatingly, this complex exhibits reduced reactivity with biomolecules, like glutathione, and it also forms more interstrand crosslinks compared to cisplatin.[98] The iminoether ligands of the *trans*-Pt(iminoether)$_2$Cl$_2$ complex (Figure 1.10) may induce steric constraints; consequently, its chloride exchange reactions are much slower. Nevertheless, a similar level of DNA platination is acquired, because the corresponding adducts are more stable.[99] In contrast to *trans*-Pt(pyridine)$_2$Cl$_2$, this complex produces mainly monofunctional DNA adducts.[100] This complex is more active than its *cis*-analogue both *in vivo* and *in vitro*.[101, 102] The *trans*-[Pt(isopropylamine)(dimethylamine)Cl$_2$] complex (Figure 1.10) also shows promising cytotoxicity against several cell lines, whereas the *cis*-analogue is found to be inactive.[103, 104] An increasing number of *trans*-platinum compounds are found to be active against a range of tumor cell lines, complementary to the ones affected by the action of cisplatin.[105, 106]

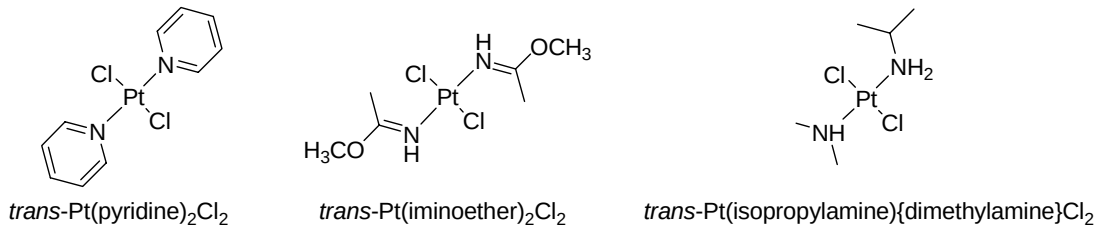

Figure 1.10 Structural formulae of three known active *trans*-platinum complexes.

Polynuclear platinum complexes are a new class of compounds aimed at interacting with DNA in a distinct way compared to cisplatin.[107] Two good examples of this class of compounds, that circumvent cisplatin-resistance, are shown in Figure 1.11. BBR3464 is a trinuclear platinum complex that can only coordinate to one other nucleophile per platinum unit. This complex forms predominantly interstrand adducts with DNA.[108, 109] The cytotoxicity profile[110] of this complex was so promising that it entered the clinical trials, but due to high toxicity, the clinical trials were abandoned at Phase-II.[110] AMPZ (Figure 1.11) is a very promising dinuclear platinum complex that is highly cytotoxic and able to overcome cisplatin resistance.[111] The complex has been designed to induce minimal DNA distortions, in order to prevent the recognition of the platinum-DNA adduct by NER proteins. Indeed, as shown by NMR, AMPZ unwinds the DNA double helix by only 10 to 15°.[112] Most likely, these small distortions account for the high activity of the complex against resistant cell lines, because the repair enzymes do not recognize the DNA damage.

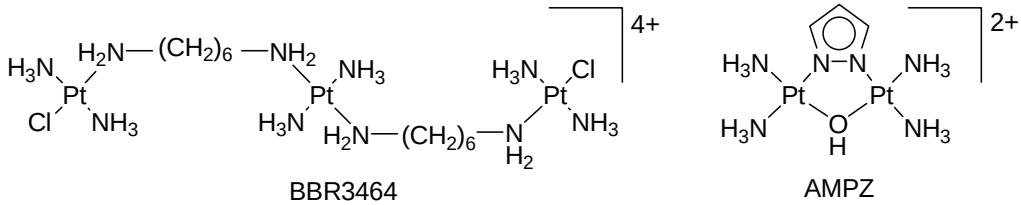

Figure 1.11 Structural formulae of the polynuclear platinum complexes BBR3464 and AMPZ.

1.7 Multifunctional platinum drugs

Another strategy to overcome the problems encountered with the use of cisplatin is to design new compounds that maintain a cisplatin activity (thanks to a cisplatin-like moiety) and which possess a second functional group.[113] For instance, a cisplatin unit can be linked to a carrier to improve the anticancer activity via a selective targeting of the cancer cells, the lessening of undesirable side effects, or an increase of their affinity for DNA. The multifunctionality is often introduced by tethering a *cis*-platinum unit to the second function. The carrier is bound to the platinum unit and is expected to target the cancer cells or to enhance the cellular uptake. Moreover, this carrier is supposed to release the drug once the target has been reached. The carrier can be attached to the leaving group of the platinum unit or linked to the amine ligands. However, the latter may change the intrinsic properties of the *cis*-platinum unit, possibly causing undesired effects inside the cell, such as the lowering of the cytotoxicity effect.

Some tumor cells are permeable for macromolecules as a result of compromised vasculature.[114] This so-called enhanced permeability and retention effect (EPR effect) can be exploited to target these cancer cells with a macromolecule bound to platinum drugs. A good example of this type of compounds is the platinum diammine unit linked to a *N*-(2-hydroxypropyl)methacrylamide polymer (Figure 1.12). Once the macromolecular compound has entered the cell, its platinum attached drug is most likely released through its hydrolysis or via the proteolyticic cleavage of the peptide bond.[115, 116] The cytotoxicity of this platinum molecule is very promising, and an activity two times higher than that of Carboplatin is observed.[113] In addition, it has been shown by *in vivo* experiments that its toxicity is six times lower than that of Carboplatin without loss of activity. This potential drug has entered Phase-I clinical trials.[117]

It is widely accepted that the antitumor properties of cisplatin result from its interaction with DNA. Nevertheless, the hydrolysis inside the cell followed by the binding to DNA is a slow process; consequently, only a small part of the platinum can reach the DNA.[11] The linkage of a platinum moiety to a drug with high DNA affinity would therefore greatly improve the rate of the reaction of the platinum unit with DNA, and increase the amount of platinum-DNA adducts formed. An additional advantage may be that the production of different platinum-DNA adducts can induce distinct DNA distortions, and thereby broaden the spectra of cancer cell lines that can efficiently be treated. For example, the affinity with DNA can be improved by introducing: (i) a positive charge in the complex, like in BBR3464, (ii) groove binders, or (iii) intercalating agents.

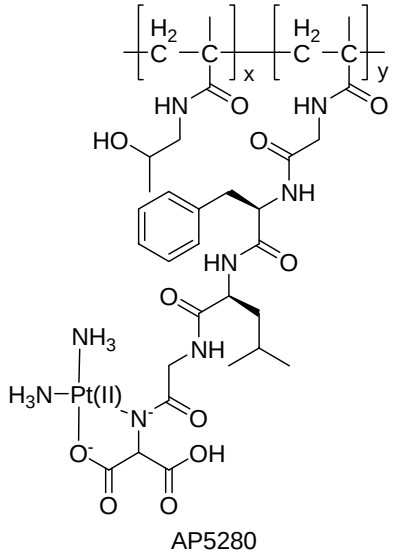

Figure 1.12 Structure of the platinum polymer AP5280.

Groove binders are compounds that are able to recognize specific sequences in the minor groove of DNA, through van der Waals attraction and formation of hydrogen bonds.[118] The two antiviral antibiotics netropsin and distamycin are good examples of this class of compounds. Both compounds have been linked to *cis*-platinum units (Figure 1.13 shows the Pt(distamycin) complex, i.e. Pt-DIST[119]).[119-121] Investigations on the Pt-DIST complex have revealed that its sequence selectivity is similar to that of cisplatin, but different DNA conformational alterations are observed as well as more interstrand cross links.[119, 121]

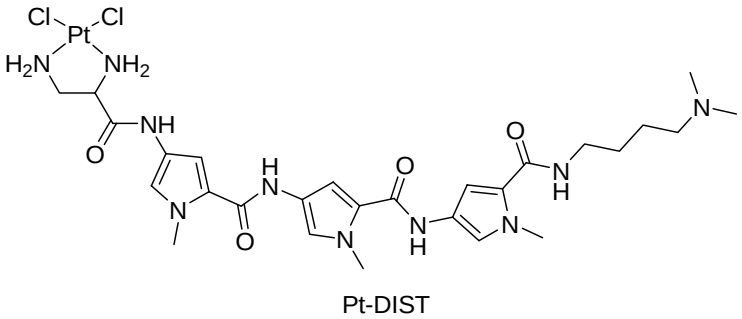

Figure 1.13 Platinum complex with the groove binder distamycin.

Intercalating agents have been used extensively to target DNA, because of their potential antitumor properties, and their very high affinity for DNA.[122, 123] The acridine family are typical examples of intercalating, antitumor active agents that bind to DNA and block Topisomerase proteins.[124] Platinum-containing units have been linked to intercalators through a flexible spacer (Figure 1.14) to achieve synergistic interactions with DNA. The complex $[Pt\{AO(CH_2)_6en\}Cl_2]^+$ (Figure 1.14) presents a *cis*-platinum unit linked to acridine orange.[125, 126] It has been shown that both units can interact with DNA, although the sequence selectivity of the platinum unit is not

significantly changed.[127] Also, this complex can be activated by light, which may induce nicks in the DNA.[126] In contrast to the latter compound, the Pt(Acridinecarboxamide)Cl_2 complex (Figure 1.14) shows a different sequence-selective binding of its platinum unit to DNA.[128] However, the major binding sites in the case of HELA cells are identical to those observed with cisplatin.[129] These results suggest that the kinetics of the platinum binding are influenced by the presence of the intercalator. The cytotoxicity of this complex against some cell lines is very promising.[130, 131] Another very promising complex is Pt-ACRAMTU (Figure 1.14). This complex possesses a very good *in vitro* antitumor activity against cisplatin-resistant cancer cell lines.[132-134] Interestingly, its platinum part can only bind to one nucleobase in DNA. Moreover, the bridge connecting the two functional groups is very short. For this reason, not only the sequence selectivity of the platinum unit but also the DNA damage are drastically different compared to cisplatin.[135-138] This bifunctional compound represents the first example in which a platinum moiety is partially directed towards the minor groove of the DNA helix.[137] Interestingly, other platinum complexes with an intercalating unit can also be followed in the cell, because the intercalator has fluorescing properties.[139, 140]

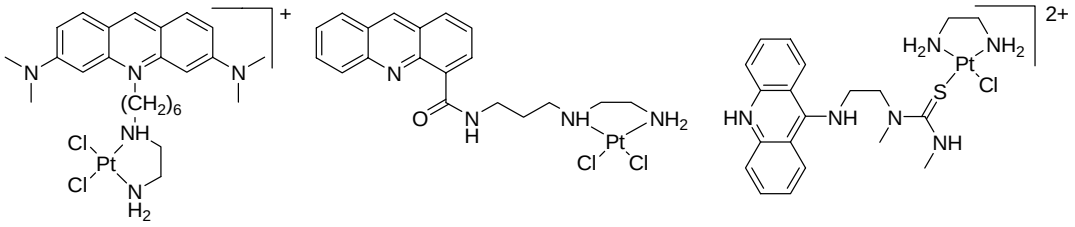

Figure 1.14 Structural formulae of bifunctional platinum complexes including an acridine group.

1.8 DNA cleavage as mechanism of action for antitumor drugs

Oxidative DNA damage is a relatively common event in cells, which may lead to mutation, cancer, and cellular or organismic death.[141] Such damage can be initiated by ionizing radiation,[142] photooxidation,[143] hydroperoxides activated by transition metals,[144, 145] hydroxyl radicals,[144] or various other oxidizing agents.[145, 146] The cellular response in living organisms to this oxidative stress includes: (i) removal of the damaged nucleotides and the restoration of the original DNA duplex, (ii) cell-cycle arrest, the reparation or prevention of the transmission of damaged or incompletely replicated chromosomes (iii) apoptosis, which results in the elimination of the damaged cell from the body. Several DNA repair mechanisms have been identified, such as: base excision repair, NER, double-strand break repair, and cross-link repair.[147]

The DNA in cancer cells can also be deliberately damaged with the aim to either kill them or to stop their proliferation. The three major pathways to induce DNA cleavage are: (i) the oxidation of the nucleobases,[148] (ii) the hydrolysis of the phosphate groups,[149-151] (iii) and the

oxidation of the deoxyribose unit.[152] Single-strand breaks of the DNA strand (SSB) or double-strand breaks in the DNA duplex (DSB) can occur. The oxidation of the nucleobases rarely leads to a direct strand scission. Indeed, often a second step is needed to break the DNA strand, which includes the use of heat, a base or an enzyme treatment.[148] The hydrolysis of the phosphate diester groups is the natural pathway to break a DNA strand. The phosphate diesters are highly stable functional groups;[153] nonetheless, some enzymes and some synthetic model compounds are known to cleave DNA via this hydrolytic pathway.[154, 155] The oxidation of the deoxyribose unit can lead to direct DNA-strand breaks. The strand scission is achieved through the initial abstraction of a hydrogen atom from the deoxyribose unit. Among the seven C–H bonds of the deoxyribose unit that can be oxidized, four point towards the minor groove, and three are located in the major groove (Figure 1.15). The ease to homolyse the C–H bond depends on the nature of the carbon considered. Thus, less energy is required to remove a H-atom from a tertiary carbon than from a secondary carbon. In addition, the orientation of the drug with regard to the sugar C–H bonds is very important. The tertiary C4'–H and C1'–H bonds (Figure 1.15) are accessible from the minor groove, while the C3'–H bond is only reachable from the major groove. The secondary C–H bonds C2' and C5' (Figure 1.15) both hold a H atom pointing in both the minor and major grooves.

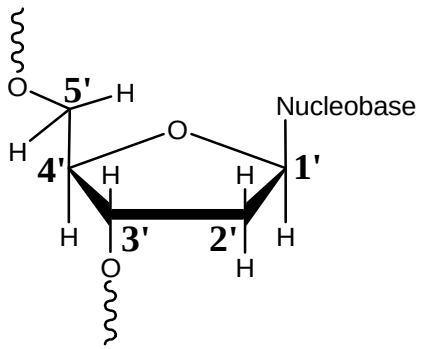

Figure 1.15 Schematical representation of the deoxyribose unit. The possible oxidation targets are indicated in bold.

The first compounds that have been found to be able to cleave DNA through the oxidation of the sugar unit are the natural products bleomycins (Figure 1.1),[156-158] neocarzinostatin,[159] calicheamicin,[160] and esperamicin.[161] Bleomycins constitute a family of compounds first isolated from *Streptomyces Verticillus* by Umezawa *et al.* in 1966.[162] They are clinically used against lymphomas, head and neck cancers, and germ-cell tumors.[157] It is generally believed that the therapeutic activity of bleomycin is due to its ability to interact with DNA and cleave it. It has been shown in early studies that bleomycin induces breaks, gaps, deletions, dicentrics and ring formation in the chromosomes, causing global morphological changes.[163] Bleomycin is formed by three domains; the bithiazole and the positively charged chain contribute to the specific binding to DNA, the disaccharide is believed to be responsible for the

accumulation of bleomycin in cancer cells, and the metal binding domain is the redox active center (Figure 1.1 in bold). The latter can coordinate metal ions such as Fe, Cu and Co. In the presence of dioxygen and a reductant, the bleomycin complexes are activated, and are capable of catalyzing the formation of SSB and DSB. Studies have indicated that both cleavage events involve the abstraction of the 4'-hydrogen atom, and that DSBs can be mediated by a single bleomycin molecule.[152]

Since the discovery of bleomycin, a variety of complexes have been synthesized to mimic its cleavage activity. The most studied synthetic complexes able to cleave DNA by oxidation of the deoxyribose unit are $[Fe^{II/III}(edta)]$[164, 165] and $[Cu^{I/II}(phen)_2]$[166] (Figure 1.16). [79]

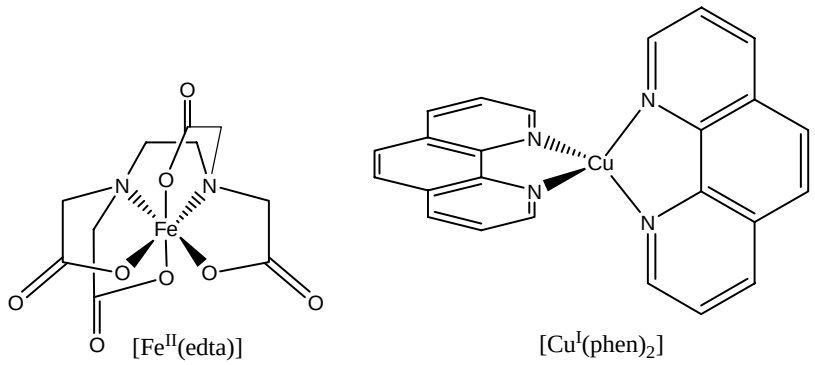

Figure 1.16 Structural formulae of the nuclease active complexes $[Fe^{II}(edta)]$ and $[Cu^{I}(phen)_2]$.

1.9 Mechanism of the cleavage mediated by $[Cu^{I/II}(phen)_2]$

The first example of a synthetic complex that exhibited nuclease activity on double stranded DNA was $[Cu^{I/II}(phen)_2]$.[166-168] This complex is able to induce SSBs on double strand DNA in the presence of a reductant and hydrogen peroxide or dioxygen. Interestingly, the nuclease activity of the $[Cu^{I/II}(phen)]$ complex is markedly lower compared to that of $[Cu^{I/II}(phen)_2]$.[145, 146, 167-169] The equilibrium constants for the binding of the first (log K_1) and second (log K_2) phenanthroline ligand to copper are respectively 10.3 and 5.5.[170] The cleavage experiments with this complex are generally performed at micromolar concentrations; therefore, a large excess of phenanthroline is required to favor the formation of the complex 2 phenanthroline/1 copper.

The $[Cu^{I}(phen)_2]$ complex exhibits a tetrahedral geometry.[171, 172] The coordination geometry of $[Cu^{I/II}(phen)_2]$ drastically changes upon oxidation of the copper ion, from a tetrahedron to a trigonal bipyramid or square pyramid. The interaction of this complex with DNA is crucial for its cleavage activity. The binding to DNA most likely results from an ordered sequential mechanism: first the non interacting $[Cu^{II}(phen)_2]$ moiety is reduced by a reductant to

$[Cu^{I}(phen)_2]$ which appears to interact better with DNA.[173] It cannot be excluded that $[Cu^{II}(phen)_2]$ is also binding to DNA. Such binding would, however, result in the very slow reduction of Cu^{2+} to Cu^{+} by $O_2^{\bullet-}$.[174] It has been found that $[Cu^{I/II}(phen)_2]$ is able to intercalate between DNA base pairs from the minor groove.[173, 175, 176] Model studies with DNA and $[Cu^{I}(phen)_2]$ have shown that one of the phenanthroline ligands is partially intercalating at the ApT, while the other one is twisted over an angle of 50° to favor interactions in the minor groove (Figure 1.17).[173, 177-179] The cleavage selectivity of this complex is to some extent sequence-dependent. $[Cu^{I}(phen)_2]$ favors the cleavage of 5'-TAT triplets and in lesser extent TGT, TAAT, TAGPyr and CAGT sequences, which reflects its preference for the minor groove. Furthermore, A-DNA is cleaved less efficiently compared to B-DNA, most likely as a result of its widened minor groove. Z-DNA and single stranded DNA are poorly cleaved by this reagent.[175, 180, 181]

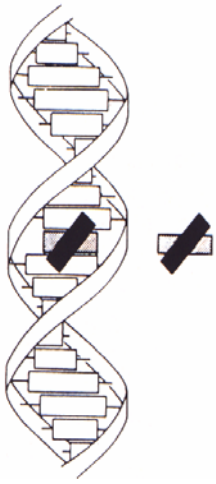

Figure 1.17 Postulated model of the intercalative binding of the $[Cu^{I}(phen)_2]$ complex to DNA.[177] The twisted black and white bars on the right of the DNA-complex model schematizes $[Cu^{I}(phen)_2]$.

Once $[Cu^{I}(phen)_2]$ is interacting with DNA, it can be activated by dihydrogen peroxide or molecular dioxygen through the formation of active "oxo" species. The exact nature of this active species is still unknown. The first chemical steps involving $[Cu^{I/II}(phen)_2]$ have been unraveled (scheme 1.1).[169] The first reaction step is the reduction of the initial complex to $[Cu^{I}(phen)_2]$. In the second step, dioxygen reversibly reacts with $[Cu^{I}(phen)_2]$, to form $[Cu^{II}(phen)_2]$ and a superoxide anion. The participation of superoxide has been established using superoxide dismutase. Indeed, superoxide dismutase is able to alter the rate of the cleavage reaction;[175] moreover, the addition of a superoxide generator in the presence of dioxygen improves the cleavage reaction.[175] Interestingly, the reaction with a superoxide generator in the absence of $[Cu^{I/II}(phen)_2]$ does not lead to any DNA cleavage, thus indicating that the superoxide anion is not directly implicated in the reaction. The involvement of generated dihydrogen peroxide (Scheme 1.1, reaction 3) has been unambiguously proven.[175] The cleavage reaction

proceeds in the presence of dihydrogen peroxide at equal rates under aerobic and anaerobic conditions. Furthermore, without dihydrogen peroxide, the cleavage reaction is markedly slower, and the addition of catalase inhibits the reaction.[169, 175] The reaction of dihydrogen peroxide with $[Cu^{I}(phen)_2]$ leads to the active species (Scheme 1.1, reaction 4). The exact nature of this species is still under debate. The cleavage products generated from the reaction of DNA with $[Cu^{I/II}(phen)_2]$ are typical for the attack of hydroxyl radicals ($OH^{\bullet}$). However, hydroxyl radical scavengers do not inhibit the cleavage reaction.[175, 182] It has been proposed that steric hindrance in the region of the DNA-$[Cu^{I/II}(phen)_2]$ adduct may prevent the radical scavengers to be able to reach the copper site where the hydroxyl radicals are generated.[183] Nonetheless, the hydroxyl radical pathway cannot be excluded. Most likely, the reactive species is a copper-bound oxygen entity, such as Cu^{3+}-hydroxide or Cu^{+}-hydrogenperoxide. A Cu^{3+}-oxido species has been proposed as well.[169]

$$[Cu^{II}(phen)_2] + e^- \longrightarrow [Cu^{I}(phen)_2] \qquad (1)$$

$$[Cu^{I}(phen)_2] + O_2 \rightleftharpoons [Cu^{II}(phen)_2] + O_2^{\bullet -} \qquad (2)$$

$$[Cu^{I}(phen)_2] + O_2^{\bullet -} + 2H^+ \longrightarrow [Cu^{II}(phen)_2] + H_2O_2 \qquad (3)$$

$$[Cu^{I}(phen)_2] + H_2O_2 \longrightarrow \text{reactive species} \qquad (4)$$

Scheme 1.1 Proposed route for the formation of the reactive species able to cleave DNA in the presence of a reductant and dioxygen.[169]

Activated $[Cu^{I/II}(phen)_2]$ is able to abstract the protons from the carbons C1', C4' and C5' of the deoxyribose unit from the minor groove of DNA.[145, 152, 169, 184] The abstraction of these protons yields unique products, which can be characterized by HPLC, PAGE or GC analysis. The proposed mechanisms for proton abstraction by $[Cu^{I/II}(phen)_2]$ are shown in scheme 1.2. The oxidation of C1' is evidenced by the detection of 5-methylene furanone (5-MF).[185] The first step in this reaction is the H1' abstraction by activated $[Cu^{I}(phen)_2]$. The resulting radical is then converted to a carbocation, probably with the help of the complex. After reaction with water,[186] the nucleobase is released, generating an oxidized abasic site. DNA deoxyribonolactone abasic sites are very stable so that normally a heating step, or an alkaline step is needed to further react and cleave the DNA strand.[187] Interestingly, in the case of $[Cu^{I/II}(phen)_2]$, the complex catalyses this step.[188, 189] Nevertheless, abasic sites could be detected by LC/ESI-MS experiments.[190] The actual cleavage of the DNA strand is realized by the first β-elimination step, thereby releasing an 5'-phosphate end. After a thermal step, the second β-elimination step is completed liberating 5-MF (Scheme 1.2). The oxidation of the carbon C1' is the major pathway of DNA cleavage mediated by $[Cu^{I/II}(phen)_2]$; therefore, the other two potential pathways have been less studied. 3'-Phosphoglycolate fragments are typically observed by PAGE experiments for the oxidation of C4'; indeed, 3'-phosphoglycolate fragments migrate faster than 3'-phosphate ones. Such

fragments have been identified in the case of [$Cu^{I/II}(phen)_2$], but no detailed mechanistic studies have so far been performed. The two most likely pathways (Scheme 1.2, **A** and **B**) for the oxidation of C4' are shown in Scheme 1.2. Both the **A** and **B** pathways start with the abstraction by [$Cu^{I/II}(phen)_2$] of the proton H4' from the deoxyribose unit. The radical mediation gives rise to a cleavage of a C–O bond in pathway **A** (Scheme 1.2), releasing the 5'-phosphorylated fragment. The resulting radical cation reacts with water, yielding a new 4'-radical. After reaction with dioxygen and a proton, a Grob rearrangement[191] occurs, and an ultimate β-elimination step gives the detectable 3'-phosphoglycolate end.[192, 193] Pathway **B** (Scheme 1.2) is proposed in the case of Fe-bleomycin.[145, 152, 156, 169] The C4' radical reacts with dioxygen to form a peroxyl radical which further reacts to produce a hydroperoxyl group. This compound undergoes a Criegee rearrangement[194]. Normally, this rearrangement is catalyzed by an acid,[194] and it is thus believed that bleomycin acts as a Lewis acid.[145] Next, the 2'-pro-R-proton and the nucleobase are consecutively eliminated to yield the 3'-phosphoglycolate end and base propenal. The C5' oxidation pathway starts with the abstraction by the $Cu^{+}(phen)_2$ complex of the proton H5' . Then, the cleavage of the 3'-phosphate end results in a direct break of the DNA strand. The heating of the ensuing C5'-aldehydic fragment under mild alkaline conditions induces two β-elimination steps with the release of the characteristic product of C5' oxidation, namely furfural. The oxidation of the carbon C5' represents a minor pathway of DNA cleavage performed by [$Cu^{I/II}(phen)_2$]. The C1' oxidation is the major pathway and accounts for about 80-90% of the cleavage events.[167]

1.10 Novel cleaving agents based on [$Cu^{I/II}(phen)_2$]

[$Cu^{I/II}(phen)_2$] has been utilized as a footprinting agent and also in biological studies.[146, 181, 195-197] However, the low binding constant of the second phenanthroline ligand and the lack of sequence selective cleavage limit its applicability. Several strategies have been employed to improve the efficiency of [Cu-phenanthroline]-based DNA cleaving agents. For instance, the second phenanthroline ligand has been replaced by various amino acids,[198, 199] NSO-donor Schiff bases,[200-204] sulfonamides,[205] or peptides.[206] In these systems, the phenanthroline/copper part is expected to bind to DNA and cleave it. The second ligand is then used to add a second functional group to the complex or to modify its interaction with DNA and thereby its biological properties. For example, the complexes with NSO-donor Schiff bases are in some cases able to perform hydrolytic,[203] or photoinduced DNA cleavage,[200-202, 204] which are not observed with the parent [$Cu^{I/II}(phen)_2$] compound.

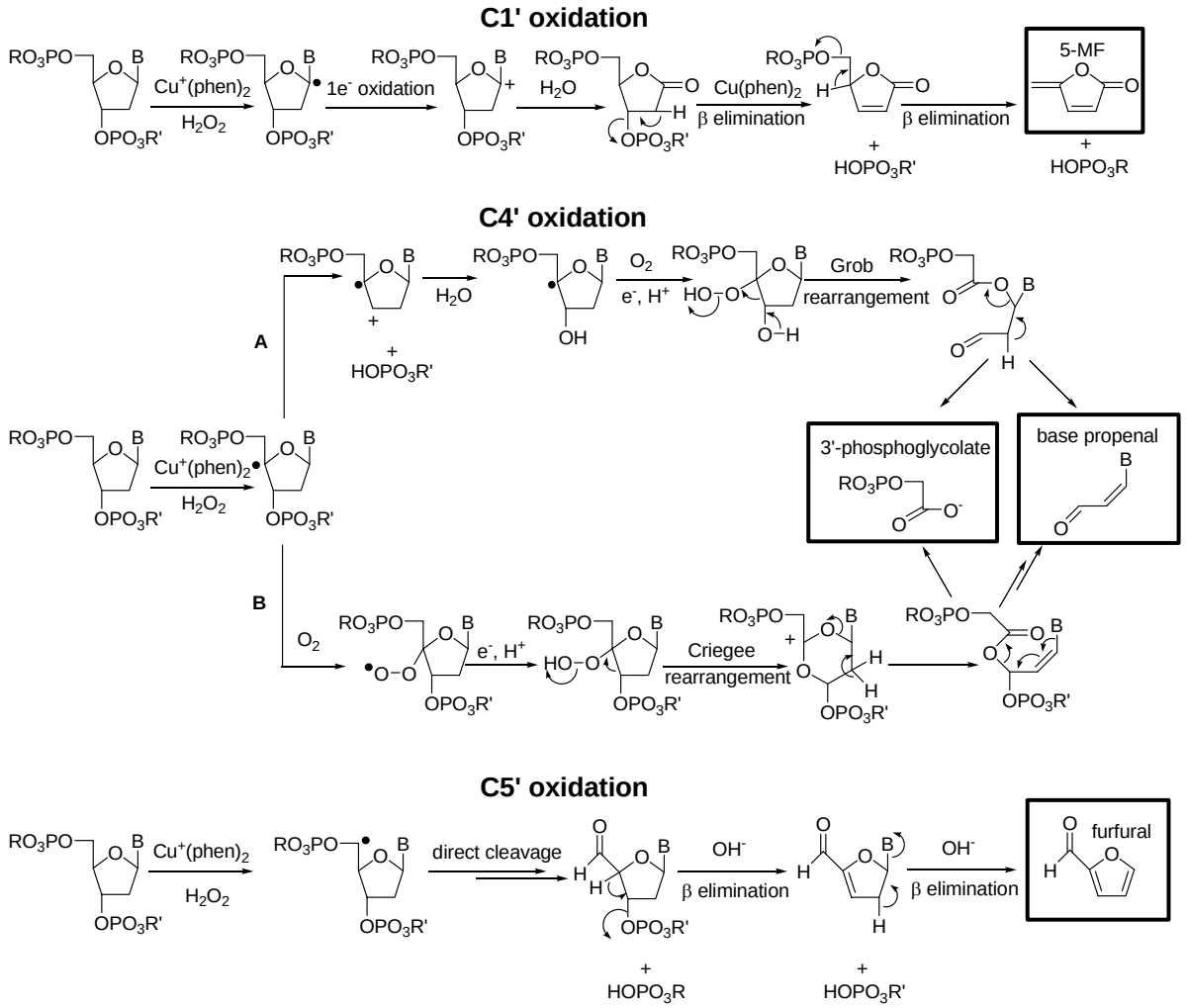

Scheme 1.2 Proposed mechanisms for the oxidation of the deoxyribose carbons C1', C4' and C5' of DNA mediated by [$Cu^{I/II}(phen)_2$]. 5-MF, 3'-phosphoglycolate, and furfural are the products that have been isolated and quantified.[169]

The induction of site specific cleavages has been achieved by connecting a phenanthroline unit to targeting compounds. Thus, phenanthroline has been linked to the DNA-binding proteins trp,[207] CAP,[208] Cro,[209] Fis,[210] and NarL[211] to investigate the target site of these proteins or to collect DNA fragments for sequencing, cloning or chromosomal mapping.[146, 184] Another strategy to induce sequence selective cleavage of single- or double-stranded DNA is to attach oligonucleotides to a phenanthroline moiety, via their 5'-end.[212-214] Similarly to platinum conjugates, phenanthroline has been connected to an intercalator,[215, 216] and a minor groove binder.[217] However, none of these strategies overcomes the problem of the decrease in cleavage activity owing to the presence of only one phenanthroline ligand.

1.11 Design and mechanism of action of Cu(Clip-Phen) and conjugates

A bridge connecting two phenanthroline ligands forces both moieties to be in the close proximity of the copper center. The bridging of phenanthroline units through a very long bridge or via two sulfur atoms has proven to be an unsuccessful strategy to improve the cleaving activity of bis-phenanthroline/copper compounds.[218, 219] The group of Meunier *et al.* has found that the connection of two phenanthroline units using a serinol bridge gives rise to an efficient system (Figure 1.18). The nuclease activity of the resulting complexes, i.e. Cu(2-Clip-Phen) and Cu(3-Clip-Phen), is increased by a factor of, respectively, 2 and 40, compared to $[Cu^{I/II}(phen)_2]$.[220, 221] Interestingly, these complexes have shown good cytostatic activities as well.[222] The ligands have been designed to fulfill the following criteria: (i) the bridge must be attached near the nitrogen donors, at the C2 or C3 position of the phenanthroline, so that the phenanthroline units are close to each other; (ii) the length of the bridge should be long and thus flexible enough to allow the conformational changes occurring during the redox cycle; (iii) the bridge must have a group that can be easily functionalized with different moieties, without altering the ability of the phenanthroline groups to coordinate copper; (iv) the C9 position of the phenanthroline should be unfunctionalized to avoid steric hindrance during the conformational changes; (v) the preparation of the ligand should be straightforward, because large quantities of an active compound will be required for any clinical application; therefore, the ligand should be symmetrical.

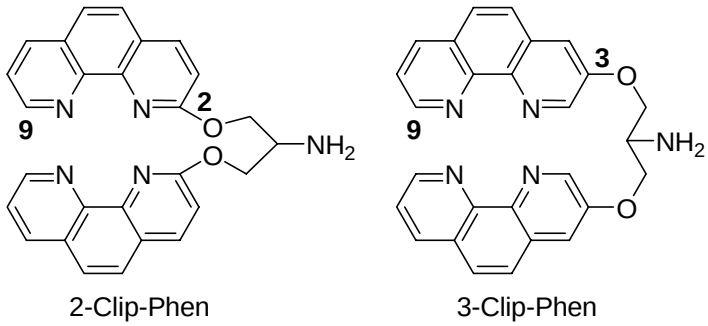

Figure 1.18 Structural formulae of 2- and 3-Clip-Phen.

Cleavage experiments performed in air in the presence of a reductant have revealed the remarkable cleaving abilities of Cu(2-Clip-Phen) and Cu(3-Clip-Phen). Quantifications of the results have shown that both complexes are typical single-strand cleaving agents. More elaborate PAGE studies have established that the mode of action of Cu(Clip-Phen) is similar to the one of $[Cu^{I/II}(phen)_2]$, since it interacts with the minor groove of DNA and cleaves without sequence selectivity. Moreover, similarly to $[Cu^{I/II}(phen)_2]$, H_2O_2 increases the cleaving activity indicating that the mode of activation is comparable.[223, 224] DFT calculations have been performed to rationalize the significant difference in cleaving activity between Cu(2-Clip-Phen) and Cu(3-Clip-Phen). It has been found that Cu(3-Clip-Phen) in both oxidation states has a more planar

geometry compared to Cu(2-Clip-Phen), which facilitates the intercalation of one of its phenanthroline units.[172] Furthermore, it has been proposed that the amine group of Cu(3-Clip-Phen) can form a double hydrogen bond in the minor groove of DNA in contrast to Cu(2-Clip-Phen) that strongly prefers to interact with the major groove (Figure 1.19).[172] It has been proposed that the amine group of Cu(2-Clip-Phen) is able to coordinate to copper, and therefore may compete with the second phenanthroline moiety.[225] The influence of the bridge length and its nature have been investigated to optimize the Clip-Phen cleavage ability.[225] Complexes with the bridge at the C3 position of the phenanthrolines are more efficient cleaving agents compared to the corresponding 2-Clip-Phen derivatives. The optimal length of the bridge has been found to be of three methylene groups.[225] Interestingly, the amine group of the serinol bridge is very important for the nuclease activity, since bridges lacking an amine function or with an acetamide group are undoubtedly less efficient.[225]

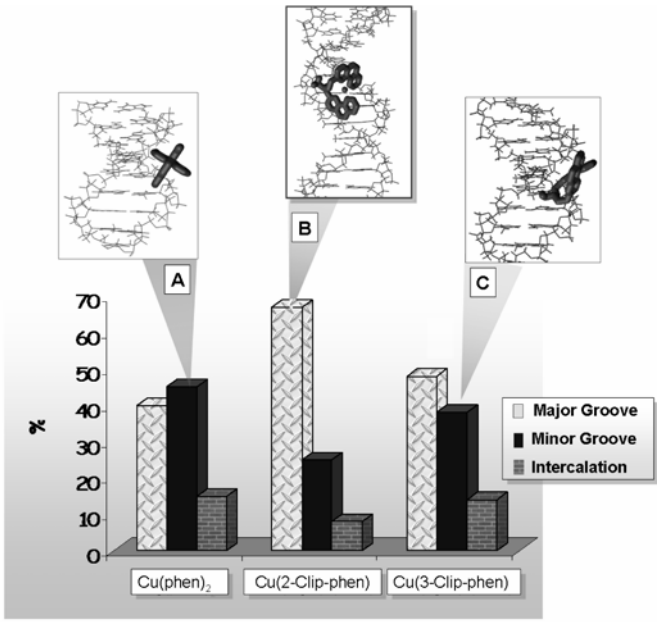

Figure 1.19 Probability of major groove binding, minor groove binding and (partial) intercalation (in %) for $[Cu^{I}(phen)_2]$, Cu^{I}(2-Clip-phen) and Cu^{I}(3-Clip-phen) adducts with a DNA oligomer (CGCTCAACTGTGATAC).[172]

The mechanism of oxidation of DNA mediated by Cu(3-Clip-Phen) has been investigated by HPLC, GC-MS and PAGE studies.[226] The direct release of nucleobases, the production of 5-MF, 3'-phosphoglycolate fragments and furfural illustrate the oxidation of DNA from the minor groove. Interestingly, the quantification of the nucleobases released through the action of Cu(3-Clip-Phen) points to a catalytic oxidation process. The oxidation of the carbon C1' has been found to be the major pathway of the DNA degradation. Nonetheless, the oxidation of the C4' and C5' atoms has been observed as well. The occurrence of the different DNA cleavage pathways has been established to be > 50% for the C1' oxidation, 15 ± 5% for C4', and 15 ± 5% for C5'.[226] In addition, Cu(3-Clip-Phen) performs direct strand cleavages similarly to

[$Cu^{I/II}(phen)_2$], in a random fashion and no direct evidence of nucleobase oxidation has been observed.

The nuclease activity of Cu(Clip-Phen) has been adjusted applying covalent association with a variety of DNA interacting agents (Figure 1.20). Cu(Clip-Phen) cleaves DNA without sequence selectivity; therefore, 2- and 3-Clip-Phen have been linked to a distamycin analogue in order to achieve a sequence selective cleavage. The cleavage patterns of these ligands in the presence of copper, air and a reductant reveal a high sequence selectivity in the close proximity of the usual binding site of distamycin.[224] The mechanism of cleavage of this bifunctional analogue confirms that the cleavage of the Cu(3-Clip-Phen) part is very similar to the one of "free" Cu(3-Clip-Phen). The only observed difference is the decrease of C1' oxidation, suggesting that the steric constraints of the bulky complex force the Cu(3-Clip-Phen) unit to act at the edge of the DNA minor groove. Spermine, a natural polyamine, exhibits a very high DNA affinity under physiological conditions. To increase the affinity of Cu(3-Clip-Phen) for DNA, and consequently its cleaving ability, Clip-Phen-sp has been prepared. The copper derivative of Clip-Phen-sp is a highly efficient cleaving agent. However, no sequence-selective cleavage has been observed with this conjugate.[223] Acridine is known to exhibit not only a high affinity for DNA, but this family of compounds can also enter cells very rapidly. 3-Clip-Phen has been therefore linked to an acridine moiety via bridges of variable lengths.[227] A series of compounds have been thus prepared which have proven to be highly efficient DNA cleaving agents in the presence of copper.[227] Also, the length of the junction arm appears to be crucial for their cleaving activity. All these rationally designed multifunctional Cu(3-Clip-Phen)-based complexes are more effective nuclease agents than Cu(3-Clip-Phen) alone.[227]

1.12 Other efficient copper-based DNA-cleaving agents.

Since the discovery of the nuclease activity of [$Cu^{I/II}(phen)_2$], many derived complexes have been synthesized that exhibit nuclease activity. Three of them are of particular interest. Redox active metal complexes are usually activated by a reductant prior to the DNA cleavage reaction. Complexes that cleave DNA by means of a hydrolytic pathway do not have to be activated. Only, a few examples have been found that can oxidize DNA without the presence of a reductant (Figure 1.21). Coordination compounds of the salen ligand with Mn^{3+}, Co^{2+}, Ni^{2+} or Cu^{2+} ions have proven to be very efficient cleaving agents in the presence of an added reductant.[148, 228-234] Interestingly, the hydroxyl-salen ligand even leads to DNA cleavage without the addition of any additive,[235] suggesting a self-activating process. The hydroxyl groups are located at the *ortho*, *meta* or *para* positions of the salen ligand. It has been found that the *ortho* and *para* isomers are able to spontaneously generate Cu^{3+} species, in contrast to the *meta* isomer. The corresponding cleaving abilities perfectly correlate with the facility to produce Cu^{3+} species,

because only the *ortho* and *para* isomers produce nuclease-active compounds. It has been suggested that the involvement of a hydroquinone system is crucial for the self-activating character of these complexes.

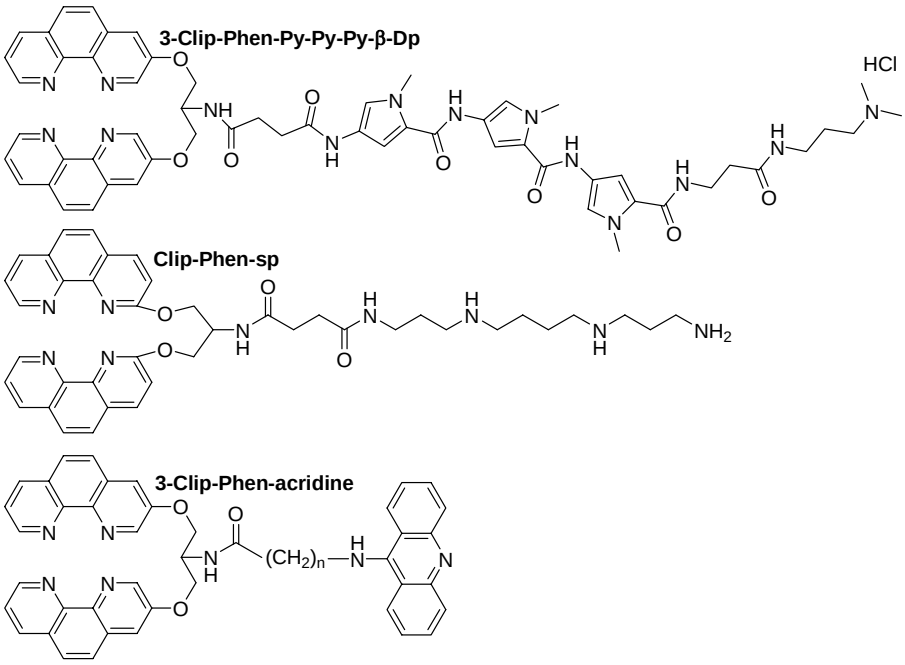

Figure 1.20 Clip-Phen complexes linked to a distamycin analogue (3-Clip-Phen-Py-Py-Py-β-Dp),[224] spermine (Clip-Phen-sp)[223] and acridine (3-Clip-Phen-acridine).[227]

A more recent example of a self-activating DNA cleavage complex is [Cu(pyrimol)Cl] (figure 1.21).[236] This complex is capable of catalytically oxidizing DNA without reductant. Fascinatingly, in the presence of reductant, the complex is even more active, but the mechanism of action is then different. Once more, a non-innocent role of the ligand is suggested. Additionally, the ligand in combination with several non-redox active Zn salts is also able to oxidatively cleave DNA, which can only be explained by the participation of the ligand.[237]

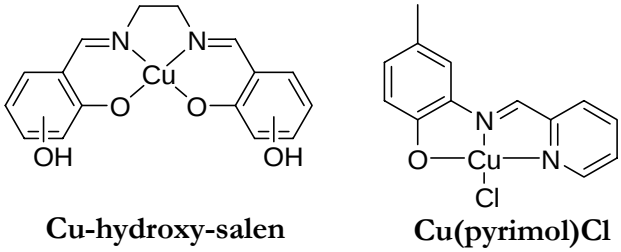

Figure 1.21 Structural formulae of the copper complexes Cu-hydroxy-salen and Cu(pyrimol)Cl complexes.[235, 236]

Karlin *et al.* have reported a trinuclear copper complex able to recognize specific junctions between single- and double-stranded DNA (Figure 1.22).[238] Thus, (Tri)Cu_3 in the presence of a

reductant and dioxygen is able to cleave a junction DNA specifically at the **Y** nucleobase at the 3'-end (Figure 1.22, right). It has been found that the complex only recognizes this position if a purine-base is at the opposite side of the **Y** nucleobase, and if the next nucleobase in the 5' direction is a guanine.[239] The three coppers are absolutely necessary to observe cleavage activity and selectivity, because the mononuclear complex does not show sequence-selective cleavage. The dinuclear copper complex is able to recognize the junction as well,[240, 241] but the sequence selectivity is different compared to the one achieved by (Tri)Cu_3. In that case (*i.e.* the dinuclear complex), the cleavage site is one base pair higher than **Y**. Also, the dinuclear complex is only active if: the purine base is an adenine, any nucleobase the guanine site in the 5' direction, and the **Y** is a guanine. Recently, other dinucleating ligand systems have been found to be able to recognize and cleave similar DNA junctions.[242, 243]

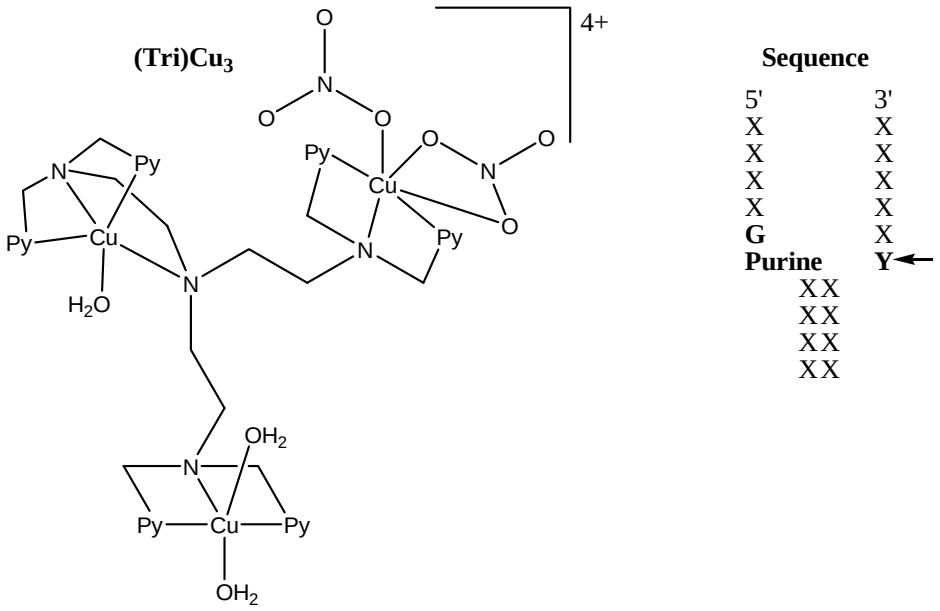

Figure 1.22 Structure of the (Tri)Cu_3 (left) where Py stands for 2-pyridyl described by Karlin et al.[238] Oligomer of DNA (right) containing a junction; X can be any nucleobase, and **Y** is the specific site of cleavage.

The natural product kanamycin in the presence of copper is able to mediate the catalytic cleavage of DNA or RNA (Figure 1.23).[244, 245] This complex is the most efficient hydrolytic and oxidative DNA cleaving agent so far reported. It has an astonishingly 50-million-fold rate enhancement in hydrolytic DNA cleavage.[154] Cu(kanamycin) is believed to generate $O_2^{\bullet-}$ or $^1O_2$ species after dioxygen activation, prior to the DNA cleavage. These species abstract selectively the H4' proton from the minor groove of DNA.[246]

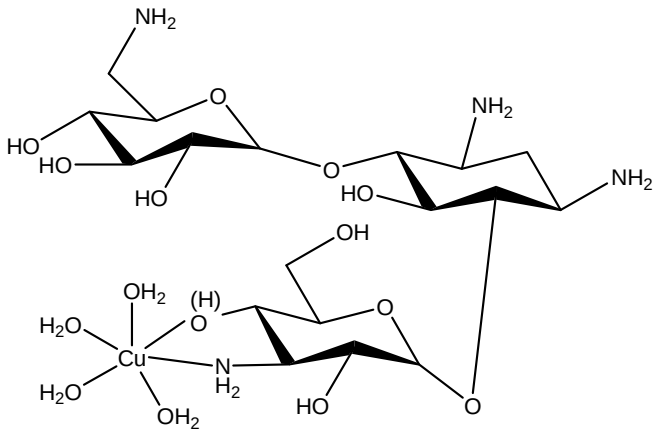

Figure 1.23 Possible structure for Cu^{II}(kanamycin).[244]

1.13 Aim and scope of this thesis.

Knowing the intrinsic qualities of the platinum unit and the Cu(3-Clip-Phen) moiety in DNA interactions a group of new heterodinuclear platinum/copper complexes has been selected to synthesize. A number of biological studies have subsequently been carried out to investigate the potential antitumor properties and cleavage activities of these complexes. The central questions of this thesis are the following:

- Is the copper moiety affecting the action of platinum unit and/or *vice versa*? In other words, do both moieties with their specific mechanism of action interact synergistically, or not?
- Does this synthetic strategy lead to platinum-containing drugs, showing different ranges of tumors that can be cured?
- Is it possible to change the DNA cleavage selectivity, the ability to induce direct DSB, or even to alter the mechanism of action of Cu(3-Clip-Phen) through its linkage to a major groove binding agent?
- Is this strategy restricted to platinum and Cu(3-Clip-Phen) or can it be applied to other multi(hetero)nuclear complex systems as well?

Chapter 2 addresses the influence of the bridge linking two phenanthroline units of 3-Clip-Phen derivatives on the activity. DFT studies have been performed to rationalize the difference in cleavage activity of a series of Cu(3-Clip-Phen)-based complexes. Chapter 3 describes the syntheses and biological activities of two heterodinuclear complexes holding unfunctionalized bridges connecting the Cu(3-Clip-Phen) unit and the platinum moiety. One complex possesses a bridge long enough to favor a major-minor groove interaction, while the other complex holds a short bridge which does not allow to cross the phosphate backbone of DNA resulting in either major or minor groove binding. Chapter 4 describes the synthesis and cleavage selectivity of a Cu(3-Clip-Phen)/platinum complex without spacer. The mechanism of the binding/cleavage of both moieties of this complex has been investigated to answer to the

question whether one of the metal centers is dominating the interaction with DNA. In chapter 5, novel complexes are reported where the platinum ion is directly coordinated to the NH_2 group of 3-Clip-Phen. Both the *cis* and the *trans* complexes have been synthesized and a comparison of their nuclease activity and cytotoxicity have been made. Chapter 6 presents the design and the syntheses of two complexes with a functionalized bridge of different length linking a platinum unit and a Cu(3-Clip-Phen) moiety. Their cleavage activity is discussed as well. Chapter 7 describes the syntheses of triazine-based multifunctional Cu(3-Clip-Phen)/platinum potential drugs. The triazine synthon is used as building block to prepare multitopic ligands. Actually, a platinum unit, Cu(3-Clip-Phen) and a fluorescent group have been successfully attached to one triazine ring. The nuclease activity and the cellular processing of complexes obtained from these triazine-based ligands are investigated. Chapter 8 shows the diversity of the multiheteronuclear strategy by linking ruthenium units with a copper-terpyridine unit. Extensive cleavage experiments have been performed to explore the capabilities of these novel complexes. Chapter 9 gives general conclusions and an outlook.

Parts of this thesis have been published, or submitted for publication.[247-250]

1.14 References

[1] www.who.int, *World Health Organization*, **2005**.

[2] www.cancer.gov, *National Cancer Institute*, **2007**.

[3] L. H. Hurley, *Nat. Rev. Cancer* **2002**, *2*, 188.

[4] L. H. Einhorn, *Proc. Natl. Acad. Sci. U. S. A.* **2002**, *99*, 4592.

[5] H. G. Kopp, M. Kuczyk, J. Classen, A. Stenzl, L. Kanz, F. Mayer, M. Bamberg, J. T. Hartmann, *Drugs* **2006**, *66*, 641.

[6] M. Peyrone, *Ann. Chem. Pharm.* **1844**, *51*, 1.

[7] B. Rosenberg, L. van Camp, T. Krigas, *Nature* **1965**, *205*, 698.

[8] B. Rosenberg, L. van Camp, J. E. Trosko, V. H. Mansour, *Nature* **1969**, *222*, 385.

[9] G. Giaccone, *Drugs* **2000**, *59*, 9.

[10] B. A. Chabner, T. G. Roberts, *Nat. Rev. Cancer* **2005**, *5*, 65.

[11] E. R. Jamieson, S. J. Lippard, *Chem. Rev.* **1999**, *99*, 2467.

[12] J. Reedijk, *Proc. Natl. Acad. Sci. U. S. A.* **2003**, *100*, 3611.

[13] D. P. Gately, S. B. Howell, *Br. J. Cancer* **1993**, *67*, 1171.

[14] M. T. Kuo, H. H. W. Chen, I. S. Song, N. Savaraj, T. Ishikawa, *Cancer Metastasis Rev.* **2007**, *26*, 71.

[15] R. Safaei, *Cancer Lett.* **2006**, *234*, 34.

[16] S. Ishida, J. Lee, D. J. Thiele, I. Herskowitz, *Proc. Natl. Acad. Sci. U. S. A.* **2002**, *99*, 14298.

[17] K. Katano, A. Kondo, R. Safaei, A. Holzer, G. Samimi, M. Mishima, Y. M. Kuo, M. Rochdi, S. B. Howell, *Cancer Res.* **2002**, *62*, 6559.

[18] R. Safaei, S. B. Howell, *Crit. Rev. Oncol./Hematol.* **2005**, *53*, 13.

[19] Y. Zhang, Z. J. Guo, X. Z. You, *J. Am. Chem. Soc.* **2001**, *123*, 9378.

[20] S. E. Miller, D. A. House, *Inorg. Chim. Acta* **1989**, *166*, 189.

[21] T. W. Hambley, *J. Chem. Soc.-Dalton Trans.* **2001**, 2711.
[22] M. S. Davies, S. J. Berners-Price, T. W. Hambley, *Inorg. Chem.* **2000**, *39*, 5603.
[23] G. Speelmans, W. Sips, R. J. H. Grisel, R. Staffhorst, A. M. J. Fichtinger-Schepman, J. Reedijk, B. deKruijff, *Biochim. Biophys. Acta-Biomembr.* **1996**, *1283*, 60.
[24] E. M. Witkin, *Proc. Natl. Acad. Sci. U. S. A.* **1967**, *57*, 1275.
[25] M. Akaboshi, K. Kawai, H. Maki, K. Akuta, Y. Ujeno, T. Miyahara, *Jpn. J. Cancer Res.* **1992**, *83*, 522.
[26] P. Boffetta, A. M. J. Fichtinger-Schepman, E. Weiderpass, H. C. M. van Dijk-Knijnenburg, G. Stoter, A. T. van Oosterom, H. J. Keizer, S. D. Fossa, J. Kaldor, P. Roy, **1998**, *9*, 125.
[27] M. J. P. Welters, A. M. J. Fichtinger-Schepman, R. A. Baan, A. J. Jacobs-Bergmans, A. Kegel, W. J. F. van der Vijgh, B. J. M. Braakhuis, *Br. J. Cancer* **1999**, *79*, 82.
[28] J. Reedijk, *Inorg. Chim. Acta* **1992**, *200*, 873.
[29] G. Natile, L. G. Marzilli, *Coord. Chem. Rev.* **2006**, *250*, 1315.
[30] M. H. Baik, R. A. Friesner, S. J. Lippard, *J. Am. Chem. Soc.* **2003**, *125*, 14082.
[31] L. A. S. Costa, T. W. Hambley, W. R. Rocha, W. B. De Almeida, H. F. Dos Santos, *Int. J. Quantum Chem.* **2006**, *106*, 2129.
[32] J. Reedijk, *Chem. Commun.* **1996**, 801.
[33] A. M. J. Fichtinger-Schepman, A. T. van Oosterom, P. H. M. Lohman, F. Berends, *Cancer Res.* **1987**, *47*, 3000.
[34] A. Eastman, *Biochemistry* **1986**, *25*, 3912.
[35] A. M. J. Fichtinger-Schepman, J. L. van der Veer, J. H. J. den Hartog, P. H. M. Lohman, J. Reedijk, *Biochemistry* **1985**, *24*, 707.
[36] A. Eastman, M. A. Barry, *Biochemistry* **1987**, *26*, 3303.
[37] J. C. Huang, D. B. Zamble, J. T. Reardon, S. J. Lippard, A. Sancar, *Proc. Natl. Acad. Sci. U. S. A.* **1994**, *91*, 10394.
[38] M. H. Fouchet, E. Guittet, J. A. H. Cognet, J. Kozelka, C. Gauthier, M. LeBret, K. Zimmermann, J. C. Chottard, *J. Biol. Inorg. Chem.* **1997**, *2*, 83.
[39] A. Gelasco, S. J. Lippard, *Biochemistry* **1998**, *37*, 9230.
[40] D. Z. Yang, S. van Boom, J. Reedijk, J. H. Van Boom, A. H. J. Wang, *Biochemistry* **1995**, *34*, 12912.
[41] P. M. Takahara, C. A. Frederick, S. J. Lippard, *J. Am. Chem. Soc.* **1996**, *118*, 12309.
[42] P. M. Takahara, A. C. Rosenzweig, C. A. Frederick, S. J. Lippard, *Nature* **1995**, *377*, 649.
[43] L. G. Marzilli, J. S. Saad, Z. Kuklenyik, K. A. Keating, Y. H. Xu, *J. Am. Chem. Soc.* **2001**, *123*, 2764.
[44] J. M. Teuben, C. Bauer, A. H. J. Wang, J. Reedijk, *Biochemistry* **1999**, *38*, 12305.
[45] C. J. van Garderen, L. P. A. van Houte, *Eur. J. Biochem.* **1994**, *225*, 1169.
[46] F. Coste, J. M. Malinge, L. Serre, W. Shepard, M. Roth, M. Leng, C. Zelwer, *Nucleic Acids Res.* **1999**, *27*, 1837.
[47] H. F. Huang, L. M. Zhu, B. R. Reid, G. P. Drobny, P. B. Hopkins, *Science* **1995**, *270*, 1842.
[48] F. Paquet, C. Perez, M. Leng, G. Lancelot, J. M. Malinge, *J. Biomol. Struct. Dyn.* **1996**, *14*, 67.
[49] Y. Jung, S. J. Lippard, *Chem. Rev.* **2007**, *107*, 1387.
[50] D. Wang, S. J. Lippard, *Nat. Rev. Drug Discov.* **2005**, *4*, 307.
[51] V. M. Gonzalez, M. A. Fuertes, C. Alonso, J. M. Perez, *Mol. Pharmacol.* **2001**, *59*, 657.
[52] J. O. Thomas, A. A. Travers, *Trends Biochem.Sci.* **2001**, *26*, 167.

[53] P. M. Pil, S. J. Lippard, *Science* **1992**, *256*, 234.
[54] U. M. Ohndorf, M. A. Rould, Q. He, C. O. Pabo, S. J. Lippard, *Nature* **1999**, *399*, 708.
[55] Q. He, C. H. Liang, S. J. Lippard, *Proc. Natl. Acad. Sci. U. S. A.* **2000**, *97*, 5768.
[56] G. Nagatani, M. Nomoto, H. Takano, T. Ise, K. Kato, T. Imamura, H. Izumi, K. Makishima, K. Kohno, *Cancer Res.* **2001**, *61*, 1592.
[57] M. Kartalou, J. M. Essigmann, *Mutat. Res.-Fundam. Mol. Mech. Mutagen.* **2001**, *478*, 1.
[58] S. G. Chaney, S. L. Campbell, E. Bassett, Y. B. Wu, *Crit. Rev. Oncol./Hematol.* **2005**, *53*, 3.
[59] H. C. Harder, R. G. Smith, A. F. Leroy, *Cancer Res.* **1976**, *36*, 3821.
[60] S. G. Chaney, S. L. Campbell, B. Temple, E. Bassett, Y. B. Wu, M. Faldu, *J. Inorg. Biochem.* **2004**, *98*, 1551.
[61] S. Prakash, R. E. Johnson, L. Prakash, *Annu. Rev. Biochem.* **2005**, *74*, 317.
[62] E. Bassett, N. M. King, M. F. Bryant, S. Hector, L. Pendyala, S. G. Chaney, M. Cordeiro-Stone, *Cancer Res.* **2004**, *64*, 6469.
[63] G. R. Gibbons, W. K. Kaufmann, S. G. Chaney, *Carcinogenesis* **1991**, *12*, 2253.
[64] L. P. Rybak, C. A. Whitworth, D. Mukherjea, V. Rarakumar, *Hear. Res.* **2007**, *226*, 157.
[65] F. E. de Jongh, R. N. van Veen, S. J. Veltman, R. de Wit, M. E. L. van der Burg, M. J. van den Bent, A. S. T. Planting, W. J. Graveland, G. Stoter, J. Verweij, *Br. J. Cancer* **2003**, *88*, 1199.
[66] B. H. Ali, M. S. Al Moundhri, *Food Chem. Toxicol.* **2006**, *44*, 1173.
[67] M. Kartalou, J. M. Essigmann, *Mutat. Res.-Fundam. Mol. Mech. Mutagen.* **2001**, *478*, 23.
[68] H. Zorbas, B. K. Keppler, *Chembiochem* **2005**, *6*, 1157.
[69] M. A. Fuertes, C. Alonso, J. M. Perez, *Chem. Rev.* **2003**, *103*, 645.
[70] C. A. Rabik, M. E. Dolan, *Cancer Treat. Rev.* **2007**, *33*, 9.
[71] L. R. Kelland, *Drugs* **2000**, *59*, 1.
[72] J. Reedijk, *Chem. Rev.* **1999**, *99*, 2499.
[73] R. P. Perez, *Eur. J. Cancer* **1998**, *34*, 1535.
[74] J. T. Reardon, A. Vaisman, S. G. Chaney, A. Sancar, *Cancer Res.* **1999**, *59*, 3968.
[75] W. Dempke, W. Voigt, A. Grothey, B. T. Hill, H. J. Schmoll, *Anti-Cancer Drugs* **2000**, *11*, 225.
[76] H. Niedner, R. Christen, X. Lin, A. Kondo, S. B. Howell, *Mol. Pharmacol.* **2001**, *60*, 1153.
[77] H. Burger, A. Capello, P. W. Schenk, G. Stoter, J. Brouwer, K. Nooter, *Biochem. Biophys. Res. Commun.* **2000**, *269*, 767.
[78] M. C. Ackley, C. G. Barry, A. M. Mounce, M. C. Farmer, B. E. Springer, C. S. Day, M. W. Wright, S. J. Berners-Price, S. M. Hess, U. Bierbach, *J. Biol. Inorg. Chem.* **2004**, *9*, 453.
[79] M. A. Jakupec, M. Galanski, B. K. Keppler, in *Reviews of Physiology, Biochemistry and Pharmacology, Vol 146,* Springer-Verlag Berlin, Berlin, **2003**, pp. 1.
[80] M. Galanski, M. A. Jakupec, B. K. Keppler, *Curr. Med. Chem.* **2005**, *12*, 2075.
[81] D. Lebwohl, R. Canetta, *Eur. J. Cancer* **1998**, *34*, 1522.
[82] A. H. Calvert, S. J. Harland, D. R. Newell, Z. H. Siddik, A. C. Jones, T. J. McElwain, S. Raju, E. Wiltshaw, I. E. Smith, J. M. Baker, M. J. Peckham, K. R. Harrap, *Cancer Chemother. Pharmacol.* **1982**, *9*, 140.
[83] T. Boulikas, M. Vougiouka, *Oncol. Rep.* **2003**, *10*, 1663.
[84] L. R. Kelland, S. Y. Sharp, C. F. O'Neill, F. I. Raynaud, P. J. Beale, I. R. Judson, *J. Inorg. Biochem.* **1999**, *77*, 111.

[85] K. Itoh, T. Yamashita, H. Wakita, Y. Watanabe, K. Kodama, H. Fujii, H. Minami, T. Ohtsu, T. Igarashi, Y. Sasaki, *Jpn. J. Clin. Oncol.* **1998**, *28*, 343.

[86] Y. Kidani, K. Inagaki, S. Tsukagoshi, *Gann* **1976**, *67*, 921.

[87] M. J. Martin, *Expert Rev. Anticancer Ther.* **2005**, *5*, 695.

[88] B. Spingler, D. A. Whittington, S. J. Lippard, *Inorg. Chem.* **2001**, *40*, 5596.

[89] S. G. Chaney, A. Vaisman, *J. Inorg. Biochem.* **1999**, *77*, 71.

[90] O. Rixe, W. Ortuzar, M. Alvarez, R. Parker, E. Reed, K. Paull, T. Fojo, *Biochem. Pharmacol.* **1996**, *52*, 1855.

[91] M. J. McKeage, *Drugs* **2007**, *67*, 859.

[92] J. Holford, F. Raynaud, B. A. Murrer, K. Grimaldi, J. A. Hartley, M. Abrams, L. R. Kelland, *Anti-Cancer Drug Des.* **1998**, *13*, 1.

[93] J. Holford, S. Y. Sharp, B. A. Murrer, M. Abrams, L. R. Kelland, *Br. J. Cancer* **1998**, *77*, 366.

[94] G. Natile, M. Coluccia, *Coord. Chem. Rev.* **2001**, *216*, 383.

[95] S. Radulovic, Z. Tesic, S. Manic, *Curr. Med. Chem.* **2002**, *9*, 1611.

[96] N. Farrell, L. R. Kelland, J. D. Roberts, M. van Beusichem, *Cancer Res.* **1992**, *52*, 5065.

[97] M. van Beusichem, N. Farrell, *Inorg. Chem.* **1992**, *31*, 634.

[98] Y. Zou, B. van Houten, N. Farrell, *Biochemistry* **1993**, *32*, 9632.

[99] M. Coluccia, A. Boccarelli, M. A. Mariggio, N. Cardellicchio, P. Caputo, F. P. Intini, G. Natile, *Chem.-Biol. Interact.* **1995**, *98*, 251.

[100] A. Boccarelli, M. Coluccia, F. P. Intini, G. Natile, D. Locker, M. Leng, *Anti-Cancer Drug Des.* **1999**, *14*, 253.

[101] M. Coluccia, A. Nassi, A. Boccarelli, D. Giordano, N. Cardellicchio, D. Locker, M. Leng, M. Sivo, F. P. Intini, G. Natile, *J. Inorg. Biochem.* **1999**, *77*, 31.

[102] M. Coluccia, A. Nassi, F. Loseto, A. Boccarelli, M. A. Mariggio, D. Giordano, F. P. Intini, P. Caputo, G. Natile, *J. Med. Chem.* **1993**, *36*, 510.

[103] E. I. Montero, S. Diaz, A. M. Gonzalez-Vadillo, J. M. Perez, C. Alonso, C. Navarro-Ranninger, *J. Med. Chem.* **1999**, *42*, 4264.

[104] E. Pantoja, A. Alvarez-Valdes, J. M. Perez, C. Navarro-Ranninger, J. Reedijk, *Inorg. Chim. Acta* **2002**, *339*, 525.

[105] E. Pantoja, A. Gallipoli, S. van Zutphen, S. Komeda, D. Reddy, D. Jaganyi, M. Lutz, D. M. Tooke, A. L. Spek, C. Navarro-Ranninger, J. Reedijk, *J. Inorg. Biochem.* **2006**, *100*, 1955.

[106] S. van Zutphen, E. Pantoja, R. Soriano, C. Soro, D. M. Tooke, A. L. Spek, H. den Dulk, J. Brouwer, J. Reedijk, *Dalton Trans.* **2006**, 1020.

[107] N. J. Wheate, J. G. Collins, *Coord. Chem. Rev.* **2003**, *241*, 133.

[108] Y. Qu, N. J. Scarsdale, M. C. Tran, N. Farrell, *J. Inorg. Biochem.* **2004**, *98*, 1585.

[109] J. Kasparkova, J. Zehnulova, N. Farrell, V. Brabec, *J. Biol. Chem.* **2002**, *277*, 48076.

[110] N. Farrell, Q. Yu, U. Bierbach, M. Valsecchi, E. Menta, Ed.: B. Lippert, Verlag CH, Basel, Switzerland, **1999**, p. 479.

[111] S. Komeda, M. Lutz, A. L. Spek, M. Chikuma, J. Reedijk, *Inorg. Chem.* **2000**, *39*, 4230.

[112] S. Teletchea, S. Komeda, J. M. Teuben, M. A. Elizondo-Riojas, J. Reedijk, J. Kozelka, *Chem.-Eur. J.* **2006**, *12*, 3741.

[113] S. van Zutphen, J. Reedijk, *Coord. Chem. Rev.* **2005**, *249*, 2845.

[114] H. Maeda, in *Advances In Enzyme Regulation, Vol 41,* Pergamon-Elsevier Science Ltd, Oxford, **2001**, pp. 189.

[115] X. Lin, Q. Zhang, J. R. Rice, D. R. Stewart, D. P. Nowotnik, S. B. Howell, *Eur. J. Cancer* **2004**, *40*, 291.

[116] E. Gianasi, M. Wasil, E. G. Evagorou, A. Keddle, G. Wilson, R. Duncan, *Eur. J. Cancer* **1999**, *35*, 994.

[117] J. M. Rademaker-Lakhai, C. Terret, S. B. Howell, C. M. Baud, R. F. de Boer, D. Pluim, J. H. Beijnen, J. H. M. Schellens, J. P. Droz, *Clin. Cancer Res.* **2004**, *10*, 3386.

[118] C. Bailly, J. B. Chaires, *Bioconjugate Chem.* **1998**, *9*, 513.

[119] H. Loskotova, V. Brabec, *Eur. J. Biochem.* **1999**, *266*, 392.

[120] M. Lee, J. E. Simpson, A. J. Burns, S. Kupchinsky, N. Brooks, J. A. Hartley, L. R. Kelland, *Med. Chem. Res.* **1996**, *6*, 365.

[121] H. Kostrhunova, V. Brabec, *Biochemistry* **2000**, *39*, 12639.

[122] N. J. Wheate, C. R. Brodie, J. G. Collins, S. Kemp, J. R. Aldrich-Wright, *Mini-Rev. Med. Chem.* **2007**, *7*, 627.

[123] K. E. Erkkila, D. T. Odom, J. K. Barton, *Chem. Rev.* **1999**, *99*, 2777.

[124] R. Martinez, L. Chacon-Garcia, *Curr. Med. Chem.* **2005**, *12*, 127.

[125] B. E. Bowler, K. J. Ahmed, W. I. Sundquist, L. S. Hollis, E. E. Whang, S. J. Lippard, *J. Am. Chem. Soc.* **1989**, *111*, 1299.

[126] B. E. Bowler, L. S. Hollis, S. J. Lippard, *J. Am. Chem. Soc.* **1984**, *106*, 6102.

[127] B. E. Bowler, S. J. Lippard, *Biochemistry* **1986**, *25*, 3031.

[128] V. Murray, H. Motyka, P. R. England, G. Wickham, H. H. Lee, W. A. Denny, W. D. McFadyen, *J. Biol. Chem.* **1992**, *267*, 18805.

[129] V. Murray, H. Motyka, P. R. England, G. Wickham, H. H. Lee, W. A. Denny, W. D. McFadyen, *Biochemistry* **1992**, *31*, 11812.

[130] H. H. Lee, B. D. Palmer, B. C. Baguley, M. Chin, W. D. McFadyen, G. Wickham, D. Thorsbournepalmer, L. P. G. Wakelin, W. A. Denny, *J. Med. Chem.* **1992**, *35*, 2983.

[131] R. J. Holmes, M. J. McKeage, V. Murray, W. A. Denny, W. D. McFadyen, *J. Inorg. Biochem.* **2001**, *85*, 209.

[132] S. M. Hess, J. G. Anderson, U. Bierbach, *Bioorg. Med. Chem. Lett.* **2005**, *15*, 443.

[133] S. M. Hess, A. M. Mounce, R. C. Sequeira, T. M. Augustus, M. C. Ackley, U. Bierbach, *Cancer Chemother. Pharmacol.* **2005**, *56*, 337.

[134] E. T. Martins, H. Baruah, J. Kramarczyk, G. Saluta, C. S. Day, G. L. Kucera, U. Bierbach, *J. Med. Chem.* **2001**, *44*, 4492.

[135] H. Baruah, U. Bierbach, *J. Biol. Inorg. Chem.* **2004**, *9*, 335.

[136] C. G. Barry, H. Baruah, U. Bierbach, *J. Am. Chem. Soc.* **2003**, *125*, 9629.

[137] C. G. Barry, C. S. Day, U. Bierbach, *J. Am. Chem. Soc.* **2005**, *127*, 1160.

[138] H. Baruah, M. W. Wright, U. Bierbach, *Biochemistry* **2005**, *44*, 6059.

[139] G. V. Kalayda, B. A. J. Jansen, C. Molenaar, P. Wielaard, H. J. Tanke, J. Reedijk, *J. Biol. Inorg. Chem.* **2004**, *9*, 414.

[140] G. V. Kalayda, B. A. J. Jansen, P. Wielaard, H. J. Tanke, J. Reedijk, *J. Biol. Inorg. Chem.* **2005**, *10*, 305.

[141] M. Valko, H. Morris, M. T. D. Cronin, *Curr. Med. Chem.* **2005**, *12*, 1161.

[142] P. Swiderek, *Angew. Chem.-Int. Edit.* **2006**, *45*, 4056.
[143] H. Urata, K. Yamamoto, M. Akagi, H. Hiroaki, S. Uesugi, *Biochemistry* **1989**, *28*, 9566.
[144] B. Demple, J. Halbrook, *Nature* **1983**, *304*, 466.
[145] G. Pratviel, J. Bernadou, B. Meunier, *Angew. Chem.-Int. Edit. Engl.* **1995**, *34*, 746.
[146] C. H. B. Chen, L. Milne, R. Landgraf, D. M. Perrin, D. S. Sigman, *Chembiochem* **2001**, *2*, 735.
[147] B. Lippert, *Cisplatin, Chemistry and Biochemistry of a leading Anticancer Drug*, Wiley-VCH, Zurich, **1999**.
[148] C. J. Burrows, J. G. Muller, *Chem. Rev.* **1998**, *98*, 1109.
[149] E. L. Hegg, J. N. Burstyn, *Coord. Chem. Rev.* **1998**, *173*, 133.
[150] J. A. Cowan, *Curr. Opin. Chem. Biol.* **2001**, *5*, 634.
[151] A. Sreedhara, J. A. Cowan, *J. Biol. Inorg. Chem.* **2001**, *6*, 337.
[152] W. K. Pogozelski, T. D. Tullius, *Chem. Rev.* **1998**, *98*, 1089.
[153] F. H. Westheimer, *Science* **1987**, *235*, 1173.
[154] A. Sreedhara, J. D. Freed, J. A. Cowan, *J. Am. Chem. Soc.* **2000**, *122*, 8814.
[155] C. L. Liu, S. W. Yu, D. F. Li, Z. R. Liao, X. H. Sun, H. B. Xu, *Inorg. Chem.* **2002**, *41*, 913.
[156] R. M. Burger, *Chem. Rev.* **1998**, *98*, 1153.
[157] J. Y. Chen, J. Stubbe, *Nat. Rev. Cancer* **2005**, *5*, 102.
[158] U. Galm, M. H. Hager, S. G. Van Lanen, J. H. Ju, J. S. Thorson, B. Shen, *Chem. Rev.* **2005**, *105*, 739.
[159] I. H. Goldberg, *Accounts Chem. Res.* **1991**, *24*, 191.
[160] B. Shen, W. Liu, K. Nonaka, *Curr. Med. Chem.* **2003**, *10*, 2317.
[161] K. C. Nicolaou, A. L. Smith, E. W. Yue, *Proc. Natl. Acad. Sci. U. S. A.* **1993**, *90*, 5881.
[162] H. Umezawa, K. Maeda, T. Takeuchi, Y. Okami, *J. Antibiot.* **1966**, *19*, 200.
[163] B. K. Vig, R. Lewis, *Mutation Res.* **1978**, *55*, 121.
[164] R. P. Hertzberg, P. B. Dervan, *J. Am. Chem. Soc.* **1982**, *104*, 313.
[165] M. W. van Dyke, R. P. Hertzberg, P. B. Dervan, *Proc. Natl. Acad. Sci. U. S. A.* **1982**, *79*, 5470.
[166] D. S. Sigman, D. R. Graham, V. Daurora, A. M. Stern, *J. Biol. Chem.* **1979**, *254*, 2269.
[167] D. S. Sigman, *Acc. Chem. Res.* **1986**, *19*, 180.
[168] D. S. Sigman, A. Mazumder, D. M. Perrin, *Chem. Rev.* **1993**, *93*, 2295.
[169] M. Pitié, C. Boldron, G. Pratviel, in *Advances In Inorganic Chemistry, Vol 58,* Elsevier Academic Press Inc, San Diego, **2006**, pp. 77.
[170] B. R. James, R. J. Williams, *J. Chem. Soc.* **1961**, 2007.
[171] J. F. Dobson, B. E. Green, P. C. Healy, C. H. L. Kennard, C. Pakawatchai, A. H. White, *Aust. J. Chem.* **1984**, *37*, 649.
[172] A. Robertazzi, A. Magistrato, P. de Hoog, P. Carloni, J. Reedijk, *Inorg. Chem.* **2007**, *46*, 5873.
[173] J. M. Veal, R. L. Rill, *Biochemistry* **1991**, *30*, 1132.
[174] S. Goldstein, G. Czapski, *J. Am. Chem. Soc.* **1986**, *108*, 2244.
[175] L. E. Marshall, D. R. Graham, K. A. Reich, D. S. Sigman, *Biochemistry* **1981**, *20*, 244.
[176] M. Kuwabara, C. Yoon, T. Goyne, T. Thederahn, D. S. Sigman, *Biochemistry* **1986**, *25*, 7401.
[177] J. C. Stockert, *J. Theor. Biol.* **1989**, *137*, 107.
[178] J. M. Veal, R. L. Rill, *Biochemistry* **1988**, *27*, 1822.
[179] J. M. Veal, R. L. Rill, *Biochemistry* **1989**, *28*, 3243.
[180] L. E. Pope, D. S. Sigman, *Proc. Natl. Acad. Sci. U. S. A.* **1984**, *81*, 3.
[181] A. Spassky, D. S. Sigman, *Biochemistry* **1985**, *24*, 8050.

[182] G. R. A. Johnson, N. B. Nazhat, *J. Am. Chem. Soc.* **1987**, *109*, 1990.
[183] M. Dizdaroglu, O. I. Aruoma, B. Halliwell, *Biochemistry* **1990**, *29*, 8447.
[184] D. S. Sigman, in *DNA and RNA Cleavers and Chemotheraphy of Cancer and Viral Diseases* Ed.: K. A. P. Dordrecht/Boston/London, **1996**, p. 119.
[185] T. E. Goyne, D. S. Sigman, *J. Am. Chem. Soc.* **1987**, *109*, 2846.
[186] M. M. Meijler, O. Zelenko, D. S. Sigman, *J. Am. Chem. Soc.* **1997**, *119*, 1135.
[187] Y. Zheng, T. L. Sheppard, *Chem. Res. Toxicol.* **2004**, *17*, 197.
[188] B. C. Bales, M. Pitie, B. Meunier, M. M. Greenberg, *J. Am. Chem. Soc.* **2002**, *124*, 9062.
[189] T. Q. Chen, M. M. Greenberg, *J. Am. Chem. Soc.* **1998**, *120*, 3815.
[190] T. Oyoshi, H. Sugiyama, *J. Am. Chem. Soc.* **2000**, *122*, 6313.
[191] G. Mehta, S. Karmakar, S. K. Chattopadhyay, *Tetrahedron* **2004**, *60*, 5013.
[192] B. Giese, X. Beyrichgraf, P. Erdmann, M. Petretta, U. Schwitter, *Chem. Biol.* **1995**, *2*, 367.
[193] B. Giese, X. Beyrichgraf, P. Erdmann, L. Giraud, P. Imwinkelried, S. N. Muller, U. Schwitter, *J. Am. Chem. Soc.* **1995**, *117*, 6146.
[194] Y. N. Ogibin, A. O. Terent'ev, A. V. Kutkin, G. I. Nikishin, *Tetrahedron Lett.* **2002**, *43*, 1321.
[195] L. Milne, D. M. Perrin, D. S. Sigman, *Methods* **2001**, *23*, 160.
[196] L. Pearson, C. B. Chen, R. P. Gaynor, D. S. Sigman, *Nucleic Acids Res.* **1994**, *22*, 2255.
[197] D. S. Sigman, A. Spassky, S. Rimsky, H. Buc, *Biopolymers* **1985**, *24*, 183.
[198] M. Chikira, Y. Tomizawa, D. Fukita, T. Sugizaki, N. Sugawara, T. Yamazaki, A. Sasano, H. Shindo, M. Palaniandavar, W. E. Antholine, *J. Inorg. Biochem.* **2002**, *89*, 163.
[199] T. Hirohama, Y. Kuranuki, E. Ebina, T. Sugizaki, H. Arii, M. Chikira, P. T. Selvi, M. Palaniandavar, *J. Inorg. Biochem.* **2005**, *99*, 1205.
[200] S. Dhar, A. R. Chakravarty, *Inorg. Chem.* **2003**, *42*, 2483.
[201] S. Dhar, D. Senapati, P. K. Das, P. Chattopadhyay, M. Nethaji, A. R. Chakravarty, *J. Am. Chem. Soc.* **2003**, *125*, 12118.
[202] A. K. Patra, S. Dhar, M. Nethaji, A. R. Chakravarty, *Chem. Commun.* **2003**, 1562.
[203] P. A. N. Reddy, M. Nethaji, A. R. Chakravarty, *Eur. J. Inorg. Chem.* **2004**, 1440.
[204] P. A. N. Reddy, B. K. Santra, M. Nethaji, A. R. Chakravarty, *J. Inorg. Biochem.* **2004**, *98*, 377.
[205] B. Macias, I. Garcia, M. V. Villa, J. Borras, M. Gonzalez-Alvarez, A. Castineiras, *J. Inorg. Biochem.* **2003**, *96*, 367.
[206] A. Garcia-Raso, J. J. Fiol, B. Adrover, V. Moreno, I. Mata, E. Espinosa, E. Molins, *J. Inorg. Biochem.* **2003**, *95*, 77.
[207] J. Pfau, D. N. Arvidson, P. Youderian, L. L. Pearson, D. S. Sigman, *Biochemistry* **1994**, *33*, 11391.
[208] P. S. Pendergrast, Y. W. Ebright, R. H. Ebright, *Science* **1994**, *265*, 959.
[209] T. W. Bruice, J. G. Wise, D. S. E. Rosser, D. S. Sigman, *J. Am. Chem. Soc.* **1991**, *113*, 5446.
[210] C. Q. Pan, R. C. Johnson, D. S. Sigman, *Biochemistry* **1996**, *35*, 4326.
[211] G. P. Xiao, D. L. Cole, R. P. Gunsalus, D. S. Sigman, C. H. B. Chen, *Protein Sci.* **2002**, *11*, 2427.
[212] J. C. Francois, C. Helene, *Biochemistry* **1995**, *34*, 65.
[213] J. C. Francois, T. Saisonbehmoaras, C. Barbier, M. Chassignol, N. T. Thuong, C. Helene, *Proc. Natl. Acad. Sci. U. S. A.* **1989**, *86*, 9702.
[214] J. S. Sun, J. C. Francois, R. Lavery, T. Saisonbehmoaras, T. Montenaygarestier, N. T. Thuong, C. Helene, *Biochemistry* **1988**, *27*, 6039.

[215] A. Zaid, J. S. Sun, C. H. Nguyen, E. Bisagni, T. Garestier, D. S. Grierson, R. Zain, *Chembiochem* **2004**, *5*, 1550.
[216] F. C. K. Chiu, R. T. C. Brownlee, K. Mitchell, D. R. Phillips, *Bioorg. Med. Chem. Lett.* **1994**, *4*, 2721.
[217] C. H. B. Chen, A. Mazumder, J. F. Constant, D. S. Sigman, *Bioconjugate Chem.* **1993**, *4*, 69.
[218] M. Hirai, K. Shinozuka, H. Sawai, S. Ogawa, *Chem. Lett.* **1992**, 2023.
[219] J. C. Francois, T. Saisonbehmoaras, M. Chassignol, N. T. Thuong, C. Helene, *J. Biol. Chem.* **1989**, *264*, 5891.
[220] M. Pitié, B. Donnadieu, B. Meunier, *Inorg. Chem.* **1998**, *37*, 3486.
[221] M. Pitié, B. Sudres, B. Meunier, *Chem. Commun.* **1998**, 2597.
[222] M. Pitié, A. Croisy, D. Carrez, C. Boldron, B. Meunier, *ChemBioChem* **2005**, *6*, 686.
[223] M. Pitié, B. Meunier, *Bioconjugate Chem.* **1998**, *9*, 604.
[224] M. Pitié, J. D. Van Horn, D. Brion, C. J. Burrows, B. Meunier, *Bioconjugate Chem.* **2000**, *11*, 892.
[225] M. Pitié, C. Boldron, H. Gornitzka, C. Hemmert, B. Donnadieu, B. Meunier, *Eur. J. Inorg. Chem.* **2003**, 528.
[226] M. Pitié, C. J. Burrows, B. Meunier, *Nucleic Acids Res.* **2000**, *28*, 4856.
[227] C. Boldron, S. A. Ross, M. Pitié, B. Meunier, *Bioconjugate Chem.* **2002**, *13*, 1013.
[228] S. Bhattacharya, S. S. Mandal, *J. Chem. Soc.-Chem. Commun.* **1995**, 2489.
[229] C. J. Burrows, S. E. Rokita, *Accounts Chem. Res.* **1994**, *27*, 295.
[230] D. J. Gravert, J. H. Griffin, *J. Org. Chem.* **1993**, *58*, 820.
[231] D. J. Gravert, J. H. Griffin, *Inorg. Chem.* **1996**, *35*, 4837.
[232] J. G. Muller, X. Y. Chen, A. C. Dadiz, S. E. Rokita, C. J. Burrows, *J. Am. Chem. Soc.* **1992**, *114*, 6407.
[233] J. G. Muller, S. J. Paikoff, S. E. Rokita, C. J. Burrows, *J. Inorg. Biochem.* **1994**, *54*, 199.
[234] S. Routier, J. L. Bernier, M. J. Waring, P. Colson, C. Houssier, C. Bailly, *J. Org. Chem.* **1996**, *61*, 2326.
[235] E. Lamour, S. Routier, J. L. Bernier, J. P. Catteau, C. Bailly, H. Vezin, *J. Am. Chem. Soc.* **1999**, *121*, 1862.
[236] P. U. Maheswari, S. Roy, H. den Dulk, S. Barends, G. van Wezel, B. Kozlevcar, P. Gamez, J. Reedijk, *J. Am. Chem. Soc.* **2006**, *128*, 710.
[237] P. U. Maheswari, S. Barends, S. Özalp-Yaman, P. de Hoog, H. Casellas, S. J. Teat, C. Massera, M. Lutz, A. L. Spek, G. van Wezel, P. Gamez, J. Reedijk, *Chem. Eur. J.* **2007**, *13*, 5213.
[238] K. J. Humphreys, K. D. Karlin, S. E. Rokita, *J. Am. Chem. Soc.* **2001**, *123*, 5588.
[239] K. J. Humphreys, K. D. Karlin, S. E. Rokita, *J. Am. Chem. Soc.* **2002**, *124*, 8055.
[240] K. J. Humphreys, A. E. Johnson, K. D. Karlin, S. E. Rokita, *J. Biol. Inorg. Chem.* **2002**, *7*, 835.
[241] K. J. Humphreys, K. D. Karlin, S. E. Rokita, *J. Am. Chem. Soc.* **2002**, *124*, 6009.
[242] L. Li, K. D. Karlin, S. E. Rokita, *J. Am. Chem. Soc.* **2005**, *127*, 520.
[243] S. Thyagarajan, N. N. Murthy, A. A. N. Sarjeant, K. D. Karlin, S. E. Rokita, *J. Am. Chem. Soc.* **2006**, *128*, 7003.
[244] A. Sreedhara, J. A. Cowan, *Chem. Commun.* **1998**, 1737.
[245] A. Sreedhara, A. Patwardhan, J. A. Cowan, *Chem. Commun.* **1999**, 1147.
[246] A. Patwardhan, J. A. Cowan, *Chem. Commun.* **2001**, 1490.
[247] P. de Hoog, C. Boldron, P. Gamez, K. Sliedregt-Bol, I. Roland, M. Pitié, R. Kiss, B. Meunier, J. Reedijk, *J. Med. Chem.* **2007**, *50*, 3148.

[248] P. de Hoog, M. Louwerse, P. Gamez, M. Pitié, E. J. Baerends, B. Meunier, J. Reedijk, *Eur. J. Inorg. Chem.* in press.

[249] P. de Hoog, M. Pitié, G. Amadei, P. Gamez, B. Meunier, R. Kiss, J. Reedijk, *submitted* .

[250] S. Özalp-Yaman, P. de Hoog, G. Amadei, M. Pitié, P. Gamez, I. Roland, B. Meunier, R. Kiss, J. Reedijk, *submitted.*

Chapter 2

Influence of the copper coordination geometry on the DNA cleavage activity of Clip-Phen complexes studied by DFT.*

Six different [$Cu^{I/II}$(3-Clip-Phen)] complexes, with or without a coordinating chloride ligand, have been investigated by DFT calculations to evaluate the influence of the length and functional substituents of the bridge linking the two phenanthroline units on the DNA cleavage activity. The changes of the structural and energetic profiles imposed by the bridge of these complexes have been analyzed by comparison with the well-studied nuclease active agent [$Cu^{I/II}(phen)_2$]. The present studies show that the bridge length of these complexes is critical for the consequent geometry, and the strain and formation energies. Upon oxidation, the geometry of [$Cu^{I}(phen)_2$] changes drastically, in contrast to the complexes with two- or three- methylene bridges. The behavior of the complexes with a 4- or 5-carbon bridge resembles the one of [$Cu^{I/II}(phen)_2$]. However, the Cu^{I} geometries are markedly different from the one of [$Cu^{I}(phen)_2$], because of the influence of the bridge.

*This chapter is based on Paul de Hoog, Manuel J. Louwerse, Patrick Gamez, Marguerite Pitié, Evert Jan Baerends, Bernard Meunier, Jan Reedijk, *Eur. J. Inorg. Chem.*, accepted

2.1 Introduction

Redox active chemical nucleases that are able to irreversibly damage DNA have received a lot of interest because of their potential application as biological tools or as drugs.[1, 2] The best studied complex systems are Fe-bleomycin,[3, 4] [Fe^{II}(edta)],[5, 6] and $Cu(phen)_2$.[7, 8] These complexes are able to oxidize the deoxyribose unit of DNA in the presence of dioxygen or dihydrogenperoxide. The mechanism of action of $Cu(phen)_2^{2+}$ allegedly involves: (i) its reduction in solution to [$Cu^{I}(phen)_2$];[9] (ii) the reversible binding to DNA;[10] (iii) the reaction with dihydrogenperoxide to form a reactive Cu-"oxo" species; (iv) the abstraction of the protons H-1', H-4' and H-5' from the deoxyribose unit in the minor groove of DNA, leading ultimately to DNA scission.[11] Unfortunately, the low binding constant of the second phenanthroline ligand limits is applicability[12], because copper complexes with only one coordinated phenanthroline are less efficient DNA-cleaving agents.[13-16] To prevail over this problem, the two phenanthroline ligands were coupled, via their C2 or C3 atom, using a serinol bridge. As a result, the nuclease activity was found to increase by a factor of 2 or 40, for 2-Clip-Phen and 3-Clip-Phen, respectively.[17, 18] A second advantage of this strategy is the possible, straightforward functionalization of the serinol bridge, allowing for example, an improvement of the sequence selectivity.[19-21] The mechanism of action of these Cu(Clip-Phen) complexes is similar to that of the $Cu(phen)_2$ complex.[20] Pitié *et al.* also investigated the influence of the length and nature of the bridge of 2- or 3-Clip-Phen derivatives on the corresponding cleavage activity.[22] The length of the bridge was varied from two to five methylene groups (Figure 2.1, complexes $\mathbf{2^{dft}}$, $\mathbf{3^{dft}}$, $\mathbf{6^{dft}}$ and $\mathbf{7^{dft}}$). For the 3-carbon bridge, the central carbon was functionalized with either an amine or an acetamide group (Figure 2.1, complexes $\mathbf{4^{dft}}$ and $\mathbf{5^{dft}}$). Interestingly, clear differences were found in the cleaving activity of these complexes, and the following order was observed: $\mathbf{4^{dft}} >> \mathbf{5^{dft}} > \mathbf{3^{dft}} > \mathbf{2^{dft}} = \mathbf{6^{dft}} >> \mathbf{7^{dft}} > \mathbf{1^{dft}}$. It was concluded that the complexes bearing an amine or an acetamide group are more active, because of an increased affinity for DNA.[22, 23] The optimal length of the bridge linking the phenanthrolines was estimated to three carbon atoms. The complexes $\mathbf{2^{dft}}$, $\mathbf{3^{dft}}$, $\mathbf{6^{dft}}$ and $\mathbf{7^{dft}}$ probably interact with DNA in a comparable manner, namely by partial intercalation of the phenanthroline unit, and no clear differences are observed in their respective Cu^{II}/Cu^{I} redox potentials, although complex $\mathbf{7^{dft}}$ shows a quasi-irreversible Cu^{II}/Cu^{I} reduction cycle.

Despite the excellent nuclease properties of these copper-phenanthroline complexes, only a few modeling and quantum chemical studies have been performed to investigate their mechanism of action.[23-30] In the present study, Cu^{I} and Cu^{II} complexes (Figure 2.1) in the presence of a coordinating chloride anion are investigated with the aid of theoretical calculations. Their geometry and electronic properties have been calculated in the gas phase by density functional theory (DFT).

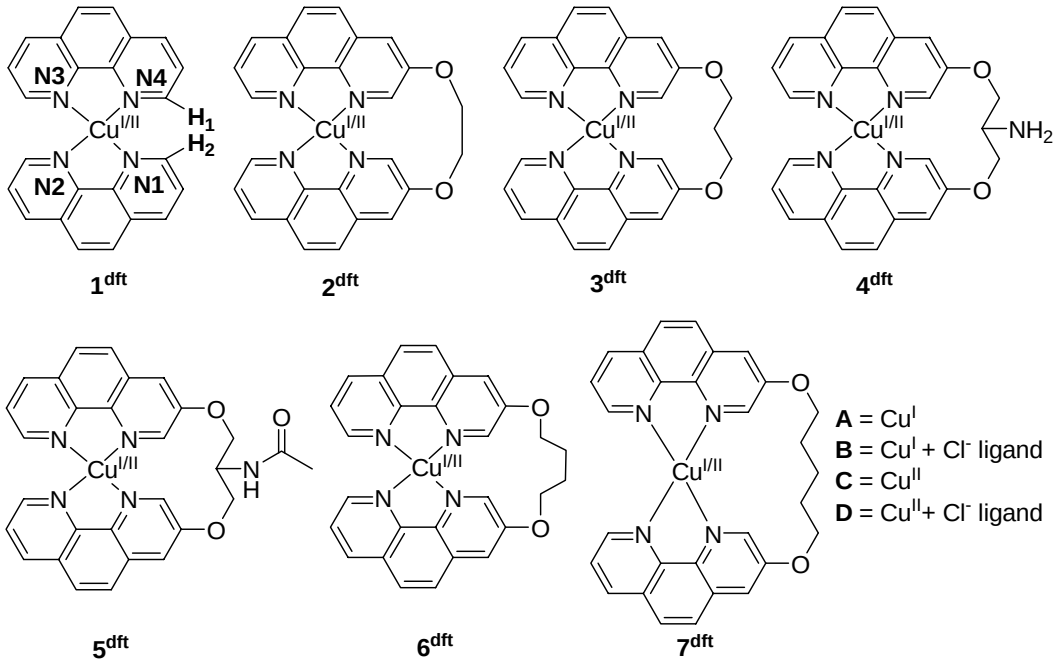

Figure 2.1 The optimized structures of complexes **1**^{dft} [$Cu^{I/II}(phen)_2$], **2**^{dft} Cu(3-ethyl-Clip-Phen), **3**^{dft} Cu(3-propyl-Clip-Phen), **4**^{dft} Cu(3-Clip-Phen), **5**^{dft} Cu(3-acetyl-Clip-Phen), **6**^{dft} Cu(3-butyl-Clip-Phen) and **7**^{dft} Cu(3-pentyl-Clip-Phen) were calculated for the two oxidation states and with or without chloride as a fifth ligand, namely Cu^{I} (**A**), Cu^{I} –Cl^{-} (**B**), Cu^{II} (**C**) and Cu^{II}–Cl^{-} (**D**). N.B. The nitrogen atoms closest to the bridges are numbered N1 and N4.

A thorough comparison of these complexes has been made in order to reveal: (i) the influence of the length of the bridge and of the substituents on the copper coordination geometry, and (ii) the variations of the redox potentials. These studies are aimed at better understanding the influence of the ligand conformation at the copper center on the cleavage activity of phenanthroline-based complexes. Such investigations are expected to be highly beneficial for the rational design and preparation of new copper-based nuclease active agents.

2.2 Results and Discussion

2.2.1 Calculations of [$Cu^{I}(phen)_2$], [$Cu(phen)_2Cl$], [$Cu^{II}(phen)_2$] and [$Cu^{I}(phen)_2Cl$]

The accuracy of the DFT calculations was validated through the comparison of the optimized, computed structures of [$Cu^{I}(phen)_2$], [$Cu^{II}(phen)_2$] and [$Cu^{II}(phen)_2Cl$] with the available experimental[31-45]and theoretical data.[23-25, 28, 30, 46] [$Cu^{I}(phen)_2$] is compared to experimental and theoretical results reported for [Cu^{I}(2,9-dimethyl-1,10-phenanthroline)$_2$], with the assumption that the effect of the additional methyl groups is negligible.[23-25, 28, 30, 41-45] The calculated bond lengths, angles and dihedral angles differ by less than respectively 0.05 Å, 6° and 7° from the crystal structures values. These small disparities may arise from intermolecular forces

in the crystal, such as strong stacking interactions, which become less important in solution. The calculated structure of $[Cu^{II}(phen)_2]$ is in good agreement with previous theoretical studies by others and us.[23, 46]

Table 2.1. Comparison between experimental and calculated parameters of $[Cu^{II}(phen)_2Cl]$.

	Experimental range	BP86/TZ2P/QZ4P (Cu only)
Cu – Cl	2.26 – 2.35 Å	2.25 Å
Cu – N1	1.98 – 2.00 Å	2.00 Å
Cu – N2	2.07 – 2.14 Å	2.11 Å
Cu – N3	1.98 – 2.01 Å	2.02 Å
Cu – N4	2.10 – 2.15 Å	2.19 Å
N1 – Cu – N3	174.0 – 176.3°	177.5°
N1 – N2 – N3 – N4	40.3 – 46.4°	46.9°

The calculated $[Cu^{II}(phen)Cl]$ geometry has been compared to distances and angles from a selection of known crystal structures (Table 2.1).[31-40] The DFT approach provides a fairly good accuracy in the calculation of such complexes; only a few values are found higher or lower than the experimental ones. These minor discrepancies may be due to strong counter ion dependence, as shown by the experimental values. From these results, it can be assumed that the DFT method employed allows a good theoretical description of the reported complexes.

2.2.2 Calculated structures of complexes $\mathbf{1}^{dft}$-$\mathbf{7}^{dft}$

The accuracy of the DFT calculations (BP86) was confirmed by comparison of the unbridged complexes $\mathbf{1A}^{dft}$, $\mathbf{1C}^{dft}$, and $\mathbf{1D}^{dft}$. Furthermore, the basis set and the relativistic effects were tested with complex $\mathbf{4A}^{dft}$. Only minor differences in the total energy are observed between the basis sets TZP, TZ2P and QZ4P (only for copper). The relativistic effects, considered by the relativistic zeroth-order regular approximation (ZORA), are very important. Indeed, calculations using the same basis set, but taking into account the relativistic effects or not, resulted in deviations of about 20 kJ mol^{-1}.

Pitié *et al.* reported several crystal structures of copper complexes with Cu^{II}(Clip-Phen). In all cases, a helical geometry with two Cu^{II} ions and two ligands (L_2/Cu_2 stoichiometry) was found. Mass spectrometry analyses demonstrated that these complexes mainly exist in solution in a 1:1 ligand-to-copper stoichiometry.[22] The minimized 1:1 L/Cu structures at the BP86/TZ2P/QZ4P level (copper only) of complexes $\mathbf{1}^{dft}$-$\mathbf{7}^{dft}$, with (**B** and **D**) or without (**A** and **C**) a chlorido ligand, and with a Cu^{I} (**A** and **B**) or a Cu^{II} (**C** and **D**) ion are shown in Figure 2.2. The chloride anion has been selected as the fifth ligand, because $CuCl_2$ is the copper salt typically used in DNA-cleavage studies.[22] Moreover, during the oxidation of DNA, a fifth ligand capable of abstracting a proton

from the deoxyribose unit is likely to bind to the copper moiety. Therefore, the structural features of such five-coordinated complexes are of special interest to rationalize the nuclease activity of copper phenanthroline compounds.

In accordance with previous reports, $[Cu^{I}(phen)_2]$ (Figure 2.2, **1A**^{dft}) has a tetrahedral geometry, which slightly deviates from the D2d symmetry.[23-25, 28, 30-46] The dihedral angle (N1−N2−N3−N4) between the two phenanthrolines amounts to 80° (Table 2.2). The coordination geometry of $Cu(phen)_2$ drastically changes upon oxidation of the copper ion. However, it has been experimentally shown that bridged Cu^{II} complexes similar to those studied in the present computational investigation are able to retain their four-coordinated environment in solution.[47] The complex $[Cu^{II}(phen)_2]$ (Figure 2.2, **1C**^{dft}) is significantly more planar than the corresponding $[Cu^{I}(phen)_2]$ complex. This structural feature results in a larger N1−Cu−N3 angle (Table 2.2, 124° for complex **1A**^{dft} and 144° for complex **1C**^{dft}) and a smaller N1−N2−N3−N4 torsion angle (Table 2.2, 80° for complex **1A**^{dft} and 40° for complex **1C**^{dft}). The Cu−N distances of **1C**^{dft} are identical, namely 2.00 Å. The $[Cu^{I}(phen)_2]$ and $[Cu^{II}(phen)_2]$ complexes holding a chlorido ligand, i.e. **1B**^{dft} and **1D**^{dft} (Figure 2.2), exhibit a trigonal bipyramidal geometry. However, the geometry of compound **1B**^{dft} is distorted. The equatorial plane is formed by a chlorido ligand and two nitrogen atoms of two different phenanthrolines. The axial positions are occupied by the other two nitrogen atoms of the phenanthroline units. The axial Cu−N distances are typically longer, as a result of the Jahn-Teller effect. The Cu−Cl distances of all complexes (**1B,D**^{dft}-**7B,D**^{dft}) amount to approximately 2.24 Å, which is in the range of experimental values.[31, 34, 38, 48, 49] Complex **1D**^{dft} displays a Cu−N3 distance of 2.19 Å, which is 0.07 Å longer than the average experimental values. The axial Cu−N lengths of the copper(I) complex **1B**^{dft} are very long, namely 2.25 Å for Cu−N1, and 2.42 Å for Cu−N3.

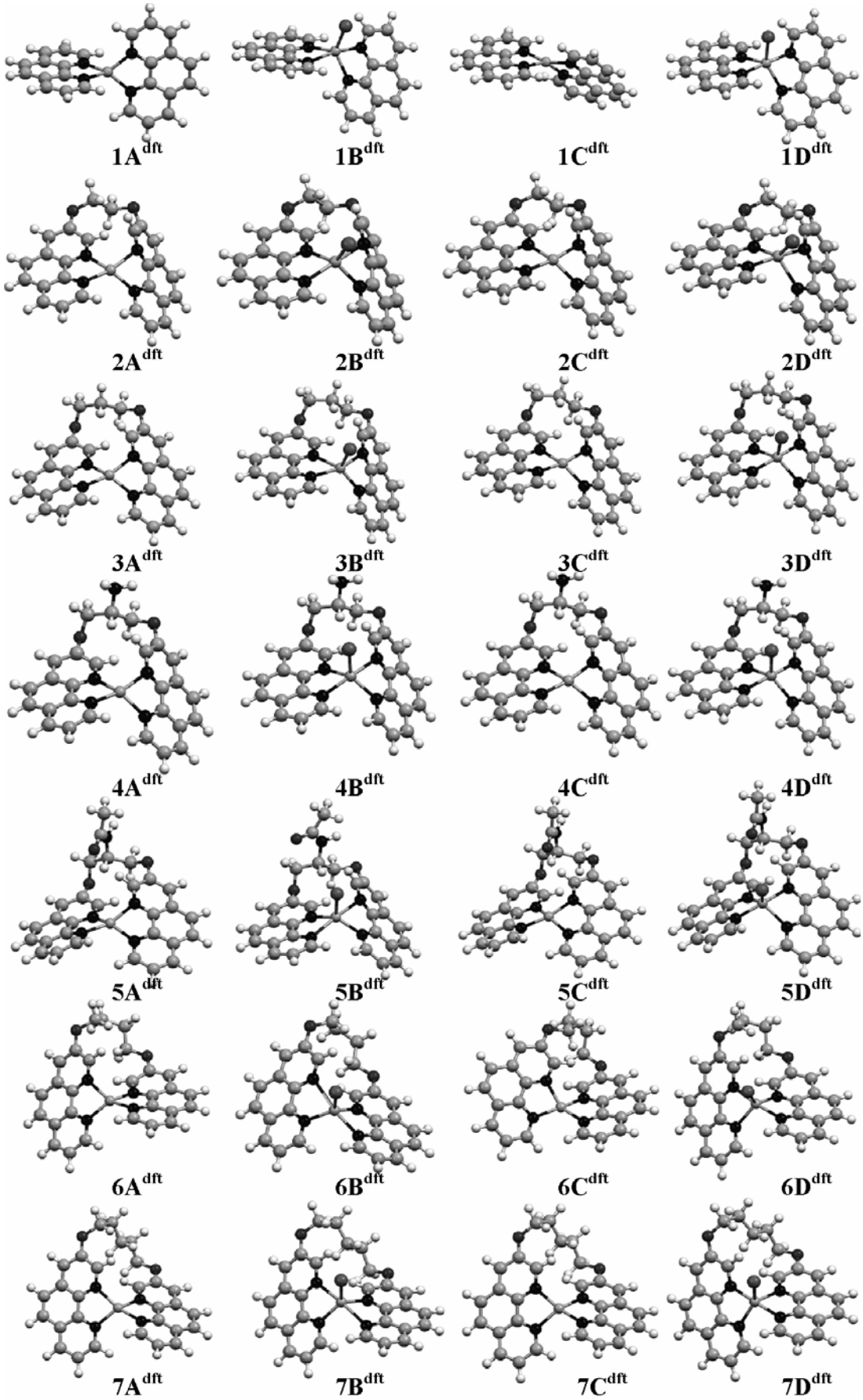

Figure 2.2 DFT optimized geometries of complexes $\mathbf{1}^{dft}$-$\mathbf{7}^{dft}$. The letters **A**, **B**, **C** and **D** symbolize the structures holding a Cu^{I}, Cu^{I}–Cl, Cu^{II} or Cu^{II}–Cl moiety, respectively.

Table 2.2 Selected bond distances and angles for complexes **1**^{dft}-**7**^{dft}.

	Distance (Å)					*Angle (°)*	*Dihedral angle (°)*	*Distance (Å)*
	Cu−N1	Cu−N2	Cu−N3	Cu−N4	Cu−Cl	N1−Cu−N3	N1−N2 −N3−N4	H1−H2
1A^{dft}	2.00	2.00	2.00	2.00		124	80	4.56
2A^{dft}	2.28	1.98	2.15	1.99		166	31	2.20
3A^{dft}	2.08	2.04	2.05	2.06		164	38	2.56
4A^{dft}	2.07	2.04	2.05	2.05		165	38	2.59
5A^{dft}	2.04	2.03	2.02	2.05		159	41	2.61
6A^{dft}	2.00	2.04	1.99	2.11		131	51	3.15
7A^{dft}	2.01	2.03	2.01	2.05		130	54	3.07
1B^{dft}	2.25	2.10	2.42	2.04	2.23	167	37	2.75
2B^{dft}	2.58	2.06	2.28	2.03	2.23	163	23	2.14
3B^{dft}	2.50	1.99	2.05	2.63	2.23	146	30	2.61
4B^{dft}	2.32	2.11	2.13	2.25	2.24	160	29	2.63
5B^{dft}	2.48	2.05	2.32	2.03	2.23	168	28	2.68
6B^{dft}	2.02	2.25	2.02	2.65	2.23	166	37	2.81
7B^{dft}	2.02	2.45	2.03	2.33	2.24	172	40	2.91
1C^{dft}	2.00	2.00	2.00	2.00		144	40	2.52
2C^{dft}	2.05	2.03	2.04	2.01		173	23	1.98
3C^{dft}	2.01	2.05	2.02	2.04		172	26	2.20
4C^{dft}	2.00	2.05	2.00	2.05		170	28	2.33
5C^{dft}	2.00	2.04	2.01	2.04		167	28	2.33
6C^{dft}	1.98	2.01	2.00	2.01		141	40	2.77
7C^{dft}	2.00	2.00	2.00	2.01		143	40	2.57
1D^{dft}	2.00	2.11	2.02	2.19	2.25	178	47	2.90
2D^{dft}	2.08	2.27	2.05	2.09	2.22	165	32	2.16
3D^{dft}	2.02	2.20	2.02	2.17	2.24	167	35	2.51
4D^{dft}	2.01	2.15	2.02	2.21	2.24	167	36	2.61
5D^{dft}	2.02	2.23	2.01	2.14	2.24	169	36	2.53
6D^{dft}	2.1	2.03	2.19	2.05	2.23	171	46	3.06
7D^{dft}	2.21	2.03	2.09	2.02	2.24	175	48	3.05

In the Clip-Phen complexes, the same characteristic is observed for the Cu−N distances of **2B**^{dft}-**7B**^{dft}. Some of these $Cu^{I}LCl^{-}$ complexes even show Cu−N distances up to 2.6 Å, which suggests a low stability. The structures of the Cu^{I} complexes **2A**^{dft}-**7A**^{dft} significantly differ from the $[Cu^{I}(phen)_2]$ one. Due to the presence of the bridge, complexes **2A**^{dft}-**7A**^{dft} can not adopt a tetrahedral geometry, as evidenced by the N1−Cu−N3 angle and the N1−N2−N3−N4 dihedral angle. The N1−Cu−N3 angle for $[Cu^{I}(phen)_2]$ is 124°, whereas this angle varies from 159° to 166° for complexes **2A**^{dft}-**5A**^{dft}. Complexes **6A**^{dft} and **7A**^{dft} possess a bridge of respectively, four and five methylene groups; therefore, the N1−Cu−N3 angle amounts to respectively 131° and 130°, which are values much closer to the one observed for $[Cu^{I}(phen)_2]$. Similarly, complexes

2A^{dft}-**7A**^{dft} exhibit torsion angles of respectively 31°, 38°, 38°, 41°, 51° and 54°, far below the value of 80° displayed by complex **1A**^{dft}.

For complex **2A**^{dft}, the small dihedral angle of 31° results in very close contacts between the protons H1 and H2 (H1···H2 = 2.20 Å), and steric repulsion can be expected. The Cu−N1 (2.28 Å) and Cu−N3 (2.15 Å) distances are also longer, compared to those of complexes with a longer bridge. This H1···H2 distance becomes even smaller upon oxidation (complex **2C**^{dft}), with a value reaching 1.98 Å. The Cu^{II} complexes with a 3-carbon bridge (complexes **3C**^{dft}-**5C**^{dft}) also show short H1···H2 contact distances, ranging from 2.20 to 2.33 Å. Due to a longer bridge, complexes **1C**^{dft}, **6C**^{dft} and **7C**^{dft} have H1···H2 separation distances of 2.52, 2.77 and 2.57 Å, respectively.

Interestingly, the geometry of the complexes with two or three methylene-bridges (complexes **2A**^{dft}-**5A**^{dft}) does not change drastically upon oxidation (complexes **2C**^{dft}-**5C**^{dft}) of the copper(I) center. The dihedral angle (N1−N2−N3−N4) decreases on average by 10°, and the N1−Cu−N3 angle experiences an increase of about 8°. 2- and 3-carbon bridges thus prevent large geometrical changes upon oxidation or reduction of the corresponding complexes, in contrast to the significant structural variations observed with longer bridges or no bridges. The complexes **1C**^{dft}, **6C**^{dft} and **7C**^{dft} present a dihedral angle (N1−N2−N3−N4) between the aromatic rings of 40°, and a N1−Cu−N3 angle of approximately 143°. The Cu−N distances of all the complexes are close to 2.00 Å.

Similar findings are noted with the $Cu^{II}Cl^{-}$ structures of complexes **2D**^{dft}-**5D**^{dft}. Due to their short bridging unit, the complexes **2D**^{dft}-**5D**^{dft} have distorted trigonal bipyramidal geometries. The torsion angle N1−N2−N3−N4 ranges from 32° to 36°, and the N1−Cu−N3 angle varies from 165° to 169° for complexes **2D**^{dft} and **5D**^{dft}, respectively. $[Cu^{II}(phen)_2Cl]$ (**1D**^{dft}) has a trigonal bipyramidal geometry, with a torsion angle N1−N2−N3−N4 of 47°, and a N1−Cu−N3 angle of 178°. Complexes **6D**^{dft} and **7D**^{dft} share their structural arrangement with complex **1D**^{dft}. The N1−N2−N3−N4 torsion angles are 46° and 48°, and the N1−Cu−N3 angles are 171° and 175° for complexes **6D**^{dft} and **7D**^{dft}, respectively. The axial positions are occupied by two nitrogen atoms from two different phenanthroline ligands, with elongated bond distances due to the Jahn-Teller effect. The axial Cu−N distances in compounds **1D**^{dft}, **3D**^{dft}-**7D**^{dft} are close to 2.20 Å, while complex **2D**^{dft} has a bond length of 2.27 Å. These values strongly differ from the calculated ones for the $Cu^{I}Cl^{-}$ structures (Cu−N bond lengths up to 2.6 Å).

It should be noted that the amine and acetamide groups of compounds **4**^{dft} and **5**^{dft} do not interact with the central copper action (the stereo-isomers in which these groups are folded to the inner sides of the bridges are sterically unfavorable and even then these functional groups

do not interact with the central copper ion). The experimentally observed effects of the functional groups in the bridge are probably caused by their interaction with the DNA strand.

2.2.3 Comparison of the calculated energies of complexes $\mathbf{1^{dft}}$*-*$\mathbf{7^{dft}}$

The ligand binding energies and the strain energies, as defined in the computational details section, are reported in Table 2.3. In general, the [Cu^{II}(Clip-Phen)] complexes have the lowest ligand binding energies and the [Cu^{I}(Clip-Phen)Cl] complexes the highest, following the net charges of the complexes. This fits with the elongated Cu-N bond lengths observed in the previous section. Furthermore, the complexes $\mathbf{2^{dft}}$-$\mathbf{6^{dft}}$ (Figure 2.1), characterized by short bridges, have higher complex ligand binding energies than complex $\mathbf{1^{dft}}$. Complex $\mathbf{2^{dft}}$ exhibits the highest ligand binding energy with one exception: the ligand binding energy is lower for $\mathbf{2B^{dft}}$ than for $\mathbf{5B^{dft}}$. A reasonable assumption to explain this higher energy obtained for $\mathbf{5B^{dft}}$ is the steric hindrance of the chloride atom by the oxygen from the acetamide group of the bridge.

Table 2.3 Ligand binding energies and strain energies (on ligand coordination) of complexes $\mathbf{1^{dft}}$-$\mathbf{7^{dft}}$.

Complex	Ligand binding energy (kJ mol^{-1})	Strain energy (kJ mol^{-1})	Complex	Ligand binding energy (kJ mol^{-1})	Strain energy (kJ mol^{-1})
$\mathbf{1A^{dft}}$	-759	0	$\mathbf{1C^{dft}}$	-1892	0
$\mathbf{2A^{dft}}$	-656	110	$\mathbf{2C^{dft}}$	-1818	95
$\mathbf{3A^{dft}}$	-692	76	$\mathbf{3C^{dft}}$	-1867	58
$\mathbf{4A^{dft}}$	-662	76	$\mathbf{4C^{dft}}$	-1838	56
$\mathbf{5A^{dft}}$	-727	69	$\mathbf{5C^{dft}}$	-1920	53
$\mathbf{6A^{dft}}$	-711	49	$\mathbf{6C^{dft}}$	-1892	35
$\mathbf{7A^{dft}}$	-730	26	$\mathbf{7C^{dft}}$	-1922	11
$\mathbf{1B^{dft}}$	-232	0	$\mathbf{1D^{dft}}$	-707	0
$\mathbf{2B^{dft}}$	-194	48	$\mathbf{2D^{dft}}$	-631	74
$\mathbf{3B^{dft}}$	-204	38	$\mathbf{3D^{dft}}$	-673	43
$\mathbf{4B^{dft}}$	-215	36	$\mathbf{4D^{dft}}$	-645	42
$\mathbf{5B^{dft}}$	-180	35	$\mathbf{5D^{dft}}$	-696	45
$\mathbf{6B^{dft}}$	-214	21	$\mathbf{6D^{dft}}$	-686	24
$\mathbf{7B^{dft}}$	-214	5	$\mathbf{7D^{dft}}$	-709	3

In order to investigate the geometrical constraints imposed by the bridge of the Clip-Phen-based complexes, the strain energy (see computational details) was also calculated (Table 2.3 and Figure 2.3). The Cu^{I} structures $\mathbf{2A^{dft}}$-$\mathbf{7A^{dft}}$ show the highest strain energies, which can be understood because the difference between the geometries of these complexes and the tetrahedral environment of [$Cu^{I}(phen)_2$] ($\mathbf{1A^{dft}}$) is substantial. Upon binding of the chloride, the

geometry of **1B**^{dft} changes drastically to a trigonal bipyramidal environment, comparable to the environment of complexes **2B**^{dft}-**7B**^{dft}. As a result, the strain energies of the $Cu^{I}Cl^{-}$ complexes **2B**^{dft}-**7B**^{dft} are much lower. The small variations in strain energy between the Cu^{II} and $Cu^{II}Cl^{-}$ structures are ascribed to the minor structural differences between **1C**^{dft} and **1D**^{dft}. As expected, complex **2**^{dft}, holding the shortest bridge, has the highest strain energy, which can be explained by steric repulsions between the protons H1 and H2 of the phenanthrolines. Strain energies are lower for the complexes with a three-methylene bridge, i.e. complexes **3**^{dft}-**5**^{dft} (Figure 2.1). No significant differences are observed between these three complexes, indicating that the functionalization of the bridge has no influence on the magnitude of the strain energy. A further increase of the bridge length leads to computed structures closely related to the one of complex **1**^{dft}. Thus, complexes **6**^{dft} and **7**^{dft} show markedly lower strain energies than complexes **2**^{dft}-**5**^{dft}. In particular, complex **7**^{dft} displays a very low strain energy, which clearly indicates that the long bridge does not induce significant geometrical constraints. The coordination characteristics of **7**^{dft} are therefore very close to those of $[Cu^{I/II}(phen)_2]$ complexes.

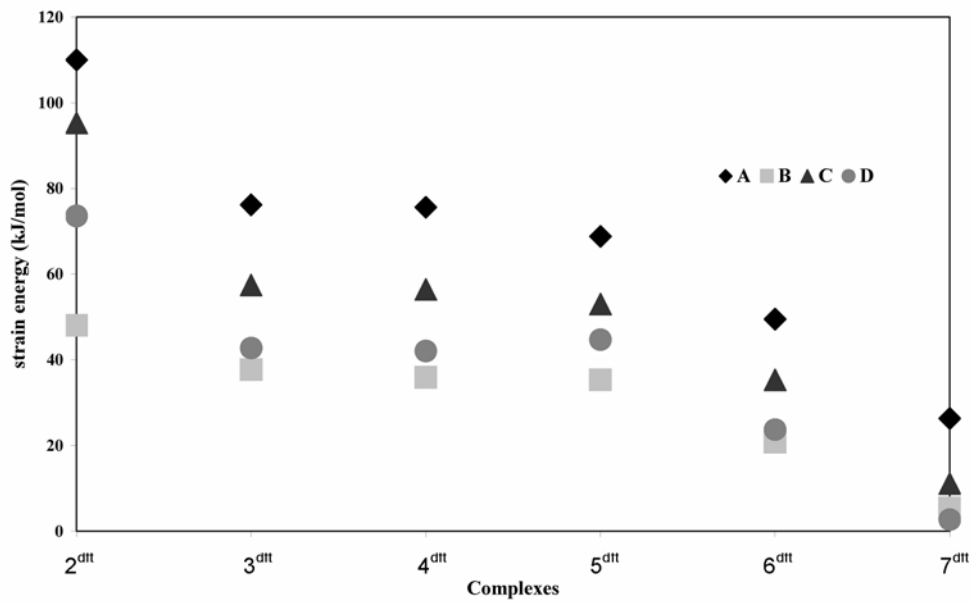

Figure 2.3 Strain energies of complexes **2**^{dft}-**7**^{dft}. The letters **A**, **B**, **C** and **D** symbolize the structures holding a Cu^{I}, Cu^{I}–Cl, Cu^{II} or Cu^{II}–Cl moiety, respectively.

The effect of the bridge on the redox properties was estimated for these complexes, by calculation of the inner-sphere reorganization energy (see computational details). The redox properties of the complexes are important, because the compounds have to go through a full redox cycle during their cleavage activity. Table 2.4 displays the λ_{red}, λ_{ox} and λ_i values of complexes **1**^{dft}-**7**^{dft} *in vacuo*. $Cu(phen)_2$ has a λ_{red} of 19 kJ mol^{-1} and a λ_{ox} of 25 kJ mol^{-1}. The sum of these components, i.e. λ_i, amounts to 44 kJ mol^{-1}. Complexes **2**^{dft}-**4**^{dft}, **6**^{dft} and **7**^{dft} have comparable inner-sphere reorganization energies; only minor differences are noticed. Complexes

3^{dft} and **4**^{dft} have a slightly lower inner-sphere reorganization energy, which can be expected, since the structural differences between the reduced and oxidized structures are less significant than for complex **1**^{dft}. Complex **2**^{dft} has a higher λ_i compared to compound **1**^{dft}, possibly due to the distorted Cu^I structure. Only the λ_i value of complex **5**^{dft} is markedly higher than those of the other complexes. In general, the complexes bearing a chlorido ligand (**1BD**^{dft}-**7BD**^{dft}) have higher λ_i values compared to the compounds without chlorido ligand (**1AC**^{dft}-**7AC**^{dft}). The highly distorted Cu^ICl^- structures of all the complexes are reflected by the large differences observed for the λ_{ox} values for the chloride-containing complexes. Consequently, it is not possible to draw any general conclusions from the differences in the λ_i values of the complexes with a chlorido ligand, other than that distortion by additional ligands can affect the redox properties rather drastically. Cyclic voltammetry experiments performed by Pitié *et al.*[22] indicated that the redox properties of the complexes **2**^{dft}-**7**^{dft} are analogous. The small differences noticed for the complexes without chlorido ligand reflect these experimental findings.

Table 2.4 Inner-sphere reorganization energies (kJ mol^{-1}) of complexes **1**^{dft}-**7**^{dft}.

Complex	λ_{red}	λ_{ox}	λ_i	Complex + Cl	λ_{red}	λ_{ox}	λ_i
1^{dft}	19	25	44	**1**^{dft} + Cl	26	50	76
2^{dft}	22	23	46	**2**^{dft} + Cl	37	40	77
3^{dft}	23	18	41	**3**^{dft} + Cl	19	60	79
4^{dft}	21	17	38	**4**^{dft} + Cl	22	34	55
5^{dft}	25	30	55	**5**^{dft} + Cl	60	78	138
6^{dft}	19	27	46	**6**^{dft} + Cl	35	48	83
7^{dft}	25	24	48	**7**^{dft} + Cl	25	63	88

2.2.4 Effect on the nuclease activity

The following nuclease activities were found[22] for complexes **1**^{dft}-**7**^{dft}: **4**^{dft} (S = 35) >> **5**^{dft} (S = 21) > **3**^{dft} (S = 15) > **2**^{dft} (S = 10) = **6**^{dft} (S = 10) >> **7**^{dft} (S = 2) > **1**^{dft} (S = 0.9), where S is a value to define the cleaving ability. The limited activity of $Cu(phen)_2^{2+}$ (**1**^{dft}) is presumably due to the loss of one phenanthroline ligand leading to the formation of $Cu(phen)^{2+}$, a much less active cleaving agent, at low complex concentrations,[11] as a result of the low binding constant of the second phenanthroline ligand. However, the difference in cleaving activity between complexes **1**^{dft} and **7**^{dft} is minor, although compound **7**^{dft} has a bridge that prevents the dissociation of the second phenanthroline. The computed coordination geometries of complexes **1**^{dft} and **7**^{dft} are comparable; only the geometry of complex **7A**^{dft} is significantly different from the one of compound **1A**^{dft}. Apparently, the geometry constraints generated by the short bridges are crucial for the nuclease activity.

Kinetic studies have demonstrated that the nuclease activity of $[Cu^{II}(phen)_2]$ proceeds by an ordered mechanism(see chapter 1, Scheme 1.1): the freely diffusing $[Cu^{II}(phen)_2]$ is first reduced to the Cu^{I} complex, $[Cu^{I}(phen)_2]$, which binds reversibly to DNA.[9] Planarity of the structures **2A**^{dft}-**7A**^{dft} (Figure 2.2) should favor the intercalation, and therefore increase the binding to DNA. A shortening of the bridge leads to a strong increase in the nuclease activity. However, complex **2**^{dft} with a two-methylene bridge is less active than complex **3**^{dft} which possesses a 3-carbon bridge. Apparently, a two-methylene bridge is too short, introducing too much strain, recognizable in elongated Cu−N distances and the very short H1−H2 distance (Table 2.2). Bridges *longer* than 3 carbons do not apply enough constraint.

Interestingly, while the calculated geometries and corresponding energies of complexes **3**^{dft}-**5**^{dft} are comparable, the cleavage activities are rather disparate, probably due to specific interactions of the amine or acetamide group with DNA. Nevertheless, it is clear that the 3-methylene bridges give the best cleavage activities, and from the present calculations it seems apparent that this is due to the planar geometry enforced by these short bridges.

2.3 Conclusions

A theoretical study has been performed with $[Cu^{I/II}(phen)_2]$ and a series of $[Cu^{I/II}$(3-Clip-Phen)] complexes whose bridge length and functionalization have been varied. The calculations have been carried out in the presence and in the absence of added chlorido ligand. This study confirms that upon oxidation of $[Cu^{I}(phen)_2]$, the structural environment of the metal center drastically changes from a tetrahedral geometry for the initial copper(I) species to a geometry in between tetrahedral and square planar for $[Cu^{II}(phen)_2]$. The coordination of a chlorido ligand results in a trigonal bipyramidal environment for $[Cu^{I/II}(phen)_2Cl]$. In general, the $Cu^{I}Cl^{-}$ structures of type **B** are highly distorted, reflected by some of their long Cu-N distances.

The complexes **6BCD**^{dft} and **7BCD**^{dft} exhibit similar structures, related to those of compounds **1BCD**^{dft}. However, complexes **6A**^{dft} and **7A**^{dft} cannot adopt an ideal tetrahedral geometry, as a result of spatial limitations induced by the bridge. The short bridges of complexes **2**^{dft}-**5**^{dft} forces the compounds to form geometries, which are distinct from the one found in complex **1**^{dft}. The Cu^{II} complexes **C** and **D** and the Cu^{I} complexes **A** and **B** show comparable geometries. The 2-carbon bridge of complex **2**^{dft} forces the phenanthroline protons next to the nitrogen atom to be in close contact (within 2 Å), which obviously instigates steric hindrance. This decrease in stability is further proven by the corresponding ligand binding energy, which is the lowest obtained. An unambiguous relation between the number of methylene groups constituting the bridge and the strain energy is observed: the highest energies are observed with the shortest bridges, and vice versa.

For the redox properties of the complexes, no correlation is observed with their cleaving abilities. The redox properties of the complexes are only mildly influenced by the bridges. Also no significant influence of the bridge length is observed on the inner-sphere reorganization energies of complexes $\mathbf{2}^{\mathbf{dft}}$-$\mathbf{7}^{\mathbf{dft}}$. A higher energy is only noted for complex $\mathbf{5}^{\mathbf{dft}}$.

The cleaving abilities of the complexes with non-functionalized bridges can be compared, because their interaction with DNA is partly achieved by intercalation. The different cleaving abilities observed, i.e. $\mathbf{3}^{\mathbf{dft}} > \mathbf{2}^{\mathbf{dft}} = \mathbf{6}^{\mathbf{dft}} > \mathbf{7}^{\mathbf{dft}}$, can be explained as follows: (i) a shortening of the bridge gives rise to an increase of the planarity of the resulting Cu^+ complexes, which is reflected by a subsequent higher affinity for DNA, and (ii) the structural changes occurring upon oxidation or reduction are less dramatic for the complexes possessing a short bridge; Accordingly, the kinetics of the cleavage reaction are enhanced. The fact that complex $\mathbf{2}^{\mathbf{dft}}$ is less active compared to compound $\mathbf{3}^{\mathbf{dft}}$ can be explained by steric interactions between the protons H1 and H2, due to the short bridge, which decreases its stability especially upon the binding of a fifth ligand. Complexes $\mathbf{3}^{\mathbf{dft}}$-$\mathbf{5}^{\mathbf{dft}}$ exhibit three methylene bridges, and complexes $\mathbf{4}^{\mathbf{dft}}$ and $\mathbf{5}^{\mathbf{dft}}$ have a substituent at the C2 position of their C3 bridge. The corresponding geometrical and energy profile disparities are minor; nonetheless significant differences are observed in the cleaving activities. Most likely, the additional functional groups on the bridge improve the interaction with DNA, and thus the nuclease activity.

The extensive DFT study herein presented investigates the structural and electronic properties of a series of bridged copper phenanthroline complexes in order to ultimately promote the rational design and synthesis of novel phenanthroline-based chemical nucleases.

2.4 Computational details

All Density Functional Theory (DFT) calculations were performed using ADF.[50-52] The complexes were subjected to full geometry optimization with Slater type (STO) basis sets of triple ζ with two polarization functions (TZ2P), and a frozen core approximation at the BP86[53, 54] level of theory. The copper ion was calculated with a basis set of quadruple ζ with four polarization functions (QZ4P). The optimizations were performed using the zeroth-order regular approximation (ZORA)[55-57] for relativistic effects. Single-point energies (SPE) were calculated with the same conditions. Open-shell Cu(II) complexes were treated with a spin-unrestricted formalism.

In order to relate the structural changes in copper complexes occurring upon the redox process with their cleavage efficiency, the reorganization energy for complexes $\mathbf{1}^{\mathbf{dft}}$-$\mathbf{7}^{\mathbf{dft}}$ was estimated. According to the Marcus theory, the rate of electron transfer is given by,

$$k_{ET} = \frac{2\pi}{h}\frac{H_{DA}^2}{\sqrt{4\pi\lambda RT}}\exp\left(\frac{-\left(\Delta G^0 + \lambda\right)^2}{4\lambda RT}\right) \qquad (1)$$

where H_{DA} is the electronic coupling element, which is a function of the overlap between the wave functions of the two states, ΔG^0 is the free energy change of the redox reaction, and λ is the reorganization energy, *i.e.,* the energy associated with relaxing the geometry of the system after electron transfer. In particular, for metal complexes, the inner-sphere reorganization energy (λ_i) is associated with the structural changes between the reduced and oxidized forms. λ_i is the sum of two contributions, λ_{red} and λ_{ox}, calculated as follows: λ_{ox} is the difference between the energy of Cu^{II} at its optimal geometry and its energy at the optimal geometry of Cu^{I}. Likewise, λ_{red} is the difference between the energy of Cu^{I} at its optimal geometry and its energy at the optimal geometry of the Cu^{II} complex.[58-62] Inner-sphere reorganization energies of coordination compounds typically range from 1 to 50 kcal/mol (4-200 kJ/mol).[58, 61]

Strain energies were calculated as the difference between the energy of $[Cu^{I/II}(phen)_2]$ at its optimal geometry and that of a $[Cu^{I/II}(phen)_2]$ fragment at the optimal geometry of the corresponding clipped complexes. Note that we define here the strain energy as the energy that would be needed to deform the $[Cu^{I/II}(phen)_2]$ complex to the geometries the ligands have in the bridged complexes.

Ligand binding energies were computed as the difference in energy between the optimal geometry of the complex, and the sum of the optimized ligand and the $Cu^{I/II}$ or (optimized) $Cu^{I/II}Cl$ complex.

2.5 References

[1] M. Pitié, A. Croisy, D. Carrez, C. Boldron, B. Meunier, *ChemBioChem* **2005**, *6*, 686.

[2] D. S. Sigman, A. Mazumder, D. M. Perrin, *Chem. Rev.* **1993**, *93*, 2295.

[3] R. M. Burger, *Chem. Rev.* **1998**, *98*, 1153.

[4] J. Y. Chen, J. Stubbe, *Nat. Rev. Cancer* **2005**, *5*, 102.

[5] R. P. Hertzberg, P. B. Dervan, *J. Am. Chem. Soc.* **1982**, *104*, 313.

[6] M. W. van Dyke, R. P. Hertzberg, P. B. Dervan, *Proc. Natl. Acad. Sci. U. S. A.* **1982**, *79*, 5470.

[7] D. S. Sigman, *Acc. Chem. Res.* **1986**, *19*, 180.

[8] D. S. Sigman, D. R. Graham, V. Daurora, A. M. Stern, *J. Biol. Chem.* **1979**, *254*, 2269.

[9] T. B. Thederahn, M. D. Kuwabara, T. A. Larsen, D. S. Sigman, *J. Am. Chem. Soc.* **1989**, *111*, 4941.

[10] J. M. Veal, R. L. Rill, *Biochemistry* **1991**, *30*, 1132.

[11] M. Pitié, C. Boldron, G. Pratviel, *Advances In Inorganic Chemistry, Vol 58,* Elsevier Academic Press Inc, San Diego, **2006**, pp. 77.

[12] L. G. Sillen, A. E. Martell, *Stability Constants of Metal-ion Complexes*, The chemical Soceity Londen Publication, Oxford, **1971**.

[13] M. M. Meijler, O. Zelenko, D. S. Sigman, *J. Am. Chem. Soc.* **1997**, *119*, 1135.

[14] W. K. Pogozelski, T. D. Tullius, *Chem. Rev.* **1998**, *98*, 1089.

[15] G. Pratviel, J. Bernadou, B. Meunier, *Angew. Chem.-Int. Edit. Engl.* **1995**, *34*, 746.

[16] A. M. Thomas, M. Nethaji, S. Mahadevan, A. R. Chakravarty, *J. Inorg. Biochem.* **2003**, *94*, 171.

[17] M. Pitié, B. Donnadieu, B. Meunier, *Inorg. Chem.* **1998**, *37*, 3486.

[18] M. Pitié, B. Sudres, B. Meunier, *Chem. Commun.* **1998**, 2597.

[19] P. de Hoog, C. Boldron, P. Gamez, K. Sliedregt-Bol, I. Roland, M. Pitié, R. Kiss, B. Meunier, J. Reedijk, *J. Med. Chem.* **2007**, *50*, 3148.

[20] M. Pitié, C. J. Burrows, B. Meunier, *Nucleic Acids Res.* **2000**, *28*, 4856.

[21] M. Pitié, B. Meunier, *Bioconjugate Chem.* **1998**, *9*, 604.

[22] M. Pitié, C. Boldron, H. Gornitzka, C. Hemmert, B. Donnadieu, B. Meunier, *Eur. J. Inorg. Chem.* **2003**, 528.

[23] A. Robertazzi, A. Magistrato, P. de Hoog, P. Carloni, J. Reedijk, *Inorg. Chem.* **2007**, *46*, 5873.

[24] L. X. Chen, G. B. Shaw, I. Novozhilova, T. Liu, G. Jennings, K. Attenkofer, G. J. Meyer, P. Coppens, *J. Am. Chem. Soc.* **2003**, *125*, 7022.

[25] P. Coppens, I. V. Novozhilova, *Int. J. Quantum Chem.* **2005**, *101*, 611.

[26] T. Hermann, H. Heumann, *RNA-Publ. RNA Soc.* **1995**, *1*, 1009.

[27] S. L. Howell, K. C. Gordon, *J. Phys. Chem. A* **2004**, *108*, 2536.

[28] Z. A. Siddique, Y. Yamamoto, T. Ohno, K. Nozaki, *Inorg. Chem.* **2003**, *42*, 6366.

[29] J. C. Stockert, *J. Theor. Biol.* **1989**, *137*, 107.

[30] M. Z. Zgierski, *J. Chem. Phys.* **2003**, *118*, 4045.

[31] A. X. Sui, G. Zhu, Z. X. Tang, *Acta Crystallogr. Sect. E.-Struct Rep. Online* **2006**, *62*, M1592.

[32] X. Q. Du, M. L. Zhu, F. Gao, *Acta Crystallogr. Sect. E.-Struct Rep. Online* **2006**, *62*, M363.

[33] W. B. Zhang, J. G. Wang, H. X. Chen, H. P. Xiao, *Acta Crystallogr. Sect. E.-Struct Rep. Online* **2005**, *61*, M2559.

[34] R. Clarke, K. Latham, C. Rix, M. Hobday, J. White, *CrystEngComm* **2005**, *7*, 28.

[35] H. Y. Mao, X. Q. Shen, G. Li, H. Y. Zhang, C. Xu, H. L. Liu, E. B. Wang, Q. A. Wu, H. W. Hou, Y. Zhu, *Polyhedron* **2004**, *23*, 1961.

[36] Y. B. Wei, P. Yang, *Acta Crystallogr. Sect. E.-Struct Rep. Online* **2004**, *60*, M429.

[37] B. Q. Ma, S. Gao, T. Yi, C. H. Yan, G. X. Xu, *Inorg. Chem. Commun.* **2000**, *3*, 93.

[38] G. Murphy, P. Nagle, B. Murphy, B. Hathaway, *J. Chem. Soc.-Dalton Trans.* **1997**, 2645.

[39] D. Boys, *Acta Crystallogr. Sect. C-Cryst. Struct. Commun.* **1988**, *44*, 1539.

[40] D. Boys, C. Escobar, S. Martinezcarrera, *Acta Crystallogr. Sect. B-Struct. Commun.* **1981**, *37*, 351.

[41] G. King, M. Gembicky, P. Coppens, *Acta Crystallogr. Sect. C-Cryst. Struct. Commun.* **2005**, *61*, M329.

[42] A. J. Blake, S. J. Hill, P. Hubberstey, W. S. Li, *J. Chem. Soc.-Dalton Trans.* **1998**, 909.

[43] J. F. Dobson, B. E. Green, P. C. Healy, C. H. L. Kennard, C. Pakawatchai, A. H. White, *Aust. J. Chem.* **1984**, *37*, 649.

[44] S. K. Hoffmann, P. J. Corvan, P. Singh, C. N. Sethulekshmi, R. M. Metzger, W. E. Hatfield, *J. Am. Chem. Soc.* **1983**, *105*, 4608.

[45] A. Y. Kovalevsky, M. Gembicky, P. Coppens, *Inorg. Chem.* **2004**, *43*, 8282.

[46] X. J. Wang, W. Wang, M. Koyama, M. Kubo, A. Miyamoto, *J. Photochem. Photobiol. A-Chem.* **2006**, *179*, 149.

[47] M. T. Miller, P. K. Gantzel, T. B. Karpishin, *Inorg. Chem.* **1998**, *37*, 2285.

[48] A. K. Chulkevich, V. I. Ponomarev, I. P. Lavrentev, L. O. Atovmyan, *Koord. Khimiya* **1987**, *13*, 1532.

[49] H. P. Xiao, M. L. Hu, X. H. Li, *Acta Crystallogr. Sect. E.-Struct Rep. Online* **2004**, *60*, M71.

[50] G. T. Velde, F. M. Bickelhaupt, E. J. Baerends, C. F. Guerra, S. J. A. Van Gisbergen, J. G. Snijders, T. Ziegler, *J. Comput. Chem.* **2001**, *22*, 931.

[51] C. F. Guerra, J. G. Snijders, G. te Velde, E. J. Baerends, *Theor. Chem. Acc.* **1998**, *99*, 391.

[52] S. ADF2005.01, Theoretical Chemistry, Vrije Universiteit, Amsterdam, The Netherlands, http://www.scm.com.

[53] A. D. Becke, *Phys. Rev. A* **1988**, *38*, 3098.

[54] J. P. Perdew, *Phys. Rev. B* **1986**, *33*, 8822.
[55] E. van Lenthe, E. J. Baerends, J. G. Snijders, *J. Chem. Phys.* **1993**, *99*, 4597.
[56] E. van Lenthe, E. J. Baerends, J. G. Snijders, *J. Chem. Phys.* **1994**, *101*, 9783.
[57] E. van Lenthe, A. Ehlers, E. J. Baerends, *J. Chem. Phys.* **1999**, *110*, 8943.
[58] X. Amashukeli, N. E. Gruhn, D. L. Lichtenberger, J. R. Winkler, H. B. Gray, *J. Am. Chem. Soc.* **2004**, *126*, 15566.
[59] M. H. M. Olsson, U. Ryde, *J. Am. Chem. Soc.* **2001**, *123*, 7866.
[60] E. Sigfridsson, M. H. M. Olsson, U. Ryde, *J. Phys. Chem. B* **2001**, *105*, 5546.
[61] U. Ryde, M. H. M. Olsson, *Int. J. Quantum Chem.* **2001**, *81*, 335.
[62] W. W. Parson, Z. T. Chu, A. Warshel, *Biophys. J.* **1998**, *74*, 182.

Chapter 3

A New Approach for the Preparation of Efficient DNA Cleaving Agents: Ditopic Copper-Platinum Complexes Based on 3-Clip-Phen and Cisplatin.*

The design and synthesis of new heterodinuclear DNA-targeting agents are described. The abilities of cisplatin and Cu(3-Clip-Phen) – an artificial DNA-cleaving agent – have been combined through their "covalent coupling". This strategy has led to bifunctional complexes, that are able to cleave the DNA in a double-stranded fashion in contrast to Cu(3-Clip-Phen) alone, and have promising cytotoxicities compared to cisplatin in several cell lines.

* This chapter is based on Paul de Hoog, Christophe Boldron, Patrick Gamez, Karen Sliedregt-Bol, Isabelle Roland, Marguerite Pitié, Robert Kiss, Bernard Meunier, and Jan Reedijk, *J. Med. Chem.* **2007**, *50*, 3148

3.1 Introduction

Among the strategies which find application in clinical anticancer chemotherapy, the cancer cells eradication induced by DNA-interacting molecules has proven its efficiency.[1, 2] First of all, cisplatin is one of the most widely used anticancer agents. It is generally accepted that the distortion of DNA generated upon binding of cisplatin is largely responsible for its antitumor properties.[3] Secondly, the therapeutic anticancer activity of the natural antibiotic bleomycin has been attributed to the ability of its metal complexes to perform oxidative DNA cleavage via oxidative degradation of the deoxyribose units.[4] This important discovery has led to the design and preparation of synthetic models of bleomycin such as 3-Clip-Phen.[5] Copper complexes of 3-Clip-Phen mediate single-strand cleavage of DNA from the minor groove, through the oxidation of the sugar moiety, albeit without sequence specificity.[5, 6]

Intrinsic or acquired drug resistance is a common problem in cisplatin chemotherapy.[7-9] Therefore, combination therapy was developed.[1] For example bleomycin, etopside and cisplatin are simultaneously used for testicular cancer treatment resulting in a curing rate of >99% if applied at the early stage of the syndrome.[10] Proceeding from this success, multifunctional drugs were developed.[11] For instance, cisplatin was combined with intercalating agents, known as Topoisomerase blockers,[12-17] and also with a photoactivated cleaving agent.[18]

The combined interest in (i) improving the DNA cleavage specificity of Cu(3-Clip-Phen) complexes together with their ability to perform double strand breaks (DSB) and (ii) circumventing drug resistance owing to the use of cisplatin,[7-9, 19, 20] has inspired the design of bifunctional molecules (Figure 3.1) containing both active entities.

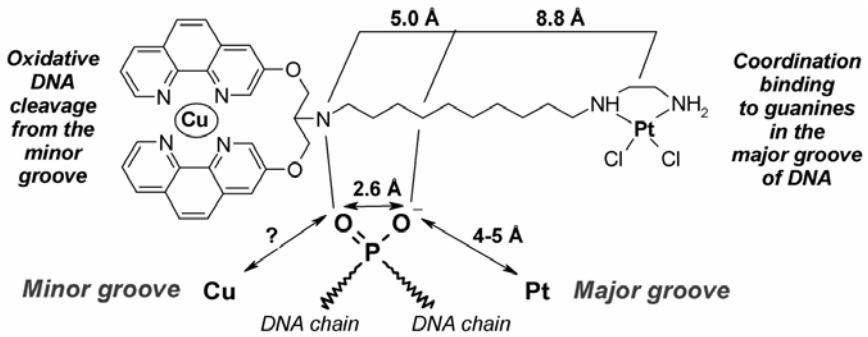

Figure 3.1 Strategy adopted for the synthesis of heterodinuclear minor/major groove interacting complexes.

Thus, compounds **Cu3CP-6-Pt** and **Cu3CP-10-Pt** have been prepared (Scheme 3.1) considering the intrinsic DNA-interaction characteristics of the two separate active metallic centers. Depending on their mutual degree of freedom, both moieties will or will not reach their preferential site of interaction simultaneously, namely the nitrogen atom N7 of guanine in the

major groove for the platinum component, and the minor groove for the copper unit.[6] The minimum separation distance required to achieve such concomitant minor-major groove interactions has been determined from the crystal structure of a DNA-cisplatin adduct.[21] The phosphate oxygen atom pointing toward the major groove and the platinum ion of cisplatin are 4-5 Å apart from each other (Figure 3.1). The distance between both oxygen atoms of the same phosphate group is about 2.6 Å.

It has been proposed that the amino group of Cu(3-Clip-Phen) could be protonated, favoring its interaction with the polyanionic structure of DNA.[22] Thus, it could interact via hydrogen bonding with the oxygen atom of the phosphate, thereby pointing toward the minor groove.[23, 24]

Compound **Cu3CP-10-Pt** has therefore been designed with a bridge long enough to allow the interaction of both metal centers with their respective preferential target site. In the case of a shorter bridge, i.e. compound **Cu3CP-6-Pt**, both moieties will be forced to sit in the same DNA groove. Nevertheless, the complex retains its flexibility during the interaction with DNA.

3.2 Results and discussion

The general synthetic pathway to prepare ligands **3CP-6-NH$_2$** and **3CP-10-NH$_2$** is depicted in Scheme 3.1. The selective and complete platination of the ethylenediamine unit using 1 equivalent of K_2PtCl_4 was monitored by ^{195}Pt NMR and UV spectroscopy (Figure 3.2). The in situ reactions of the so-obtained platinum derivatives **3CP-6-Pt** and **3CP-10-Pt** with 2 equivalents of $CuCl_2$ yielded the heterobimetallic complexes **Cu3CP-6-Pt** and **Cu3CP-10-Pt,** respectively. The UV-Vis spectrum recorded for the solution of **3CP-6-NH$_2$** or **3CP-10-NH$_2$** exhibits the typical features for the free 3-Clip-Phen ligand. The spectrum recorded for the solution of **3CP-6-Pt** or **3CP-10-Pt** is comparable to the one of the solution of **3CP-6-NH$_2$** or **3CP-10-NH$_2$**. As expected, platinum(II) does not coordinate to the Clip-Phen part of **3CP-6-NH$_2$**, but to the ethylenediamine part as clearly indicated by the ^{1}H NMR and ^{195}Pt NMR studies. No significant shift of the 3-Clip-Phen peaks were observed by ^{1}H-NMR, and the ^{195}Pt-NMR peak around –2310 ppm corresponds to the coordination of platinum to the ethylenediamine moiety.[25-27] The spectrum recorded for a solution of **Cu3CP-6-Pt** or **Cu3CP-10-Pt** is typical for a Cu(3-Clip-Phen) complex.[5] As anticipated, Copper(II) coordinates to the Clip-Phen moiety of the platinum complex.

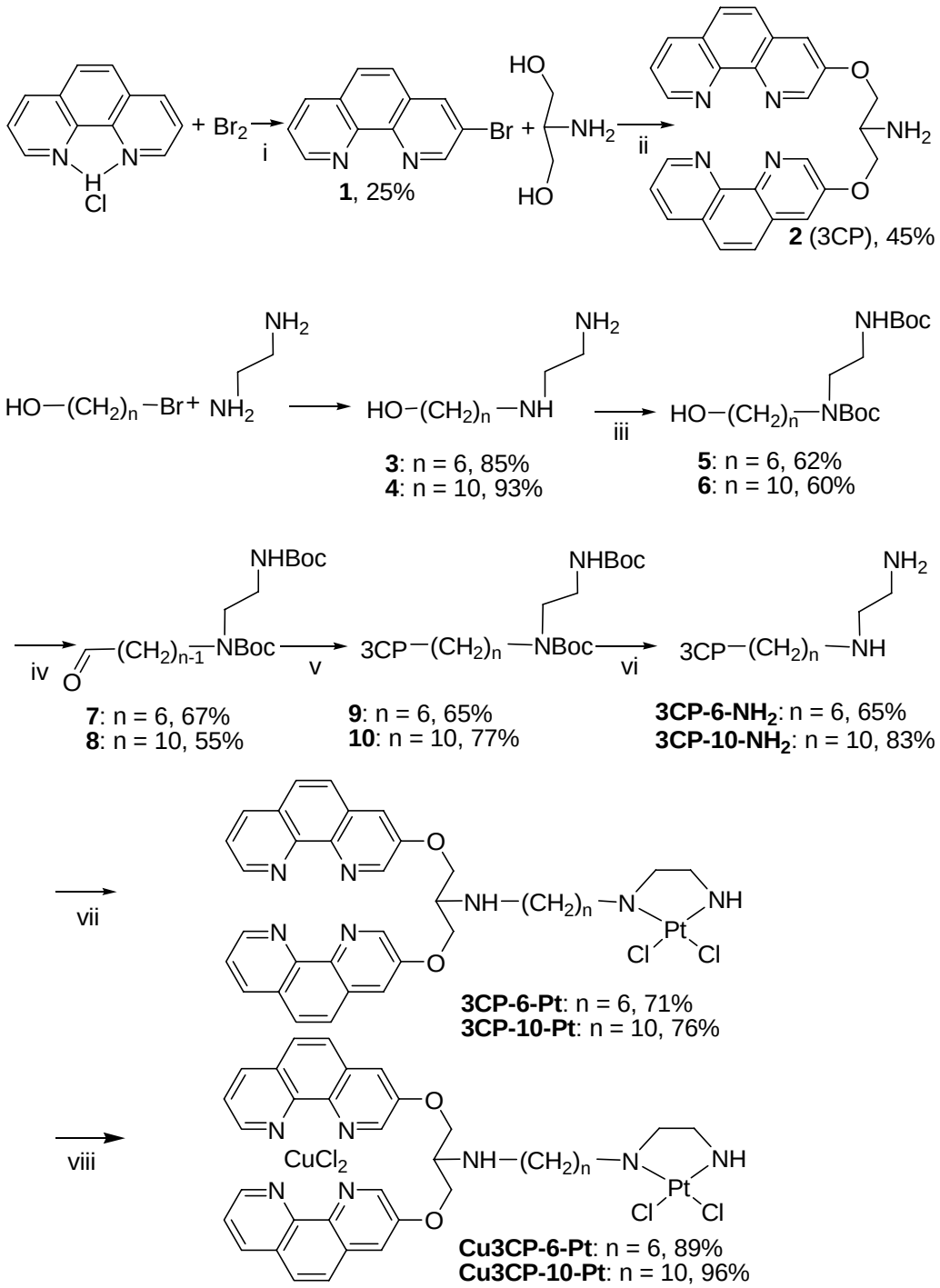

Scheme 3.1 Reagents and conditions: (i) 140 °C, nitrobenzene; (ii) 50 °C, NaH, 2,6-di-*tert*-butyl-4-methylphenol, DMF; (iii) (1) NaH, Boc_2O, THF, overnight, (2) K_2CO_3, MeOH, reflux, 1 h; (iv) pyridinium chloridotrioxidochromate (PCC), CH_2Cl_2, 2 h; (v) (1) 3-Clip-Phen (**2**), MeOH, reflux, 2 h, (2) $NaBH_4$, reflux, 2 h; (vi) TFA, 0 °C, 1 h; (vii) K_2PtCl_4, MeOH/H_2O, 5 h; (viii) $CuCl_2$, DMF, 50 °C.

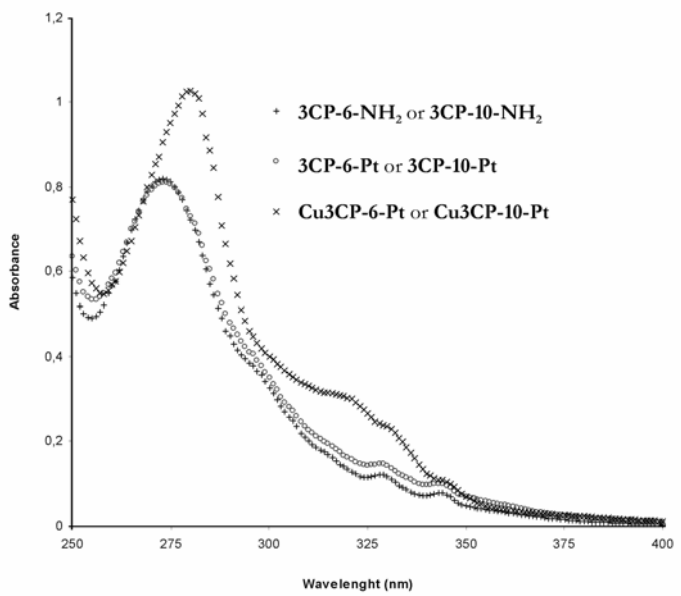

Figure 3.2 UV-Vis spectroscopic studies of a solution of ligand **3CP-6-NH$_2$** or **3CP-10-NH$_2$**, a solution of **3CP-6-Pt** or **3CP-10-Pt**, and a solution of **Cu3CP-6-Pt** or **Cu3CP-10-Pt**. The UV-vis spectra were recorded after dilution of the solutions with H_2O to a concentration of 20.8 μM.

The relaxation of supercoiled circular ΦX174 DNA (form I) into the relaxed (form II) and the linear (form III) conformations is monitored in order to compare the aerobic cleavage abilities of complexes **Cu3CP-6-Pt**, **Cu3CP-10-Pt** and Cu(3-Clip-Phen) in the presence of a reducing agent (Figure 3.3). The bifunctional complexes are incubated for 20 h in order to allow the formation of platinum-DNA adducts. The nuclease activity is subsequently initiated by the addition of 5 mM mercaptopropionic acid (MPA) in air.

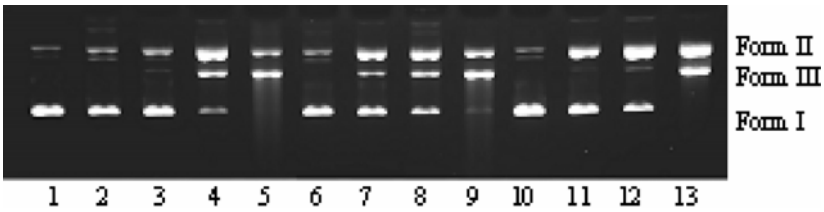

Figure 3.3 Comparison of the oxidative cleavage of ΦX174 plasmid DNA performed by **Cu3CP-6-Pt**, **Cu3CP-10-Pt** and Cu(3-Clip-Phen) in the presence of 5 mM MPA. Lane 1: control DNA. Lane 2: 250 nM **Cu3CP-6-Pt** without MPA. Lane 3: 100 nM **Cu3CP-6-Pt**. Lane 4: 150 nM **Cu3CP-6-Pt**. Lane 5: 250 nM **Cu3CP-6-Pt**. Lane 6: 250 nM **Cu3CP-10-Pt** without MPA. Lane 7: 100 nM **Cu3CP-10-Pt**. Lane 8: 150 nM **Cu3CP-10-Pt**. Lane 9: 250 nM **Cu3CP-10-Pt**. Lane 10: 250 nM Cu(3-Clip-Phen) without MPA. Lane 11: 100 nM Cu(3-Clip-Phen). Lane 12: 150 nM Cu(3-Clip-Phen). Lane 13: 250 nM Cu(3-Clip-Phen).

Lanes 4, 8 and 12 clearly show that the nuclease activities of **Cu3CP-6-Pt** and **Cu3CP-10-Pt** are higher than the one achieved with Cu(3-Clip-Phen), and more linear DNA is formed. Indeed, quantifications show that **Cu3CP-6-Pt** and **Cu3CP-10-Pt** cleaved the largest quantities of form I (starting material). Using the same experimental conditions (lanes 4, 8 and

12), Form III is generated by the platinum/copper complexes and not by Cu(3-Clip-Phen). Moreover, smears (resulting from multi-fragmented DNA) are observed when using complexes **Cu3CP-6-Pt** or **Cu3CP-10-Pt** at 250 nM concentration, which is not the case with Cu(3-Clip-Phen) (lanes 5, 9 and 13). The most striking feature observed for these hybrid platinum/copper complexes is that form III already appears while form I is still present. This result obviously indicates that the heterobimetallic complexes are able to perform direct double strand cuts, whereas Cu(3-Clip-Phen) is only capable of carrying out successive single strand cuts.[5] Time-course studies of the cleavage of the complexes **Cu3CP-6-Pt**, **Cu3CP-10-Pt** and Cu(3-Clip-Phen) have been performed to further investigate the direct double strand cleavage (Figure 3.4). From these studies, it appears that linear DNA is formed for both complexes **Cu3CP-6-Pt** and **Cu3CP-10-Pt** directly from the start of the reaction in contrast to Cu(3-Clip-Phen). Even after most of the supercoiled DNA has disappeared in the reaction with Cu(3-Clip-Phen), only less then 8% of linear DNA has formed. Also, these studies confirm the higher cleaving activities of complexes **Cu3CP-6-Pt** and **Cu3CP-10-Pt** compared to Cu(3-Clip-Phen) alone, since a fast disappearance of form I, associated with the appearance of form III is observed with these bifunctional molecules. If the concentration of Cu(3-Clip-Phen) is increased to 250 nM, the full disappearance of the supercoiled DNA is observed (Figure 3.4d). Although, small quantities of linear DNA are still observed before the complete disappearance of supercoiled DNA, its amount is inferior to the one noticed with complexes **Cu3CP-6-Pt** and **Cu3CP-10-Pt**. In addition, more than 80 % of circular DNA is formed, while the reaction with complexes **Cu3CP-6-Pt** and **Cu3CP-10-Pt** only generate a maximum of 60 % of form II.

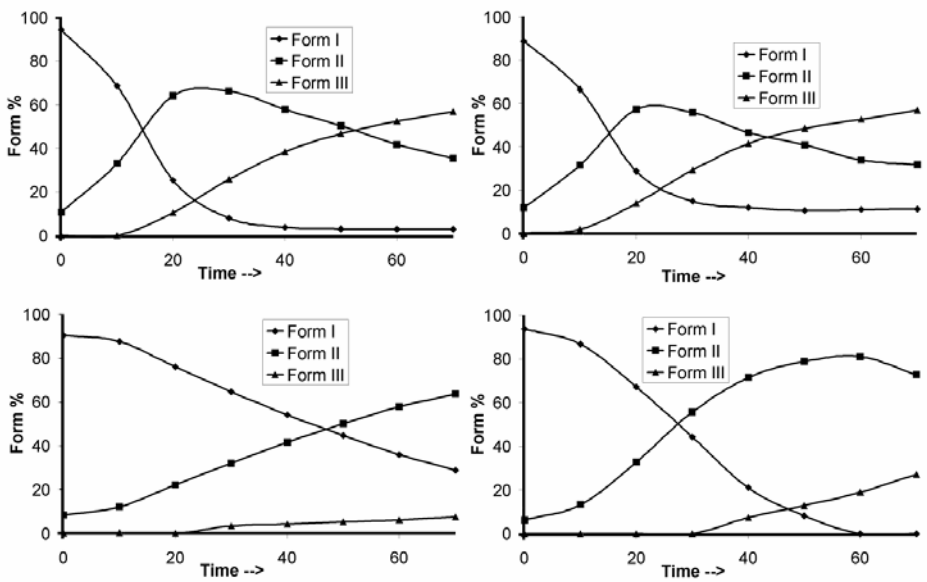

Figure 3.4 Time-course experiments of DNA cleavage (20 μM base pairs) over a period of 70 minutes in the presence of 5 mM MPA and air. Before addition of the reductant, the complexes were incubated for 24 h. (a) 200 nM **Cu3CP-6-Pt**, (b) 200 nM **Cu3CP-10-Pt**, (c) 200 nM Cu(3-Clip-Phen), (d) 250 nM Cu(3-Clip-Phen).

The DSB formation was further explored by a statistical test developed by Povirk *et al.*, which has been used to assay other complexes such as bleomycin.[28, 29] This test assumes a Poisson distribution of strand cuts, and allows calculating the average number of DSB per molecule, n_2. n_2 is obtained from the fraction of linear DNA after cleavage, and the total average number of single- plus double-strand breaks ($n_1 + n_2$), from the fraction of remaining supercoiled DNA after reaction. In order to determine n_1 and n_2 both supercoiled and linear DNA should be present in the experiments. For complexes **Cu3CP-6-Pt** and **Cu3CP-10-Pt**, the n_1/n_2 values determined at 20 minutes (Figure 3.4), amounts to respectively 10.5 and 6.8 and respectively 5.8 and 3.1 at 30 minutes. The n_1/n_2 values for Cu(3-Clip-Phen) at 40 and 50 minutes are respectively 18.5 and 16.4. The DSB values of **Cu3CP-6-Pt** and **Cu3CP-10-Pt** are in the range of bleomycin,[29] while the cleavage occurs in a more random manner for Cu(3-Clip-Phen). These results emphasize the ability of complexes **Cu3CP-6-Pt** and **Cu3CP-10-Pt** to induce direct double stranded cuts.

Therefore, it appears that the platinum moiety of complexes **Cu3CP-6-Pt** and **Cu3CP-10-Pt** acts as an anchor to DNA through a kinetically inert coordination bond. Subsequently, the Cu(3-Clip-Phen) component can function as a cleaving agent only in the close proximity of the platinum moiety, thereby favoring double stranded scissions.

To further investigate the platinum coordination of the complexes to DNA, high resolution analyses with a 36 bp DNA fragment were performed (Figure 3.5a). This fragment contains the two major platination sites on the 5'-end-labelled ODN I strand (highlighted in bold in Figure 3.5a). Complexes able to coordinate to DNA retard the migration rate of the complexed DNA during denaturing polyacrylamide gel electrophoresis (PAGE), as a result of the increase in molecular weight and the change of the overall charge. Therefore, complexes **3CP-6-Pt**, **3CP-10-Pt**, **Cu3CP-6-Pt** and **Cu3CP-10-Pt** were incubated for 24 h with the 36 bp DNA fragment, followed by PAGE in order to detect the platinum-DNA adducts (Figure 3.5b). The complexes are all able to coordinate to ODN I, because free ODN I has partially disappeared and clear bands have emerged above the free ODN fragment (Figure 3.5b). Cisplatin has almost fully reacted, and a clear band corresponding to the adducts is observed (Figure 3.5b, lane 2). Complexes **3CP-6-Pt**, **3CP-10-Pt**, **Cu3CP-6-Pt** and **Cu3CP-10-Pt** have partially reacted with the ODN fragment with the following order of efficiency: **3CP-6-Pt** ≈ **3CP-10-Pt** > **Cu3CP-6-Pt** = **Cu3CP-10-Pt**. In contrast to cisplatin, the products engendered by complexes **3CP-6-Pt**, **3CP-10-Pt**, **Cu3CP-6-Pt** and **Cu3CP-10-Pt** give rise to a smear (Figure 3.5b). This is especially true for complexes **Cu3CP-6-Pt** and **Cu3CP-10-Pt** whose copper moieties are coordinated. No clear bands can be observed (lanes 4 and 6), possibly as the result of unselective DNA binding of the platinum part caused by the Cu(3-Clip-Phen) moiety, which preferentially coordinates in the minor groove of DNA.

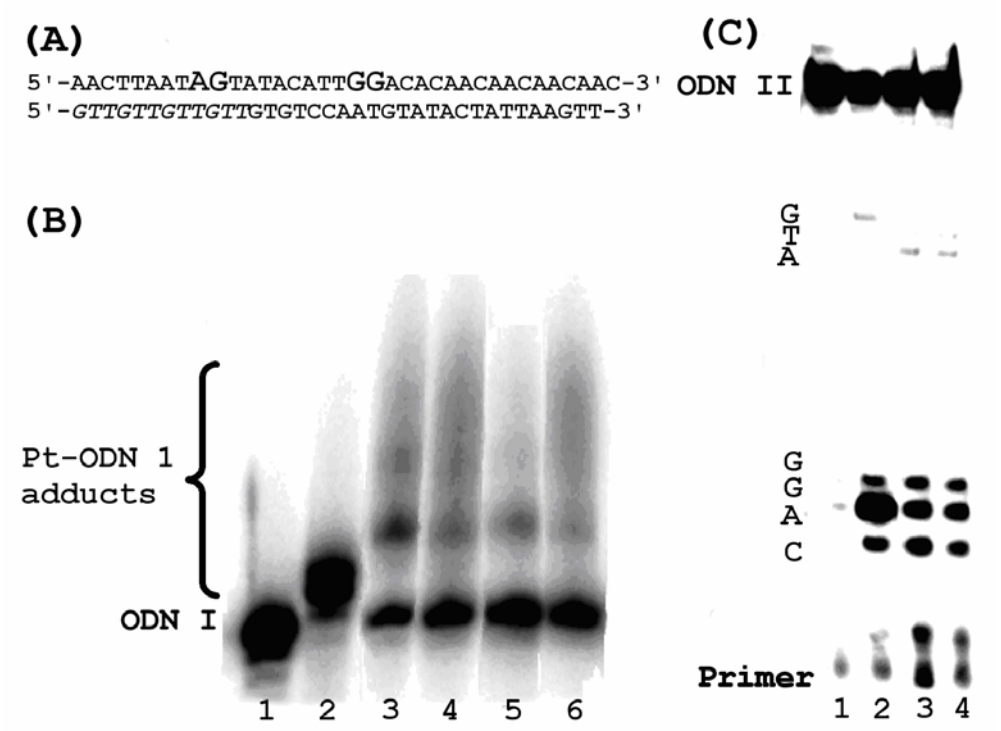

Figure 3.5. (a) 36 bp DNA fragment used for these studies. The two major platination sites are shown in bold and the primer is visualized in italic on ODN II. (b) PAGE analysis of the platinum-ODN I adducts. ODN I-ODN II duplex was ^{32}P-labeled on the 5'-end of ODN I. The complexes were incubated for 24 h with the ODN I-ODN II duplex before analyses. Lane 1: ODN I. Lane 2: 3 μM cisplatin. Lane 3: 10 μM **3CP-6-Pt**. Lane 4: 10 μM **Cu3CP-6-Pt**. Lane 5: 10 μM **3CP-10-Pt**. Lane 6: 10 μM **Cu3CP-10-Pt**. (c) Phosphor image of a DNA sequencing gel comparing the sequence specificity of cisplatin, **3CP-6-Pt** and **3CP-10-Pt** with primer extension. ODN I-ODN II duplex was incubated with platinum-complexes then precipitated to remove unlinked complexes. 5'-end labeled primer was added and all the samples were extended using TAQ polymerase, starting from the 5'-end-labelled primer. Lane 1: blank experiment. Lane 2: 3 μM cisplatin Lane 3: 10 μM **3CP-6-Pt**. Lane 4: 10 μM **3CP-10-Pt**. Note that the AG and GG sites give the sequence of the opposite strand.

Primer extension experiments are performed to investigate the sequence selective binding of platinum complexes to DNA.[30-36] TAQ polymerase has proven to effectively stop at platination sites, and is therefore used for these studies.[37-39] The cisplatin-specific damage sites are the GG and AG sites, but the majority of cisplatin is detected at the GG site. Complexes **3CP-6-Pt** and **3CP-10-Pt** lead to similar results, suggesting that the platinum part is interacting with its preferred site (Figure 4c). However, the bulkiness of the complexes also affects the bases in the close proximity of the adduct. Therefore, the stops of the TAQ polymerase are also influenced by this steric issue. In the experiment with cisplatin, the polymerization is halted at the GG site, primarily on the A before the GG spot, but also at the cytosine before the adenine, and at the first guanine. Near the AG site, the TAQ polymerase mainly stops at the G base. For complexes **3CP-6-Pt** and **3CP-10-Pt**, the enzyme halts at the GG site are equally distributed

between the GAC nucleobases. At the AG site, the damage is mainly observed at the A base. However, no stops are detected at the G base.

The cytotoxic activities of complexes **3CP-6-Pt**, **3CP-10-Pt**, **Cu3CP-6-Pt**, **Cu3CP-10-Pt**, Cu(3-Clip-Phen) and cisplatin have been determined for breast (MCF7 and EVSA-T), colon (WIDR), ovarian (IGROV), melanoma (M19), renal (A498), non-small lung (H226), two glioblastomas (Hs683 and U373), two colorectal (HCT-15 and LoVo) and lung (A549) cancer cell lines. The results of the most relevant activities are summarized in Table 3.1. The cytotoxicities of all complexes are insignificant for the cell lines HCT-15, Hs683, LoVo and A498. Therefore, the corresponding values have been excluded from Table 3.1. Indeed, a complex with an IC_{50} value higher than 10 μM (>10) is considered to be inactive.[40]

Table 3.1 In vitro cytotoxicity assays for **3CP-6-Pt**, **3CP-10-Pt**, **Cu3CP-6-Pt**, **Cu3CP-10-Pt**, Cu(3-Clip-Phen), and cisplatin, against a selection of cancer cell lines.

	IC_{50}[a] values (μM)					
Cell lines	**3CP-6-Pt**	**3CP-10-Pt**	**Cu3CP-6-Pt**	**Cu3CP-10-Pt**	Cu(3-Clip-Phen)	Cisplatin
WIDR	3.7	3.6	7.0	>10	0.58	3.2
EVSA-T	5.6	4.0	1.6	2.7	0.53	1.4
H226	3.0	4.1	5.1	>10	1.6	>10
A549	>10	7.4	>10	>10	>10	1.5
MCF-7	0.9	5.4	3	>10	>10	9
M19	6.0	5.2	0.86	0.37	0.30	1.9
IGROV	>10	>10	7.7	>10	5.4	0.56
U373	>10	6.5	7.1	>10	>10	5

[a]IC_{50} = concentration of drug required to eradicate 50% of the cancer cells.

The IC_{50} values observed for Cu(3-Clip-Phen) are in some cases superior to those achieved with cisplatin (Table 3.1, WIDR, EVSA-T, H226 and M19). The significant antiproliferative activity of 3-Clip-Phen and the corresponding copper complex has been previously measured on the L1210 murine leukemia cell line.[28] These good activities confirm the high potential of Cu(3-Clip-Phen) as an antitumor agent, and strengthen the potential of our strategy to prepare hybrid Cu(3-Clip-Phen)/cis-Pt derivatives. The IC_{50} values obtained with the copper-free complexes (**3CP-6-Pt** and **3CP-10-Pt**) are similar or higher compared to the ones achieved with cisplatin, for the cell lines WIDR, H226, and MCF-7. Complex **3CP-6-Pt** is even ten times more active than cisplatin for the cell line MCF-7, where Cu(3-Clip-Phen) has been found to be inactive. Interestingly, in some cell lines, the cytotoxicities of **3CP-6-Pt** or

3CP-10-Pt are even higher than those reached with **Cu3CP-6-Pt** or **Cu3CP-10-Pt**. However, for the EVSA-T and M19 cell lines, the hybrid platinum/copper complexes are more active, which is in agreement with the known activity of Cu(3-Clip-Phen). However, Cu(3-Clip-Phen) is equally good or better in both cell lines. In most cases, compound **3CP-10-Pt** is more active than **3CP-6-Pt,** and surprisingly, **Cu3CP-6-Pt** is more efficient than **Cu3CP-10-Pt**.

3.3 Conclusions

The new synthetic approach to produce highly efficient DNA-cleaving agents herein reported now also offers the prospect to improve the nuclease activity of well-known effective drugs through their synergistic combination within a single molecule. The resulting ditopic (or even multitopic) bio-active molecules thus expand the mechanism of action of its well established antitumor-active components. The fine-tuning of the cleaving ability of such Cu-Pt complexes by further varying the nature and the length of the bridge between the platinum and the Cu(3-Clip-Phen) moieties is reported in chapters 4 and 5. Investigations on the cleavage mechanism with these potential anticancer drugs are reported in chapter 4.

3.4 Experimental section

Synthesis of 3-bromo-1,10-phenanthroline (1) The synthesis of **1** was previously reported,[41] but the purification has been optimized. 45 mL of nitrobenzene were added to 1,10-phenantroline hydrochloride (25 g, 107.5 mmol) into a two necked flask and heated at 140 °C. Then a solution of bromine (8.25 mL, 160 mmol) in 23 mL of nitrobenzene was added drop wise to the flask using a dropping funnel. The total amount of the bromine was added over a period of one hour. The mixture was left for three hours at 140 °C and the mixture was cooled to room temperature. The precipitate was filtered and 100 mL of 25% aqueous NH_4OH were added to the filtrate. The solution was extracted three times with 50 mL of CH_2Cl_2. The organic layer was dried over Na_2SO_4 and the solvent was evaporated under reduced pressure. The raw product was purified by column chromatography (SiO_2, DCM:MeOH, 99:1) to eliminate 1,10-phenanthroline and obtain a mixture of multi-bromo-phenanthroline products. This solid mixture (3-bromo-phenanthroline (43.3 mmol)) was dissolved in 280 mL of DMF and heated to 100 °C to dissolve it. After dissolution, the mixture was cooled to room temperature and 150 mL H_2O were added. The resulting solution was allowed to stand in the refrigerator for two days. The precipitate was filtered and the solvent was evaporated under reduced pressure yielding the pure product. Yield 25%.

Synthesis of 1,3-di(1,10-phenanthrolin-3-yloxy)propan-2-amine (2) The synthesis of **2** was previously reported,[5] but the synthetic procedure has been optimized. Serinol (0.352 g, 3.86 mmol) was dissolved in 64 mL of DMF under argon. Then 2,6-di-*tert*-butyl-4-methylphenol (0.851 g, 3.86 mmol) and NaH (60% dispersion in mineral oil, 1.85 g, 46.4 mmol) were added. The mixture was allowed to react for 20 minutes at RT and at 4 °C for further 20 minutes with an ice bath. **1** (2 g, 7.7 mmol) was added as a solid at once to the mixture and the wall of the flask were rinsed with 32 mL of DMF. The mixture was stirred for 20 minutes at 4 °C and for 30 minutes at room temperature. Then the reaction mixture was

stirred for 40 hours at 50 °C. 100 mL of water were added to quench the excess of NaH and the mixture was extracted with 3 × 100 mL of CH_2Cl_2. The organic layer was dried over Na_2SO_4 and the solvent was evaporated under reduced pressure leading to a dark brownish oil. This oil was purified by column chromatography (SiO_2, DCM:MeOH:NH_4OH, 95:5:0.5) giving the desired compound. Yield 45%.

Synthesis of 6-(2-Amino-ethylamino)-hexan-1-ol (3) and 10-(2-Amino-ethylamino)-decan-1-ol (4) 6-Bromohexan-1-ol or 10-bromohexan-1-ol (3.74 mmol) was added to 2 mL of ethylenediamine (30.00 mmol) at 4 °C over a period of 2 h. The reaction mixture was then stirred for 1 h at RT, and 10 mL of ethyl acetate were added. The resulting solution was further stirred for 15 min. After overnight decantation, the ethyl acetate phase was separated, evaporated under reduced pressure, and stirred under vacuum during 2 h at 50 °C, in order to remove the residual ethylenediamine starting material. Data for **3**: Color less oil (yield = 85%). ^{1}H NMR ($DCCl_3$, 300 MHz) δ 3.59 (t, 2H, *J* = 6.52 Hz), 2.79 (m, 2H), 2.52-2.70 (m, 4H), 1.51 (m, 4H), 1.35 (m, 4H) ppm. Low resolution MS (ESI >0) *m/z* 161.2 [$(M+H)^+$; calcd for $C_8H_{21}N_2O^+$: 161.3]. Data for **4**: Color less oil (yield = 93%). ^{1}H NMR ($DCCl_3$, 300 MHz) δ 3.56 (t, 2H, *J* = 6.61 Hz), 2.76 (t, 2H, *J* = 5.97 Hz), 2.63 (t, 2H, *J* = 6.02 Hz), 2.56 (t, 2H, *J* = 7.15 Hz), 1.48 (m, 4H), 1.25 (m, 12H) ppm.

Synthesis of (2-*tert*-Butoxycarbonylamino-ethyl)-(6-hydroxy-hexyl)-carbamic acid *tert*-butyl ester (5) and (2-*tert*-Butoxycarbonylamino-ethyl)-(10-hydroxy-decyl)-carbamic acid *tert*-butyl ester (6). NaH (0.830 g, 20.8 mmol) was added in portions to a solution of **3** or **4** (4.6 mmol) in 6 mL of THF. The solution was then heated to 50 °C during 1 h under argon. The heterogeneous reaction mixture was cooled down to 4 °C using an ice bath, and di-*tert*-butylcarbonate (Boc_2O) (4.5 g, 20.8 mmol) in 20 mL of THF was added dropwise over a period of 30 min. The ice bath was removed and the mixture was allowed to react overnight at RT. The excess of NaH was neutralized carefully with 50 mL of water, and the resulting solution was extracted with diethyl ether (3 × 50 mL). The pooled organic phases were dried over sodium sulfate, and the solvent was evaporated under reduced pressure. The crude residue was refluxed with 5 g of K_2CO_3 in 50 mL of MeOH during 1 h. The reaction mixture was cooled down to RT and filtered. The filtrate was extracted with heptane (2 × 20 mL). After evaporation of the solvent, the residue was dissolved in 50 mL of DCM, washed with distilled water (3 × 50 mL), dried over sodium sulfate, and the solvent was evaporated under reduced pressure. Data for **5**: Color less oil (yield = 62%).^{1}H NMR ($DCCl_3$, 300 MHz) δ 5.10-4.60 (br, 1H), 3.62 (m, 2H), 3.35-3.10 (m, 6H), 1.60-1.25 (m, 26H) ppm. ^{13}C NMR ($DCCl_3$, 75 MHz) δ 63.45, 47.08, 40.38, 33.37, 29.19, 27.30, 26.21 ppm. Low resolution MS (ESI >0) *m/z* 383.2 [$(M+Na)^+$; calcd for $C_{18}H_{37}N_2NaO_5^+$: 383.5]. Data for **6**: Color less oil (yield = 60%). ^{1}H NMR ($DCCl_3$, 300 MHz) δ 3.63 (t, 2H, *J* = 6.59 Hz), 3.35-3.10 (m, 6H), 1.60-1.15 (m, 34H) ppm. ^{13}C NMR ($DCCl_3$, 75 MHz) δ 63.1, 47.7, 46.4, 39.7, 32.8, 29.5, 29.4, 29.3, 28.4, 26.8, 25.7 ppm. Low resolution MS (ESI >0) *m/z* 417.2 [$(M+H)^+$; calcd for $C_{22}H_{45}N_2O_5^+$: 417.6].

Synthesis of 2-*tert*-Butoxycarbonylamino-ethyl)-(6-oxo-hexyl)-carbamic acid *tert*-butyl ester (7) and (2-*tert*-Butoxycarbonylamino-ethyl)-(6-oxo-decyl)-carbamic acid *tert*-butyl ester (8). **5** or **6** (0.96 mmol) and pyridinium chloridotrioxidochromate (PCC, 0.310 g, 1.44 mmol) were stirred separately during 15 min in 4.5 mL of DCM containing 0.5 g of activated powdered molecular sieves. The solution of alcohol **5** or **6** was added to the solution of PCC using a cannula. The resulting reaction mixture was stirred during 1.5 h. Diethyl ether (10 mL) was then added and the solid materials were separated by filtration over celite. The filtrate was evaporated under reduced pressure to afford **7** or **8** as

color less oils. Data for **7**: Color less oil (yield = 67 %). ^{1}H NMR ($DCCl_3$, 300 MHz) δ 9.76 (s, 1H), 3.35-3.10 (m, 6H), 2.44 (t, 2H, *J* = 6.60 Hz), 1.70-1.20 (m, 24H) ppm. ^{13}C NMR ($DCCl_3$, 75 MHz) δ 202.2, 156.1, 79.7, 47.4, 46.4, 43.5, 39.5, 28.3, 26.2, 21.7 ppm. Low resolution MS (ESI >0) *m/z* 381.2 [$(M+Na)^+$; calcd for $C_{18}H_{34}N_2O_5Na^+$: 381.5]. Data for **8**: Color less oil (yield = 55 %). ^{1}H NMR ($DCCl_3$, 300 MHz) δ 9.76 (s, 1H), 3.35-3.10 (m, 6H), 2.41 (t, 2H, *J* = 7.33 Hz), 1.75-1.15 (m, 32H) ppm. ^{13}C NMR ($DCCl_3$, 75 MHz) δ 202.7, 79.5, 47.6, 46.3, 43.8, 39.6, 29.2, 29.0, 28.3, 26.7, 22.0 ppm. Low resolution MS (ESI >0) *m/z* 437.3 [$(M+Na)^+$; calcd for $C_{22}H_{42}N_2O_5Na^+$: 437.6].

Synthesis of (2-*tert*-Butoxycarbonylamino-ethyl)-{6-[3-Clip-Phen]-hexyl}-carbamic acid *tert*-butyl ester (9) and (2-*tert*-Butoxycarbonylamino-ethyl)-{10-(3-Clip-Phen)-decyl}-carbamic acid *tert*-butyl ester (10). **7** or **8** (0.86 mmol), 3-Clip-Phen (**2**) (0.38 g, 0.86 mmol) and 1 g of molecular sieves were stirred under argon in 20 mL of MeOH under reflux during 3 hours. After cooling down to 4 °C, $NaBH_4$ (0.063 g, 1.72 mmol) was added and the reaction mixture was further stirred for 2 h. 50 mL of DCM were added and the molecular sieves were removed by filtration. The filtrate was transferred in a separating funnel, washed with water (2 × 50 mL), dried over sodium sulfate, and evaporated under reduced pressure. The crude product was purified by column chromatography (SiO_2, DCM:MeOH:NH_4OH, 95:5:0.5). Data for **9**: Light brown powder (yield = 65 %). ^{1}H NMR ($DCCl_3$, 300 MHz) δ 9.13 (dd, 2H, *J* = 4.30, 1.49 Hz), 8.94 (d, 2H, *J* = 2.70 Hz), 8.19 (dd, 2H, *J* = 8.05, 1.49 Hz), 7.76 and 7.70 (AB, 4H, *J* = 8.86 Hz), 7.61 (d, 2H, *J* = 2.70 Hz), 7.56 (dd, 2H, *J* = 8.05, 4.30 Hz), 4.99 (br, 0.5H), 4.78 (br, 0.5H), 4.40 (m, 4H), 3.60 (m, 1H), 3.00-3.40 (m, 7H), 2.86 (t, 2H, *J* = 7.15 Hz), 1.10-1.70 (m, 26H) ppm. ^{13}C NMR ($DCCl_3$, 75 MHz) δ 153.9, 150.2, 146.1, 142.5, 140.5, 135.8, 129.4, 127.2, 126.0, 122.0, 115.1, 67.5, 56.5, 47.8, 46.3, 39.5, 30.3, 28.3, 26.9, 26,6 ppm. Low resolution MS (ESI >0) *m/z* 812.57 [$(M+Na)^+$; calcd for $C_{45}H_{55}N_7NaO_6^+$: 812.95], 828.55 [$(M+K)^+$; calcd for $C_{45}H_{55}N_7KO_6^+$: 829.06], 790.57 [$(M+H)^+$; calcd for $C_{45}H_{56}N_7O_6^+$: 790.97]. Anal. Calcd for $C_{45}H_{55}N_7O_6 \cdot 0.7$ CH2Cl2: C, 64.62; H, 6.69; N, 11.54. Found: C, 44.62; H, 6.93; N, 11.81. Data for **10**: Light brown powder (yield = 77%). ^{1}H NMR ($DCCl_3$, 300 MHz) δ 9.02 (dd, 2H, *J* = 4.34, 1.65 Hz), 8.85 (d, 2H, *J* = 2.83 Hz), 8.06 (dd, 2H, *J* = 8.05, 1.65 Hz), 7.62 and 7.57 (AB, 4H, *J* = 8.88 Hz), 7.49 (d, 2H, *J* = 2.83 Hz), 7.42 (dd, 2H, *J* = 8.05, 4.34 Hz), 5.03 (br, 0.5H), 4.79 (br, 1H), 4.30 (m, 4H), 3.47 (m, 1H), 2.95-3.30 (m, 7H), 2.75 (t, 2H, *J* = 7.06 Hz), 1.00-1.60 (m, 34H) ppm. ^{13}C NMR ($DCCl_3$, 75 MHz) δ 154.7, 151.0, 146.9, 143.3, 141.3, 136.6, 130.2, 128.0, 126.8, 122.8, 115.9, 68.4, 57.2, 48.7, 48.5, 47.1, 40.4, 31.1, 30.2, 30.0, 29.1, 28.0, 27,5 ppm. Low resolution MS (ESI >0) *m/z* 868.4 [$(M+Na)^+$; calcd for $C_{49}H_{63}N_7NaO_6^+$: 869.1], 846.4 [$(M+H)^+$; calcd for $C_{49}H_{64}N_7O_6^+$: 847.1]. Anal. Calcd for $C_{49}H_{63}N_7O_6 \cdot 1.5$ CH_2Cl_2: C, 62.31; H, 6.83; N, 10.07. Found: C, 62.03; H, 7.33; N, 10.44.

Synthesis of [N*1*-{6-[3-Clip-Phen]-hexyl}-ethane-1,2-diamine] (3CP-6-NH_2) and N*1*-{10-[3-Clip-Phen]-decyl}-ethane-1,2-diamine (3CP-10-NH_2). **9** or **10** (0.1 mmol) was dissolved in 2 mL of trifluoroacetic acid (TFA) at 4 °C, and stirred during 1 h. The TFA was then evaporated under reduced pressure and the crude product was purified by column chromatography (SiO_2, DCM:MeOH:NH_4OH, 90:10:1). Data for **3CP-6-NH_2**: Light brown powder (yield = 65 %). NB: the NMR spectra chemical shifts are dependent on the sample concentration. ^{1}H NMR (MeOD-d_3, 300 MHz) δ 9.03 (d, 2H, *J* = 2.83 Hz), 8.91 (d, 2H, *J* = 2.84 Hz), 8.40 (d, 2H, *J* = 6.56 Hz), 7.92 (d, 2H, *J* = 2.83 Hz), 7.89 (d, 2H, *J* = 8.95 Hz), 7.83 (d, 2H, *J* = 8.92 Hz), 7.69 (dd, 2H, *J* = 8.09, 4.48 Hz), 4.78 (m, 4H), 4.31 (m, 1H), 3.44 (t, 2H, *J* = 7.66), 3.35 (m, 4H), 3.04 (t, 2H, *J* = 7.49), 1.90 (m, 2H), 1.71 (m, 2H), 1.48 (br, 4H) ppm. ^{13}C NMR ($DCCl_3$, 75 MHz) δ 153.1, 149.1, 144.6, 141.6, 139.4, 136.8, 129.5, 127.5, 127.2, 126.1,

122.5, 116.0, 64.7, 56.4, 44.5, 35.6, 25.3, 25.1 ppm. Low resolution MS (ESI >0) *m/z* 590.37 [(M+H)$^+$; calcd for $C_{35}H_{40}N_7O_2^+$: 590.74], 295.98 [(M+2H)$^{2+}$; calcd for $C_{35}H_{41}N_7O_2^{2+}$: 295.86]. Data for **3CP-10-NH$_2$**: Light brown powder (yield = 83 %). NB: the NMR spectra chemical shifts are dependent on the sample concentration. ^{1}H NMR (MeOD-d$_3$, 300 MHz) δ 8.98 (dd, 2H, *J* = 4.41, 1.61 Hz), 8.84 (d, 2H, *J* = 2.82 Hz), 8.34 (dd, 2H, *J* = 8.12, 1.62 Hz), 7.90 (d, 2H, *J* = 2.83), 7.85 (d, 2H, *J* = 8.98 Hz), 7.80 (d, 2H, *J* = 8.93 Hz), 7.65 (dd, 2H, *J* = 8.09, 4.45 Hz), 4.60 (d, 4H, *J* = 4.75), 3.87 (br, 1H), 3.10 (m, 6H), 2.84 (m, 2H), 1.70 (m, 2H), 1.54 (m, 2H), 1.41-1.16 (m, 12H) ppm. ^{13}C NMR (DCCl$_3$, 75 MHz) δ 154.7, 151.0, 146.9, 143.3, 141.3, 136.6, 130.2, 128.0, 126.8, 122.8, 115.9, 68.4, 57.2, 48.7, 48.5, 47.1, 40.4, 31.1, 30.2, 30.0, 29.1, 28.0, 27.5 ppm. Low resolution MS (ESI >0) *m/z* 646.3 [(M+H)$^+$; calcd for $C_{39}H_{48}N_7O_2^+$: 646.8], 323.8 [(M+2H)$^{2+}$; calcd for $C_{39}H_{49}N_7O_2^{2+}$: 323.9]. Anal. Calcd for $C_{39}H_{47}N_7O_2 \cdot 2CH_2Cl_2$: C, 60.37; H, 6.30; N, 12.02. Found: C, 60.44; H, 6.16; N, 11.87.

Synthesis of Pt[N*1*-{6-[3-Clip-Phen]-hexyl}-ethane-1,2-diamine]Cl$_2$ (3CP-6-Pt) and Pt[N*1*-{10-[3-Clip-Phen]-decyl}-ethane-1,2-diamine]Cl$_2$ (3CP-10-Pt). A solution of K_2PtCl_4 (0.1 mmol) in 3 mL of H_2O was added dropwise to a solution of **3CP-6-NH$_2$** or **3CP-10-NH$_2$** (0.1 mmol) in 6 mL of MeOH over a period of 2 min. The resulting off-white precipitate was filtered after a reaction time of 5 h. The product was washed consecutively with 3 × 10 mL of H_2O, 3 × 10 mL of MeOH, and 2 × 20 mL of diethyl ether. The coordination compounds were dried overnight at 50 °C under reduced pressure. The integrals of the ^{1}H-NMR peaks around 4.60 ppm may be inaccurate due to the suppression of the water signal by the program used during the scanning of the sample. Also, the signal owing to DMSO, used to dissolve the samples, is partially overlapping the peaks in the 2.70 ppm region. Data for **3CP-6-Pt**: Off-white powder (yield = 71 %). ^{1}H NMR (DMSO-d$_6$ and D$_2$O, 300 MHz) δ 8.82 (br, 2H), 8.64 (br, 2H), 8.42 (br, 2H), 7.78 (br, 2H), 7.64-7.54 (br, 6 H), 4.84 (br, 1H), 4.57-4.53 (br, 2H) 4.15 (br, 1H), 3.07-2.69 (m, 6H), 1.80 (br, 2H), 1.67 (br, 2H), 1.41 (br, 4H) ppm. ^{13}C NMR (DMSO-d$_6$, 75 MHz) δ 153.7, 148.2, 142.4, 139.3, 137.4, 129.9, 127.5, 127.1, 123.0, 116.4, 65.2, 55.3, 46.7, 46.0, 44.2, 35.4, 25.3 ppm. ^{195}Pt NMR (DMSO-d$_6$, 300 MHz) δ –2308 (complex) and –2949 (complex with coordinated DMSO) ppm. MS (MALDI-TOF) *m/z* 898.6, 897.6, 899.6, 900.6, 901.6, 902.6 [(M+DMSO(solvent)–Cl$^-$)$^+$; calcd for $C_{37}H_{45}ClN_7O_3PtS^+$:898.3, 897.3, 899.3, 900.3, 901.3,902.3], 784.4, 785.4, 783.4, 786.4, 787.5, 788.4 [(M –HCl –Cl$^-$)$^+$; calcd for $C_{35}H_{38}N_7O_2Pt^+$:784.3, 785.3, 783.3, 786.3, 787.3, 788.3]. Data for **3CP-10-Pt**: Off-white powder (yield = 76 %). ^{1}H NMR (DMSO-d$_6$ and D$_2$O, 300 MHz) δ 8.78 (br, 2H), 8.68 (br, 2H), 8.23 (br, 2H), 7.67-7.49 (m, 4H), 4.81 (br, 1H), 4.58 (br, 3H), 4.11 (br, 2H), 2.82-2.69 (br, 7H), 1.76 (br, 16H) ppm. ^{13}C NMR (DMSO-d$_6$, 75 MHz) δ 154.5, 150.7, 145.5, 143.3, 138.5, 130.8, 128.5, 127.8, 123.9, 117.4, 66.4, 56.7, 53.2, 48.0, 47.4, 36.6, 29.9, 27.4-26.8 ppm. ^{195}Pt NMR (DMF-d$_7$, 300 MHz) δ -2329 ppm. MS (MALDI-TOF) *m/z* 839.1, 840.1, 838.1, 841.1, 842.1, 843.1 [(M –HCl –Cl$^-$)$^+$; calcd for $C_{39}H_{46}N_7O_2Pt^+$:839.3, 840.3, 838.3, 841.3, 842.3, 843.3]. ICP-AES Pt to K ratio = 1:0.37. Anal. Calcd for $C_{39}H_{47}Cl_2N_7O_2Pt \cdot 0.37\ KCl \cdot 6H_2O$: C, 44.72; H, 5.68; N, 9.36. Found: C, 44.25; H, 5.04; N, 9.19.

Synthesis of CuPt[N*1*-{6-[3-Clip-Phen]-hexyl}-ethane-1,2-diamine]Cl$_4$ (Cu3CP-6-Pt) and CuPt[N*1*-{10-[3-Clip-Phen]-decyl}-ethane-1,2-diamine]Cl$_4$ (Cu3CP-10-Pt). $CuCl_2$ (0.1 mmol) was added as a solid to a suspension of **3CP-6-Pt** or **3CP-10-Pt** (0.05 mmol) in DMF (25 mL). The reaction was stirred overnight at 50 °C. The DMF was partially evaporated under reduced pressure, and the crude was precipitated in 100 mL of diethyl ether. The solid material was filtered and washed with 3 × 20 mL of diethyl ether and dried overnight at 50 °C under reduced pressure. The resolution of the mass measurements was not sufficient enough, because only broadened peaks were observed. Data for

Cu3CP-6-Pt: MS (MALDI-TOF) m/z 954.1 [(M–Cl⁻)⁺; calcd for $C_{35}H_{39}Cl_3N_7O_2PtCu^+$: 954.7], UV-Vis (DMSO/$H_2O$ 10/90) λ_{max}/nm (ε/dm³ mol⁻¹ cm⁻¹): 281 (41500), 318 (14400), 346 (5700), Data for **Cu3CP-10-Pt**: MS (MALDI-TOF) m/z 1055.1 [(M + DMSO –2Cl⁻)⁺; calcd for $C_{41}H_{53}Cl_2N_7O_3SPtCu^+$: 1053.5], 1077.1 [(M + DMSO –2Cl⁻)⁺; calcd for $C_{41}H_{53}Cl_2N_7O_3SNaPtCu^+$: 1076.5], UV-Vis (DMSO/$H_2O$ 10/90) λ_{max}/nm (ε/dm³ mol⁻¹ cm⁻¹): 282 (43600), 319 (17500), 347 (8000)

Cleavage studies. Complexes were prepared as 1 mM solutions in DMSO, and diluted to respectively 400, 600 and 1000 nM with MilliQ water. 5 μL of complex solution were added to 10 μL of supercoiled ΦX174 DNA ((Invitrogen)7 nM, 40 μM base pairs) in 6 mM NaCl, 20 mM sodium phosphate buffer (pH 7.2), and incubated for 20 h at 37 °C. To initiate the cleavage, 5 μL of a 20 mM mercaptopropionic acid solution in water were added, and the resulting reaction mixture was incubated at 37 °C for 1 h. The reaction was quenched at 4 °C, followed by the addition of 4 μL of loading buffer (bromophenol blue) prior to its loading on a 0.8 % agarose gel containing 1 μg mL⁻¹ of ethidium bromide. The gels were run at a constant voltage of 70 V for 90 minutes in TBE buffer containing 1 μg mL⁻¹ of ethidium bromide. The gels were visualized under a UV transilluminator, and the bands were quantified using a BioRad Gel Doc 1000 apparatus interfaced with a computer. A correction factor of 1.47 has been applied to quantify the amount of supercoiled DNA (form I) present in all samples.

Time-course experiments of DNA cleavage: the solutions of the different complexes were prepared as 1 mM solutions in DMSO, which were subsequently diluted to respectively 800 and 1000 nM (only Cu(3-Clip-Phen) with MilliQ water. 50 μL of complex solution were added to 100 μL of supercoiled ΦX174 DNA ((Invitrogen) 7 nM, 40 μM base pair) in 6 mM NaCl, 20 mM sodium phosphate buffer (pH 7.2), and the resulting reaction mixture was incubated for 20 h at 37 °C. To initiate the cleavage, 50 μL of a 20 mM mercaptopropionic acid were added, and a sample was taken out every 10 minutes. 4 μL of loading buffer (bromophenol blue) were added, and the sample was directly frozen in liquid nitrogen. When all samples were collected they were loaded on a 0.8% agarose gel containing 1 μg mL⁻¹ of ethidium bromide.

The DSB formation was calculated from a test developed by Povirk *et al.*[28, 29] which assumes a Poisson distribution of strand cuts, and allows to calculate the average number of DSB per molecule, n_2. n_2 is obtained from the fraction of linear DNA after cleavage, and the total average number of single- plus double-strand breaks ($n_1 + n_2$), from the fraction of remaining supercoiled DNA after reaction. In order to determine n_1 and n_2 both supercoiled and linear DNA should be present in the experiments. The fraction of linear DNA after scission chemistry, form III = $n_2\exp(-n_2)$. The supercoiled fraction remaining after treatment is form I = $\exp[-(n_1 + n_2)]$.[29]

Analysis of platinum adducts by high resolution polyacrylamide gel electrophoresis. (Experiments have been performed at the CNRS in Toulouse) The ODNs I, II and the primer were purchased from Eurogentec, and purified on a 15% polyacrylamide gel. Concentrations of single-stranded ODNs were determined by UV titration at 260 nm.[42] The ODNs were end-labeled with ^{32}P using standard procedures with T_4 polynucleotide kinase (New England BioLabs) and [γ-^{32}P]ATP for the 5'-end, before being purified on a MicroSpin G25 column (Pharmacia).[43]

Analysis of the platinum-DNA adducts: The 36mer ODN I-ODN II duplex target (2 μM, 5'-end labeled on ODN I) was annealed in 1100 μL of Tris-HCl (20 mM, pH 7.2) by heating to 90 °C for 5 minutes, followed by slow cooling to room temperature. Samples were divided in shares of 60 μL before addition of 60 μL of complex solution (6 μM cisplatin or 20 μM of complexes **3CP-6-Pt**, **3CP-10-Pt**, **Cu3CP-6-Pt** and **Cu3CP-10-Pt**). Samples were incubated for 20 hours at 37 °C, and subsequently precipitated with 100 μL of sodium acetate buffer (3M, pH 5.2), and 1300 μL of cold ethanol. The resulting pellets were rinsed twice with 200 μL of cold ethanol, and then lyophilized. The samples dissolved in 5 μL of a bromophenol blue/xylene cylenol/formamide solution were separated by denaturing 20 % polyacrylamide gel electrophoresis.

Primer extension experiments: The 36mer ODN I-ODN II duplex target (2 μM) was annealed in 1100 μL of Tris-HCl (20 mM, pH 7.2) by heating to 90 °C for 5 minutes, followed by slow cooling to room temperature. Samples were divided in shares of 60 μL before the addition of 60 μL of complex solution (6 μM cisplatin or 20 μM complex **3CP-6-Pt** and **3CP-10-Pt**). Samples were incubated for 20 hours at 37 °C, and then precipitated with 100 μL of sodium acetate buffer (3M, pH 5.2), and 1300 μL of cold ethanol. The resulting pellets were rinsed twice with 200 μL of cold ethanol, and then were lyophilized. The samples were dissolved in MilliQ H_2O to a 1.25 μM concentration of ODN I/ODN II. To 2 μL of this solution, was added 1 μL of enzyme 10 × buffer, 2 μL of primer/ODN I solution (1 equivalent of 5'-end labeled primer + 1 equivalent of ODN I) and 2 μL of MilliQ H_2O. The samples were hybridized by heating to 90 °C for 5 minutes, followed by slow cooling to RT. To this solution, 2 μL of a 250 μM dGTP, dCTP, dATP and dTTP solution were added and 1 μL of enzyme (2.5 units TAQ polymerase). The reaction time with the TAQ polymerase was 30 minutes at 37 °C. TAQ polymerase is a thermally stable enzyme; therefore, the samples were directly frozen in liquid nitrogen. 5 μL of a bromophenol blue/xylene cylenol/formamide solution were added to a 5 μL sample, followed by separation by denaturing 20 % polyacrylamide gel electrophoresis. Maxam and Gilbert sequencing scale, where the 3'-phosphate ends of the resulting fragments were removed with polynucleotide kinase, was used to analyze DNA fragments.[44]

Cytotoxicity tests. (Experiments have been performed in the group of R. Kiss in Brussels) The following human tumor cell lines were used to determine the cytotoxic abilities of the compounds prepared:

MCF7	breast cancer
EVSA-T	breast cancer
WIDR	colon cancer
IGROV	ovarian cancer
M19 MEL	melanoma
A498	renal cancer
H226	non-small cell lung cancer
Hs683	glioblastomas
U-373MG	glioblastomas
HCT-15	colorectal cancer
LoVo	colorectal cancer
A549	lung cancer

The experimental procedure reported below has been followed for the cell lines: MCF7, EVSA-T, WIDR, IGROV, M19 MEL, A498 and H226. The test and reference compounds were dissolved to reach a concentration of 250000 ng mL^{-1} in the full medium, by a 20 fold dilution of a stock solution containing 1 mg compound/200 μL. The complexes were dissolved in DMSO. The cytotoxicity of the different compounds was estimated via the microculture sulforhodamine B (SRB) test. The experiment was started on day 0 when 150 μL of trypsinized tumor cells (1500 – 2000 cells/well) were plated in 96-wells flat bottom microtiter plates (falcon 3072, BD). The plates were preincubated for 48 h at 37 °C, with 8.5 % CO_2 to allow the cells to adhere.

On day 2, a three-fold dilution sequence of ten steps was performed in the full medium, starting with the 250000 ng mL^{-1} stock solution. Every dilution was used in quadruplicate by adding 50 μL to a column of four wells. This procedure resulted in the highest concentration of 62500 ng mL^{-1} for column 12. Column 2 was used for the blank. PBS was added to column 1 in order to diminish interfering evaporation.

On day 7, the incubation was terminated by washing the plate twice with PBS. Subsequently, the cells were fixed with 10% trichloroacetic acid in PBS and placed at 4 °C for one hour. After five washing steps with tap water, the cells were stained for at least 15 minutes with 0.4% SRB dissolved in 1% acetic acid. After staining, the cells were washed with 1% acetic acid to remove the free stain. The plates were air-dried and the bound stain was dissolved in 150 μL of 10 mM Tris-base. The absorbance was read at 540 nm using an automated microplate reader (Labsystems Multiskan MS). The data were processed for the construction of concentration-response curves and the determination of the ID_{50} value, using the Deltasoft 3 software.

The experimental procedure described below has been used for the following cell lines: Hs683, U373MG, HCT-15, LoVo, and A549. The cells were cultured at 37 °C in sealed (airtight) Falcon plastic dishes (Nunc, Gibco, Belgium) containing Eagle's minimal essential medium (MEM, Gibco) supplemented with 5 % fetal calf serum (FCS). All the media were supplemented with a mixture of 0.6 mg mL^{-1} glutamine (Gibco), 200 IU mL^{-1} penicillin (Gibco), 200 IU mL^{-1} streptomycin (Gibco), and 0.1 mg mL^{-1} gentamycin (Gibco). The FCS was heat-inactivated for 1 h at 56 °C.

The MTT test is an indirect technique, which allows the rapid measurement (5 days) of the effect of a given product on the global growth of a cell line.[40] This test is based on the measurement of the number of metabolically active living cells able to transform the yellowish MTT product (3-(4,5-dimethylthiazol-2-yl)-2,5 diphenyl tetrazolium bromide) into the blue product, formazan, via mitochondrial reduction performed by living cells.[40] The amount of formazan obtained at the end of the experiment is measured with a spectrophotometer, and is therefore directly proportional to the number of living cells at that moment. The measurement of the OD (Optical density) provides a quantitative measurement of the effect of the product investigated as compared to control (untreated cells), and enables it to be compared to other reference products.[40]

The cells are put to grow in flat-bottomed 96-well micro-wells with 100 μL of cell suspension per well and between 1,000 and 5,000 cells/well depending on cell type. Each cell line is seeded in its own cell culture medium. After a 24-hour period of incubation at 37 °C, the culture medium is replaced by 100 μL

of fresh medium in which the substance to be tested has been dissolved at the different concentrations required. In our experiments, we tested the 6 compounds (**3CP-6-Pt**, **3CP-10-Pt**, **Cu3CP-6-Pt**, **Cu3CP-10-Pt**, Cu-3-Clip-Phen and cisplatin) at 10^{-5} M to 10^{-9} M by ½ log step. Each experimental condition is carried out in six different wells. After 72 hours of incubation at 37 °C with the drug (experimental conditions) or without the drug (control), the medium is replaced by 100 μL MTT at the concentration of 1 mg mL^{-1} dissolved in RPMI. The micro-wells are then incubated for 3 h at 37 °C and centrifuged at 400 G for 10 minutes. The MTT is removed and the formazan crystals formed are dissolved in 100 μL of DMSO. The micro-wells are then shaken for 5 minutes and read on a spectrophotometer at 2 wavelengths (570 nm: the maximum formazan absorbance wavelength; 630 nm: the background noise wavelength).[40]

The IC_{50} value of the 3-Clip-Phen ligand is for: Hs683; 8.4 μM, U373MG; 1 μM, HCT-15 > 10 μM, LoVo; 8.6 μM, A549; 5 μM and MCF-7; 4.5 μM.

3.5 References

[1] B. A. Chabner, T. G. Roberts, *Nat. Rev. Cancer* **2005**, *5*, 65.

[2] L. H. Hurley, *Nat. Rev. Cancer* **2002**, *2*, 188.

[3] J. Reedijk, *Proc. Natl. Acad. Sci. U. S. A.* **2003**, *100*, 3611.

[4] J. Y. Chen, J. Stubbe, *Nat. Rev. Cancer* **2005**, *5*, 102.

[5] M. Pitié, B. Sudres, B. Meunier, *Chem. Commun.* **1998**, 2597.

[6] M. Pitié, C. J. Burrows, B. Meunier, *Nucleic Acids Res.* **2000**, *28*, 4856.

[7] M. A. Fuertes, C. Alonso, J. M. Perez, *Chem. Rev.* **2003**, *103*, 645.

[8] M. Kartalou, J. M. Essigmann, *Mutat. Res.-Fundam. Mol. Mech. Mutagen.* **2001**, *478*, 23.

[9] M. Kartalou, J. M. Essigmann, *Mutat. Res.-Fundam. Mol. Mech. Mutagen.* **2001**, *478*, 1.

[10] H. G. Kopp, M. Kuczyk, J. Classen, A. Stenzl, L. Kanz, F. Mayer, M. Bamberg, J. T. Hartmann, *Drugs* **2006**, *66*, 641.

[11] S. van Zutphen, J. Reedijk, *Coord. Chem. Rev.* **2005**, *249*, 2845.

[12] H. Baruah, C. L. Rector, S. M. Monnier, U. Bierbach, *Biochem. Pharmacol.* **2002**, *64*, 191.

[13] B. E. Bowler, K. J. Ahmed, W. I. Sundquist, L. S. Hollis, E. E. Whang, S. J. Lippard, *J. Am. Chem. Soc.* **1989**, *111*, 1299.

[14] C. Cullinane, G. Wickham, W. D. McFadyen, W. A. Denny, B. D. Palmer, D. R. Phillips, *Nucleic Acids Res.* **1993**, *21*, 393.

[15] B. D. Palmer, H. H. Lee, P. Johnson, B. C. Baguley, G. Wickham, L. P. G. Wakelin, W. D. McFadyen, W. A. Denny, *J. Med. Chem.* **1990**, *33*, 3008.

[16] L. C. Perrin, P. D. Prenzler, C. Cullinane, D. R. Phillips, W. A. Denny, W. D. McFadyen, *J. Inorg. Biochem.* **2000**, *81*, 111.

[17] J. Whittaker, W. D. McFadyen, G. Wickham, L. P. G. Wakelin, V. Murray, *Nucleic Acids Res.* **1998**, *26*, 3933.

[18] B. E. Bowler, L. S. Hollis, S. J. Lippard, *J. Am. Chem. Soc.* **1984**, *106*, 6102.

[19] R. J. Holmes, M. J. McKeage, V. Murray, W. A. Denny, W. D. McFadyen, *J. Inorg. Biochem.* **2001**, *85*, 209.

[20] E. T. Martins, H. Baruah, J. Kramarczyk, G. Saluta, C. S. Day, G. L. Kucera, U. Bierbach, *J. Med. Chem.* **2001**, *44*, 4492.

[21] P. M. Takahara, A. C. Rosenzweig, C. A. Frederick, S. J. Lippard, *Nature* **1995**, *377*, 649.

[22] M. Pitié, C. Boldron, H. Gornitzka, C. Hemmert, B. Donnadieu, B. Meunier, *Eur. J. Inorg. Chem.* **2003**, 528.

[23] C. A. Detmer, F. V. Pamatong, J. R. Bocarsly, *Inorg. Chem.* **1997**, *36*, 3676.

[24] F. V. Pamatong, C. A. Detmer, J. R. Bocarsly, *J. Am. Chem. Soc.* **1996**, *118*, 5339.

[25] J. F. Hartwig, P. M. Pil, S. J. Lippard, *J. Am. Chem. Soc.* **1992**, *114*, 8292.

[26] H. H. Lee, B. D. Palmer, B. C. Baguley, M. Chin, W. D. McFadyen, G. Wickham, D. Thorsbournepalmer, L. P. G. Wakelin, W. A. Denny, *J. Med. Chem.* **1992**, *35*, 2983.

[27] M. S. Robillard, S. van Alphen, N. J. Meeuwenoord, B. A. J. Jansen, G. A. van der Marel, J. H. van Boom, J. Reedijk, *New J. Chem.* **2005**, *29*, 220.

[28] L. F. Povirk, C. W. Houlgrave, *Biochemistry* **1988**, *27*, 3850.

[29] L. F. Povirk, W. Wubker, W. Kohnlein, F. Hutchinson, *Nucleic Acids Res.* **1977**, *4*, 3573.

[30] M. E. Budiman, R. W. Alexander, U. Bierbach, *Biochemistry* **2004**, *43*, 8560.

[31] M. D. Temple, W. D. McFadyen, R. J. Holmes, W. A. Denny, V. Murray, *Biochemistry* **2000**, *39*, 5593.

[32] E. Bassett, A. Vaisman, J. M. Havener, C. Masutani, F. Hanaoka, S. G. Chaney, *Biochemistry* **2003**, *42*, 14197.

[33] A. Vaisman, S. G. Chaney, *J. Biol. Chem.* **2000**, *275*, 13017.

[34] J. M. Woynarowski, W. G. Chapman, C. Napier, M. C. S. Herzig, P. Juniewicz, *Mol. Pharmacol.* **1998**, *54*, 770.

[35] Y. Zou, B. van Houten, N. Farrell, *Biochemistry* **1994**, *33*, 5404.

[36] J. Kasparkova, O. Novakova, N. Farrell, V. Brabec, *Biochemistry* **2003**, *42*, 792.

[37] V. Murray, H. Motyka, P. R. England, G. Wickham, H. H. Lee, W. A. Denny, W. D. McFadyen, *Biochemistry* **1992**, *31*, 11812.

[38] V. Murray, H. Motyka, P. R. England, G. Wickham, H. H. Lee, W. A. Denny, W. D. McFadyen, *J. Biol. Chem.* **1992**, *267*, 18805.

[39] M. D. Temple, P. Recabarren, W. D. McFadyen, R. J. Holmes, W. A. Denny, V. Murray, *Biochim. Biophys. Acta-Gene Struct. Expression* **2002**, *1574*, 223.

[40] L. Ingrassia, P. Nshimyumukiza, J. Dewelle, F. Lefranc, L. Wlodarczak, S. Thomas, G. Dielie, C. Chiron, C. Zedde, P. Tisnes, R. van Soest, J. C. Braekman, F. Darro, R. Kiss, *J. Med. Chem.* **2006**, *49*, 1800.

[41] D. Tzalis, Y. Tor, S. Failla, J. S. Siegel, *Tetrahedron Lett.* **1995**, *36*, 3489.

[42] G. Fasman, *Handbook of biochemistry and molecular biology: nucleic acids, Vol. 3rd edn.*, Boca Raton, p175, **1975**.

[43] J. Sambrook, E. F. Fritsch, T. Maniatis, *Molecular Cloning: A Laboratory Manuel, Vol. 2nd Edn.*, Cold Spring Harbor Laboratory Press, Cold Spring Harbor, NY, **1989**.

[44] A. M. Maxam, W. Gilbert, *Proc. Natl. Acad. Sci. U. S. A.* **1977**, *74*, 560.

Chapter 4

DNA Cleavage and binding selectivity of a heterodinuclear Pt-Cu(3-Clip-Phen) complex.*

The synthesis and nuclease activity of a new bifunctional heterodinuclear platinum-copper complex are reported. The design of this ditopic coordination compound is based on the specific mode of action of each component, namely cisplatin and Cu(3-Clip-Phen). Cisplatin is not only able to direct the Cu(3-Clip-Phen) part to the GG or AG site, but also acts as a kinetically inert DNA anchor. The nuclease activity of this complex has been investigated on supercoiled DNA. The dinuclear compound is not only more active than Cu(3-Clip-Phen), but is also capable to induce direct double-strand breaks. The sequence selectivity of the mononuclear platinum complex has been investigated by primer extension experiments, which reveal that its interaction with DNA occurs at the same sites as cisplatin. The Taq polymerase recognizes the resulting DNA damage as different from unmodified cisplatin. The sequence selective cleavage has been investigated by high-resolution gel electrophoresis on a 36 bp DNA fragment. Sequence selective cleavages are observed in the close proximity of the platinum sites for the strand exhibiting the preferential platinum binding sites. The platinum moiety also coordinates to the other DNA strand, most likely leading only to mono guanine or adenine adducts.

* This chapter is based on Paul de Hoog, Marguerite Pitié, Giulio Amadei, Patrick Gamez, Bernard Meunier, Robert Kiss, and Jan Reedijk, *submitted*

4.1 Introduction

DNA is a target for numerous anti-tumor drugs.[1, 2] Reversible or irreversible modifications of the nucleic acids can lead to disruption of the transcription and/or replication, initiating ultimately the death of cancer cells. Cisplatin[3] and the iron, copper or cobalt complex of bleomycin are among these efficient anticancer drugs.[4] The mechanism of action is different for both drug substances; cisplatin primarily induces distortions upon binding to DNA, whereas bleomycin is able to generate DNA strand scissions.

Since the discovery of bleomycin,[5] numerous metal complexes have been synthesized that are able to produce DNA cleavage. Typical examples are [Fe^{II}(edta)] complexes, manganese(III)-porphyrin and Cu, Co, Ru and Rh complexes with phenanthroline.[6-9] For instance, [$Cu^{I}(phen)_2$] (Figure 1.16, chapter 1) in the presence of dihydrogen peroxide efficiently cleaves double-stranded DNA through the oxidative attack on deoxyribose units from the minor groove.[10, 11] The consequent DNA-cleavage products include 5'- and 3'-monophosphate ester termini, free bases, 5-methylene-furanone, and a small amount of 3'-phosphoglycolate.[12-14] Dihydrogen peroxide can be generated by [$Cu^{II}(Phen)_2$] in close proximity to the DNA strands, in the presence of a reductant and molecular oxygen. The nuclease activity of $Cu(phen)_2$ has been enhanced with the synthesis of 3-Clip-Phen based on the covalent linkage of two phenanthroline units through either their 3-position, leading to an increase of 60 times compared to the nuclease activity of $Cu(phen)_2$ itself.[15] However, similarly to $Cu(phen)_2$, the copper complexes of 3-Clip-Phen have no sequence selectivity, and cleave the double stranded DNA in a single-stranded fashion. The amine group of 3-Clip-Phen have been functionalized with different groups, such as a distamycin analog or various DNA intercalators.[16, 17] Thus, the resulting complexes show enhanced cleaving activities, and the complexes with the distamycin analog exhibit excellent targeting properties toward A·T boxes.[18]

In chapter 3, it has been shown that Cu(3-Clip-Phen) attached to a cisplatin motif is able to perform direct double-strand cuts, thanks to the DNA-anchoring platinum moiety.[19] Platinum complexes have received a considerable attention since the discovery of the anti-proliferate activity of cisplatin in 1969.[20] It is generally accepted that the distortion of DNA generated upon binding of cisplatin is largely responsible for its antitumor properties.[3] Subsequent drug activation via intracellular aquation reactions results in a variety of stable bifunctional DNA-platinum(II) adducts. 1,2-Intrastrand crosslinks between two adjacent guanine bases d(GG) or between an adenine and a guanine residues d(AG) are primarily formed. The platinum centre of complexes with a *cis*-motif preferentially coordinates to the N7 position of both adenine and guanine in the major groove of DNA.[21-24]

In the present chapter, the preparation of a bifunctional complex (**Cu3CP-0-Pt**) containing both a *cis*-bis(amine)Pt(II) moiety and a nuclease active Cu(3-Clip-Phen) group is reported (Figure 4.1). The bridge connecting the platinum and copper moieties is very short and therefore rigid, in contrast to the compounds reported in chapter 3, where the complexes have flexible linkers in order to have a major-minor groove interaction.[19] The platinum component plays two roles: (i) it acts as a DNA anchor, thus allowing the Cu(3-Clip-Phen) moiety to perform cleavages in the close proximity of the Pt-DNA adducts, and (ii) it induces a sequence selective binding of the heterodinuclear complex. Accordingly, the achievement of double strand breaks is potentially increased, because the single-strand cuts are in the close proximity of the platinum adduct and sequence selective cleavage may be expected.

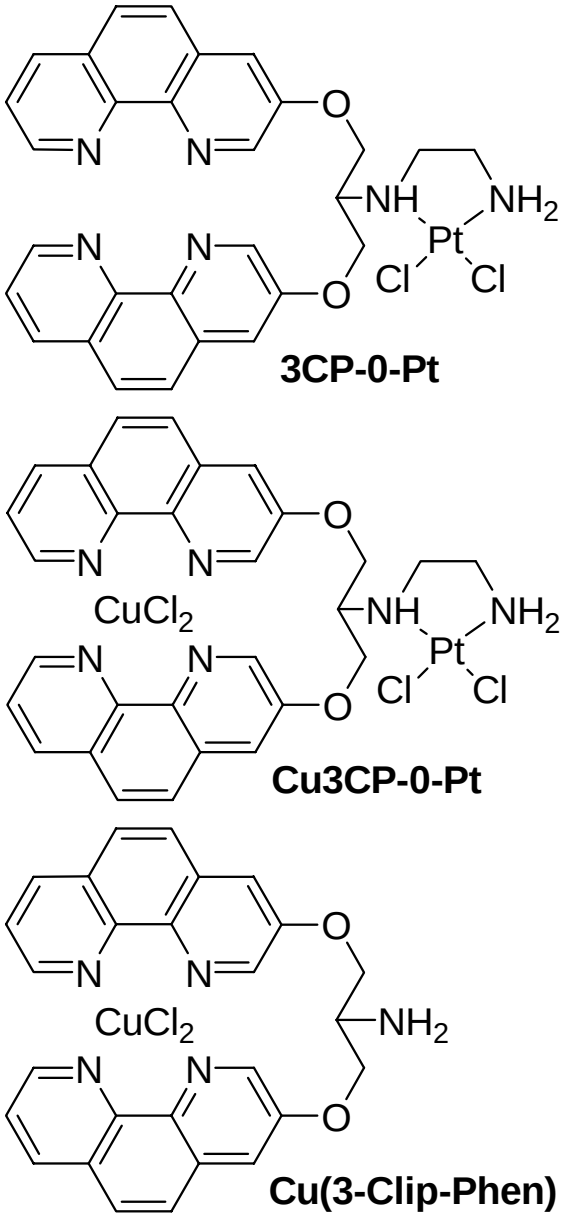

Figure 4.1 Schematic representations of **3CP-0-Pt**, **Cu3CP-0-Pt** and Cu(3-Clip-Phen).

In the present study, the platinum and the 3-Clip-Phen adjacent parts are separated by a relatively short linker preventing that both bind in different grooves. Consequently, either the platinum species or the 3-Clip-Phen moiety cannot interact with its preferential site (the major and the minor groove, respectively). The binding property of the platinum moiety and the cleavage selectivity and activity of this novel heterodinuclear complex **Cu3CP-0-Pt** have been investigated by agarose gel electrophoresis and high-resolution analysis with a 36 bp DNA fragment (Figure 4.2). The results obtained are compared to those achieved with cisplatin and Cu(3-Clip-Phen) complex.

```
                 ▼▼           ▼▼
5'-AACTTAATAGTATACATTGGACACAACAACAACAAC-3'  ODN I
3'-TTGAATTATCATATGTAACCTGTGTTGTTGTTGTTG-5'  ODN II
      ▲▲
3'-TTGTTGTTGTTG-5'                          PRIMER
```

Figure 4.2 Nucleobase sequences of ODN I, ODN II and the primer used for the binding experiments. The known preferential binding sites of cisplatin are indicated by arrows.

4.2 Results and discussion

4.2.1 Design and synthesis of a heterodinuclear platinum-copper complex

A ditopic ligand, i.e. **3CP-0-NH$_2$**, has been designed to favor the simultaneous coordination of a platinum and a copper entities. Hence, the resulting bifunctional complex would combine the ability to form a kinetically inert coordination bond with DNA, thanks to its *cis*-Pt moiety, with the cleavage properties of Cu(3-Clip-Phen). Two coordination compounds, namely the platinum complex **3CP-0-Pt**, and the heterodinuclear platinum/copper complex **Cu3CP-0-Pt** (Figure 4.1) have been prepared with the ligand **3CP-0-NH$_2$**. The binding ability of the platinum unit and the cleavage selectivity of the Cu(3-Clip-Phen) moiety have been investigated. The results have been compared with the known Cu(3-Clip-Phen). The short separation between the Pt and the Cu centers in **Cu3CP-0-Pt** most likely affects the preference for Pt to bind in the major groove, and in the minor groove for Cu. Accordingly, the coordination of the platinum moiety in the major groove will force the Cu(3-Clip-Phen) component to bind in the major groove, and *vice versa*.

The general synthetic pathway to prepare **3CP-0-Pt** and **Cu3CP-0-Pt** is depicted in Scheme 4.1. The selective and complete platination of the ethylenediamine unit using one equivalent of K_2PtCl_4 is monitored by ^{195}Pt NMR and ^{1}H NMR. The *in situ* reaction of the resulting platinum derivative **3CP-0-Pt** with one equivalent of $CuCl_2$ produces the heterobimetallic complex **Cu3CP-0-Pt**.

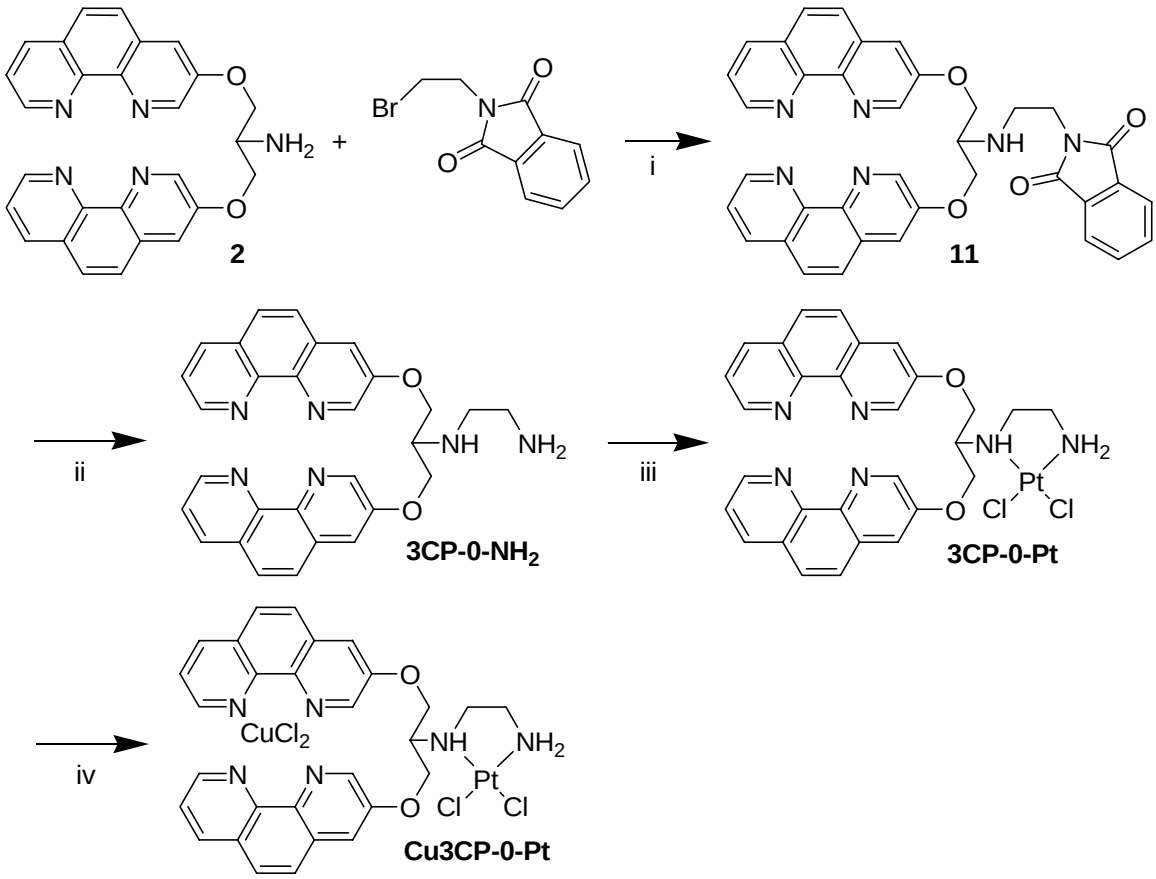

Scheme 4.1 Preparation of **3CP-0-Pt** and **Cu3CP-0-Pt**. Reagents and conditions: (i) DMF, diisopropylethylamine (DIPEA), 100 °C, 2 days; (ii) ethanol, $H_2N{-}NH_2$, reflux, overnight; (iii) K_2PtCl_4, methanol/water, room temperature, 6 h; (iv) $CuCl_2$, DMF, 50 °C, overnight.

4.2.2 Cleavage of supercoiled DNA

The relaxation of supercoiled circular ΦX174 DNA (form I) into its relaxed (form II) and linear (form III) conformations has been monitored to compare the aerobic cleavage abilities of **Cu3CP-0-Pt** and Cu(3-Clip-Phen), in the presence of a reducing agent (Figure 4.3). First, the complexes are incubated for 20 h, to allow the formation of platinum-DNA adducts. The nuclease activity is subsequently initiated by the addition of 5 mM MPA. Complex **Cu3CP-0-Pt** exhibits a markedly higher nuclease activity than Cu(3-Clip-Phen). Indeed, at complex concentrations of 100 nM, most supercoiled DNA has reacted to circular and linear DNA in the case of **Cu3CP-0-Pt**, while Cu(3-Clip-Phen) only generates a small amount of form II (Figure 4.3, lanes 4 and 8). Moreover, almost all the supercoiled DNA has reacted to form smaller DNA fragments (migrating as a smear) at a complex concentration of 250 nM for **Cu3CP-0-Pt** (Figure 4.3, lane 5), whereas no smear is observed for Cu(3-Clip-Phen) (Figure 4.3, lane 9). Interestingly, at a concentration of 100 nM for **Cu3CP-0-Pt**, form III is already detected before the total disappearance of form I (Figure 4.3, lane 4).[19] This result indicates that the heterodinuclear platinum/copper complex is able to perform direct double-strand cuts, since form I is still

detected in the reaction. Such double-stranded breaks are highly cytotoxic, since the cells have difficulties to repair such damage.[25, 26] Cu(3-Clip-Phen) is only able to perform repetitive single-strand cuts.[15]

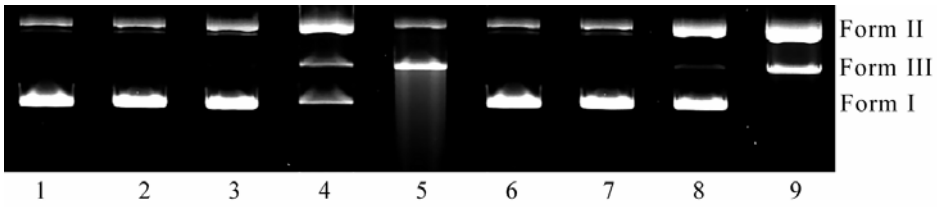

Figure 4.3 Comparative experiments of the oxidative cleavage of ΦX174 plasmid DNA performed by **Cu3CP-0-Pt** and Cu(3-Clip-Phen), in the presence of 5 mM MPA. Lane 1: control DNA. Lane 2: 250 nM solution of **Cu3CP-0-Pt** without MPA. Lane 3: 50 nM **Cu3CP-0-Pt**. Lane 4: 100 nM **Cu3CP-0-Pt**. Lane 5: 250 nM **Cu3CP-0-Pt**. Lane 6: 250 nM Cu(3-Clip-Phen) without MPA. Lane 7: 50 nM Cu(3-Clip-Phen). Lane 8: 100 nM Cu(3-Clip-Phen). Lane 9: 250 nM Cu(3-Clip-Phen).

Time-course studies of DNA cleavage by **Cu3CP-0-Pt** and Cu(3-Clip-Phen) have been carried out to further investigate the direct double-strand cleavage event (Figure 4.4). Thus, Cu(3-Clip-Phen) at a concentration of 250 nM generates a maximum of 80% of circular DNA (form II) after a reaction time of about 1 h, see chapter 3.[19] Around 20% of linear DNA (form III) is produced via the action of Cu(3-Clip-Phen) after 70 min. Remarkably, the formation of form III is only observed after a reaction time of 30 min when already 60% of form II has been produced. For a 150 nM solution of **Cu3CP-0-Pt**, linear DNA (form III) is generated from the initial stages of the cleavage reaction, with supercoiled DNA (form I) still present (Figure 4.4). Also, only a maximum of 60% of form II is generated. These features reflect the ability of **Cu3CP-0-Pt** to perform direct double-strand breaks, most likely as a result of the binding of the platinum moiety to DNA, allowing the catalytic copper part to achieve more than one oxidative cleavage in the close proximity of the Pt coordination site.

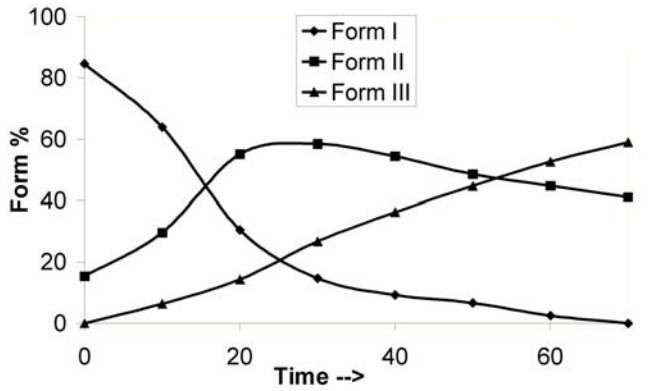

Figure 4.4 Time-course experiments of DNA cleavage (20 μM in base pairs) over a period of 70 min, in the presence of 5 mM MPA and air. Before addition of the reductant, 150 nM **Cu3CP-0-Pt** was incubated for 24 h with the DNA solution.

4.2.3 Analysis of the platinum adducts on ODN I of the ODN I/ODN II duplex target

High-resolution analyses with a 36 bp DNA duplex (ODNI/ODN II) have been performed to investigate the coordination of the platinum component of the bifunctional complexes to DNA, (Figure 4.5a). The sequence of this duplex was chosen to include GG and AG sites (which are the two major binding sites of *cis*-Pt(II) complexes) on one strand (ODN I). The results obtained after incubation of the complexes with the duplex labeled on the 5'-end of ODN I for 24 h are analyzed by PAGE under denaturing conditions and are shown in Figure 5a. Denaturing conditions allowed the analysis of the platinum-DNA adducts on the ODN I of the duplex.

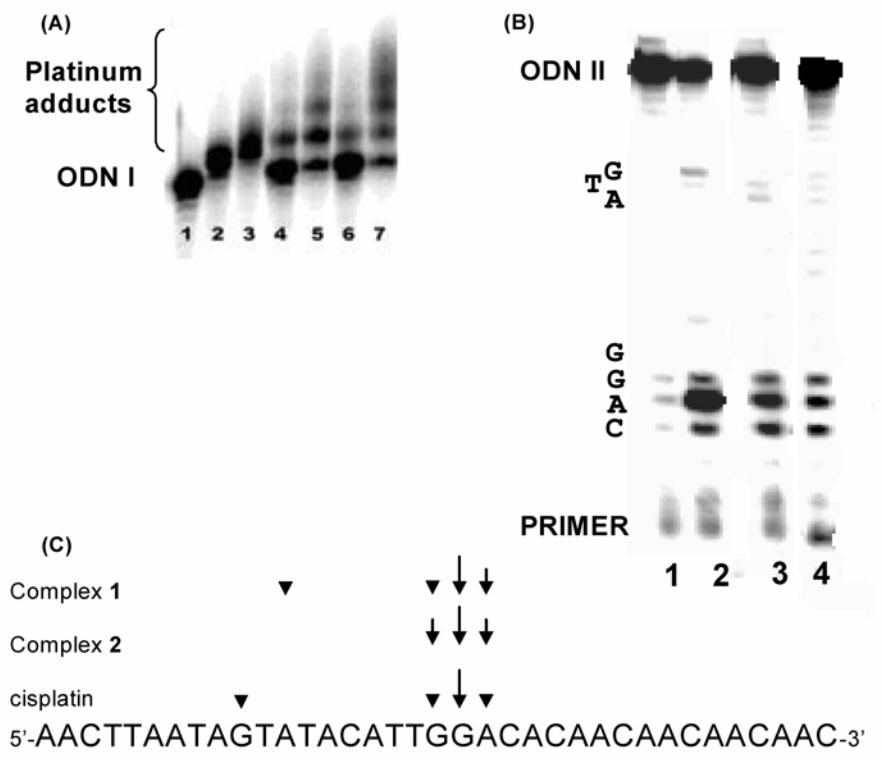

Figure 4.5 (A) PAGE analysis of the platinum-ODN I adducts of ODN I/ODN II duplex target (1 μM). ODN I was 5'-end-labelled with ^{32}P-phosphate. The complexes were incubated with the DNA for 24 h before analyses. Lane 1: ODN I. Lane 2: 3 μM cisplatin. Lane 3: 10 μM cisplatin. Lane 4: 3 μM **3CP-0-Pt**. Lane 5: 10 μM **3CP-0-Pt**. Lane 6: 3 μM **Cu3CP-0-Pt**. Lane 7: 10 μM **Cu3CP-0-Pt**. (B) Phosphorimager data of a DNA sequencing gel comparing the sequence specificity of cisplatin, **3CP-0-Pt** and **Cu3CP-0-Pt**. All the samples were extended using Taq polymerase, starting from the 5'-end-labelled primer. Lane 1: blank experiment; Lane 2: 3 μM of cisplatin; Lane 3: 10 μM of **3CP-0-Pt**. Lane 4: 10 μM of **2**. It is noteworthy that the GTA and GGAC sites give the sequence of the opposite strand that induced the stop of the primer extension. (C) Nucleobase sequence of ODN I, and indication of the damage sites induced by cisplatin, **3CP-0-Pt** and **Cu3CP-0-Pt**. Large and small arrows represent, respectively, major and minor stop sites.

Molecules able to irreversibly bind to DNA will retard the rate of migration of the modified ODN, compared to the free ODN. Therefore, ODN-Pt adducts appear as retarded bands on gels. The incubation with three equivalents of cisplatin clearly reveals an impeded mobility of the ensuing cisplatin-ODN I adduct (Figure 4.5a, lane 2). Only traces of free ODN I are detected, 89% of the ODN I has been modified. The incubation of the DNA duplex with 10 equivalents of cisplatin results in a total conversion of the ODN I (Figure 4.5a, lane 3). Complex **3CP-0-Pt** shows the formation of platinum-ODN I adducts (Figure 4.5a, lanes 4 and 5). Two distinct bands are clearly observed when 10 equivalents of **3CP-0-Pt** are incubated with the DNA target, indicating the formation of platinum-ODN I adducts. The quantification of free ODN I reveals that as much as 84% of this DNA fragment has reacted. The use of **Cu3CP-0-Pt** leads to comparable results, with the conversion of 88% of the initial ODN I (Figure 4.5a, lane 7). However, the reaction between ODN I and **Cu3CP-0-Pt** produces a smear (i.e. a range of products) on the gel.

*4.2.4 Sequence selective binding of **3CP-0-Pt** and **Cu3CP-0-Pt** compared to cisplatin*

Primer extension experiments have been performed to investigate the sequence selective binding of the platinum units to the ODN I fragment of the ODN I/ODN II DNA duplex (Figures 4.5b and 4.5c). The platinum complexes that did not react with DNA were removed prior to the start of the primer extension experiments. Nevertheless, it is possible to have more than one platinum moiety coordinating the ODN strand, since the concentration of cisplatin, **3CP-0-Pt** and **Cu3CP-0-Pt** were respectively 3 and 10 times higher compared to the ODN I/ODN II DNA duplex. Taq polymerase has proven to be a valuable tool for the determination of the sequence selectivity of various platinum complexes.[23, 27-36] Cisplatin inhibits the enzymatic polymerization at the anticipated GG and AG sites (Figure 4.5b and 4.5c), but the majority of cisplatin is detected at the GG site. It should be noted, that once the ODN I strand contains two Pt-adducts on both the GG and AG sites, the enzyme stops only at the GG site. Therefore, it is possible that the amount of modified AG sites is underestimated. Nevertheless, not all of the ODN I has been modified by the complexes (see Figure 4.5a). It is therefore reasonable to say that the majority of the ODN I contains only one Pt-adduct and that the AG-site is indeed the minor site of interaction. The stop sites observed for **3CP-0-Pt** are also located for a major part at the GG and, for a minor part, at AG base pairs. Complex **Cu3CP-0-Pt** shows only stops at the GG binding site. These results indicate that the platinum moiety interacts with its preferential binding site. The difference between cisplatin and **3CP-0-Pt** and **Cu3CP-0-Pt** is the precise point at which the peak intensity occurs at the damaged site. The stops of the Taq polymerase are mainly located at the A base before the GG site for cisplatin, **3CP-0-Pt** and **Cu3CP-0-Pt**. However, the damage induced at the GG site is more equally distributed among the GAC site in the cases of **3CP-0-Pt** and **Cu3CP-0-Pt** (Figures 4.5b and 4.5c; the size of the arrows are an

indication of the damage intensity). The binding of **3CP-0-Pt** and **Cu3CP-0-Pt** apparently produces bulky adducts, thus allowing a partial stop at the second nucleotide before the classical position, at the GG adduct, since an increase of the reaction time with the enzyme (from 30 to 120 min, Figure 4.6; **3CP-0-Pt**) induces a bypass of the stop at the C base (associated to a decrease of the peak intensity when compared to G). The difference between cisplatin and **3CP-0-Pt** is more pronounced at the AG site. Although it is the minor binding site, the damage induced by cisplatin is almost exclusively taking place at the G base, at the 5'-end of ODN I. The Taq polymerase stops for **3CP-0-Pt** are mainly observed at the A base.

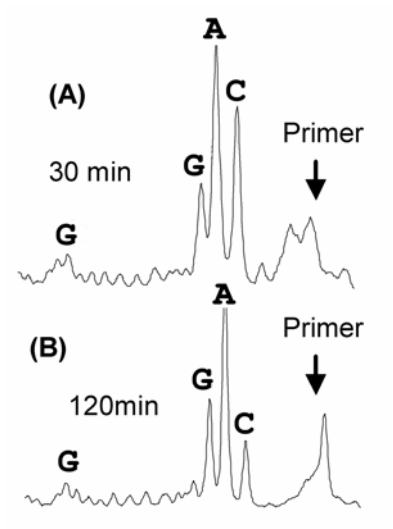

Figure 4.6 Bypass of the stop at the adenine of the AGG site of ODN I when the incubation time with Taq polymerase was increased from 30 min (A) to 120 min (B). Primer extensions were performed as on Figure 4.5 from ODN I-platinum adducts induced by **3CP-0Pt**.

4.2.5 Cleavage of the ODN I strand of the ODN I/ODN II duplex

The cleavage of the ODN I-ODN II duplex with **3CP-0-Pt**, **Cu3CP-0-Pt** and Cu(3-Clip-Phen) has been investigated by polyacrylamide gel electrophoresis, the target being labeled on the 5'-end of ODN I (Figure 4.7). These preliminary results are sufficiently important, because detailed studies of such bifunctional complexes are to the best of our knowledge reported only once.[37] **3CP-0-Pt** and **Cu3CP-0-Pt** are pre-incubated for 20 h to allow the coordination of the platinum moiety to the DNA target. For **3CP-0-Pt**, the pre-incubation is subsequently followed by the coordination of 1 equivalent of copper, since the copper-free complex does not show any nuclease activity. The non-coordinated complexes are removed by precipitation before the cleavage is initiated by the addition of ascorbic acid (0.2 mM) under aerobic conditions. Additional treatments (HEPES pH 8.0 and piperidine) have been carried out.

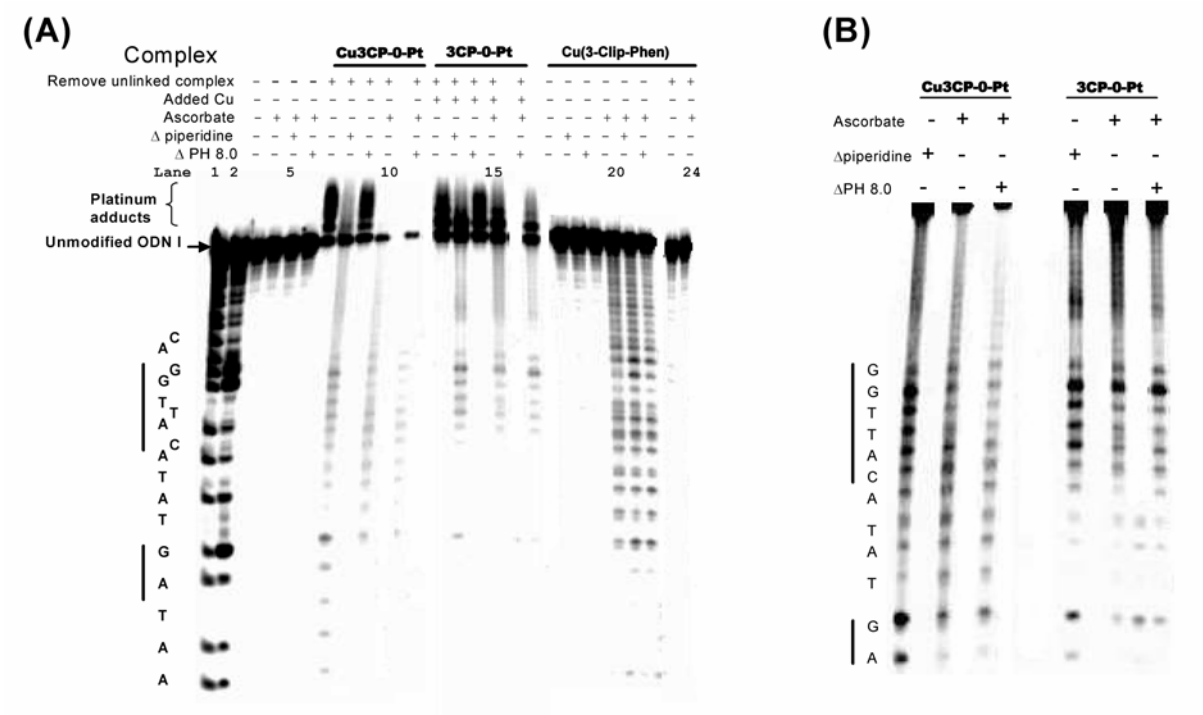

Figure 4.7 (A) PAGE analysis of cleavage of ODN I of the ODN I-ODN II duplex (1 μM) by compounds **3CP-0-Pt**, **Cu3CP-0-Pt** and Cu(3-Clip-Phen) (10 μM when unspecified). The cleavage reactions were initiated with ascorbate (200 μM) in aerobic conditions or by heating 30 min at 90 °C in aqueous piperidine 0.2 M. The Maxam-Gilbert sequencing reactions A + G (lane 1) and G (lane 2) were performed to determine the cleavage sites. On the top of the gel are indicated the conditions used during the experiments (details are given in the experimental part). Lanes 3-6: controls without complexes. Lanes 17-22: experiments were performed in the presence of 1 μM of Cu(3-Clip-Phen). (B) High contrast picture of the lanes 8, 10, 11, 13, 15 and 16 of figure A allowing observing more easily the cleavage pattern. ΔpH 8 was a heating step of 30 min at 90 °C in HEPES·NaOH buffer (0.1 M, pH 8.0). Unlinked complexes were removed by a precipitation step with ethanol before the induction of cleavage.

The non-covalent interaction of Cu(3-Clip-Phen) with DNA permits its abstraction from the ODNs by a simple precipitation step. A ten-fold excess of Cu(3-Clip-Phen) (compared to the ODNs) does not generate cleavage products after the precipitation step (Figure 4.7, lane 24), while 1 equivalent of Cu(3-Clip-Phen) without precipitation exhibits significant cleavage (Figure 4.7, lane 20). The platinum-containing complexes **3CP-0-Pt** and **Cu3CP-0-Pt** form kinetically inert bonds with DNA, and therefore cannot be removed from the ODN during the precipitation step. In contrast, the unreacted complexes are eliminated.

As expected, the cleavage pattern of Cu(3-Clip-Phen) is non-specific,[18] as about 20% of the target is oxidized at all nucleotides (Figure 4.7, lane 20). The cleavage achieved by **Cu3CP-0-Pt** in the presence of ascorbic acid, results in the full and partial disappearance of respectively, the platinum-ODN I adducts and the ODN I band (Figure 4.7, lane 10). The total cleavage amounts to nearly 80%, and its pattern is different compared to the features resulting from the action of Cu(3-Clip-Phen), but no clear sequence selectivity is observed. Accordingly, a

smear of products is noted in contrast to Cu(3-Clip-Phen), suggesting that the mechanism of the cleavage is different. This observation may be explained by either of the following possibilities: (i) some cuts are due to platinum adducts of **Cu3CP-0-Pt** positioned on the other strand of the duplex (ODN II); (ii) the extensive cleavage observed most likely indicates that the ODN I fragment experiences more than one cut; therefore, **Cu3CP-0-Pt** should have been released after repetitive cuts from the ODN I and able to cut the free ODN.

To verify this hypothesis, the experimental conditions have been adjusted to introduce less platinum adducts on the target (20% against the 80% of modification of ODN I showed on Figure 4.7), and less ascorbate (100 μM) has been used to limit the re-cleavage events. However, the resulting cleavage pattern appears to be similar to the one observed with the former conditions (Figure 4.9).

One equivalent of $CuCl_2$ has been added to **3CP-0-Pt**, after the formation of platinum-DNA adducts, to analyze the cleavage selectivity of the resulting compound. A comparatively less efficient cleavage is achieved using **3CP-0-Pt** with extra added $CuCl_2$, when compared to **Cu3CP-0-Pt** (compare lanes 10 and 15 on Figure 4.7), possibly as a result of the partial coordination of the copper ions to **3CP-0-Pt**. Similarly to **Cu3CP-0-Pt**, the cleavage pattern obtained with **3CP-0-Pt** is found to be significantly different to the one of Cu(3-Clip-Phen) (Figure 4.7, lane 20). Interestingly, the free ODN I is not affected during the cleavage process, as only the ODN fragments containing platinum adducts are cleaved. Furthermore, a sequence selective cleavage (associated to the formation of fragments of ODN I including probably 3'-phosphate end, since they co-migrated as Maxam and Gilbert sequencing fragments) is observed in the close vicinity of the GG and AG sites (indicated as black bars in Figure 4.7, left). The intensity of the bands is much stronger at the GG site, reflecting the results of the primer extension experiments previously obtained. The four base pairs neighboring the GG site in the 5'-direction are also affected by the cleavage of **3CP-0-Pt**. In the 3'-direction, no clear bands, but a smear is observed, which can be explained as follows: the cleavage products remain coordinated to the complex and have therefore a totally different mobility, compared to the Maxam-Gilbert sequencing. The apparent smear observed in the 3'-direction supports this assumption, since such behaviour is observed for ODN I-platinum adducts including the copper complex (Figure 4.5A, lane 6), and can be therefore expected for cleavage fragments that coordinate to the complex.

A heating step in HEPES buffer (90 °C; pH 8.0) is often used to cleave the meta-stable products resulting from the oxidation of the deoxyribose. This treatment on the cleavage products obtained with **3CP-0-Pt**, **Cu3CP-0-Pt** and Cu(3-Clip-Phen) do not show a strong increase of the DNA cuts (Figure 4.7, respective comparisons between lanes 15, 16 and 10 and 11, 20 and 22). Therefore, products of strand cleavage are essentially observed during this

analysis. However, the smears observed in lanes 10 and 15 are partially converted into bands, indicating that some cleavage products, originating from the oxidation of the deoxyribose, are sensitive to alkaline conditions.

More drastic alkaline heating (as with piperidine) allows to detect the oxidations of the nucleobases that do not induce direct DNA cleavage.[6] Surprisingly, when this treatment is applied to **3CP-0-Pt** (with addition of 1 equivalent of copper) and **Cu3CP-0-Pt**, clear cleavages are observed, although the systems have not been incubated with ascorbate (Figure 4.7, lanes 13 and 8, respectively). This phenomenon is dependant of the presence of copper ion, since it is not observed for ODN I-platinum adducts with **3CP-0-Pt** without the addition of $CuCl_2$ (results not shown). Therefore, these alkaline conditions are sufficient to induce a redox activity of the copper complex part of the hybrid molecule (this phenomenon has not been observed with Cu(3-Clip-Phen) that can be removed during a precipitation step preceding the heating in the presence of piperidine). Interestingly, only the platinum-ODN I adducts are cleaved; none of the free ODN I is degraded and selective cleavages are observed around the position of adducts detected during primer extension experiments. Unfortunately, this activity of the copper complexes covalently linked to the target does not disclose whether or not the dual platinum/copper complexes perform the oxidation of nucleobases.

4.2.6 Cleavage of ODN II strand of the ODN I-ODN II duplex

The same experiments have been performed with ODNI/ODNII duplex labeled on the 5'-end of ODN II (Figure 4.8). Similar amounts of platinum-ODN II adducts are formed with **3CP-0-Pt** (Figure 4.8, lane 8) and **Cu3CP-0-Pt** (Figure 4.8, lane 3). Most likely, only parts of the platinum components of **3CP-0-Pt** and **Cu3CP-0-Pt** are bound on the ODN II at the preferential AG site, and the cleavages do not seem to be restricted to one selective site. Other adducts are probably also present. The occurrence of platinum-guanine mono-adducts on the ODN II (that is particularly rich in guanine bases) may explain the results observed. Further research investigations are required to confirm these proposals.

Both **3CP-0-Pt** with added copper and **Cu3CP-0-Pt** show extensive cleavage activities in the presence of ascorbic acid in air (Figure 4.8, lanes 11 and 6, respectively). In the experiments with **Cu3CP-0-Pt**, the platinum-ODN II adducts have fully reacted, while the free ODN II is only partly altered. The cleavage fragments are poorly resolved on the gel (a smear is essentially observed), and treatment with HEPES or piperidine fail to improve their analysis. These cleavage fragments are composed of modified DNA. It can be reasonably proposed that the fragments include ODN II-platinum adducts and that these adducts produce a smear during the migration in PAGE. All these results indicate that the platinum moieties of **3CP-0-Pt** and **Cu3CP-0-Pt**

bind, as expected, to the preferential Pt-site on ODN II, but also and mainly to single A and G nucleobases.

In the same conditions, the complex Cu(3-Clip-Phen) performs clear cleavages on ODN II with some sequence selectivity (lane 16-18), since A_{17} is specially targeted.

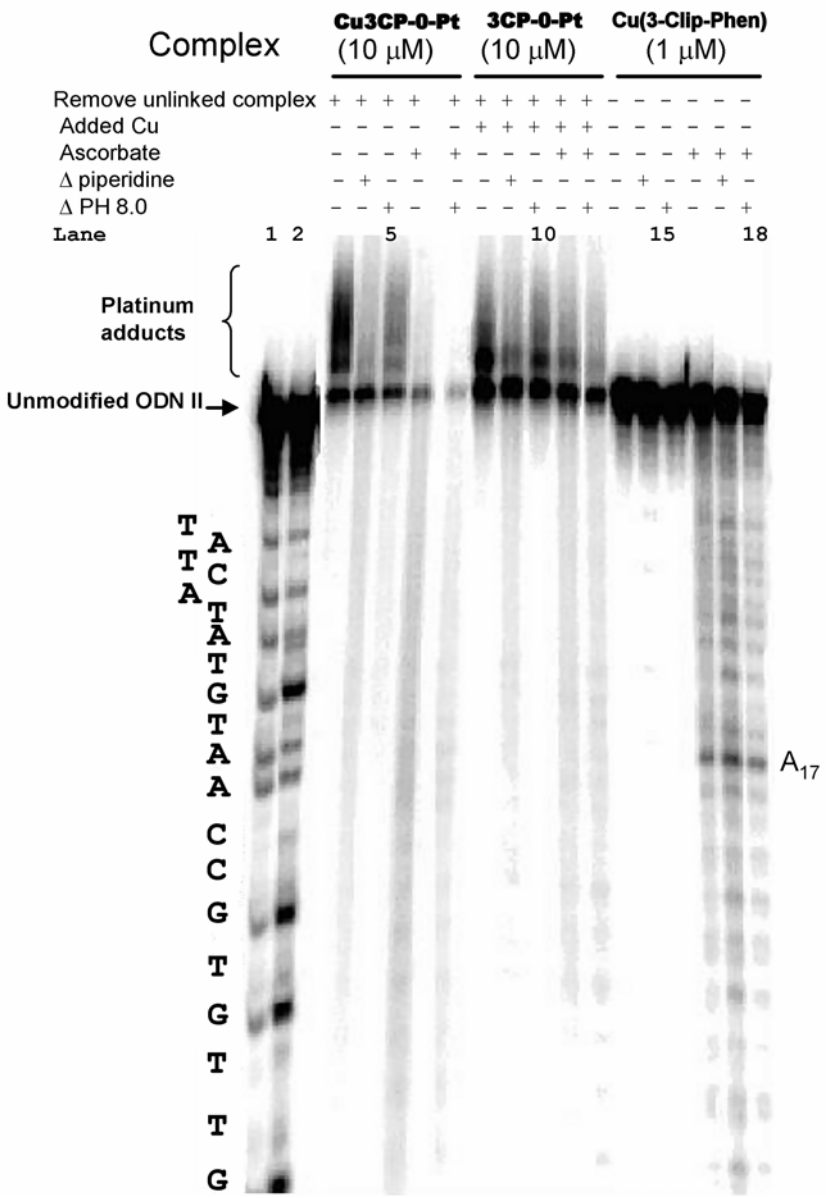

Figure 4.8 PAGE analysis of the cleavage of ODN II of the ODN I-ODN II duplex (1 μM) by compounds **3CP-0-Pt**, **Cu3CP-0-Pt** and Cu(3-Clip-Phen). The cleavage reactions were initiated with ascorbate (200 μM) in aerobic conditions or by heating 30 min at 90 °C in aqueous piperidine 0.2 M. The Maxam-Gilbert sequencing reactions A + G (lane 1) and G (lane 2) were performed to determine the cleavage sites. On top of the gel are indicated the conditions used during the experiments (details are given in the experimental part). ΔpH 8 was a heating step of 30 min at 90 °C in HEPES·NaOH buffer 0.1 M pH 8.0. Unlinked complexes were removed by a precipitation step with ethanol before the induction of cleavage.

A comparison between the cleavage patterns resulting from the action of complex **Cu3CP-0-Pt** on a single-stranded ODN I and on the duplex ODN I-ODN II has been made to appraise the influence of the formation of platinum-ODN II adducts on the resulting cleavage (Figure 4.9). ODN I-platinum adducts are formed when the single strand is used, and these adducts are essentially positioned at the GG site of the ODN I (the results of the primer extension are not shown). For this study, only 20% of the platinum adducts on the ODN I of the duplex, and 40% of the platinum adducts on the single strand are created in order to have a maximum of one adduct per DNA target, and thus simplify the analysis. The cleavage is induced by the addition of a small quantity of ascorbate (100 μM) to disfavor re-cleavage events.

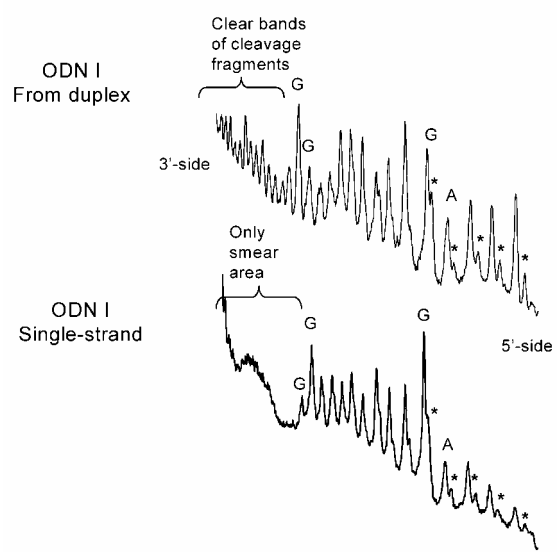

Figure 4.9 Phosphorimager scanning of the PAGE-cleavage patterns of ODN I by **Cu3CP-0-Pt**. The cleavage was performed on either the duplex ODN I-ODN II duplex (5'-end labeled on the ODN I) or on the single-stranded ODN I. Cleavage was induced by the addition of ascorbate (100 μM) after the removing of the unlinked complex during a precipitation step with ethanol. The clear bands on the 3'-side of GG site of the duplex are probably due to covalent adduct of **Cu3CP-0-Pt** on ODN II (the complementary strand of the duplex). 3'-Phosphoglycolate cleavage fragments are labeled with an asterisk. The other clear bands were attributed to fragments of ODN I including 3'-phosphate ends.

The cleavage of the ODN I fragment of the duplex results in a cleavage pattern exhibiting various moderate peaks in the 3'- region of the GG base pair of ODN I. The cleavage of single-stranded ODN I by complex **Cu3CP-0-Pt** gives rise to a smear in the same region. The smears observed characterize cleaved ODN I products that are still coordinated to complex **Cu3CP-0-Pt**. Accordingly, the weak peaks in this region of the DNA sequence are most likely due to the cleavage of complex **Cu3CP-0-Pt**-ODN II adducts on both strands. Since the conditions used favor a maximum of one ODN-platinum adduct per duplex, these cleavages on non-modified ODN I probably originate from complex **Cu3CP-0-Pt**-ODN II adducts.

The results are summarized in Figure 4.10. Importantly, the cleavage of the ODN I by ODN II-platinum adducts appears to be partially responsible of the observed non-selective cleavage of the duplex by the complex **Cu3CP-0-Pt**.

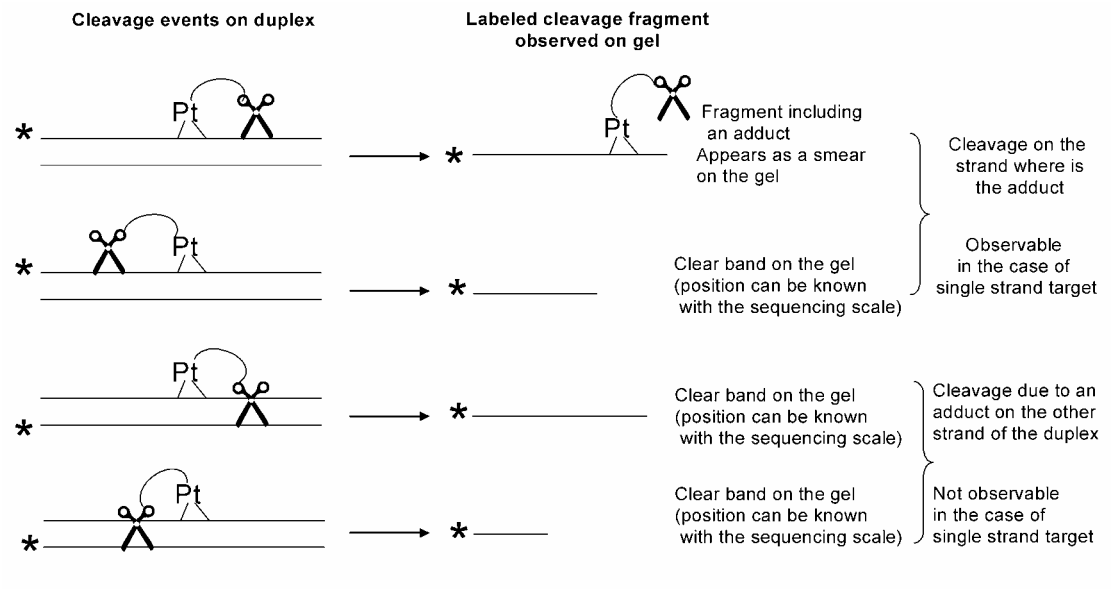

Figure 4.10 Summary of cleavage events due to platinum/copper dual complex **Cu3CP-0-Pt** on double-stranded DNA. The labelled strand of the DNA duplex that can be observed from denaturing PAGE experiment is labelled with an asterisk.

Interestingly, the weak peaks observed on the 5'-side of the cleavage fragments (and showed with an asterisk in Figure 4.9) probably correspond to DNA fragments with 3'-phosphoglycolate extremities. Indeed, these species are observed at the position of the cleavage products of the duplex produced by the action of complex Cu(3-Clip-Phen), and which have been previously characterized.[15] Such fragments have been earlier identified as the result of the oxidation of the C4' position of the 2-deoxyribose. Further research investigations are required to confirm these proposals.

The cytotoxicity of the complexes **3CP-0-Pt** and **Cu3CP-0-Pt** have been determined for breast (MCF7), two glioblastomas (Hs683 and U373), two colorectal (HCT-15 and LoVo) and lung (A549) cancer cell lines. Unfortunately, both complexes are not cytotoxic for most cell lines (a compound with an IC_{50} value higher than 10 μM is considered to be inactive). The only cell lines affected by complex **3CP-0-Pt** are U373 (IC_{50} value 4.6 μM) and A549 (IC_{50} value 9 μM). Complex **Cu3CP-0-Pt** is active in the U373 (IC_{50} value 4.4 μM) cell line. The IC_{50} value for cisplatin is comparable or lower in both cell lines.

4.3 Conclusions

The novel heterodinuclear platinum/copper complex **Cu3CP-0-Pt** with a short linker exhibits improved nuclease activity, compared to its parent compound Cu(3-Clip-Phen), and is able to perform double-strand breaks. The platinum moiety acts as an anchor to DNA, forcing the Cu(3-Clip-Phen) group to generate cuts in close proximity to the platinum-DNA adducts, hence even allowing direct double-strand breaks. Mechanistic investigations on a 36 bp DNA fragment (ODN I-ODN II) reveal that platinum adducts are indeed formed with both **3CP-0-Pt** and **Cu3CP-0-Pt**. The platinum moiety of complexes **3CP-0-Pt** and **Cu3CP-0-Pt** is binding to GG (primarily) and AG sites, like cisplatin. Nevertheless, the Taq polymerase enzyme stops at different base pairs for cisplatin and **3CP-0-Pt** and **Cu3CP-0-Pt**. This feature suggests that **3CP-0-Pt** and **Cu3CP-0-Pt** induce different distortions (compared to cisplatin) upon their binding to DNA, most likely owing to the bulkiness of the 3-Clip-Phen moiety. **3CP-0-Pt** with added copper (1 equivalent) shows a sequence selective cleavage, in the close proximity to the platinum adducts. A sequence selective cleavage is also observed for **Cu3CP-0-Pt**, but to a lesser extent compared to **3CP-0-Pt**. The opposite strand also contains platinum-DNA adducts, but no clear sequence selectivity is observed, most likely due to the lack of preferential platinum binding sites. These atypical platinum adducts lead to the partial damage of the other DNA strand, as is clearly evidenced by comparison of the cleavage products on a single stranded or duplex DNA.

Interestingly, it has been found that piperidine is also able to activate the Cu(3-Clip-Phen) component of the bifunctional platinum/copper complexes, a feature so far not reported. Thus, a good sequence selective cleavage is observed upon treatment of **3CP-0-Pt** with piperidine. Reasonable sequence selectivity is achieved with **Cu3CP-0-Pt**. The investigation of the mechanism of cleavage by **Cu3CP-0-Pt** has to be performed.

4.4 Experimental

Preparation of complexes 1 and 2: All reagents and solvents were commercially available and used without further purification. Cu(3-Clip-Phen) was prepared as previously described.[15]

2-(2-(3-(1,10-phenanthrolin-3-yl-oxy)-1-(1,10-phenanthrolin-8-yl-oxy)propan-2-ylamino)ethyl)isoindoline-1,3-dione (11): 3-Clip-Phen (**2**) (100 mg, 0.22 mmol) was dissolved in DMF (5 mL). One equivalent of *N*-(2-bromoethyl)phthalimide (56.7 mg, 0.22 mmol) and one equivalent of DIPEA (38 μL, 0.22 mmol) were added to **2**. The reaction mixture was heated to 100 °C for 2 days. After cooling down to RT, 10 mL of dichloromethane were added, and the organic phase was washed three times with 10 mL of distilled H_2O. After drying over Na_2SO_4 and evaporation under reduced pressure, the resulting crude product was purified by column chromatography (SiO_2, DCM/MeOH/NH_4OH, 95:5:0.5), to yield **11** as an off-white powder (yield = 34%). ^{1}H NMR ($DCCl_3$, 300 MHz) δ 9.05 (dd, 2H, J = 4.32, 1.67 Hz), 8.81 (d, 2H, J = 2.83 Hz), 8.10 (dd, 2H, J = 8.07, 1.62 Hz), 7.72 (dd, 2H, J = 5.43, 3.05 Hz), 7.67

(d, 2H, J = 8.88 Hz), 7.62 (d, 2H J = 8.86 Hz), 7.54 (dd, 2H, J = 6.09, 4.74 Hz), 7.48 (m, 4H), 4.27 (d, 4H, J = 5.18 Hz), 3.84 (t, 2H, J = 6.06 Hz), 3.54 (m, 1H), 3.13 (t, 2H, J = 6.12 Hz) ppm. ^{13}C NMR ($DCCl_3$, 75 MHz) δ 168.4, 153.7, 150.1, 146.0, 142.4, 140.3, 135.73, 133.8, 132.0, 129.3, 127.1, 125.9, 123.0, 122.0, 114.9, 67.3, 55.6, 45.4, 37.8 ppm. Low-resolution MS (ESI >0) m/z 621.00 [$(M+H)^+$; calcd for $C_{37}H_{29}N_6O_4^+$: 621.66], 642.94 [$(M+Na)^+$; calcd for $C_{37}H_{28}N_6O_4Na^+$: 643.65] Anal. Calcd for $C_{37}H_{28}N_6O_4 \cdot 1.6\ H_2O$: C, 68.42; H, 4.84; N, 12.94. Found: C, 68.34; H, 4.86; N, 13.21

***N*^{1}-(3-(1,10-phenanthrolin-3-yl-oxy)-1-(1,10-phenanthrolin-8-yl-oxy)propan-2-yl)ethane-1,2-diamine (3CP-0-NH$_2$):** 2 equivalents of hydrazine (15.6 µL, 0.32 mmol) were added to a solution of **11** (100 mg, 0.16 mmol) in 5 mL of pure ethanol. The mixture was refluxed overnight. The ethanol was evaporated under reduced pressure, and the crude product was purified by column chromatography (SiO_2, DCM/MeOH/NH_4OH, 90:10:1) to give **3CP-0-NH$_2$** as a light brown powder (yield = 73%). ^{1}H NMR (MeOD-d$_3$, 300 MHz) δ 9.00 (dd, 2H, J = 4.41, 1.63 Hz), 8.84 (d, 2H, J = 2.84 Hz), 8.34 (dd, 2H, J = 8.10, 1.67 Hz), 7.90 (d, 2H, J = 2.86 Hz), 7.83 (m, 4H), 7.65 (dd, 2H, J = 8.10, 3.26 Hz), 4.51 (d, 2H, J = 4.47 Hz), 3.58 (m, 1H), 3.07 (t, 2H, J = 5.64 Hz), 2.97 (t, 2H, J = 5.23) ppm. ^{13}C NMR (MeOD-d$_3$, 75 MHz) δ 155.6, 150.6, 146.3, 143.0, 140.5, 137.6, 131.0, 128.7, 128.2, 127.4, 123.5, 116.7, 69.1, 57.5, 41.9 ppm. Low resolution MS (ESI >0) m/z 490.98 [$(M+H)^+$; calcd for $C_{29}H_{27}N_6O_2^+$: 491.56] Anal. Calcd for $C_{29}H_{26}N_6O_2 \cdot 1.9\ CH_2Cl_2$: C, 56.93; H, 4.61; N, 12.89. Found: C, 56.79; H, 5.13; N, 13.23

Platinum[*N*^{1}-(3-(1,10-phenanthrolin-3-yl-oxy)-1-(1,10-phenanthrolin-8-yl-oxy)propan-2-yl)ethane-1,2-diamine]dichloride (3CP-0-Pt): To a solution of **3CP-0-NH$_2$** (70.4 mg, 0.14 mmol) in 6.5 mL of DMF was added a solution of 0.8 equivalent of K_2PtCl_4 (47.69 mg, 0.11 mmol) in 3.25 mL of de-ionized H_2O. The reaction mixture was stirred for 6 h at room temperature. The off-white precipitate was filtered and washed with 30 mL of de-ionized H_2O, 30 mL of methanol and 20 mL of diethyl-ether to give **3CP-0-Pt** as an off-white powder (yield = 42%).^{1}H NMR (DMSO-d$_6$, 300 MHz) δ 9.04 (d, 2H, J = 2.77 Hz), 8.88 (d, 2H, J = 2.45 Hz), 8.45 (d, 2H, J = 8.00 Hz), 8.05 (br, 2H), 7.95 (m, 4H), 7.70 (dd, 2H, J = 7.99, 4.35 Hz), 4.49 (br, 4H), 4.07 (br, 5H) ppm. ^{195}Pt NMR (DMSO-d$_6$) δ −2317 (complex), −3292 (complex with one DMSO coordinated) ppm. IR (neat): ν = 3049 (br), 1591 (s), 1506 (s), 1424 (s), 1236 (s), 1198 (s), 1102 (s), 1018 (s), 876 (s), 834 (s), 728 (s), 332 (s), 325 (s) cm^{-1} Anal. Calcd for $C_{29}H_{26}Cl_2N_6O_2Pt \cdot DMF$: C, 46.33; H, 4.01; N, 11.82 Found: C, 47.54; H, 4.43; N, 11.70

CuPt[N^1-(3-(1,10-phenanthrolin-3-yl-oxy)-1-(1,10-phenanthrolin-8-yl-oxy)propan-2-yl)ethane-1,2-diamine]Cl$_4$ (Cu3CP-0-Pt): $CuCl_2$ (17.0 mg, 0.1 mmol) was added as a solid to a suspension of **3CP-0-Pt** (75.7 mg, 0.1 mmol) in DMF (25 mL). The reaction was stirred overnight at 50 °C. DMF was partially evaporated under reduced pressure, and the crude compound was precipitated in 100 mL of diethyl ether. The solid material was filtered and washed with 3 × 20 mL of diethyl ether, and dried overnight at 50 °C under reduced pressure to give **Cu3CP-0-Pt** as a green powder (yield = 93%). X-Band EPR (solid state): g = 2.1191. UV-Vis (H_2O) λmax/nm: 282 (40100), 321 (12500), 333 (10100) and 347 (3280). HRMS (m/z): [2M –2Cl] calcd for $(C_{58}H_{52}Cl_6N_{12}O_4Pt_2Cu_2)^{2+}$ 853.00852, 853.5096, 854.0097, 854.5087, 855.0088, 855.5072, 856.0073, 856.5083, 857.0100, 857.5067 found 853.0117, 853.5117, 854.0114, 854.5110, 855.0107, 855.5105, 856.0103, 856.5101, 857.0098, 857.5097

Solutions of complexes for experiments with DNA: 1 mM DMSO solutions of the complexes investigated were prepared, and subsequently diluted with MilliQ water.

Nuclease activity on supercoiled DNA: 1 mM DMSO solutions of the complexes investigated were diluted to respectively 200, 400 and 1000 nM with MilliQ water. 5 μL of the complex solution were added to 10 μL of supercoiled ΦX174 DNA (Invitrogen, 7 nM, 40 μM base pairs) in 6 mM NaCl, 20 mM sodium phosphate buffer (pH 7.2), and incubated for 20 h at 37 °C. To initiate the cleavage, 5 μL of a 20 mM mercaptopropionic acid solution in water were added, and the resulting reaction mixture was incubated at 37 °C for 1 h. The reaction was quenched at 4 °C, followed by the addition of 4 μL of loading buffer (glycerol with bromophenol blue) prior to its loading on a 0.8% agarose gel containing 1 μg mL^{-1} of ethidium bromide. The gels were run at a constant voltage of 70 V for 90 min in TBE buffer containing 1 μg mL^{-1} of ethidium bromide. The gels were visualized under a UV trans-illuminator, and the bands were quantified using a BioRad Gel Doc 1000 apparatus interfaced with a computer. A correction factor of 1.47 has been applied to quantify the amount of supercoiled DNA (form I) present in all samples.

Time-course experiments of DNA cleavage: 50 μL of complex solution were added to 100 μL of supercoiled ΦX174 DNA (Invitrogen, 7 nM, 40 μM base pairs) in 6 mM NaCl, 20 mM sodium phosphate buffer (pH 7.2), and the resulting reaction mixture was incubated for 20 h at 37 °C. To initiate the cleavage, 50 μL of 20 mM mercaptopropionic acid were added, and a sample was taken out every 10 min. 4 μL of loading buffer (glycerol with bromophenol blue) were added, and the sample was directly frozen in liquid nitrogen. When all samples were collected, they were loaded on a 0.8% agarose gel containing 1 μg mL^{-1} of ethidium bromide.

Analyses with 5'-^{32}P-end-labeled DNA: The ODNs I, II and the primer (Figure 4.2) were purchased from Eurogentec, and purified on a 15% polyacrylamide gel. Concentrations of single-stranded ODNs were determined by UV titration at 260 nm.[38] The ODNs were end-labeled with ^{32}P using standard procedures with T_4 polynucleotide kinase (New England BioLabs) and [γ-^{32}P]ATP for the 5'-end, before being purified on a MicroSpin G25 column (Pharmacia).[39]

Comparison of the platinum-ODN adducts formed with the different complexes: 5'-end labeled ODN I (2 μM) was annealed to 1 equivalent of its complementary strand ODN II in 1100 μL of Tris-HCl (20 mM, pH 7.2) by heating to 90 °C for 5 min, followed by slow cooling to room temperature. Then, 60 μL of this solution was incubated with 60 μL of complex solution (6 μM or 20 μM) for 20 h at 37 °C followed by precipitation with 100 μL of sodium acetate buffer (3 M, pH 5.2) and 1300 μL of cold ethanol. Pellets were rinsed with ethanol and lyophilized. Platinum-DNA adducts were analyzed by denaturing 20% polyacrylamide gel electrophoresis then by phosphorimagery.

Comparison of the sequence selective binding by primer extension experiments with Taq polymerase: ODN I (2 μM) was annealed to ODN II (2 μM) in 1100 μL of Tris-HCl (20 mM, pH 7.2) by heating to 90 °C for 5 min, followed by slow cooling to room temperature. 60 μL of this solution were then incubated with 60 μL of complex solution (6 μM or 20 μM) for 20 h at 37 °C followed by precipitation with 100 μL of sodium acetate buffer (3 M, pH 5.2) and 1300 μL of cold ethanol. Pellets were rinsed with ethanol and lyophilized. For primer extension, an aliquot of this solution (0.25 μM) was annealed with 5'end labeled primer (0.25 μM) and 1 equiv of ODN I (0.25 μM) in the enzyme buffer (the buffer contains a small amount of reductant, but not enough to induce DNA cleavage by complex **Cu3CP-0-Pt**) before the addition of 250 μM dGTP, dCTP, dATP and dTTP and 2.5 units Taq

polymerase (final concentrations are given, the total volume was 10 μL). One equivalent of unmodified ODN I was added in order to displace the ODN II from the duplex and replace it with the labeled primer. The samples were reacted at 37 °C for 30 min, and 1 μL of edta (0.2 M) was subsequently added. 5 μL of sample were then analyzed by denaturing 20% polyacrylamide gel electrophoresis and phosphorimagery. Maxam and Gilbert sequencing scale,[40] including a final scale of T4 polynucleotide kinase digestion to remove 3'end-phosphates, was used to analyze the DNA fragments.

Comparison of the cleavage patterns of ODN I-ODN II induced by the copper complexes: The 5'-end labeled 36mer target (2 μM) was annealed to 1 equiv of its complementary strand in 1100 μL of Tris-HCl (20 mM, pH 7.2) by heating to 90 °C for 5 min, followed by slow cooling to room temperature. To 60 μL of this solution were added 60 μL of complex **3CP-0-Pt**, **Cu3CP-0-Pt** or Cu(3-Clip-Phen) solutions (20 μM). Parts of the samples involving complex **Cu3CP-0-Pt** were incubated for 19 h, followed by the addition of 1 equivalent of $CuCl_2$ per complex and subsequent incubation (1 h). The other samples were incubated for 20 h at 37 °C. Next, all samples were precipitated with 100 μL of sodium acetate buffer (3 M, pH 5.2) and 1300 μL of cold ethanol. Pellets were rinsed with ethanol and lyophilized then dissolved to 1.33 μM in Tris-HCl buffer (13.3 mM, pH 7.4). For the cleavage experiments, to 15 μL of this solution was added 5 μL of a 0.8 mM ascorbate solution (5 μL of water were added to the controls). The samples were incubated at 37 °C for 1 h, followed by precipitation in 20 μL of sodium acetate buffer (3 M, pH 5.2) containing 1 μg of salmon testes DNA and 180 μL of cold ethanol. Pellets were rinsed with ethanol and lyophilized. In order to study the DNA cleavage mechanism, additional treatments were performed on some samples: (i) heating at 90 °C in 50 μL of HEPES-NaOH buffer (0.1 M, pH 8.0) for 30 min, followed by ethanol precipitation; (ii) heating at 90 °C in 50 μL of piperidine (0.2 M in water) for 30 min, followed by lyophilization. Samples were analyzed by denaturing 20% polyacrylamide gel electrophoresis then phosphorimagery. Maxam and Gilbert sequencing scale was used to analyze DNA fragments.[40]

Cytotoxicity tests. The experimental procedure described below has been used for the following cell lines: Hs683, U373MG, HCT-15, LoVo, MCF-7 and A549.

- Hs683 and U-373MG: glioblastomas
- HCT-15 and LoVo: colorectal cancers
- A549: lung cancer
- MCF-7: breast cancer

The cells were cultured at 37 °C in sealed (airtight) Falcon plastic dishes (Nunc, Gibco, Belgium) containing Eagle's minimal essential medium (MEM, Gibco) supplemented with 5 % fetal calf serum (FCS). All the media were supplemented with a mixture of 0.6 mg mL^{-1} glutamine (Gibco), 200 IU mL^{-1} penicillin (Gibco), 200 IU mL^{-1} streptomycin (Gibco), and 0.1 mg mL^{-1} gentamycin (Gibco). The FCS was heat-inactivated for 1 h at 56 °C.

The MTT test is an indirect technique, which allows the rapid measurement (5 days) of the effect of a given product on the global growth of a cell line.[41] This test is based on the measurement of the number of metabolically active living cells able to transform the yellowish MTT product (3-(4,5-dimethylthiazol-2-yl)-2,5 diphenyl tetrazolium bromide) into the blue product, formazan, via mitochondrial reduction performed by living cells.[41] The amount of formazan obtained at the end of the

experiment is measured with a spectrophotometer, and is therefore directly proportional to the number of living cells at that moment. The measurement of the OD (Optical density) provides a quantitative measurement of the effect of the product investigated as compared to control (untreated cells), and enables it to be compared to other reference products.[41]

The cells are put to grow in flat-bottomed 96-well micro-wells with 100 μL of cell suspension per well and between 1,000 and 5,000 cells/well depending on cell type. Each cell line is seeded in its own cell culture medium. After a 24-hour period of incubation at 37 °C, the culture medium is replaced by 100 μL of fresh medium in which the substance to be tested has been dissolved at the different concentrations required. In our experiments, we tested the 4 compounds **3CP-0-Pt**, **Cu3CP-0-Pt**, Cu(3-Clip-Phen) and cisplatin) at 10^{-5} M to 10^{-9} M concentrations with ½ log steps. Each experimental condition is carried out in six different wells. After 72 hours of incubation at 37 °C with the drug (experimental conditions) or without the drug (control), the medium is replaced by 100 μL MTT at the concentration of 1 mg mL^{-1} dissolved in RPMI. The micro-wells are then incubated for 3 h at 37 °C and centrifuged at 400 G for 10 minutes. The MTT is removed, and the formazan crystals formed are dissolved in 100 μL of DMSO. The micro-wells are then shaken for 5 minutes and read on a spectrophotometer at 2 wavelengths (570 nm: the maximum formazan absorbance wavelength; 630 nm: the background noise wavelength).[41]

4.5 References

[1] B. A. Chabner, T. G. Roberts, *Nat. Rev. Cancer* **2005**, *5*, 65.

[2] L. H. Hurley, *Nat. Rev. Cancer* **2002**, *2*, 188.

[3] J. Reedijk, *Proc. Natl. Acad. Sci. U. S. A.* **2003**, *100*, 3611.

[4] J. Y. Chen, J. Stubbe, *Nat. Rev. Cancer* **2005**, *5*, 102.

[5] H. Umezawa, K. Maeda, T. Takeuchi, Y. Okami, *J. Antibiot.* **1966**, *19*, 200.

[6] C. J. Burrows, J. G. Muller, *Chem. Rev.* **1998**, *98*, 1109.

[7] M. Pitié, C. Boldron, G. Pratviel, *Advances In Inorganic Chemistry, Vol. 58*, Elsevier Academic Press Inc, San Diego, **2006**, pp. 77.

[8] G. Pratviel, J. Bernadou, B. Meunier, *Angew. Chem.-Int. Edit. Engl.* **1995**, *34*, 746.

[9] D. S. Sigman, A. Mazumder, D. M. Perrin, *Chem. Rev.* **1993**, *93*, 2295.

[10] L. E. Marshall, D. R. Graham, K. A. Reich, D. S. Sigman, *Biochemistry* **1981**, *20*, 244.

[11] J. M. Veal, R. L. Rill, *Biochemistry* **1991**, *30*, 1132.

[12] O. Zelenko, J. Gallagher, D. S. Sigman, *Angew. Chem.-Int. Edit.* **1997**, *36*, 2776.

[13] T. E. Goyne, D. S. Sigman, *J. Am. Chem. Soc.* **1987**, *109*, 2846.

[14] M. Kuwabara, C. Yoon, T. Goyne, T. Thederahn, D. S. Sigman, *Biochemistry* **1986**, *25*, 7401.

[15] M. Pitié, B. Sudres, B. Meunier, *Chem. Commun.* **1998**, 2597.

[16] C. Boldron, S. A. Ross, M. Pitié, B. Meunier, *Bioconjugate Chem.* **2002**, *13*, 1013.

[17] M. Pitié, J. D. Van Horn, D. Brion, C. J. Burrows, B. Meunier, *Bioconjugate Chem.* **2000**, *11*, 892.

[18] M. Pitié, C. J. Burrows, B. Meunier, *Nucleic Acids Res.* **2000**, *28*, 4856.

[19] P. de Hoog, C. Boldron, P. Gamez, K. Sliedregt-Bol, I. Roland, M. Pitié, R. Kiss, B. Meunier, J. Reedijk, *J. Med. Chem.* **2007**, *50*, 3148.

[20] B. Rosenberg, L. Vancamp, J. E. Trosko, V. H. Mansour, *Nature* **1969**, *222*, 385.

[21] E. R. Jamieson, S. J. Lippard, *Chem. Rev.* **1999**, *99*, 2467.

[22] H. Kostrhunova, V. Brabec, *Biochemistry* **2000**, *39*, 12639.

[23] M. S. Robillard, N. P. Davies, G. A. van der Marel, J. H. van Boom, J. Reedijk, V. Murray, *J. Inorg. Biochem.* **2003**, *96*, 331.

[24] M. D. Temple, W. D. McFadyen, R. J. Holmes, W. A. Denny, V. Murray, *Biochemistry* **2000**, *39*, 5593.

[25] J. E. Haber, *Trends Genet.* **2000**, *16*, 259.

[26] P. Karran, *Curr. Opin. Genet. Dev.* **2000**, *10*, 144.

[27] M. C. Ackley, C. G. Barry, A. M. Mounce, M. C. Farmer, B. E. Springer, C. S. Day, M. W. Wright, S. J. Berners-Price, S. M. Hess, U. Bierbach, *J. Biol. Inorg. Chem.* **2004**, *9*, 453.

[28] E. Bassett, A. Vaisman, J. M. Havener, C. Masutani, F. Hanaoka, S. G. Chaney, *Biochemistry* **2003**, *42*, 14197.

[29] A. M. Galea, V. Murray, *Biochim. Biophys. Acta-Gene Struct. Expression* **2002**, *1579*, 142.

[30] J. Kasparkova, O. Novakova, N. Farrell, V. Brabec, *Biochemistry* **2003**, *42*, 792.

[31] V. Murray, H. Motyka, P. R. England, G. Wickham, H. H. Lee, W. A. Denny, W. D. McFadyen, *Biochemistry* **1992**, *31*, 11812.

[32] V. Murray, H. Motyka, P. R. England, G. Wickham, H. H. Lee, W. A. Denny, W. D. McFadyen, *J. Biol. Chem.* **1992**, *267*, 18805.

[33] M. D. Temple, P. Recabarren, W. D. McFadyen, R. J. Holmes, W. A. Denny, V. Murray, *Biochim. Biophys. Acta-Gene Struct. Expression* **2002**, *1574*, 223.

[34] A. Vaisman, S. G. Chaney, *J. Biol. Chem.* **2000**, *275*, 13017.

[35] J. M. Woynarowski, W. G. Chapman, C. Napier, M. C. S. Herzig, P. Juniewicz, *Mol. Pharmacol.* **1998**, *54*, 770.

[36] Y. Zou, B. van Houten, N. Farrell, *Biochemistry* **1994**, *33*, 5404.

[37] A. Petitjean, J. K. Barton, *J. Am. Chem. Soc.* **2004**, *126*, 14728.

[38] G. Fasman, *Handbook of biochemistry and molecular biology: nucleic acids, Vol. 3rd edn.*, Boca Raton, p175, **1975**.

[39] J. Sambrook, E. F. Fritsch, T. Maniatis, *Molecular Cloning: A Laboratory Manuel, Vol. 2nd Edn.*, Cold Spring Harbor Laboratory Press, Cold Spring Harbor, NY, **1989**.

[40] A. M. Maxam, W. Gilbert, *Proc. Natl. Acad. Sci. U. S. A.* **1977**, *74*, 560.

[41] L. Ingrassia, P. Nshimyumukiza, J. Dewelle, F. Lefranc, L. Wlodarczak, S. Thomas, G. Dielie, C. Chiron, C. Zedde, P. Tisnes, R. van Soest, J. C. Braekman, F. Darro, R. Kiss, *J. Med. Chem.* **2006**, *49*, 1800.

Chapter 5

Platinated copper(3-Clip-Phen) complexes as effective DNA-cleaving and cytotoxic agents.*

The synthesis and biological activity of three heteronuclear platinum-copper complexes based on 3-Clip-Phen are reported. These rigid complexes have been designed to alter the intrinsic mechanism of action of both the platinum moiety and the Cu(3-Clip-Phen) unit. The platinum centres of two of these complexes are coordinated to a 3-Clip-Phen moiety, an ammine ligand and two chlorides, which are either cis or trans to each other. The third complex comprises two 3-Clip-Phen units and two chloride ligands bound in a trans fashion to the platinum ion. DNA cleavage experiments show that the complexes are highly efficient nuclease agents. In addition, a markedly difference in their aptitude to perform direct double-strand cleavage is observed, which appears to be strongly related to the ability of the platinum unit to coordinate to DNA. Indeed, the ***Cu(Sym-trans)*** *complex is unable to coordinate to DNA, which is reflected by its incapability to carry out DSBs. Nonetheless, the DNA cleavage activity of this complex is very high, and its cytotoxicity is high for several cell lines.* ***Cu(Sym-trans)*** *shows better anti-proliferate activity than both cisplatin and Cu(3-Clip-Phen), in most cancer cell lines. Furthermore, the cytotoxicity observed for* ***Asym-cis*** *is in most cell lines close to that of cisplatin, or even better.*

* Parts of this chapter are submitted for publication (Paul de Hoog, Şeniz Özalp-Yaman, Giulio Amadei, Janique Dewelle, Tatjana Mijatovic, Marguerite Pitié, Patrick Gamez, Bernard Meunier, and Jan Reedijk)

5.1 Introduction

Among the different therapeutic strategies to eradicate cancer cells, the development of DNA-targeting drugs is a rising topic of investigations in bio-inorganic chemistry.[1, 2] The interaction of such drugs with DNA often gives rise to the formation of coordination, covalent or non-covalent adducts, thereby disrupting the transcription and/or replication. Cisplatin and bleomycin are well-known representatives of this category of highly efficient antitumor agents.[3, 4] The spectra of tumors cured by cisplatin and bleomycin are complementary; in some cases, their combined use is more effective, like for testicular cancer therapy.[5]

After the discovery of the antitumor activities of cisplatin in 1965,[6, 7] a great deal of effort has been accomplished to determine its mechanism of action. Nowadays, the main target of cisplatin is generally accepted to be DNA. The main adduct formed is the very stable intrastrand GpG cross-link located in the major groove, which is likely to be responsible for the antitumor properties of cisplatin.[8] However, cisplatin treatment is still accompanied by severe side effects, and by both intrinsic and acquired resistance to the drug.[9-11]

The bleomycin family was isolated from *Streptomyces verticillus* for the first time in 1966.[12] Associated to iron(II) or copper(I), and in the presence of a reductant, the resulting complexes can catalyze the formation of single-strand and double-strand DNA lesions, which are lethal for the cancer cells.[4] This finding has led to the design and preparation of synthetic bleomycin models, such as Cu(3-Clip-Phen) and derivatives.[13-15] Due to strong interactions with DNA, dominated both by electrostatic interactions and partial intercalation, these Clip-Phen derivatives show very high nuclease activities. However, Cu(3-Clip-Phen) is not capable of performing a direct double-strand break (DSB), and it is also not sequence selective.[16, 17]

Several strategies have been developed to overcome cisplatin resistance, like the use of polynuclear platinum complexes,[18, 19] compounds exhibiting a *trans* geometry,[20, 21] or derivatives containing a second functionality.[22] In the present chapter, a new approach aimed at reducing, or even annihilating cisplatin resistance, is reported where platinum is directly coordinated to the amine group of the DNA-cleaving moiety in Cu(3-Clip-Phen) (Figure 5.1).[23] As a result, the platinum unit plays two roles: it acts (i) as an antitumor drug and (ii) as an anchor to DNA, thus allowing the Cu(3-Clip-Phen) moiety to perform cleavages in the close proximity to the Pt-DNA adducts. Consequently, the possibilities to achieve DSBs, which are highly cytotoxic, are enhanced. Cu(3-Clip-Phen) typically abstracts protons from the minor groove of DNA,[16] while cisplatin normally binds in the major groove of DNA. These hybrid complexes exhibit short distances between the metallic entities and are obviously not able to interact with the major and the minor grooves at the same time. Therefore, either the platinum moiety or the Cu(3-Clip-Phen) part will not interact with its ideal site of interaction, thereby changing its

intrinsic mechanism of action. Two asymmetric complexes and one symmetric complex, having *cis* or *trans* geometries and containing both active entities, have been synthesized and their nuclease activity and cytotoxicity have been evaluated.

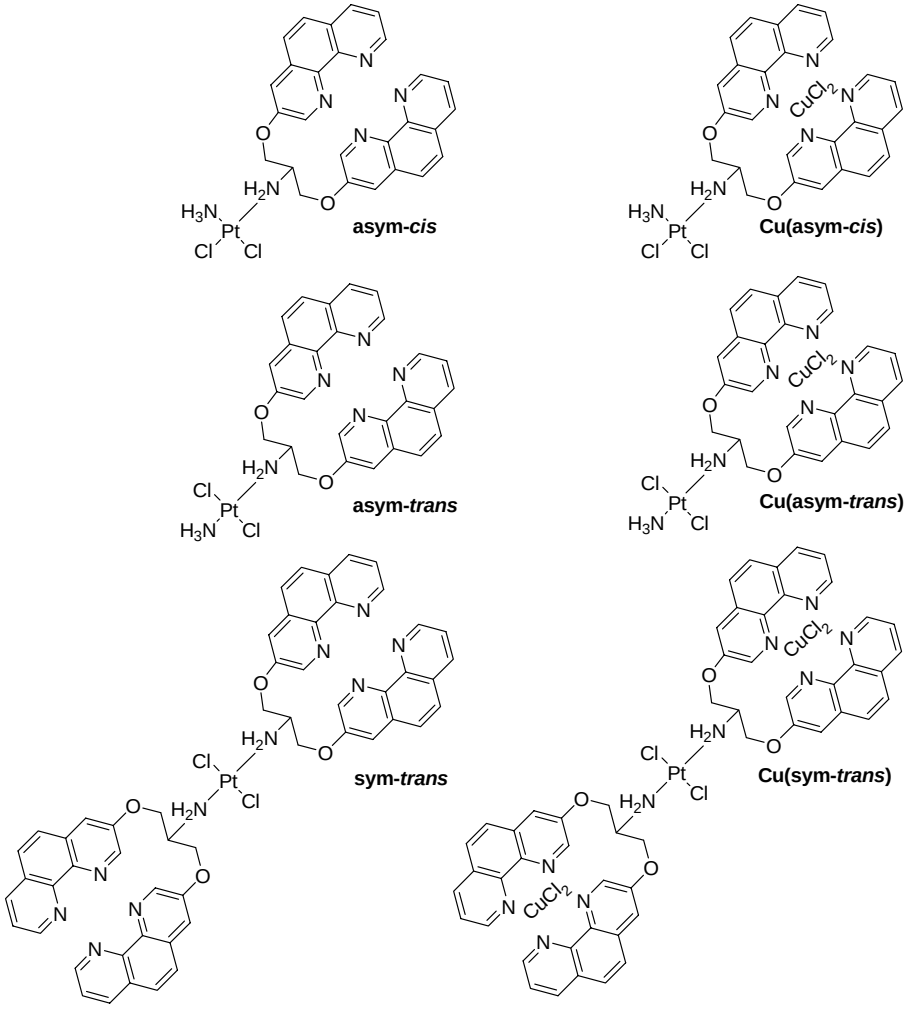

Figure 5.1 Schematic representations of the platinum complexes **asym-*cis***, **asym-*trans***, **sym-*trans*** and the heteronuclear platinum-copper complexes **Cu(asym-*cis*)**, **Cu(asym-*trans*)**, **Cu(sym-*trans*)**.

5.2 Results and Discussion

The synthetic pathway for the preparation of the hybrid platinum/copper complexes is depicted in Scheme 5.1. **Asym-*cis*** is obtained through a two-step process with the initial synthesis of the intermediate species $(NBu_4)[Pt(NH_3)Cl_3]$ (**12**).[24] The second step then consists of the addition of 1 equivalent of 3-Clip-Phen to **12**, giving rise to the precipitation of pure product **Asym-*cis***. The preparation of compound **Asym-*trans*** first requires the activation of cisplatin via the removal of one chloride anion using 1 equivalent of $AgNO_3$. Next, 3-Clip-Phen is reacted for 2 days at room temperature with the resulting Pt moiety, producing the complex $[Pt(3\text{-Clip-Phen})(NH_3)_2Cl]NO_3$ (**13**) as a precipitate. The final step involves the treatment of **13**

with a large excess of HCl at 85 °C for 6 hours, as earlier described.[25] The pure **Asym-*trans*** precipitates after neutralization of the reaction mixture with NaOH. Complex **Sym-*trans*** is prepared in three synthetic steps. First, $K_2[PtCl_4]$ is treated with $AgNO_3$ to substitute three chloride ligands by water molecules. Reaction of the resulting complex $[Pt(H_2O)_3Cl](NO_3)$ (**14**) with an excess of 3-Clip-Phen at 50 °C for 24 hours, yields the compound [Pt(3-Clip-Phen)$_3$Cl](NO_3) (**15**) via ligand exchange. **15** is isolated by filtration and washed extensively with water, methanol and diethyl ether, to remove the unreacted products. **15** is subsequently treated with a large excess of HCl at 85 °C for 6 hours. Neutralization using NaOH results in the precipitation of the HCl salt of **Sym-*trans***. The coordination of compounds **Asym-*cis***, **Asym-*trans*** and **Sym-*trans*** to copper is achieved *in situ* with one equivalent of copper(II) chloride per 3-Clip-Phen residue, which produces the heteronuclear complexes **Cu(Asym-*cis*)**, **Cu(Asym-*trans*)** and **Cu(Sym-*trans*)**.

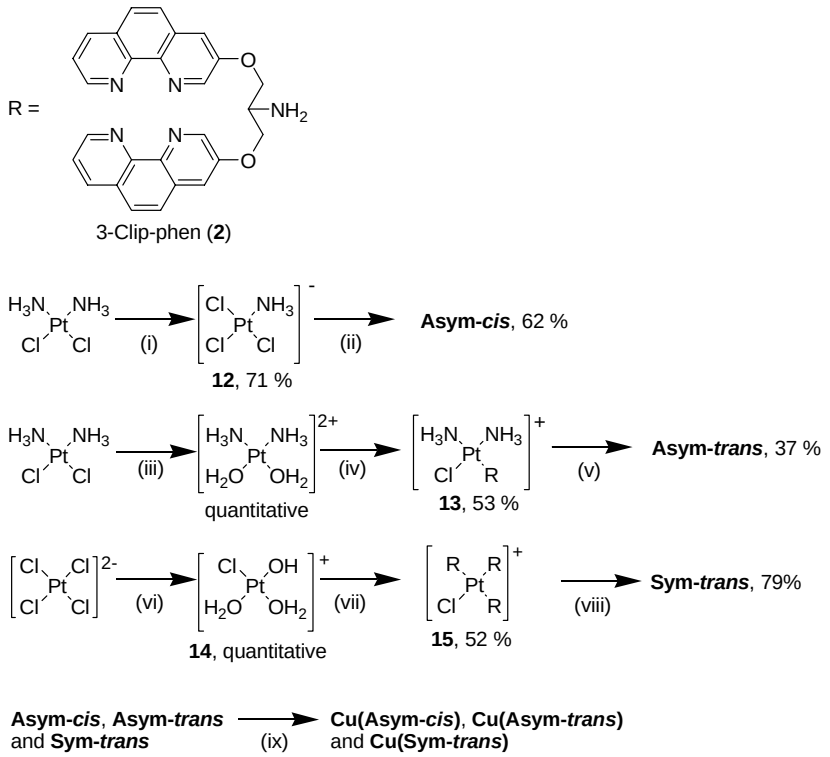

Scheme 5.1 Reagents and conditions: (i) 100 °C, $(C_4H_9)_4N)Cl$, dimethylacetamide, 6 h; (ii) 3-Clip-Phen, DMF, 2.5 h; (iii) $AgNO_3$, H_2O, 24 h; (iv) 3-Clip-Phen, DMF, 48 h (v) 85 C, HCl, DMF, 6 h; (vi) $AgNO_3$, H_2O, 24 h; (vii) 50 °C, 3-Clip-Phen, DMF, 24 h; (viii) 85 C, HCl, DMF, 6 h; (ix) $CuCl_2$, *in situ* preparation.

Relaxation experiments of supercoiled ΦX174 DNA (form I) into the circular (form II) and the linear (form III) forms have been performed (agarose gel electrophoresis) to monitor the relative cleavage activities of complexes **Cu(Asym-*cis*)**, **Cu(Asym-*trans*)** and **Cu(Sym-*trans*)** in the presence of a reducing agent, in air. For this purpose, the different complexes are pre-incubated for 20 hours with supercoiled DNA to allow the binding of the platinum moiety. The

cleavage reaction is initiated via the addition of mercaptopropionic acid (MPA) in aerobic conditions (Figure 5.2).

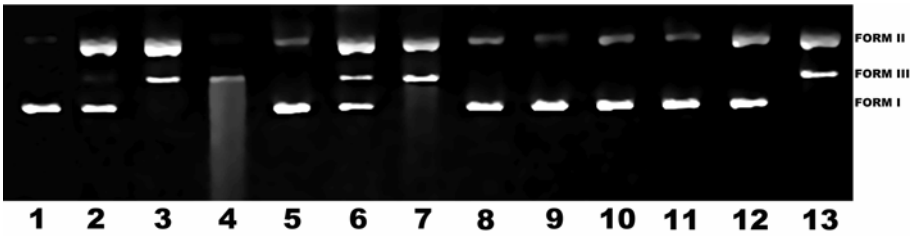

Figure 5.2 Comparative oxidative cleavage experiments of ΦX174 plasmid DNA for complexes **Cu(Asym-*cis*)**, **Cu(Asym-*trans*)**, **Cu(Sym-*trans*)** and Cu(3-Clip-Phen) in the presence of 5 mM MPA. Lane 1: control DNA. Lane 2: 50 nM **Cu(Sym-*trans*)**. Lane 3: 100 nM **Cu(Sym-*trans*)**. Lane 4: 250 nM **Cu(Sym-*trans*)**. Lane 5: 50 nM **Cu(Asym-*cis*)**. Lane 6: 100 nM **Cu(Asym-*cis*)**. Lane 7: 250 nM **Cu(Asym-*cis*)**. Lane 8: 50 nM **Cu(Asym-*trans*)**. Lane 9: 100 nM **Cu(Asym-*trans*)**. Lane 10: 250 nM **Cu(Asym-*trans*)**. Lane 11: 50 nM Cu(3-Clip-Phen). Lane 12: 100 nM Cu(3-Clip-Phen). Lane 13: 250 nM Cu(3-Clip-Phen).

The absence of nuclease activity for all complexes investigated is observed when no reductant is added. In the presence of MPA, the following order of cleaving ability is observed for 100 nM solutions of the various complexes (Figure 5.2): **Cu(Sym-*trans*)** (lane 3) >> **Cu(Asym-*cis*)** (lane 6) > Cu(3-Clip-Phen) (lane 12) >> **Cu(Asym-*trans*)** (lane 9). In addition, at a complex concentration of 250 nM, a smear (multi-fragmented DNA) is observed for compounds **Cu(Sym-*trans*)** and in lesser extent for **Cu(Asym-*cis*)** (Figure 5.2, lanes 4 and 7). In the same experimental conditions, i.e. 250 nM, the activity of complex **Cu(Asym-*trans*)** is comparatively reduced (Figure 5.2, lane 10); however, a 500 nM solution of **Cu(Asym-*trans*)** leads to the cleavage of supercoiled DNA into its circular and linear forms (Figure 5.3, lane 3). Interestingly, at this concentration, complex **Cu(Asym-*trans*)** generates DNA form III fragments, while the Form I is still present (Figure 5.3, lane 3). The same feature is observed with complex **Cu(Asym-*cis*)** at a concentration of 100 nM (Figure 5.3, lane 2).

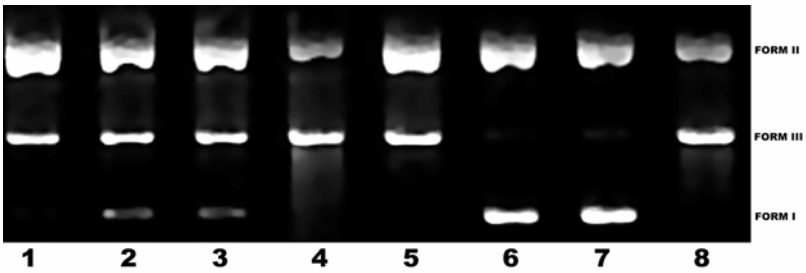

Figure 5.3 Comparative oxidative cleavage experiments of ΦX174 plasmid DNA for complexes **Cu(Asym-*cis*)**, **Cu(Asym-*trans*)**, **Cu(Sym-*trans*)** and Cu(3-Clip-Phen) in the presence of 5 mM MPA, with and without incubation time (20 hours). Lane 1: 100 nM **Cu(Sym-*trans*)** with 20 h. pre-incubation time. Lane 2: 100 nM **Cu(Asym-*cis*)** with 20 h. pre-incubation time. Lane 3: 500 nM **Cu(Asym-*trans*)** with 20 h. pre-incubation time. Lane 4: 250 nM Cu(3-Clip-Phen) with 20 h. pre-incubation time. Lane 5: 100 nM **Cu(Sym-*trans*)**. Lane 6: 100 nM **Cu(Asym-*cis*)**. Lane 7: 500 nM **Cu(Asym-*trans*)**. Lane 8: 250 nM Cu(3-Clip-Phen).

These important results clearly indicate that these complexes are able to perform direct double-strand cuts.[23] In contrast, Cu(3-Clip-Phen) and the complex **Cu(Sym-*trans*)** do not show this form I/form III pattern (Figure 5.3), suggesting that both complexes are only capable of performing repetitive single-strand cuts. Cleavage experiments with or without pre-incubation times (20 hours) have been carried out to further investigate the influence of the platinum-DNA adduct formation on the cleaving activities of the corresponding heteronuclear complexes (Figure 5.3). The coordination of platinum to DNA is a slow process, which typically requires several hours. A pre-incubation time is thus needed to ensure that the platinum moiety of the heteronuclear compound is effectively bound to DNA. Complexes **Cu(Asym-*cis*)** (Figure 5.3, lanes 2 and 6) and **Cu(Asym-*trans*)** (lanes 3 and 7) show a very strong decrease in activity when no pre-incubation is performed. These remarkable results reveal that the coordination of the platinum moiety to DNA is crucial for their cleaving ability.

In contrast, Cu(3-Clip-Phen) (Figure 5.3, lanes 4 and 8), and complex **Cu(Sym-*trans*)** (Figure 5.3, lanes 1 and 5) do not show any noticeable differences between the experiments with or without pre-incubation times. The DNA cleavage behavior exhibited by complex **Cu(Sym-*trans*)** is comparable to the one of Cu(3-Clip-Phen), thus suggesting that the platinum moiety of the bulky complex **Cu(Sym-*trans*)** does not coordinate to DNA. The steric hindrance due to the two coordinated 3-Clip-Phen units and the less reactive *trans*-platinum moiety most likely prohibit the coordination of the platinum ion to the DNA molecule. As a result, the cleaving ability of complex **Cu(Sym-*trans*)** is solely dominated by its two Cu(3-Clip-Phen) entities. This hypothesis is corroborated by the absence of direct double-strand cleavage induced by **Cu(Sym-*trans*)**. Indeed, contrary to complexes **Cu(Asym-*cis*)** and **Cu(Asym-*trans*)**, compound **Cu(Sym-*trans*)** is not able to directly generate form-III fragments of DNA (see Figure 5.3, lanes 5-7), showing that, similarly to Cu(3-Clip-Phen), the compound **Cu(Sym-*trans*)** more or less behaves as a 'free' cleaving agent.

To further investigate the coordination of the complexes to DNA through their platinum group, high resolution analyses on a 36 bp (base pairs) ODN I – ODN II DNA fragment (Figure 5.4) have been performed. The sequence of this duplex was chosen to have GG and AG sequences included (which are the two major binding sites of *cis*-Pt(II) complexes) on the ODN I strand. The complexes were incubated for 20 or 96 hours in order to allow the platinum to coordinate to the DNA duplex.

ODN I 5′-AACTTAAT**AG**TATACATT**GG**ACACAACAACAACAAC-3′
ODN II 3′-TTGAATTATCATATGTTACCTGTGTTGTTGTTGTTG-5′

Figure 5.4 The 36 bp fragment used for the analysis. The major cisplatin binding sites are identified with bold letters. The sequence of the primer used during these experiments corresponds to the underlined region of ODN II.

Molecules able to irreversibly bind to DNA will retard the rate of migration of the modified ODN, compared to the free ODN; therefore, ODN-Pt adducts appear as retarded bands on PAGE. Hence, the amount of formed platinum-ODN I can be quantified. The error of the quantifications is between 5 and 10 percent. Complexes **Asym-*cis***, **Cu(Asym-*cis*)**, **Asym-*trans***, **Cu(Asym-*trans*)**, **Sym-*trans*** and **Cu(Sym-*trans*)** form respectively 15-20 %, 15-20 %, 10-15 %, 10-15 %, 5-10 % and 5-10 % platinum-ODN I adducts after an incubation time of 20 hours. After 96 hours, complexes **Asym-*cis***, **Cu(Asym-*cis*)**, **Asym-*trans***, **Cu(Asym-*trans*)**, and **Sym-*trans*** form respectively 50-60 %, 70-80 %, 15-20 %, 5-10 %, 5-10 % platinum-ODN I adducts, while the quantity of **Cu(Sym-*trans*)** is below the detection limit. The amounts of platinum-ODN I adducts developed show that complexes **Asym-*cis*** and **Cu(Asym-*cis*)** are the most reactive. Moreover, a significant enhancement of the formation of platinum-ODN I adducts is observed when the incubation time is increased. Comparatively, complexes **Asym-*trans*** and **Cu(Asym-*trans*)** are much less reactive, and a significant increase in incubation time does not result in an increase of platinum-ODN I adducts. In the case of complexes **Sym-*trans*** and **Cu(Sym-*trans*)**, their platinum parts can be considered as non-binding, since only insignificant quantities (within the experimental error) of platinum-ODN I adducts could be detected. Even after an incubation time of 96 hours, the action of complex **Cu(Sym-*trans*)** does not yield any detectable amounts of platinum-ODN I adducts.

Primer extension experiments have been performed to investigate the sequence selective binding of platinum complexes **Asym-*cis***, **Asym-*trans*** and **Sym-*trans*** to DNA (Figure 5.5).[26-31] Taq polymerase has proven to effectively stop at platination sites, and is therefore used for these studies. The use of cisplatin results in clear stops of the Taq polymerase at the expected preferential binding sites (of cisplatin), *i.e.* mainly at the GG, but also at the AG site (Figure 5.5, lane 4). The stop is mainly observed on the adenosine preceding the GG site. The binding of complexes **Asym-*cis*** and **Asym-*trans*** to DNA also results in Taq polymerase stops at the G and A nucleobases near the GG binding site. The results obtained with complex **Sym-*trans*** confirm previous observations revealing that the use of **Sym-*trans*** does not lead to Taq polymerase stops; therefore, the platinum moiety of **Sym-*trans*** is evidently not capable of binding to the DNA fragment.

The cytotoxic activities of complexes **Asym-*cis***, **Asym-*trans***, **Sym-*trans***, **Cu(Asym-*cis*)**, **Cu(Asym-*trans*)** , **Cu(Sym-*trans*)**, Cu(3-Clip-Phen), and cisplatin have been determined for breast (MCF7), two glioblastomas (Hs683 and U373), two colorectal (HCT-15 and LoVo) and lung (A549) cancer cell lines. The results of the activities are summarized in Table 5.1. A complex with an IC_{50} value higher than 10 μM (>10) is considered as being inactive.

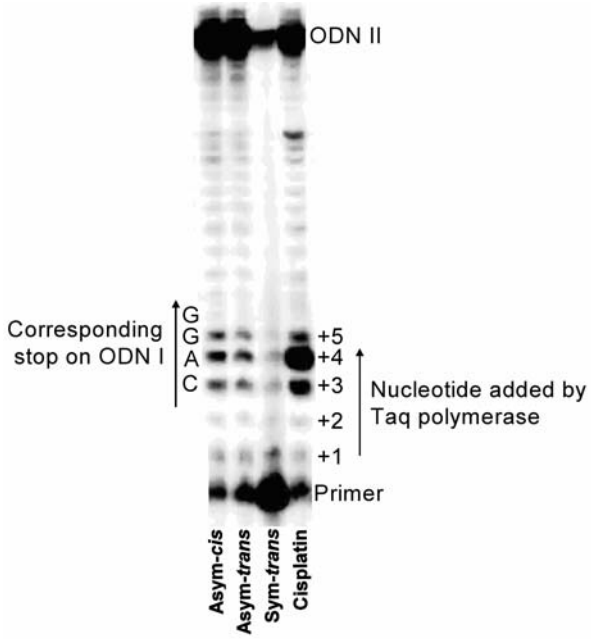

Figure 5.5 Phosphor image of a DNA-sequencing gel comparing the sequence specificity of cisplatin, **Cu(Asym-*cis*)**, **Cu(Asym-*trans*)** and **Cu(Sym-*trans*)**. All the samples were extended using Taq polymerase, starting from the 5'-end-labelled primer. Lane 1: 10 μM **Cu(Asym-*cis*)**; Lane 2: 10 μM **Cu(Asym-*trans*)**; Lane 3: 10 μM **Cu(Sym-*trans*)**. Lane 4: 3 μM cisplatin. It is noteworthy that the GT and GGAC sites give the sequence of the opposite strand that induced the stop of the primer extension.

Table 5.1 In vitro cytotoxicity assays for **Asym-*cis***, **Asym-*trans***, **Sym-*trans***, **Cu(Asym-*cis*)**, **Cu(Asym-*trans*)**, **Cu(Sym-*trans*)**, Cu(3-Clip-Phen), and cisplatin, against several cancer cell lines.

IC_{50} values[a] (μM)						
	Cell lines					
Complexes	Hs683	U373	HCT-15	Lovo	A549	MCF-7
Asym-*cis*	7.2	3.3	4.5	4.4	1.2	1.1
Asym-*trans* [b]	> 10	7.7	> 10	> 10	> 10	5.8
Sym-*trans* [b]	> 10	5.4	> 10	> 10	6.2	2.5
Cu(Asym-*cis*) [b]	> 10	8.3	> 10	> 10	> 10	1.9
Cu(Asym-*trans*) [b]	> 10	> 10	> 10	> 10	> 10	0.9
Cu(Sym-*trans*)	2.7	0.6	4.6	0.4	0.9	1.6
Cu(3-Clip-Phen) [b]	> 10	> 10	> 10	> 10	> 10	> 10
cisplatin	0.4	5	10	0.3	1.5	9

[a] IC_{50} = concentration of drug required to eradicate 50% of the cancer cells.
[b] An IC_{50} value higher than10 μM (> 10) is indicative of an inactive compound.

Although unmodified Cu(3-Clip-Phen) shows antiproliferative activities in a number of cell lines,[23, 32] the IC_{50} values herein reported for distinct cell lines are higher than 10 μM (Table 5.1). Major differences in the cytotoxic activities of the complexes described in the present report are observed. The copper-free complex **Asym-*cis*** exhibits IC_{50} values comparable to, or in some cases better than those achieved with cisplatin (Table 5.1, cell lines U373, HCT-15, A549 and MCF-7). The Pt-complex **Asym-*cis*** is drastically more cytotoxic than Cu(3-Clip-Phen) on these cell lines; however, the corresponding Pt-Cu(3-Clip-Phen) complex, **Cu(Asym-*cis*)**, shows low cytotoxic activities (except for the MCF-7 cell line), suggesting that its action is mostly governed by its copper component. The IC_{50} values determined for the *trans* complexes **Asym-*trans*** and **Cu(Asym-*trans*)** are generally inferior to the ones of cisplatin. However, for the MCF-7 cell line, compound **Cu(Asym-*trans*)** is about ten times more cytotoxic than cisplatin. The *trans*-platinum complex **Sym-*trans*** bearing two 3-Clip-Phen ligands shows antiproliferative activities comparable to those of cisplatin in the U373 and MCF-15 cell lines (Table 5.1). If copper is coordinated to both 3-Clip-Phen units of complex **Sym-*trans***, the resulting complex **Cu(Sym-*trans*)** becomes a highly efficient cytotoxic agent. Indeed, compound **Cu(Sym-*trans*)** is more cytotoxic than cisplatin in many cell lines studied (Table 5.1). Remarkably, the IC_{50} value for the cell line U373 is ten times higher, compared to cisplatin. Interestingly, the complex **Cu(Sym-*trans*)** is the most effective DNA cleaving agent (Figure 5.2, lanes 3 and 4), which is in total agreement with the cytotoxicity assays. In the same way, the cytotoxicities achieved with complex **Cu(Asym-*trans*)** corroborate its DNA cleaving abilities, as DNA cuts are only observed at very high concentrations (Figure 5.2, lanes 8-10). The coordination of copper to complexes **Asym-*cis*** and **Sym-*trans***, respectively producing complexes **Cu(Asym-*cis*)** and **Cu(Sym-*trans*)**, induces major diversities regarding the corresponding cytotoxic activities. These variations could be explained by, either the permeability of the cells, and/or the cellular distribution is affected by the presence of copper ions.

5.3 Conclusions

Three bifunctional Pt-Cu complexes are reported. These complexes contain a (a)symmetric platinum moiety with different geometries (*cis* or *trans*) which can bind to DNA, and one or two Cu(3-Clip-Phen) groups that can cleave the DNA strands. The three complexes show excellent DNA-cleavage activities. Complex **Cu(Sym-*trans*)** is the pre-eminent nuclease active agent, whose activity is significantly superior to the one of Cu(3-Clip-Phen). The platinum moieties of the two latter complexes are able to bind to the DNA strands, whereas complex **Sym-*trans*** probably acts as two single Cu(3-Clip-Phen) units, probably owing to well-known lower activities of *trans* complexes combined with the bulkiness of the two 3-Clip-Phen ligands. Complexes **Asym-*cis*** and **Asym-*trans*** show binding specificities analogous to the ones of cisplatin, thus preferentially binding at the GG site. Complex **Cu(Sym-*trans*)** appears to be the

most active cleaving agent. In addition, its cytotoxicity is superior to the ones of all other complexes, including cisplatin.

5.4 Experimental

Synthesis of the complex *cis*-[Pt(3-Clip-Phen)(NH_3)Cl_2] (Asym-*cis*) The preparation of {$(C_4H_9)_4N$}[Pt(NH_3)Cl_3] (**12**) was carried out as previously described.[24] {$(C_4H_9)_4N$}[Pt(NH_3)Cl_3] (**12**) (0.433 g, 0.77 mmol) and $(C_4H_9)_4N$)Cl (0.36 g, 1.30 mmol) were dissolved in 4 mL of MeOH. One equivalent of 3-Clip-Phen (**2**) (0.346 g, 0.77 mmol) dissolved in 3 mL of DMF was added, resulting in an immediate precipitation of a yellow compound. The suspension was stirred for 1 h 30 at room temperature in the dark. The precipitate was isolated on a glass filter and washed with methanol (3 × 10 mL) and diethyl ether (2 × 10 mL). The yellow product was dried in air. Yellow powder; yield = 62 %; ^{1}H NMR (DMF-d^7, 300 MHz) δ 9.11 (br, 2H), 8.92 (br, 2H), 8.46 (br, 2H), 8.19 (br, 2H), 7.71 (br, 2H), 4.90 (d, 4H) 4.13 (m, 1H) ppm; ^{195}Pt NMR (DMF-d^7) δ –2161 ppm; Elemental analyses $C_{27}H_{24}Cl_2N_6O_2Pt \cdot ((C_4H_9)_4N)Cl)_{0.2}$, fnd (calc): C, 46.58 (46.14); H, 4.26 (4.00); N, 11.14 (11.05).

Synthesis of the complex *trans*-[Pt(3-Clip-Phen)(NH_3)Cl_2] (**Asym-*trans***)

Step 1: synthesis of [Pt(3-Clip-Phen)$(NH_3)_2$Cl]Cl (**13**). Cisplatin (0.400 g, 1.33 mmol) was dissolved in 100 mL of MilliQ water in the dark. Two equivalents of $AgNO_3$ (0.456 g, 2.66 mmol) were added drop wise. The solution was stirred overnight in the dark. The white AgCl precipitate was filtered off. **2** (0.717 g, 1.60 mmol) dissolved in 5 mL of dimethylformamide was added dropwise to the filtrate, and the resulting reaction mixture was stirred during 2 days in the dark. The greenish precipitate [Pt$(NH_3)_2$(3-Clip-Phen)Cl]NO_3 was collected and washed respectively with 3 × 15 mL of CH_2Cl_2/methanol mixture (5% methanol), 3 × 15 mL of ethanol, and 3 × 15 mL of diethyl ether to remove unreacted reagents. Greenish powder; yield = 53 %; ^{1}H NMR (DMSO-d^6, 300 MHz) δ 9.07 (d, 2H, J = 8.94 Hz), 8.88 (d, 2H, J = 2.60 Hz), 8.44 (d, 2H, J = 8.02 Hz), 8.06 (d, 2H, J = 2.73 Hz), 7.99-7.92 (m, 4H), 7.70 (dd, 2H, J = 7.99, 4.32 Hz), 4.63 (br, 4H), 4.26 (br, 1H) ppm; ^{195}Pt NMR (DMSO-d^6) δ -2403 ppm

Step 2: synthesis of *trans*-[Pt(3-Clip-Phen)(NH_3)Cl_2] (**Asym-*trans***).
13 (0.1231 g, 0.16 mmol) was dissolved in 3 mL of DMF. 33 equivalents of HCl (37 % in water) (0.437 mL, 5.28 mmol) were added to this solution in the dark. A precipitate occurred instantly. The suspension was refluxed at 85 °C for 6 hours in the dark. After cooling the reaction, NaOH was added in excess to neutralize the HCl. The orange precipitate was filtered off and washed 3 times with respectively 5 mL of MilliQ H_2O, 5 mL of methanol, and 5 mL of diethyl ether. Orange powder; yield = 37 %; ^{1}H NMR (DMF-d^7, 300 MHz) δ 9.09 (br, 2H), 8.94 (br, 2H), 8.48 (br, 3H), 8.19 (br, 1H), 7.72 (br, 2H), 5.17-4.92 (br, 4H), 4.46 (br, 1H) ppm; ^{195}Pt NMR (DMF-d^7) δ -2169 ppm ESI-MS m/z 734.0, 735.0, 736.0, 737.0, 738.0 [(M –Cl + H_2O + Na)$^+$; calcd for $C_{27}H_{24}N_6O_2Pt^+$:735.0, 736.0, 737.0, 738.0, 739.0 Elemental analyses $C_{27}H_{24}Cl_2N_6O_2Pt \cdot 4HCl$, fnd (calc): C, 37.09 (37.00); H, 3.45 (3.22); N, 9.09 (9.59).

Synthesis of the complex *trans*-[Pt(3-Clip-Phen)$_2$$Cl_2$] (**Sym-*trans***)

Step 1: synthesis of [Pt(3-Clip-Phen)$_3$Cl]NO_3 (**15**). K_2PtCl_4 (500 mg, 1.20 mmol) was dissolved in 3mL of MilliQ water. A solution of 4 equivalents of $AgNO_3$ in 7 mL of MilliQ H_2O (818 g, 4.80 mmol)

was added. The resulting solution was stirred in the dark overnight. The precipitate of AgCl was removed and the clear yellowish filtrate was evaporated until the yellow product $[Pt(H_2O)_3Cl](NO_3)$ (**14**) precipitated. The complex was filtered and washed with 5 mL of cold MilliQ water, 3 times 5 mL of ethanol, and 3 times 5 mL of diethyl ether. 6.5 equivalents of **2** (864 mg, 1.93 mmol) were dissolved in 10 mL of DMF. A solution of $[Pt(H_2O)_3Cl](NO_3)$ (**14**) (111 mg, 0.32 mmol) dissolved in 20 mL of MilliQ H_2O was added drop wise to the 3-Clip-Phen solution in the dark. A yellow precipitate immediately appeared. The mixture was stirred at room temperature for about 3.30 h, before being heated to 50 °C with an oil bath. The reaction mixture was stirred for 21 hours at this temperature, in the dark. The dense yellow precipitate was filtered and washed respectively with 3 × 10 mL of MilliQ H_2O, 3 × 10 mL of methanol, and 3 × 10 mL of diethyl ether. The compound turned brown during the drying under reduced pressure. Brown powder; yield = 52%; ^{1}H NMR (DMSO-d^6, 300 MHz) δ 9.02 (d, 2H, J = 3.06 Hz), 8.81 (br, 2H), 8.48 (d, 2H, J = 7.86 Hz), 8.06 (br, 2H), 7.98-7.89 (m, 4H), 7.74 (dd, 2H, J = 7.91, 4.42 Hz), 4.40 (br, 4H), 3.74 (br, 1H) ppm; ^{195}Pt NMR (DMSO-d^6) δ –3064 ppm (1 solvent DMSO coordinated) Important IR absorptions (neat): υ = 3368 (br), 1590 (s), 1428 (s), 1326 (br), 1238 (s), 1039 (s), 1014 (s) cm^{-1}.

Step 2: Synthesis of the complex *trans*-$[Pt(3\text{-Clip-Phen})_2Cl_2]$ (**Sym-*trans***). $[Pt(3\text{-Clip-Phen})_3Cl](NO_3)$ (**15**) (148.5 mg, 0.09 mmol) was suspended in 3 mL of DMF. 23 equivalents of HCl (200 μL, 1.53 mmol) were added to this solution. The remaining solution was heated at 85 °C for 6 h in the dark. The HCl was neutralized with NaOH. The consequent brown precipitate was filtered and washed with 3 × 10 mL of MilliQ H_2O, 3 × 10 mL of methanol, and 3 × 10 mL of diethyl ether, and dried in air. Brown powder; yield = 79%; ^{1}H NMR (DMSO-d^6, 300 MHz) δ 9.03 (d, 2H, J = 3.03 Hz), 8.81 (d, 2H, J = 2.55 Hz), 8.46 (d, 2H, J = 7.96 Hz), 8.09 (br, 2H), 7.95 (m, 4H), 7.72 (dd, 2H, J = 8.00, 4.33 Hz), 4.55 (br, 4H), 4.06 (br, 1H) ppm; ^{195}Pt NMR (DMSO-d^6) δ –3488 ppm (2 solvent molecules DMSO coordinated) Important IR absorptions (neat): υ = 3370 (br), 1590 (s), 1428 (s), 1359 (s), 1328 (s), 1240 (s), 1040 (s), 1021 (s) cm^{-1}. Elemental analyses $C_{54}H_{42}Cl_2N_{10}O_4Pt \cdot 8HCl$, fnd (calc): C, 43.45 (44.65); H, 3.44 (3.47); N, 9.88 (9.64).

Cleavage studies. The solutions of the complexes were prepared as 1 mM solutions in DMSO, and diluted to the appropriate concentration with water, typically corresponding to a concentration 4 times higher than the final concentration of the cleavage experiment. 5 μL of complex solution were added to 10 μL of supercoiled ΦX174 DNA ((Invitrogen)7 nM, 40 μM base pairs) in 6 mM NaCl, 20 mM sodium phosphate buffer (pH 7.2), and incubated for 20 h at 37 °C. To initiate the cleavage, 5 μL of a 20 mM mercaptopropionic acid solution in water were added, and the resulting reaction mixture was incubated at 37 °C for 1 h. The reaction was quenched at 4 °C, followed by the addition of 4 μL of loading buffer (bromophenol blue) prior to its loading on a 0.8 % agarose gel containing 1 μg mL^{-1} of ethidium bromide. The gels were run at a constant voltage of 70 V for 90 minutes in TBE buffer containing 1 μg mL^{-1} of ethidium bromide. The gels were visualized under a UV transilluminator, and the bands were quantified using a BioRad Gel Doc 1000 apparatus interfaced with a computer. A correction factor of 1.47 has been applied to quantify the amount of supercoiled DNA (form I) present in all samples.

Analysis of platinum adducts by high resolution polyacrylamide gel electrophoresis. (Experiments have been performed at the CNRS in Toulouse) The ODNs I, II and the primer were purchased from Eurogentec, and purified on a 15% polyacrylamide gel. The concentrations of single-stranded ODNs were determined by UV titration at 260 nm.[33] The ODNs were end-labeled with ^{32}P using standard procedures with T4 polynucleotide kinase (New England BioLabs) and [γ-^{32}P]ATP for the 5'-end, before being purified on a MicroSpin G25 column (Pharmacia).[34]

Analysis of the platinum-DNA adducts. 5'-end labeled ODN I (2 μM) was annealed to 1 equiv of its complementary strand ODN II in 1100 μL of Tris-HCl (20 mM, pH 7.2) by heating to 90 °C for 5 minutes, followed by slow cooling to room temperature. Then, 60 μL of this solution was incubated with 60 μL of complex solution (6 μM cisplatin or 20 μM of complexes **Asym-*cis***, **Asym-*trans*** and **Sym-*trans***) for 20 or 96 hours at 37 °C, followed by precipitation with 100 μL of sodium acetate buffer (3 M, pH 5.2) and 1300 μL of cold ethanol. Pellets were rinsed with ethanol and lyophilized. Platinum-DNA adducts were analyzed by denaturing 20 % polyacrylamide gel electrophoresis followed by phosphor imagery.

Primer extension experiments. ODN I (2 μM) was annealed to ODN II (2 μM) in 1100 μL of Tris-HCl (20 mM, pH 7.2) by heating to 90 °C for 5 minutes, followed by slow cooling to room temperature. Then, 60 μL of this solution was incubated with 60 μL of complex solution (6 μM cisplatin or 20 μM complex **Asym-*cis***, **Asym-*trans*** and **Sym-*trans***) for 20 hours at 37 °C, followed by precipitation with 100 μL of sodium acetate buffer (3 M, pH 5.2) and 1300 μL of cold ethanol. Pellets were rinsed with ethanol and lyophilized. For primer extension, an aliquot of this solution (0.25 μM) was annealed with 5'-end labeled primer (0.25 μM) and 1 equiv of ODN I (0.25 μM) in the enzyme buffer before the addition of 250 μM dGTP, dCTP, dATP and dTTP and 2.5 units Taq polymerase (final concentrations are given, the total volume was 10 μL). The samples were reacted at 37 °C for 120 minutes then the samples received 1 μL of Na_2H_2edta (0.2 M) then 5 μL of sample were analyzed by denaturing 20 % polyacrylamide gel electrophoresis then phosphorimagery. Maxam and Gilbert sequencing scale, including a final scale of T4 polynucleotidekinase digestion to remove 3'-end-phosphates, was used to analyze DNA fragments.[35]

Cytotoxicity tests. (Experiments have been performed in the group of R. Kiss in Université Libre de Bruxelles in Brussels) The experimental procedure described below has been used for the following cell lines: Hs683, U373MG, HCT-15, LoVo, MCF-7 and A549.

- Hs683 and U-373MG: glioblastomas
- HCT-15 and LoVo: colorectal cancers
- A549: lung cancer
- MCF-7: breast cancer

The cells were cultured at 37 °C in sealed (airtight) Falcon plastic dishes (Nunc, Gibco, Belgium) containing Eagle's minimal essential medium (MEM, Gibco) supplemented with 5 % fetal calf serum (FCS). All the media were supplemented with a mixture of 0.6 mg mL^{-1} glutamine (Gibco), 200 IU mL^{-1} penicillin (Gibco), 200 IU mL^{-1} streptomycin (Gibco), and 0.1 mg mL^{-1} gentamycin (Gibco). The FCS was heat-inactivated for 1 h at 56 °C.

The MTT test is an indirect technique, which allows the rapid measurement (5 days) of the effect of a given product on the global growth of a cell line.[36] This test is based on the measurement of the number of metabolically active living cells able to transform the yellowish MTT product (3-(4,5-dimethylthiazol-2-yl)-2,5 diphenyl tetrazolium bromide) into the blue product, formazan, via mitochondrial reduction performed by living cells.[36] The amount of formazan obtained at the end of the experiment is measured with a spectrophotometer, and is therefore directly proportional to the number of living cells at that moment. The measurement of the OD (Optical density) provides a quantitative measurement of the effect of the product investigated as compared to control (untreated cells), and enables it to be compared to other reference products.[36]

The cells are put to grow in flat-bottomed 96-well micro-wells with 100 μL of cell suspension per well and between 1,000 and 5,000 cells/well depending on cell type. Each cell line is seeded in its own cell culture medium. After a 24-hour period of incubation at 37 °C, the culture medium is replaced by 100 μL of fresh medium in which the substance to be tested has been dissolved at the different concentrations required. In our experiments, the 6 compounds (**Asym-*cis***, **Asym-*trans***, **Sym-*trans***, **Cu(Asym-*cis*)**, **Cu(Asym-*trans*)**, **Cu(Sym-*trans*)**, Cu-3-Clip-Phen and cisplatin) were tested at 10^{-5} M to 10^{-9} M concentrations with ½ log steps. Each experimental condition is carried out in six different wells. After 72 hours of incubation at 37 °C with the drug (experimental conditions) or without the drug (control), the medium is replaced by 100 μL MTT at the concentration of 1 mg mL^{-1} dissolved in RPMI. The micro-wells are then incubated for 3 h at 37 °C and centrifuged at 400 G for 10 minutes. The MTT is removed, and the formazan crystals formed are dissolved in 100 μL of DMSO. The micro-wells are then shaken for 5 minutes and read on a spectrophotometer at 2 wavelengths (570 nm: the maximum formazan absorbance wavelength; 630 nm: the background noise wavelength).[36]

5.5 References

[1] B. A. Chabner, T. G. Roberts, *Nat. Rev. Cancer* **2005**, *5*, 65.

[2] L. H. Hurley, *Nat. Rev. Cancer* **2002**, *2*, 188.

[3] E. R. Jamieson, S. J. Lippard, *Chem. Rev.* **1999**, *99*, 2467.

[4] J. Y. Chen, J. Stubbe, *Nat. Rev. Cancer* **2005**, *5*, 102.

[5] L. H. Einhorn, *Proc. Natl. Acad. Sci. U. S. A.* **2002**, *99*, 4592.

[6] B. Rosenberg, L. Vancamp, T. Krigas, *Nature* **1965**, *205*, 698.

[7] B. Rosenberg, L. Vancamp, J. E. Trosko, V. H. Mansour, *Nature* **1969**, *222*, 385.

[8] A. M. J. Fichtinger-Schepman, J. L. van der Veer, J. H. J. den Hartog, P. H. M. Lohman, J. Reedijk, *Biochemistry* **1985**, *24*, 707.

[9] M. A. Fuertes, C. Alonso, J. M. Perez, *Chem. Rev.* **2003**, *103*, 645.

[10] Y. P. Ho, S. C. F. Au-Yeung, K. K. W. To, *Med. Res. Rev.* **2003**, *23*, 633.

[11] Z. H. Siddik, *Oncogene* **2003**, *22*, 7265.

[12] H. Umezawa, K. Maeda, T. Takeuchi, Y. Okami, *J. Antibiot.* **1966**, *19*, 200.

[13] C. Boldron, S. A. Ross, M. Pitié, B. Meunier, *Bioconjugate Chem.* **2002**, *13*, 1013.

[14] M. Pitié, C. Boldron, H. Gornitzka, C. Hemmert, B. Donnadieu, B. Meunier, *Eur. J. Inorg. Chem.* **2003**, 528.

[15] M. Pitié, B. Sudres, B. Meunier, *Chem. Commun.* **1998**, 2597.

[16] M. Pitié, C. J. Burrows, B. Meunier, *Nucleic Acids Res.* **2000**, *28*, 4856.

[17] M. Pitié, J. D. Van Horn, D. Brion, C. J. Burrows, B. Meunier, *Bioconjugate Chem.* **2000**, *11*, 892.

[18] S. Komeda, *PhD thesis*, Leiden University (Leiden), **2002**.

[19] T. D. McGregor, A. Hegmans, J. Kasparkova, K. Neplechova, O. Novakova, H. Penazova, O. Vrana, V. Brabec, N. Farrell, *J. Biol. Inorg. Chem.* **2002**, *7*, 397.

[20] S. Radulovic, Z. Tesic, S. Manic, *Curr. Med. Chem.* **2002**, *9*, 1611.

[21] S. van Zutphen, E. Pantoja, R. Soriano, C. Soro, D. M. Tooke, A. L. Spek, H. den Dulk, J. Brouwer, J. Reedijk, *Dalton Trans.* **2006**, 1020.

[22] H. Baruah, C. L. Rector, S. M. Monnier, U. Bierbach, *Biochem. Pharmacol.* **2002**, *64*, 191.

[23] P. de Hoog, C. Boldron, P. Gamez, K. Sliedregt-Bol, I. Roland, M. Pitié, R. Kiss, B. Meunier, J. Reedijk, *J. Med. Chem.* **2007**, *50*, 3148.

[24] F. P. Intini, A. Boccarelli, V. C. Francia, C. Pacifico, M. F. Sivo, G. Natile, D. Giordano, P. De Rinaldis, M. Coluccia, *J. Biol. Inorg. Chem.* **2004**, *9*, 768.

[25] A. Martinez, J. Lorenzo, M. J. Prieto, R. de Llorens, M. Font-Bardia, X. Solans, F. X. Aviles, V. Moreno, *Chembiochem* **2005**, *6*, 2068.

[26] M. E. Budiman, R. W. Alexander, U. Bierbach, *Biochemistry* **2004**, *43*, 8560.

[27] M. D. Temple, W. D. McFadyen, R. J. Holmes, W. A. Denny, V. Murray, *Biochemistry* **2000**, *39*, 5593.

[28] M. C. Ackley, C. G. Barry, A. M. Mounce, M. C. Farmer, B. E. Springer, C. S. Day, M. W. Wright, S. J. Berners-Price, S. M. Hess, U. Bierbach, *J. Biol. Inorg. Chem.* **2004**, *9*, 453.

[29] A. Vaisman, S. G. Chaney, *J. Biol. Chem.* **2000**, *275*, 13017.

[30] J. M. Woynarowski, W. G. Chapman, C. Napier, M. C. S. Herzig, P. Juniewicz, *Mol. Pharmacol.* **1998**, *54*, 770.

[31] Y. Zou, B. van Houten, N. Farrell, *Biochemistry* **1994**, *33*, 5404.

[32] M. Pitié, A. Croisy, D. Carrez, C. Boldron, B. Meunier, *ChemBioChem* **2005**, *6*, 686.

[33] G. Fasman, *Handbook of biochemistry and molecular biology: nucleic acids, Vol. 3rd edn.*, Boca Raton, p175, **1975**.

[34] J. Sambrook, E. F. Fritsch, T. Maniatis, *Molecular Cloning: A Laboratory Manuel, Vol. 2nd Edn.*, Cold Spring Harbor Laboratory Press, Cold Spring Harbor, NY, **1989**.

[35] A. M. Maxam, W. Gilbert, *Proc. Natl. Acad. Sci. U. S. A.* **1977**, *74*, 560.

[36] L. Ingrassia, P. Nshimyumukiza, J. Dewelle, F. Lefranc, L. Wlodarczak, S. Thomas, G. Dielie, C. Chiron, C. Zedde, P. Tisnes, R. van Soest, J. C. Braekman, F. Darro, R. Kiss, *J. Med. Chem.* **2006**, *49*, 1800.

Chapter 6

Change of the bridge linking a platinum moiety and the DNA-cleaving agent Cu(3-Clip-Phen).*

New heterodinuclear platinum-copper complexes have been designed, prepared and tested for their nuclease activity. These complexes are based on the specific DNA-binding properties of its two components, i.e. a platinum moiety and Cu(3-Clip-Phen). The platinum moiety interacts with the major groove of DNA while the Cu(3-Clip-Phen) unit targets the minor groove of DNA. In order to have a major-minor groove interaction a long and flexible bridge is needed between the platinum and the Cu(3-Clip-Phen) moieties to cross the phosphate backbone. In the present chapter, complexes bearing a bridge holding an amino group are presented, which are expected to interact through hydrogen bonding with the phosphate backbone of DNA. The length of the bridge has been varied to aim for the best interaction with both the amine/phosphate backbone and to favor the major-minor groove interactions. Both complexes show similar nuclease activity, since the equal amounts of circular and linear DNA are formed at the same experimental conditions. However, these complexes show lower cleaving abilities than a related complex (mentioned in Chapter 3) whose bridge lacks the amine function, since less supercoiled DNA has reacted to circular and linear DNA at the same complex concentrations.

* Parts of this chapter will be submitted for publication (Andrea Vanossi, Liselotte Bouquerel, Paul de Hoog, Marguerite Pitié, Patrick Gamez, Bernard Meunier, and Jan Reedijk)

6.1 Introduction

Cisplatin and bleomycin are examples of DNA-targeting drugs.[1-6] Both compounds are very effective agents in clinical use and have significantly improved the survival of cancer patients. The use of cisplatin and bleomycin is believed to induce reversible or irreversible modifications of the nucleic acids, which influences the transcription and/or replication of DNA inside the cancer cells, initiating ultimately the cell death. Both agents are used in combination for the treatment of testicular cancer. The curing rate for this disease is approaching 100%.[7]

The anti-proliferate activity of cisplatin was discovered by Rosenberg *et al.* in 1965.[8] Cisplatin is believed to form kinetically inert coordination bonds with DNA, thereby disrupting its transcription and replication.[5] Cisplatin binds to two neighboring guanines in the major groove of DNA. This bonding interaction results in the bending of the DNA double helix towards the major groove and the concomitant opening of the minor groove.[9, 10] Despite the success of cisplatin, the drug has severe side effects; moreover, the cancer cells can develop resistance to the treatment.[11-13]

Bleomycin was first isolated from *Streptomyces Verticillus* by Umezawa *et al.* in 1966.[14] Bleomycin is able to cleave DNA in the presence of copper, iron or cobalt ions. The potential of this compound has inspired many research groups to develop a number of biomimetic models. For instance, the group of Sigman has found that $[Cu^{I/II}(phen)_2]$ shows good nuclease activity.[15, 16] The cleavage activity of this complex was increased drastically by the linkage of both phenanthroline ligands through their C3-position, producing Cu(3-Clip-Phen).[17, 18] Cu(3-Clip-Phen) was designed to improve the cleaving activity by decreasing the dissociation of the ligand. In addition, the bridge connecting the Phen ligands possesses an amino group which can be used to link this cleaving agent to other DNA interacting molecules. For example, Cu(3-Clip-Phen) moiety has been functionalized with a distamycin analog or a platinum moiety.[19, 20]

Mixed platinum-Cu(3-Clip-Phen) complexes have been designed to form kinetically inert bonds with DNA and to cleave the strands in the close proximity of the platinum-DNA adduct.[19] Indeed, the platinum part of the heterodinuclear complex may act as an anchor to DNA, forcing the Cu(3-Clip-Phen) moiety to remain in its proximity. In chapter 3, two complexes have been synthesized: (i) **Cu3CP-6-Pt** was designed to have a flexible bridge between the platinum group and the Cu(3-Clip-Phen) moiety; however, the linker is not long enough to allow a major-minor groove interaction with DNA, (ii) **Cu3CP-10-Pt** has been designed to favor a minor-major groove interaction with DNA. Both complexes are able to induce direct double strand cuts.

The influence of the length of the bridging unit of the bifunctional complexes on the nuclease activity has now been investigated by taking two different lengths of the spacer (Figure 6.1), and the results are reported in the present chapter. An amino group has been introduced in the bridge aimed at improving the interaction with DNA, as well as the solubility of the complex in water, since the amino group is protonated at physiological conditions.[21] The ability of the Cu(3-Clip-Phen) part of the heterodinuclear conjugates to mediate direct double strand cuts is expected to be retained in these complexes designed to direct the platinum and the Cu(3-Clip-Phen) moieties to their preferential site of interaction, namely the major and minor groove, respectively. The distance between the Pt and the Cu ions is varied, but in both complexes, the 3-Clip-Phen unit is separated by six methylene groups from the amine function. The length of the bridge linking the secondary amine group to the platinum unit corresponds to either six or ten methylene groups.

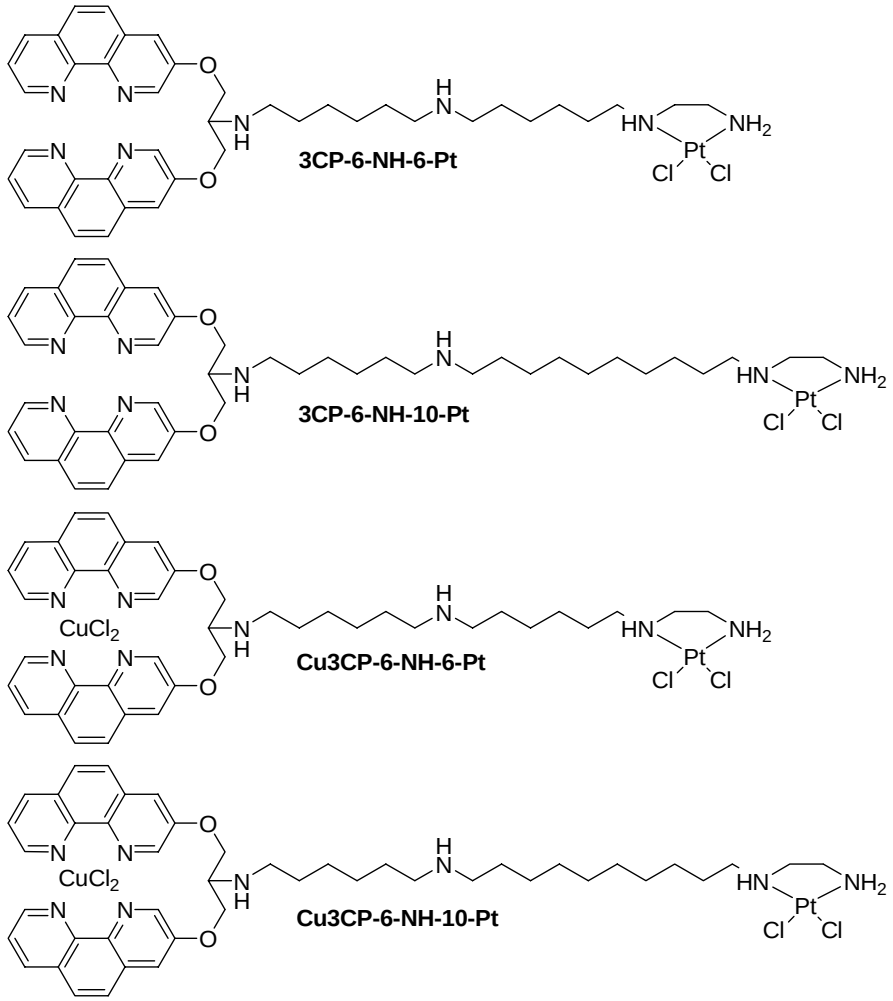

Figure 6.1 Schematic representations of the platinum complexes **3CP-6-NH-6-Pt**, **3CP-6-NH-10-Pt**, and the heterodinuclear platinum-copper complexes **Cu3CP-6-NH-6-Pt**, **Cu3CP-6-NH-10-Pt**.

6.2 Results and discussion

6.2.1 Synthesis and characterization of the heterodinuclear complexes

The synthetic pathways for the preparation of **3CP-6-NH-6-Pt**, **3CP-6-NH-10-Pt**, **Cu3CP-6-NH-6-Pt** and **Cu3CP-6-NH-10-Pt** are depicted in Schemes 6.1-6.5. The bridge connecting the platinum and the Cu(3-Clip-Phen) moieties is composed of two parts. The first fragment is the unit between the Cu(3-Clip-Phen) entity and the NH group near the middle of the bridge, and the second fragment is the unit between the NH group and the platinum unit. The synthetic strategy to generate **Cu3CP-6-NH-6-Pt** and **Cu3CP-6-NH-10-Pt** consists in preparing three building blocks that can be coupled by reductive amination reactions. The first building block can be obtained using two slightly different pathways, starting from 6-aminohexanol (Scheme 6.1). Two different synthetic pathways have been employed, because the Fmoc group is unstable in the synthesis of compound **22**. Actually, the amino group can be protected by either a Fmoc group yielding 83% of (9H-fluoren-9-yl)methyl-6-hydroxyhexylcarbamate (**16**), or by a Boc generating 92% of *Tert*-butyl 6-hydroxyhexylcarbamate (**18**).

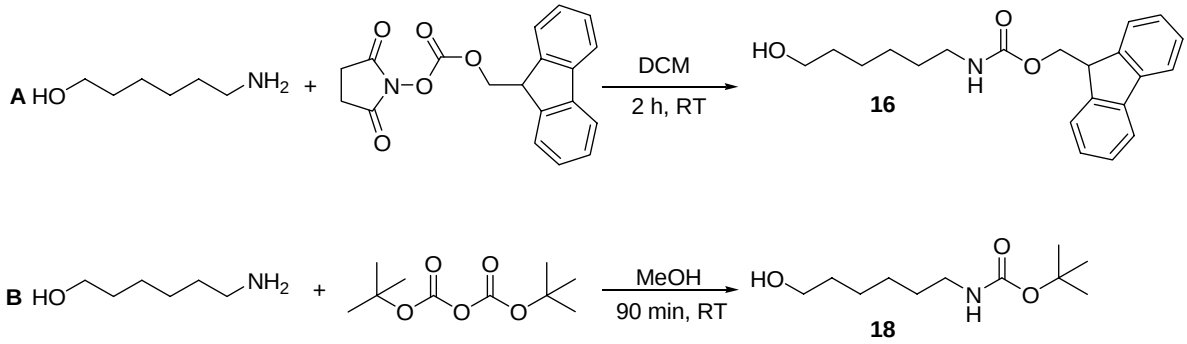

Scheme 6.1 Synthesis of intermediates **16** and **18**, which are two precursors of the first fragment of the bridge. In route **A**, the amine moiety is protected by a (9H-fluoren-9-yl)methylcarbamate (Fmoc) group; in route **B**, the amine moiety is protected by a Boc group.

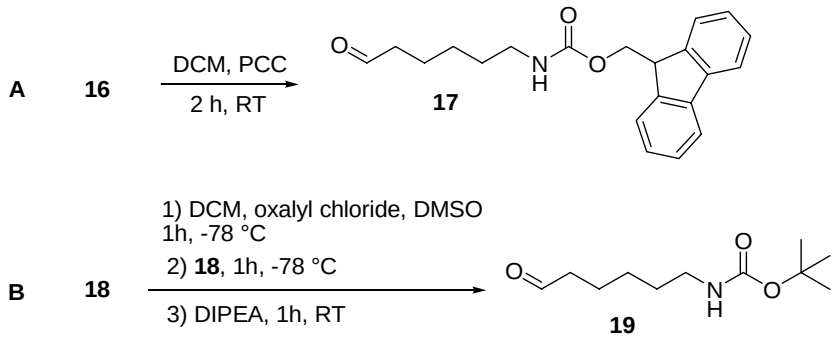

Scheme 6.2 Synthesis of **17** and **19**. In route **A**, compound **16** is oxidized with Pyridinium ChloridotrioxidoChromate (PCC); in route **B**, compound **18** is obtained applying the Swern oxidation method.

The alcoholic function of **16** and **18** can be oxidized in two different ways (Scheme 6.2). (9H-fluoren-9-yl)methyl 5-formylpentylcarbamate (**17**) has been obtained by reaction of **16** with pyridinium chloridotrioxidochromate (PCC) in dichloromethane at RT, yielding 63% of the desired product. The conversion of **18** to *tert*-butyl-5-formylpentylcarbamate (**19**) was efficiently carried out using Swern oxidation.[22] In this way, **19** was obtained with a yield of 98%.

The coupling of compound **17** with 3-Clip-Phen in methanol by reductive amination yields both (9H-fluoren-9-yl)-6-(3-(1,10-phenanthrolin-3-yloxy)-1-(1,10-phenanthrolin-8-yloxy)propan-2-ylamino)methyl hexylcarbamate (**21**) and *N'*-(3-(1,10-phenanthrolin-3-yloxy)-1-(1,10-phenanthrolin-8-yloxy)propan-2-yl)hexane-1,6-diamine (**22**) (Scheme 6.3). After removal of the methanol solvent, the resulting mixture is reacted with piperidine overnight to obtain compound **21** with a yield of 53%. The coupling of compound **19** with 3-Clip-Phen by reductive amination yields *tert*-butyl-6-(3-(1,10-phenanthrolin-3-yloxy)-1-(1,10-phenanthrolin-8-yloxy)propan-2-ylamino)hexylcarbamate (**20**) with a yield of 30%. The desired compound **22** is obtained quantitatively after deprotection of the Boc group by reaction of **20** with TFA at 0 °C during 30 minutes.

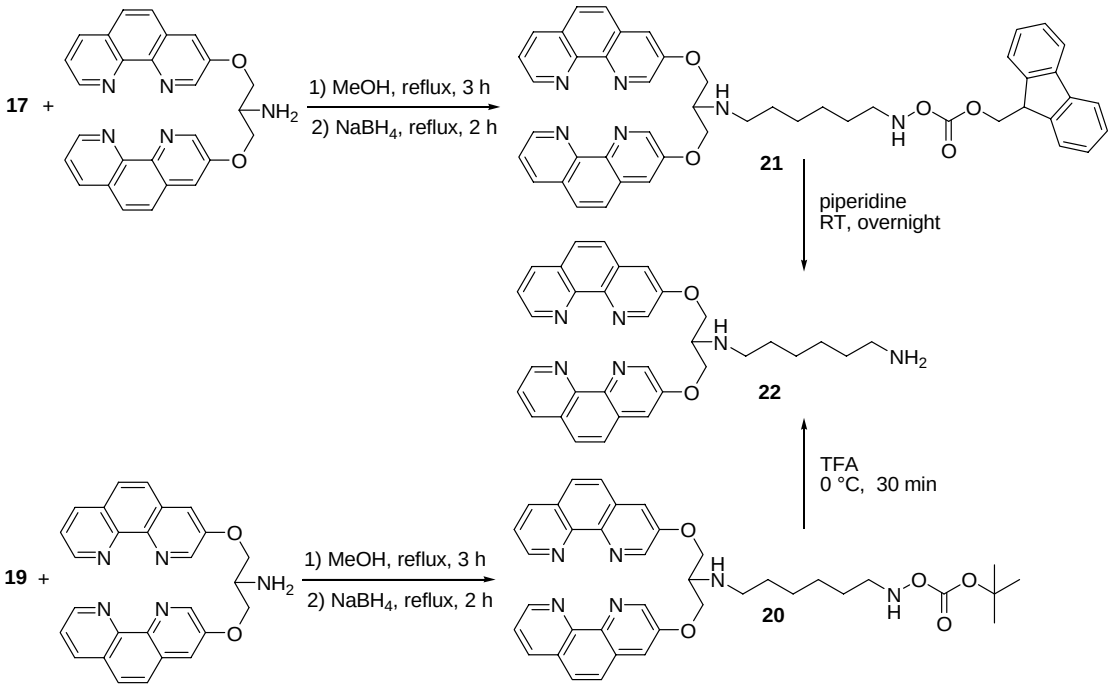

Scheme 6.3 Synthesis of **20**, **21** and **22**.

The synthetic procedures to generate the building blocks **7** and **8** (Figure 6.2), which represent the functional part for the binding of platinum, have been described in detail in chapter 3. The couplings of **22** with **7** or **8** by reductive amination in methanol yield respectively *N*-(3-(1,10-phenanthrolin-3-yloxy)-1-(1,10-phenanthrolin-8-yloxy)propan-2-yl)-*N*6-(6-(2-amino-*tert*-butylacetate-ethylamino-*tert*-butyl acetate)hexyl)hexane-1,6-diamine (**23**) (with a yield of 42%) and N-(6-(3-(1,10-phenanthrolin-3-yloxy)-1-(1,10-phenanthrolin-8-yloxy)propan-2-ylamino)hexyl)-

*N*10-[(2-amino-*tert*-butylacetate)*tert*-butylacetate-ethyl]decane-1,10-diamine (**24**) (with a yield of 22%) (Scheme 6.4).

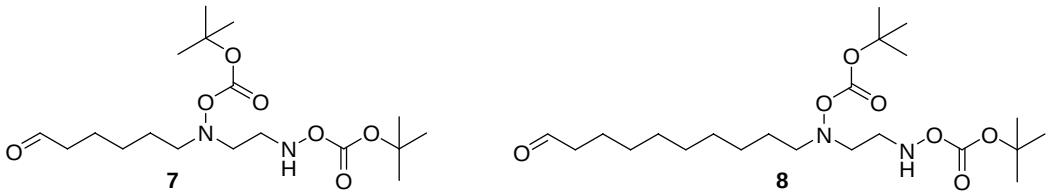

Figure 6.2 Structural formulae of building blocks **7** and **8**.

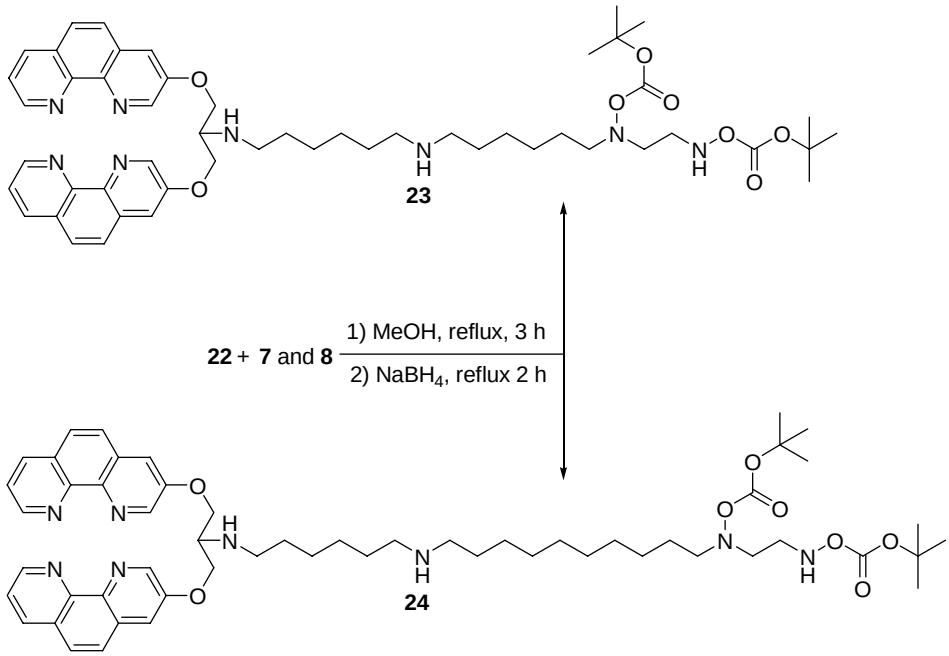

Scheme 6.4 Synthesis of **23** and **24**.

Prior to the coordination experiments, the amino groups of ligands **23** and **24** have to be deprotected (Scheme 6.5). The Boc groups are removed using TFA at 0 °C, leading to the free amines within a reaction time of 1 hour. The excess of TFA is evaporated under reduced pressure. The terminal ethylenediamine moiety is subsequently platinated with K_2PtCl_4 stoichiometrically in a methanol-water mixture at RT overnight. Tetra-*N*-butylammonium chloride (Pt:Cl ratio 1:10) is added to prevent the hydrolysis of the platinum coordination unit in the methanol-water solution. The compound rapidly precipitates and can be isolated by filtration. The crude product is washed with methanol and water to remove the remaining starting materials. The yields for **3CP-6-NH-6-Pt** and **3CP-6-NH-10-Pt** are respectively 74% and 63%. The copper-platinum complexes are obtained in two steps starting with the reaction of **3CP-6-NH-6-Pt** and **3CP-6-NH-10-Pt** in DMF with $CuCl_2$ at 50 °C overnight (Scheme 6.5). The desired multifunctional products **Cu3CP-6-NH-6-Pt** and **Cu3CP-6-NH-10-Pt** are isolated by precipitation in diethyl ether and characterized and analyzed by IR, UV-Vis and EPR.

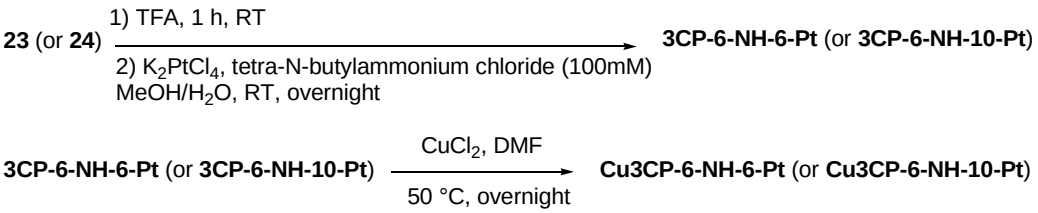

Scheme 6.5 Preparation of the complexes **3CP-6-NH-6-Pt**, **3CP-6-NH-10-Pt**, **Cu3CP-6-NH-6-Pt** and **Cu3CP-6-NH-10-Pt**. **3CP-6-NH-6-Pt** and **3CP-6-NH-10-Pt** have been characterized by ^{1}H-NMR, ^{195}Pt-NMR, IR, Mass and UV-Vis. **Cu3CP-6-NH-6-Pt** and **Cu3CP-6-NH-10-Pt** have been characterized by IR, UV-Vis and EPR.

The preparation of species **Cu3CP-6-NH-6-Pt** and **Cu3CP-6-NH-10-Pt** as depicted in Scheme 6.5 are freshly dissolved in DMSO/H_2O (1/9) prior to the DNA-cleavage experiments. All parent solutions have a concentration of 1 mM. Frozen-solution EPR spectra have been recorded for the parent solutions and compared to the spectrum of Cu^{2+} in DMSO. The EPR spectra of **Cu^{II}3CP-6-NH-6-Pt** (Figure 6.2) and **Cu3^{II}CP-6-NH-10-Pt** (Figure 6.3) show broad peaks that in part overlap with those of a blank of Cu^{2+} in DMSO. It appears that under these dilute conditions part of the copper dissociates from **Cu^{II}3CP-6-NH-10-Pt** and **Cu^{II}3CP-6-NH-6-Pt** in DMSO/H_2O to produce $[Cu(DMSO)_x(H_2O)_{6-x}]^{2+}$ species (see black circles in Figure 6.2 and Figure 6.3, respectively) or part of the copper has not been coordinated during the synthesis of **Cu3CP-6-NH-10-Pt** and **Cu3CP-6-NH-6-Pt**. Nonetheless, some unique peaks for other species are observed, which are indicated by open grey squares in Figure 6.2 and Figure 6.3. These peaks correspond to copper species coordinating one, two or more nitrogen ligands. The EPR spectrum of **Cu^{II}3CP-6-NH-10-Pt** shows even a third Cu^{II} species that is coordinating one or more nitrogen ligands, which is indicated by a light grey asterisk in Figure 6.3.

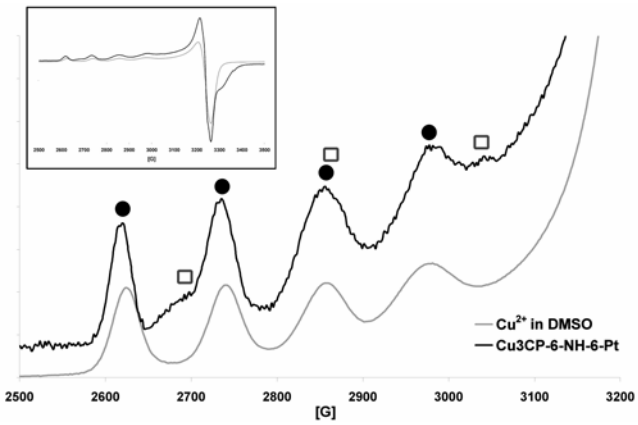

Figure 6.2 Enlargement of the hyperfine splittings of the frozen-solution EPR spectra of Cu^{2+} in DMSO (grey line), and of **Cu3CP-6-NH-6-Pt** in DMSO/H_2O (1/9, 1mM) (black line). The inset shows the full spectrum of the frozen EPR spectra of Cu^{2+} in DMSO (grey line), and of **Cu3CP-6-NH-6-Pt** in DMSO/H_2O (1/9, 1mM) (black line). The black dots represent the hyperfine splittings of the spectrum of Cu^{2+} in DMSO. The open grey squares symbolize a second Cu^{II} species present in the frozen solution of **Cu3CP-6-NH-6-Pt** in DMSO/H_2O.

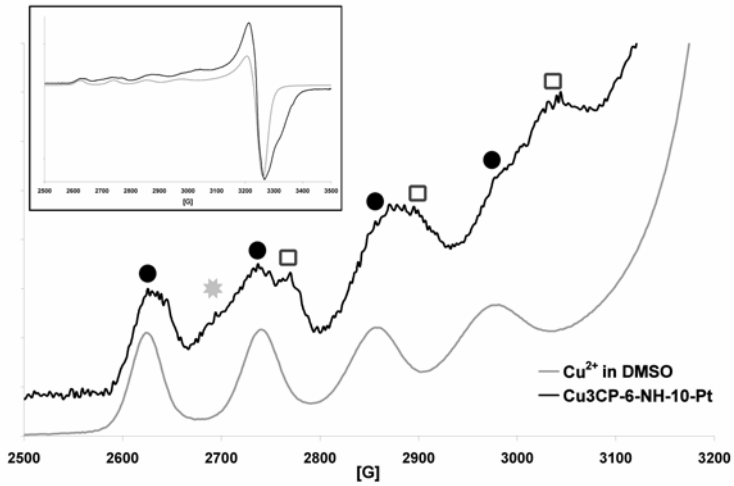

Figure 6.3 Enlargement of the hyperfine splittings of the frozen-solution EPR spectra of Cu^{2+} in DMSO (grey line), and of **Cu3CP-6-NH-10-Pt** in DMSO/H_2O (1/9, 1mM) (black line). The inset shows the full spectrum of the frozen EPR spectra of Cu^{2+} in DMSO (grey line), and of **Cu3CP-6-NH-10-Pt** in DMSO/H_2O (1/9, 1mM) (black line). The black dots represent the hyperfine splittings of the spectrum of Cu^{2+} in DMSO. The open grey squares symbolize a second, the light grey stars the third Cu^{II} species in the frozen solution of **Cu3CP-6-NH-10-Pt** in DMSO/H_2O.

6.2.2 Cleavage of supercoiled DNA

The conversion of supercoiled circular ΦX174 DNA (form I) into the relaxed (form II) and the linear (form III) conformations has been monitored to compare the aerobic cleavage abilities of complexes **Cu3CP-6-Pt**, **Cu3CP-6-NH-6-Pt** and **Cu3CP-6-NH-10-Pt** in the presence of a reducing agent (Figure 6.4). For this purpose, the complexes have been incubated for 20 h to allow the formation of platinum-DNA adducts. The nuclease activity is subsequently initiated by the addition of 5 mM mercaptopropionic acid (MPA) in air. **Cu3CP-6-Pt** described in chapter 3 has been used as a reference, since it has also one platinum unit and one Cu(3-Clip-Phen) moiety, and a flexible bridge. In addition, **Cu3CP-6-Pt** showed a higher nuclease activity compared to the **Cu3CP-10-Pt** as also described in chapter 3. The complexes **Cu3CP-6-NH-6-Pt** and **Cu3CP-6-NH-10-Pt** show comparable nuclease activities. At a complex concentration of 500 nM, both **Cu3CP-6-NH-6-Pt** and **Cu3CP-6-NH-10-Pt** show the formation of circular DNA, but no linear DNA is generated (compare lanes 6 and 10, Figure 6.4). At a complex concentration of 750 nM, circular and linear DNA are visible, even though supercoiled DNA is still present (compare lanes 7 and 11, Figure 6.4). These results suggest that the complexes are able to perform direct double-strand cuts, most likely as a result of multiple single-strand cuts in the close proximity of the platinum adduct. However, **Cu3CP-6-Pt** (reported in chapter 3) cleaves DNA more effectively. At a **Cu3CP-6-Pt** concentration of 250 nM, the amounts of cleavage products observed are comparable to those achieved with the experiments using **Cu3CP-6-NH-6-Pt** and **Cu3CP-6-NH-10-Pt** concentrations of 750 nM. The

EPR spectra of these complexes have shown that a fraction of the copper dissociates from the 3-Clip-Phen moiety in an aqueous DMSO solution. So, for this reason it is possible that the cleaving ability of these complexes is impeded. It should be realized that, the EPR spectra have been recorded in DMSO/H_2O (10%/90%), whereas the DNA cleavage solutions are diluted with a minimum of 1000 times (complex concentration 1 μM) with water, so they contain 0.01 % DMSO. Thus, the dissociation of the copper from the 3-Clip-Phen moiety observed in the EPR spectra is not necessarily occurring in the DNA cleavage solutions, or at least not to the same degree.

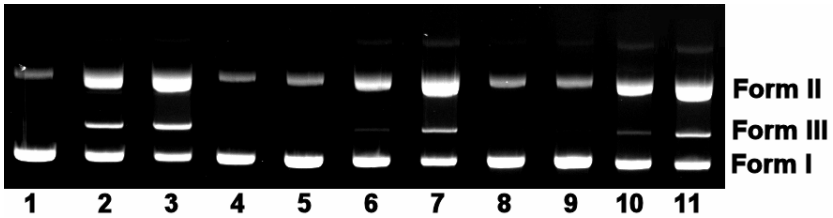

Figure 6.4 Comparison of the oxidative cleavage of ΦX174 plasmid DNA mediated by **Cu3CP-6-Pt**, **Cu3CP-6-NH-6-Pt** and **Cu3CP-6-NH-10-Pt** in the presence of 5 mM MPA. Lane 1: control DNA. Lane 2: 250 nM **Cu3CP-6-Pt**. Lane 3: 500 nM **Cu3CP-6-Pt**. Lane 4: 750 nM **Cu3CP-6-NH-6-Pt** without MPA. Lane 5: 250 nM **Cu3CP-6-NH-6-Pt**. Lane 6: 500 nM **Cu3CP-6-NH-6-Pt**. Lane 7: 750 nM **Cu3CP-6-NH-6-Pt**. Lane 8: 750 nM **Cu3CP-6-NH-10-Pt** without MPA. Lane 9: 250 nM **Cu3CP-6-NH-10-Pt**. Lane 10: 500 nM **Cu3CP-6-NH-10-Pt**. Lane 11: 750 nM **Cu3CP-6-NH-10-Pt**.

6.3 Conclusions

Cu3CP-6-NH-6-Pt and **Cu3CP-6-NH-10-Pt**, two heterodinuclear complexes bearing an amino group in the bridge linking the metallic units, have been designed and successfully synthesized with the aim to favor a triple interaction with DNA, namely with the major groove (platinum unit), the minor groove (copper unit) and the phosphate backbone (amine function). In addition, the aqueous solubility of the complexes is enhanced, thanks to this central amino group which is protonated at physiological conditions. It appears that the copper in the DMSO/H_2O solution of **Cu3CP-6-NH-6-Pt** and **Cu3CP-6-NH-10-Pt** is partially dissociated from the complexes in order to form the $[Cu(DMSO)_x(H_2O)_{6-x}]^{2+}$ species. Unfortunately, the incorporation of an amine function in the bridge in these complexes does not give rise to an improvement of the nuclease activity, because the complexes are less efficient than the amine-free **Cu3CP-6-Pt** complex, has which has been reported in Chapter 3.

6.4 Experimental

General procedures and materials: All NMR measurements were performed on a 300 MHz Bruker DPX300 spectrometer with a 5 mm multi-nucleus probe. The temperature was kept constant at

298 K using a variable temperature unit. Chemical shifts are reported in δ (parts per million) relative to the solvent peak or tetramethylsilane (TMS) as reported for each compound. MS spectra were taken on a ThermoFinnegan AQA ESI-MS. Sample solutions (in CH_2Cl_2 or methanol) were introduced in the ESI source by using a Dionex ASI-100 automated sampler injector and an eluent running at 0.2 mL/minute. Reagents were purchased from Aldrich or Acros, unless otherwise stated. Solvents were obtained from Applied Biosystems Inc. C, H and N analyses were carried out using an automatic Perkin-Elmer 2400 series II CHNS/O micro analyzer. X-band powder EPR spectra were obtained on a Bruker-EMX*plus* electron spin resonance spectrometer (Field calibrated with DPPH; g = 2.0036).

(9H-fluoren-9-yl)methyl-6-hydroxyhexylcarbamate (16). Commercially available 6-aminohexanol (3.77 g, 32.20 mmol) was dissolved 130 mL of DCM. The resulting solution was cooled to 0 °C and a solution of *N*-(9-Fluorenylmethoxycarbonyloxy)succinimide (Fmoc-Osu) (5.39 g, 15.97 mmol) in DCM (74 mL) was added drop-wise over a period of 30 minutes. During the addition, a white precipitate formed. The suspension was stirred for 1 h 30 at RT. The precipitate was filtered off through a glass filter. The filtrate was extracted with 0.5 M aqueous HCl (3 × 200 mL). The pooled organic layer was dried over Na_2SO_4. The white product (**16**) was dried in air. White powder; yield = 83 %; ^{1}H NMR ($CDCl_3$, 300 MHz) δ 1.38 (m, 2H), 1.57 (t, 2H, J = 9.7 Hz), 3.20 (t, 2H, J = 6.5 Hz), 3.65 (t, 2H, J = 6.2 Hz), 4.22 (t, 1H, J = 6.7 Hz), 4.40 (d, 2H, J = 6.8 Hz), 4.75 (s, 1H), 7.31 (dd, 2H, J = 1.1 Hz, 7.4 Hz), 7.40 (t, 2H, J = 7.3 Hz), 7.59 (d, 2H, J = 7 Hz), 7.76 (d, 2H, J =7.5 Hz) ppm. ^{13}C NMR ($CDCl_3$, 300 MHz) δ 25.3, 26.3, 29.9, 32.5, 40.8, 47.3, 62.7, 66.4, 119.9, 124.9, 127.0, 127.7, 141.3, 143.8, 157.3 ppm. Low resolution MS (ESI >0) m/z 362.08 [$(M+Na)^+$; calcd for $C_{21}H_{25}NO_3Na^+$: 362.42]. Anal. Calcd for $C_{21}H_{25}NO_3$: C 74.31, H 7.42, N 4.13; found: C 74.08, H 7.64, N 4.13.

(9H-fluoren-9-yl)methyl 5-formylpentylcarbamate (17). A solution of **16** (2.26 g, 6.67 mmol) in 70 mL of DCM containing activated molecular sieves was stirred for 30 minutes at RT. PCC (2.16 g, 10.01 mmol) was added at once and the resulting mixture was stirred for 2 h at RT. The reaction mixture was then filtered and absorbed on 3 g of silica. The crude was purified by column chromatography (SiO_2, DCM:MeOH, 95:5). Data for **17**: white powder (Yield = 63 %). ^{1}H NMR ($CDCl_3$, 300 MHz) δ 1.36 (m, 2H), 1.62-1.43 (m, 4H), 2.42 (t, 2H, J = 6.7 Hz), 3.20 (t, 2H, J = 6.5 Hz), 4.21 (t, 1H, J = 7 Hz), 4.40 (d, 2H, J = 6.8 Hz), 7.32 (dd, 2H, J = 1.1 Hz, 7.4 Hz), 7.40 (t, 2H, J = 7.4 Hz), 7.59 (d, 2H, J = 7.24 Hz), 7.76 (d, 2H, J = 7.5 Hz) ppm. ^{13}C NMR ($CDCl_3$, 300 MHz) δ 21.6, 26.2, 29.8, 40.7, 43.7, 47.3, 66.5, 119.9, 125.0, 127.0, 127.6, 141.3, 144.0, 156.4, 202.3 ppm. Low resolution MS (ESI >0) m/z 352.07 [$(M+OH)^+$; calcd for $C_{21}H_{24}NO_4^+$ during the measurement the aldehyde oxidized; the observed peak corresponds to the acid]. Anal.calcd for ($HOOC_6NHFmoc$) $C_{21}H_{23}NO_3$: C 74.75, H 6.87, N 4.15; found: C 74.76, H 7.67, N 4.18. The high percentage of H is not understood.

***Tert*-butyl 6-hydroxyhexylcarbamate (18)**. 6-Amino-1-hexanol (2.08 g, 17.7 mmol) and di-*tert*-butyl dicarbonate (4.23 g, 19.4 mmol) were dissolved in 40 mL of MeOH. The resulting reaction mixture was stirred for 90 minutes at RT. The solvent was removed under reduced pressure and the solid residue was purified by column chromatography (SiO_2, DCM:MeOH, 98:2). Data for **18**: color less oil (Yield = 92 %). ^{1}H NMR ($CDCl_3$, 300 MHz) δ 1.35 (m, 4H), 1.43 (s, 9H), 1.47-1.58 (m, 4H), 3.09 (t, 2H, J = 6.78 Hz), 3.62 (t, 2H, J = 6.44 Hz), 4.73 (br, 1H) ppm.

***Tert*-butyl-5-formylpentylcarbamate (19)**. The oxidation of **18** was performed using Swern conditions.[22] A solution of oxalyl chloride (3.6 mL, 42.5 mmol) in 60 mL of CH_2Cl_2 was stirred for one hour at –78 °C under an atmosphere of argon. Next, DMSO (3 mL, 42.5 mmol) was added to the reaction mixture. After 10 minutes, a solution of **18** (3.1 g, 14.2 mmol) in 150 mL of CH_2Cl_2 was added drop-wise and the reaction mixture was stirred at –78 °C for 1 hour. Diisopropylethylamine (DIPEA) (14 mL, 84.71 mmol) was added and the resulting solution was warmed to RT over a period of one hour. The crude was extracted with H_2O (3 × 150 mL). The pooled organic layer was dried over Na_2SO_4, and the solvent was evaporated under reduced pressure, yielding a light yellow oil (Yield = 98 %). ^{1}H NMR ($CDCl_3$, 300 MHz) δ 0.96-1.00 (m, 2H), 1.03 (s, 9H), 1.10-1.30 (m, 4H), 2.06 (m, 2H), 2.70 (m, 2H), 5.11 (br, 1H), 9.35 (s, 1H) ppm.

***Tert*-butyl-6-(3-(1,10-phenanthrolin-3-yloxy)-1-(1,10-phenanthrolin-8-yloxy)propan-2-ylamino)hexylcarbamate (20)**. To a solution of **2** (450 mg, 1.01 mmol) in 5 mL dry MeOH (distilled over magnesium) was added a solution of **19** (216.5 mg, 1.01 mmol) in 5 mL dry MeOH on activated molecular sieves. The resulting reaction mixture was refluxed for 3 h at 96 °C. Then, the solution was cooled down to 0 °C and $NaBH_4$ (80.23 mg, 2.12 mmol) was added. The resulting suspension was refluxed for two more hours. The molecular sieves were filtered off and 10 mL of H_2O were added to the filtrate to quench the excess of $NaBH_4$. The mixture was extracted with CH_2Cl_2 (3 × 50 mL). The pooled organic layer was dried over Na_2SO_4 and the solvent was evaporated under reduced pressure. The crude was purified by column chromatography (SiO_2, DCM:MeOH:NH_4OH, 97:3:0.3). Data for **20**: light brown powder (Yield = 30 %). ^{1}H NMR ($CDCl_3$, 300 MHz) δ 1.21-1.35 (m, 6H), 1.39 (s, 9H), 1.56 (m, 2H), 1.95 (br, 1H), 2.82 (t, 2H, J = 6.95 Hz), 3.06 (m, 2H), 3.55 (m, 1H), 4.37 (d, 4H, J = 5.14 Hz), 4.52 (br, 1H), 7.51 (dd, 2H, J = 8.03, 4.34 Hz), 7.57 (d, 2H, J = 2.84 Hz), 7.66 (d, 2H, J = 8.87 Hz), 7.71 (d, 2H, J = 8.85 Hz), 8.14 (dd, 2H, J = 8.08, 1.62 Hz), 8.91 (d, 2H, J = 2.73 Hz), 9.09 (dd, 2H, J = 4.32, 1.61 Hz) ppm. ^{13}C NMR ($CDCl_3$, 300 MHz) δ 27.4-27.7, 29.2, 30.5-31.0, 41.2, 48.6, 57.3, 68.4, 79.8, 115.9, 122.9, 126.9, 128.1, 130.3, 136.7, 141.6, 143.4, 146.9, 151.3, 154.8, 156.8 ppm. Low resolution MS (ESI >0) m/z 646.94 [$(M+H)^+$; calcd for $C_{38}H_{43}N_6O_4^+$: 647.79] Anal. Calcd for $C_{38}H_{42}N_6O_4 \cdot 1.3\ CH_2Cl_2$: C 62.34, H 5.94, N 11.10; found: C 62.55, H 6.08, N 10.78.

***N*$^{\eta}$-(3-(1,10-phenanthrolin-3-yloxy)-1-(1,10-phenanthrolin-8-yloxy)propan-2-yl)hexane-1,6-diamine (22)**. 6 mL of TFA were added to **20** (185 mg, 0.29 mmol) at 0 °C. The resulting solution was stirred at 0 °C for 30 minutes. The excess of TFA was evaporated under reduced pressure and the crude was purified by column chromatography (SiO_2, DCM:MeOH:NH_4OH, 90:10:1).

21 can also be prepared starting from compound **17**. To a solution of **2** (450 mg, 1.01 mmol) in 5 mL of dry MeOH (distilled over magnesium) was added a solution of **17** (340.78 mg, 1.01 mmol) in 5 mL of dry MeOH on activated molecular sieves. The mixture was refluxed for 3 h at 96 °C. The reaction mixture was cooled down to 0 °C and $NaBH_4$ (80.23 mg, 2.12 mmol) was added. The resulting suspension was refluxed for two more hours. Next, the molecular sieves were filtered off and 10 mL of H_2O were added to the filtrate to quench the excess of $NaBH_4$. The reaction mixture was extracted with CH_2Cl_2 (3 × 50 mL). The pooled organic layer was dried over Na_2SO_4 and the solvent was evaporated under reduced pressure yielding 53% of (9H-fluoren-9-yl)-6-(3-(1,10-phenanthrolin-3-yloxy)-1-(1,10-phenanthrolin-8-yloxy)propan-2-ylamino)methyl hexylcarbamate (**21**) 5 mL of piperidine were added, and the solution was stirred overnight. Diethyl ether was added to the mixture to precipitate the crude compound which was isolated by filtration. This solid was dissolved in 40 mL of CH_2Cl_2 and the resulting organic solution was

washed with water (3 × 40 mL). The organic layer was dried over Na_2SO_4 and the solvent was evaporated under reduced pressure.
The solid residue was purified by column chromatography (SiO_2 DCM:MeOH, 95:5 starting eluent, DCM:MeOH:NH_4OH, 85:15:1.5 final eluent). Data for **22**: light brown powder (Yield = quantitative). ^{1}H NMR ($CDCl_3$, 300 MHz) δ 1.24 (m, 4H), 1.53 (t, 2H, J = 6.9 Hz), 2.75 (t, 2H, J = 6.9 Hz), 2.87 (t, 2H, J = 6.9 Hz), 3.58 (m, 1H), 4.39 (m, 4H), 7.59 (m, 4H), 7.74 (m, 4H), 8.20 (d, 2H, J = 5.4 Hz), 8.99 (d, 2H, J = 2.8 Hz), 9.14 (d, 2H, J = 2.6 Hz) ppm. ^{13}C NMR ($CDCl_3$, 300 MHz): δ 26.7, 27.0, 30.3, 32.9, 41.8, 47.8, 56.5, 67.7, 115.2, 122.1, 126.1, 127.3, 129.5, 135.9, 140.5, 142.6, 146.1, 150.3, 154.0 ppm. Exact mass (ESI >0) m/z 547.28160 [$(M+H)^+$; calcd for $C_{33}H_{35}N_6O_2^+$: 547.28215], 569.26309 [$(M+Na)^+$; calcd for $NaC_{33}H_{34}N_6O_2^+$: 569.26409] Anal. Calcd: for $C_{33}H_{34}N_6O_2 \cdot 3H_2O$: C 65.98, H 6.71, N 13.99. found: C 65.43, H 6.37, N 13.65.

***N*-(3-(1,10-phenanthrolin-3-yloxy)-1-(1,10-phenanthrolin-8-yloxy)propan-2-yl)-*N*6-(6-(2-amino-*tert*-butyl acetate-ethylamino-*tert*-butyl acetate)hexyl)hexane-1,6-diamine (23) and N-(6-(3-(1,10-phenanthrolin-3-yloxy)-1-(1,10-phenanthrolin-8-yloxy)propan-2-ylamino)hexyl)-*N*10-[(2-amino-*tert*-butylacetate)*tert*-butylacetate-ethyl]decane-1,10-diamine (24)**. To a solution of **22** (99 mg, 0.18 mmol) in 5 mL of dry MeOH (distilled over magnesium) was added a solution of **7** or **8** (0.18 mmol) in 5 mL of dry MeOH on activated molecular sieves. The resulting reaction mixture was refluxed for 3 h at 96 °C. The reaction mixture was then cooled down to 0 °C and $NaBH_4$ (13.62 mg, 0.36 mmol) was added. The mixture was refluxed for two more hours. The molecular sieves were filtered off and 10 mL of H_2O were added to the filtrate to quench the excess of $NaBH_4$. The resulting solution was extracted with CH_2Cl_2 (3 × 50 mL). The pooled organic layer was dried over Na_2SO_4 and the solvent was evaporated under reduced pressure. The crude compound was purified by column chromatography (SiO_2 DCM:MeOH:NH_4OH, 90:10:1) Data for (**23**): light brown powder (Yield = 42 %). ^{1}H NMR ($CDCl_3$, 300 MHz) δ 1.33-1.45 (br, 34H), 2.60-2.84 (br, 4H), 3.18 (br, 8H), 3.56 (m, 1H), 4.39 (m, 4H), 7.57 (m, 4H), 7.73 (m, 4H), 8.19 (dd, 2H, J = 1.6 and 8 Hz), 8.95 (d, 2H, J = 2.8 Hz), 9.13 (br, 2H) ppm. ^{13}C NMR ($CDCl_3$, 300 MHz) δ 26.6-28.4, 39.6, 47.8, 49.7, 56.5, 67.7, 115.1, 122.2, 126.1, 127.3, 129.5, 135.9, 140.5, 142.6, 146.2, 150.4, 154.0 ppm. Low resolution MS (ESI >0): m/z 889.31 [$(M+H)^+$; calcd for $C_{51}H_{69}N_8O_6^+$: 890.14] Anal. Calcd for $C_{51}H_{68}N_8O_6 \cdot 1H_2O$: C 67.52, H 7.78, N 12.35; found: **C** 67.20, H 7.58, N 12.10. Data for (**24**): light brown powder (Yield = 22%). ^{1}H NMR ($CDCl_3$, 300 MHz) δ 1.20-.1.24 (m, 22H), 1.42 (br, 18H), 1.62 (m, 2H), 1.99 (br, 2H), 2.74-2.84 (m, 4H), 3.14-3.24 (m, 8H), 3.54 (m, 1H), 4.40 (br, 4H), 5.03 (br, 1H), 7.57 (dd, 2H, J = 8.00, 4.31 Hz), 7.63 (d, 2H, J = 2.75 Hz), 7.72 (d, 2H, J = 8.87 Hz), 7.77 (d, 2H, J = 8.80 Hz), 8.20 (d, 2H, J = 6.77 Hz), 8.98 (d, 2H, J = 2.72 Hz), 9.14 (d, 2H, J = 2.88 Hz) ppm. ^{13}C NMR ($CDCl_3$, 300 MHz) δ 27.6-31.1, 29.2, 40.4, 47.1, 48.5, 49.2, 57.4, 68.4, 80.0, 80.4, 116.0, 123.0, 126.9, 128.1, 130.4, 136.8, 141.5, 143.3, 146.9, 151.1, 154.8, 156.2 ppm. Low resolution MS (ESI >0): m/z 945.31 [$(M+H)^+$; calcd for $C_{55}H_{77}N_8O_6^+$: 946.25] Anal. Calcd for $C_{55}H_{76}N_8O_6 \cdot 1CH_2Cl_2$: C 65.29, H 7.63, N 10.88; found: C 65.81, H 8.09, N 8.14.

***N*1-(3-(1,10-phenanthrolin-3-yloxy)-1-(1,10-phenanthrolin-8-yloxy)propan-2-yl)-*N*6-(6-(2-aminoethylamino)hexyl)hexane-1,6-diamine, (25) or *N*1-(6-(3-(1,10-phenanthrolin-3-yloxy)-1-(1,10-phenanthrolin-8-yloxy)propan-2-ylamino)hexyl)-*N*10-(2-aminoethyl)decane-1,10-diamine (26).** Compound **24** or **25** (34.8 μmol) was added to 1 mL of TFA and the resulting reaction mixture was stirred for 1 hour at RT. The excess of TFA was evaporated under reduced pressure. The yield could not be accurately calculated, since the amount of TFA molecules interacting with the target compound could not

be estimated. Data for **25**, brown solid. ^{1}H NMR (MeOD, 300 MHz) δ 1.44 (m, 8H), 1.71 (m, 8H), 3.07 (m, 8H), 3.27-3.33 (m, 4H), 4.31 (m, 1H), 4.82 (m, 4H), 8.12-8.24 (m, 8H), 9.00-9.26 (m, 6H) ppm. ^{13}C NMR (MeOD, 300 MHz) δ 24.0, 33.9, 46.02, 57.1, 64.5, 105.4, 114.5, 121.7, 124.5, 127.8, 141.4, 142.3, 144.6, 158.1, 158.5, 159.0 ppm. Low resolution MS (ESI >0): m/z 689.21 [(M+H)$^+$; calcd for $C_{41}H_{53}N_8O_2^+$: 689.91]. Data for **26**, brown solid. ^{1}H NMR (MeOD, 300 MHz) δ 1.27-1.52 (m, 16 H), 1.69 (m, 8H), 2.93-3.08 (m, 8H), 3.29-3.40 (m, 4H), 4.40 (m, 1H), 4.83 (m, 4H), 8.23 (m, 8H), 9.07 (m, 2H), 9.17-9.23 (m, 4H) ppm. ^{13}C NMR (MeOD, 300 MHz) δ 26.6, 29.5, 36.4, 45.0, 57.1, 65.9, 117.0, 124.2, 126.9, 130.0, 132.4, 144.1, 144.5, 146.5, 154.3, 156.4, 161.8 ppm. Low resolution MS (ESI >0): m/z 745.21 [(M+H)$^+$; calcd for $C_{45}H_{61}N_8O_2^+$: 746.02].

[Pt(*N*1-(3-(1,10-phenanthrolin-3-yloxy)-1-(1,10-phenanthrolin-8-yloxy)propan-2-yl)-*N*6-(6-(2-aminoethylamino)hexyl)hexane-1,6-diamine)Cl$_2$], (3CP-6-NH-6-Pt) or [Pt(*N*1-(6-(3-(1,10-phenanthrolin-3-yloxy)-1-(1,10-phenanthrolin-8-yloxy)propan-2-ylamino)hexyl)-*N*10-(2-aminoethyl)decane-1,10-diamine)Cl$_2$], (3CP-6-NH-10-Pt). To a 100 mM methanolic solution of tetra-N-butylamonium chloride (8 mL) were added 77.9 μmol of **25** or **26**. A solution of K_2PtCl_4 (32.3 mg, 77.8 μmol) in 2.6 mL MilliQ H_2O was subsequently added, resulting in an immediate precipitation . The mixture was stirred in the dark at RT overnight. The precipitate obtained was isolated by filtration and washed respectively with MilliQ H_2O (2 × 20 mL), MeOH (2 × 20 mL) and diethyl ether (2 × 20 mL). Data for **3CP-6-NH-6-Pt**, off white powder (Yield = 74 %). ^{1}H NMR (DMSO-d^6, 300 MHz) δ 1.10-.1.80 (br, 16H), 4.22 (m, 1H), 4.68 (m, 4H), 8.04 (br, 2H), 8.21 (br, 2H), 8.67 (br, 4H), 8.79 (br, 2H), 8.88 (br, 2H), 9.04 (br, 2H) ppm. ^{195}Pt NMR (DMSO-d$_6$, 300 MHz) δ –2312 (**3CP-6-NH-6-Pt**) and –2952 (**3CP-6-NH-6-Pt** with coordinated DMSO) ppm. Exact mass (ESI >0) m/z 953.32969, 954.33218, 955.33194, 956.33016, 957.33039 [(M+H)$^+$; calcd for $C_{41}H_{53}N_8O_2PtCl_2^+$: 953.32891, 954.33135, 955.33048, 956.33069, 957.32819], IR (neat, cm^{-1}): 3412, 3052, 2935, 1596, 1436, 1254, 1176, 1104, 1042, 1021, 888, 837, 714. UV-Vis (DMSO/H_2O 10/90) λ_{max}/nm (ε/dm^3 mol^{-1} cm^{-1}): 276 (21754). Data for **3CP-6-NH-10-Pt**, off white powder (Yield = 63 %). ^{1}H NMR (DMSO-d^6, 300 MHz) δ 1.23-.1.61 (br, 24H), 2.95 (m, 8H), 4.32 (m, 1H), 4.89 (m, 4H), 7.92 (br, 2H), 8.09 (br, 2H), 8.24 (br, 4H), 8.78 (br, 2H), 8.97 (br, 2H), 9.12 (br, 2H) ppm. ^{195}Pt NMR (DMSO-d$_6$, 300 MHz) δ –2307 (**3CP-6-NH-10-Pt**) and –2952 (**3CP-6-NH-10-Pt**) with coordinated DMSO) ppm. Exact mass (ESI >0) m/z 1009.39295, 1010.39509, 1011.39470, 1012.39372, 1013.39473 [(M+H)$^+$; calcd for $C_{45}H_{61}N_8O_2PtCl_2^+$: 1009.39151, 1010.39397, 1011.39322, 1012.39348, 1013.3933], IR (neat, cm^{-1}): 3420, 3052, 2928, 2856, 1652, 1436, 1253, 1176, 1110, 1086, 1043, 888, 838, 718, 707. UV-Vis (DMSO/H_2O 10/90) λ_{max}/nm (ε/dm^3 mol^{-1} cm^{-1}): 280 (17571).

[PtCu(*N*1-(3-(1,10-phenanthrolin-3-yloxy)-1-(1,10-phenanthrolin-8-yloxy)propan-2-yl)-*N*6-(6-(2-aminoethylamino)hexyl)hexane-1,6-diamine)Cl$_4$], (Cu3CP-6-NH-6-Pt) or [PtCu(*N*1-(6-(3-(1,10-phenanthrolin-3-yloxy)-1-(1,10-phenanthrolin-8-yloxy)propan-2-ylamino)hexyl)-*N*10-(2-aminoethyl)decane-1,10-diamine)Cl$_4$], (Cu3CP-6-NH-10-Pt). To a suspension of **3CP-6-NH-6-Pt** or **3CP-6-NH-10-Pt** (24.7 μmol) in 12 mL of DMF was added $CuCl_2$ (4.64 mg, 27.2 μmol). This mixture was heated at 50 °C overnight. The volume of the green solution was reduced to 5 mL and 25 mL of diethyl ether were subsequently added causing the precipitation of the complex. The green precipitate was isolated by filtration and washed with diethyl ether (3 × 20 mL). Data for **Cu3CP-6-NH-6-Pt,** green powder (Yield = 89 %). IR (neat, cm^{-1}): 3412, 3052, 2935, 1596, 1436, 1254, 1176, 1104, 1042, 1021, 888, 837, 714. UV-Vis (DMSO/H_2O 1/9) λ_{max}/nm (ε/dm^3 mol^{-1} cm^{-1}): 326 (10697), 282 (25456). X-Band

EPR (frozen DMSO/H_2O (1/9) solution): $[Cu(DMSO)_x(H_2O)_{6-x}]^{2+}$ $g_\perp$ = 2.07, $g_{//}$ = 2.41, $A_{//}$ = 10.0 mT; Second species $g_\perp$ = 2.07, $g_{//}$ = 2.29, $A_{//}$ = 14.8 mT. Data for **Cu3CP-6-NH-10-Pt,** green powder (Yield = 86 %). IR (neat, cm^{-1}): 3420, 3052, 2928, 2856, 1652, 1436, 1253, 1176, 1110, 1086, 1043, 888, 838, 718, 707. UV-Vis (DMSO/H_2O 10/90) λ_{max}/nm (ε/dm^3 mol^{-1} cm^{-1}): 330 (7938), 283 (19745). X-Band EPR (frozen DMSO/H_2O (1/9) solution): $[Cu(DMSO)_x(H_2O)_{6-x}]^{2+}$ $g_\perp$ = 2.08, $g_{//}$ = 2.41, $A_{//}$ = 10.0 mT; Second species $g_\perp$ = 2.08, $g_{//}$ = 2.26, $A_{//}$ = 11.8 mT.; The third species cannot be assigned, since most peaks fully overlap with the other two species. Note: since all the peaks partially overlap the error of these values is significantly increased compared to an EPR spectrum with only one species.

6.5 References

[1] B. A. Chabner, T. G. Roberts, *Nat. Rev. Cancer* **2005**, *5*, 65.

[2] L. H. Hurley, *Nat. Rev. Cancer* **2002**, *2*, 188.

[3] R. M. Burger, *Chem. Rev.* **1998**, *98*, 1153.

[4] J. Y. Chen, J. Stubbe, *Nat. Rev. Cancer* **2005**, *5*, 102.

[5] E. R. Jamieson, S. J. Lippard, *Chem. Rev.* **1999**, *99*, 2467.

[6] J. Reedijk, *Proc. Natl. Acad. Sci. U. S. A.* **2003**, *100*, 3611.

[7] L. H. Einhorn, *Proc. Natl. Acad. Sci. U. S. A.* **2002**, *99*, 4592.

[8] B. Rosenberg, L. van Camp, T. Krigas, *Nature* **1965**, *205*, 698.

[9] P. M. Takahara, A. C. Rosenzweig, C. A. Frederick, S. J. Lippard, *Nature* **1995**, *377*, 649.

[10] J. M. Teuben, C. Bauer, A. H. J. Wang, J. Reedijk, *Biochemistry* **1999**, *38*, 12305.

[11] M. A. Fuertes, C. Alonso, J. M. Perez, *Chem. Rev.* **2003**, *103*, 645.

[12] Y. P. Ho, S. C. F. Au-Yeung, K. K. W. To, *Med. Res. Rev.* **2003**, *23*, 633.

[13] Z. H. Siddik, *Oncogene* **2003**, *22*, 7265.

[14] H. Umezawa, K. Maeda, T. Takeuchi, Y. Okami, *J. Antibiot.* **1966**, *19*, 200.

[15] D. S. Sigman, D. R. Graham, V. Daurora, A. M. Stern, *J. Biol. Chem.* **1979**, *254*, 2269.

[16] D. S. Sigman, A. Mazumder, D. M. Perrin, *Chem. Rev.* **1993**, *93*, 2295.

[17] M. Pitié, C. Boldron, G. Pratviel, *Advances in Inorganic Chemistry, Vol. 58*, Elsevier Academic Press Inc, San Diego, **2006**.

[18] M. Pitié, B. Sudres, B. Meunier, *Chem. Commun.* **1998**, 2597.

[19] P. de Hoog, C. Boldron, P. Gamez, K. Sliedregt-Bol, I. Roland, M. Pitié, R. Kiss, B. Meunier, J. Reedijk, *J. Med. Chem.* **2007**, *50*, 3148.

[20] M. Pitié, J. D. Van Horn, D. Brion, C. J. Burrows, B. Meunier, *Bioconjugate Chem.* **2000**, *11*, 892.

[21] M. Pitié, B. Meunier, *Bioconjugate Chem.* **1998**, *9*, 604.

[22] A. J. Mancuso, S. L. Huang, D. Swern, *J. Org. Chem.* **1978**, *43*, 2480.

Chapter 7

Triazine as a building block for the generation of multifunctional heteronuclear platinum/copper complexes.*

The design and preparation of multifunctional anti-tumor drugs is a topic of growing interest. The synthetic approach reported in this chapter is based on the differential reactivity of the chloride atoms of 2,4,6-trichloro-1,3,5-triazine. Indeed, the chlorine atoms of the triazine building block can be substituted by a nucleophile at different temperatures, allowing the straightforward synthesis of compounds with a maximum of three distinct functions. Herein, triazine-based complexes have been prepared that can bind to DNA through a platinum unit and cleave DNA, thanks to a Cu(3-Clip-Phen) moiety. Moreover, a trifunctional complex is reported that includes a platinum unit, a Cu(3-Clip-Phen) moiety, and a fluorescent group so that the cellular processing of the complex can be followed. The cleavage activities of the complexes are compared to the complex reported in chapter 3. It is observed that the cleavage of the complex with one Cu(3-Clip-Phen) and one platinum unit shows the highest nuclease activity, followed by the complex with one Cu(3-Clip-Phen), one platinum unit and the fluorophore. The complex with two platinum and one Cu(3-Clip-Phen) moiety does not show any nuclease activity at the used experimental conditions.

* Parts of this chapter will be submitted for publication (Paul de Hoog, Teresa Estruch Millet, Angel Garcia Ramos, Patricia Marqués Callego, Ganna Kalayda, Marguerite Pitié, Patrick Gamez, Bernard Meunier, and Jan Reedijk)

7.1 Introduction

Multifunctional anti-tumor drug design is a topic of growing interest.[1, 2] The multifunctional drugs can have an anti-tumor active moiety linked to a group that targets cancer cells,[3, 4] or linked to a group that aims the cellular target.[5-8] In addition, the multifunctional drugs can link two different moieties with known activities; to induce a synergistic anti-tumor effect or to expand the cytotoxic spectrum compared to the two single agents.[9-12] A straightforward synthetic procedure to introduce multi-functionality is indispensable for the design of such drugs.

The 1,3,5-triazine unit has been used in a number of applications such as medicinal chemistry,[13] herbicides,[14] catalysis[15] or polymer chemistry.[16] The *s*-triazine synthon is used efficiently to prepare multidentate ligands for the preparation of supramolecular assemblies.[17-21] A wide variety of sophisticated *s*-triazine derivatives can be easily prepared from low-cost cyanuric chloride, i.e. 2,4,6-trichloro-1,3,5-triazine. The advantage of cyanuric chloride is the differential reactivity of its three chloride atoms. They can be substituted by nucleophiles at different temperatures in the presence of a base (Figure 7.1). The first substitution of one of the chlorides is an exothermic reaction; therefore, the reaction mixture should be cooled and maintained at 0 °C. The second chloride substitution can be carried out at room temperature. The last chloride can be substituted under reflux in THF. The yield of each substitution often exceeds 95% and the trisubstituted derivatives can be obtained in a one-pot synthesis. Compounds with a maximum of three functions can be synthesized in a good yield. Numerous *s*-triazine derivatives have been prepared using this synthetic route.[22-25]

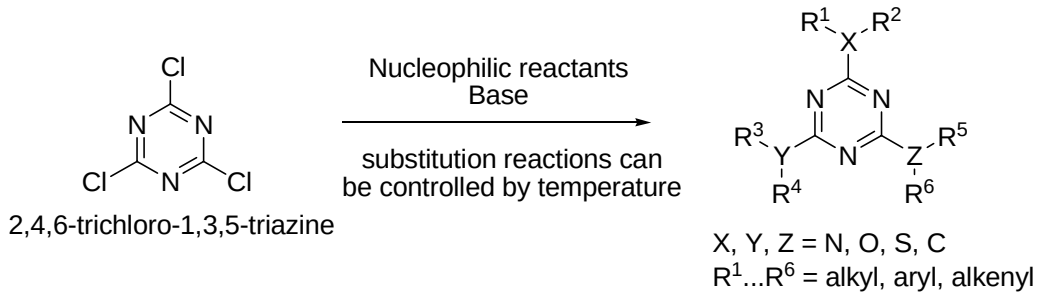

Figure 7.1 General preparation of multifunctional *s*-triazine derivatives.

DNA is the cellular target of many anti-cancer drugs.[26] The interaction of such drugs with DNA often gives rise to the formation of coordination, covalent or non-covalent adducts, thereby disrupting the transcription and/or replication. For example, cisplatin and bleomycin are believed to grant their cytotoxic effect from their interaction with DNA.[27, 28] The anti-proliferate activity of cisplatin was discovered by Rosenberg *et al.* in 1965.[29] Since then a great deal of research has focussed on; finding the cellular target, and identifying the mode of interaction of cisplatin with the target.[30] It was found that cisplatin is able to form a kinetically inert bond

between two neighboring guanines in DNA. This bonding interaction results in a local distortion of the DNA,[31] which is believed to be the reason for the anti-tumor properties of cisplatin.

Bleomycins constitute of a family of compounds first isolated from *Streptomyces Verticillus* by Umezawa *et al.* in 1966.[32] This family of ligands is able to cleave DNA in the presence of iron(II) or copper(II) ions and a reductant.[27, 33] Since the discovery of bleomycin,[32] numerous metal complexes have been synthesized that are able to cleave DNA as well, such as Cu(3-Clip-Phen).[34] Cu(3-Clip-Phen) cleaves DNA in a single-strand fashion by oxidation of the deoxyribose unit.[35] Moreover, 3-Clip-Phen ligand has an amine group on the second carbon of the bridge linking the two phenanthroline moieties. By attachment of a DNA targeting moiety to this amine function, the cleaving activity can be modulated. For instance, in order to induce sequence selectivity and direct double strand cuts, Cu(3-Clip-Phen) has been attached already to a platinum moiety[9] and also to a distamycin derivative[36]. Interestingly, the linkage of Cu(3-Clip-Phen) to other active moieties does change its interaction with DNA, but does not alter its excellent cleaving abilities.

In the present chapter, the 1,3,5-triazine unit is used as a building block for the preparation of multifunctional anti-tumor drugs. The particular reactivity of cyanuric chloride have been utilized to prepare a bifunctional (**Cu3CP-triz-Pt**) and two trifunctional (**Cu3CP-triz-2Pt** and **Cu3CP-triz-F-Pt**) complexes (Figure 7.2). In principle, the platinum unit of these compounds is able to anchor the complex to DNA at two neighboring guanines,[9] whereas the Cu(3-Clip-Phen) can cleave the DNA strands in the close proximity of the Pt-DNA adducts. The complexes have been prepared with the *cis*-platinum motive, due to its higher activity towards DNA compared to *trans*-platinum compounds. **Cu3CP-triz-Pt** has one Cu(3-Clip-Phen) unit and one platinum function. Hence, the Cu(3-Clip-Phen) group is flexible enough to move in the groove of DNA, while the platinum unit is coordinated to DNA. **Cu3CP-triz-2Pt** has one Cu(3-Clip-Phen) group and two platinum functions. As a result, the Cu(3-Clip-Phen) is unable to reposition itself in the DNA when the two platinum units coordinate to DNA. The third complex **Cu3CP-triz-F-Pt** has three distinct functions, namely a Cu(3-Clip-Phen) moiety, a platinum group and the third position of the triazine is labeled with a fluorophore. This complex is expected to coordinate to DNA and cleave it, and the complex will be followed inside the cell by fluorescence microscopy. The high affinity for DNA of the fluorescent group is an additional complication and perhaps an advantage for the interaction with DNA of the designed complex.

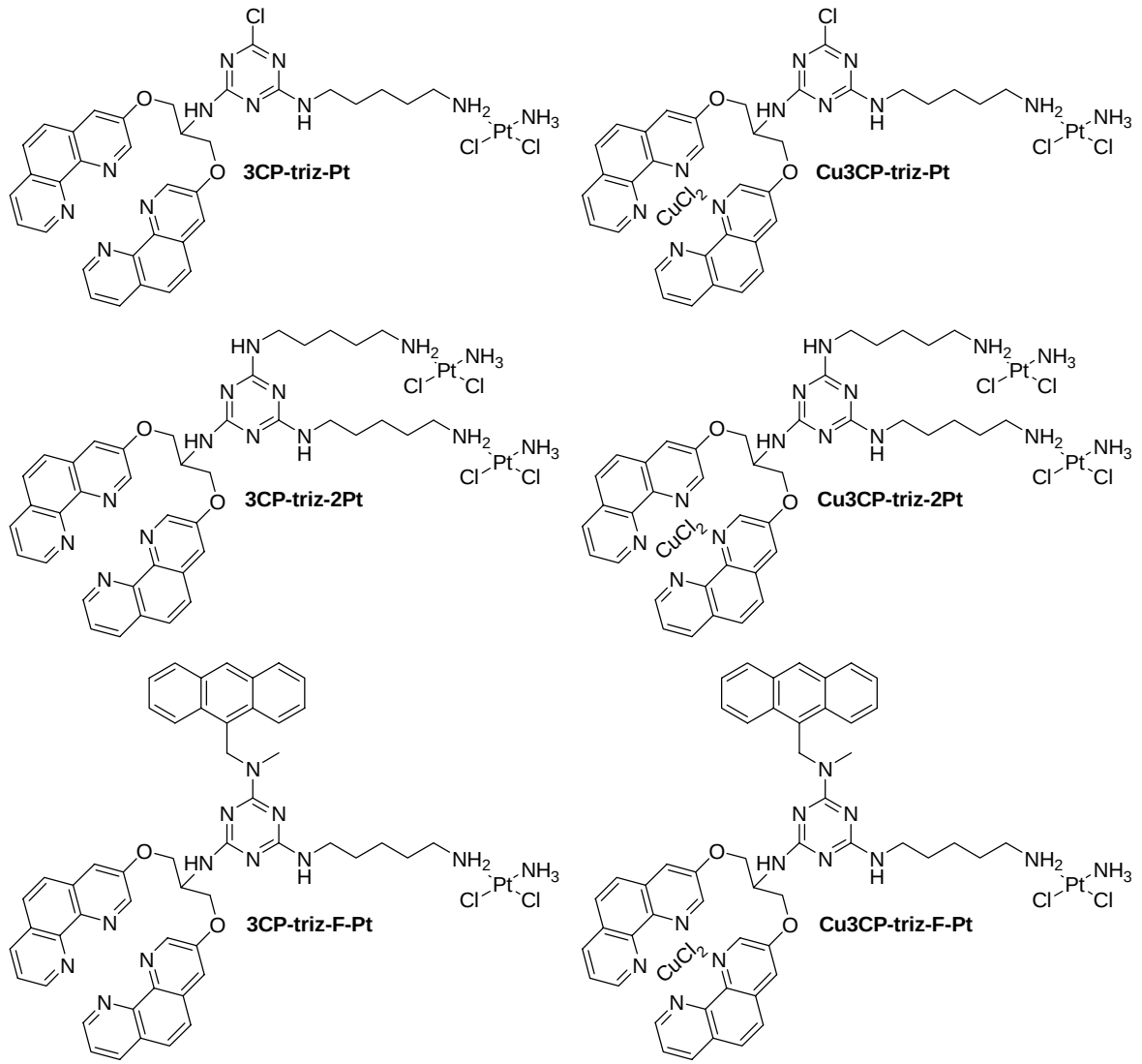

Figure 7.2 Schematic representations of the platinum complexes **3CP-triz-Pt**, **3CP-triz-2Pt**, **3CP-triz-F-Pt** and the heteronuclear platinum-copper complexes **Cu3CP-triz-Pt**, **Cu3CP-triz-2Pt**, **Cu3CP-triz-F-Pt**.

7.2 Results and discussion

The synthetic pathway for the synthesis of the triazine-based platinum/copper complexes is depicted in Schemes below. The 1,5-diaminopentane moiety is employed to coordinate platinum. First, one of the amine groups is protected with a Boc moiety, to obtain *tert*-butyl-5-aminopentylcarbamate (**27**) (Scheme 7.1).

A bifunctional triazine ligand, 2-{1,3-bis-(1,10-phenanthroline-3-yloxy)-propan-2-ylamino}-4-{tert-butyl-5-(1-ylamino)pentylcarbamate}-6-chloro-1,3,5-triazine (**28**), has been obtained using the synthetic pathway depicted in Scheme 7.2. The first step consists of the preparation of the s-triazine derivative with one 3-Clip-Phen unit. Reaction of 3-Clip-Phen (**2**) with 2,4,6-trichloro-1,3,5-triazine in the presence of diisopropylethylamine (DIPEA) in THF

heating slowly from 0 °C to room temperature overnight, yielded quantitatively the desired product. Without further purification, one equivalent of **27** was added and the reaction was continued at 30 °C for one additional night. The desired product **28** was obtained after purification by column chromatography (with a yield of 74 %).

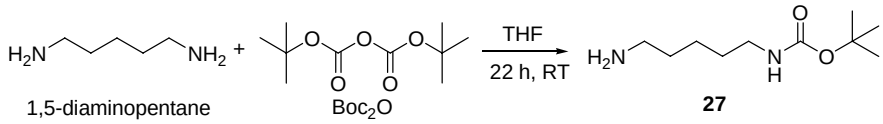

Scheme 7.1 Synthesis scheme for the building block **27**.

Interestingly, unexpected peaks are observed in the ^{1}H-NMR spectrum of **28** (the ^{1}H-NMR spectrum is partly shown in Figure 7.3 on top of the 2D ^{1}H COSY NMR). The peaks between 6.2-6.6 ppm and 5.4-6.0 ppm, as well as the broadening or the splitting of the peaks at 5.0-5.1 ppm, 4.4-4.7 ppm and 3.0-3.1 ppm, have never been observed before in such systems. 2D ^{1}H COSY NMR experiments allowed assigning these peaks. An expansion of the area from 1 to 6.7 ppm is shown in Figure 7.3. The chemical shifts of the phenanthroline entity are as expected in the range 7−9.5 ppm. The peaks at 4.4,-4.7 ppm and at 5.0-5.1 ppm are assigned to the protons *(1)*, *(3)* and *(2)* respectively by comparison with the spectrum of 3-Clip-Phen. The interaction between the proton (*10*) and the proton of the adjacent carbon (*2*) is expected to generate a doublet and one cross peak. In fact, the spectrum displays three cross peaks in the 6.2-6.6 ppm range (which are all doublets) and a broad peak with a shoulder at 5.0-5.1 ppm. Hence, the signals between 6.2 and 6.6 ppm are attributed to the proton (*10*). The signals of the protons (*4*) and (*8*) appear at 3.3 and 3.0-3.1 ppm, respectively. The −NH− group (*11*) connected to the triazine is more deshielded than the amidic −NH− group (*12*) adjacent to (*8*) (see Figure 7.3). The couplings of the proton (*11*) with the protons of the adjacent carbon (*4*) are visualized between 5.4 and 6.0 ppm. The integral value at 4.5 ppm in the 1D ^{1}H spectrum suggests the presence of one more proton than anticipated. Furthermore, the 2D ^{1}H NMR spectrum reveals that the protons at 4.5 ppm are coupled to the protons (*8*); consequently, the signal is attributed to (*12*). The three peaks observed for (*10*) and (*11*) are most likely due to intra-molecular interactions, resulting from more than one conformation of the ligand in solution. Therefore, most of the proton signals are split and broadened.

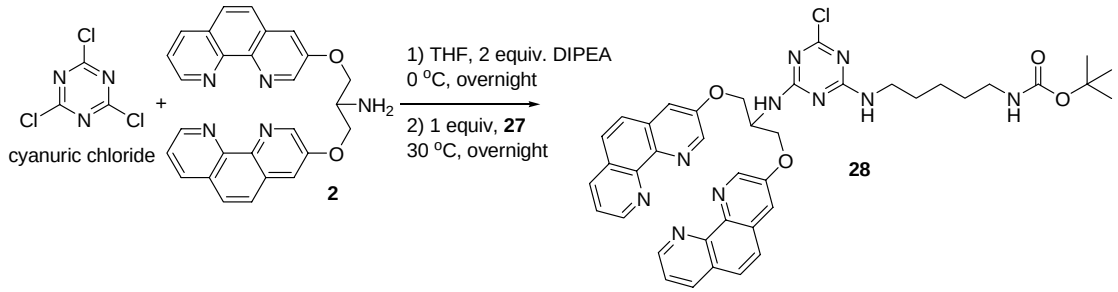

Scheme 7.2 Synthesis scheme of the ligand **28**.

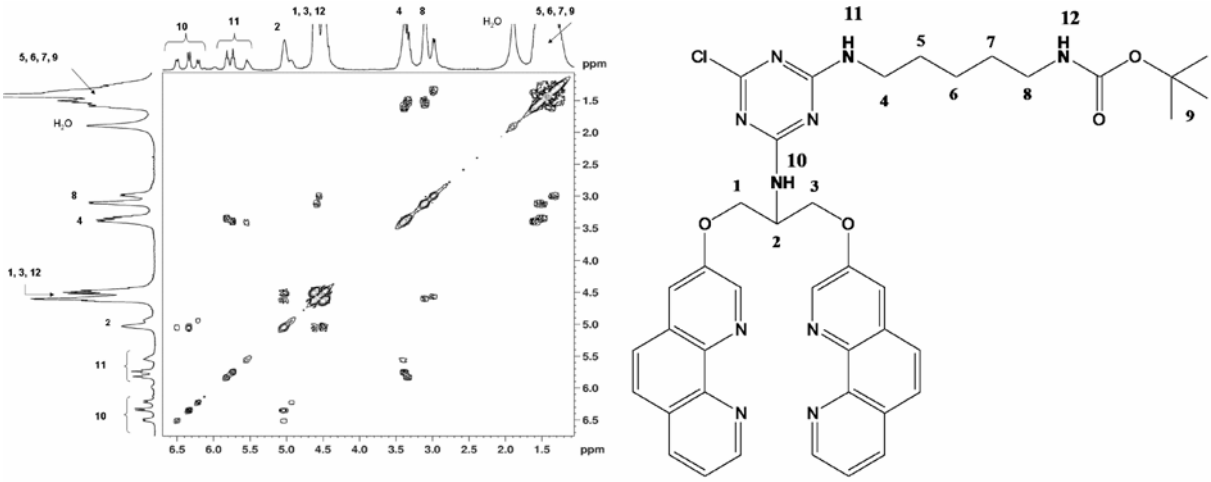

Figure 7.3 Left: 2D ^{1}H COSY NMR spectrum of **28** in $CDCl_3$ with the assignments. Right: schematic representation of **28** with the corresponding numbering of the assigned peaks. The ^{1}H COSY NMR peaks of the phenanthroline moiety are comparable to those of free 3-Clip-Phen, and are therefore omitted for clarity.

Next, a ligand with two platinum binding moieties and one 3-Clip-Phen group, 2-{1,3-bis(1,10-phenanthrolin-3-yloxy)-propan-2-ylamino}-4,6-bis-{tert-butyl-5-(1-ylamino)pentylcarbamate}-1,3,5-triazine (**29**), has been prepared (Scheme 7.3). As for the previous ligand, the first step of the synthesis is the reaction between 2,4,6-trichloro-1,3,5-triazine and 3-Clip-Phen in THF in the presence of three equivalents of DIPEA. Afterwards, two equivalents of **26** are added. The resulting reaction is refluxed overnight under argon and the pure, desired compound is obtained after column chromatography with a yield of 34 %.

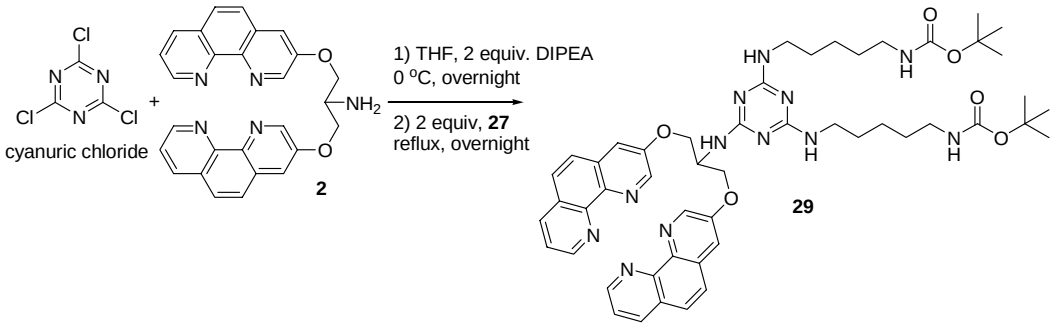

Scheme 7.3 Synthesis scheme of the ligand **29**.

The trifunctional ligand 2-{1,3-bis-(1,10-phenantrolin-3-yloxy)-propan-2-ylamino}-4-{tert-butyl-5-(1-ylamino)-pentylcarbamate}-6-{9-(methylamminomethyl)-antracene}-1,3,5-triazine (**30**) was then prepared from ligand **28** (Scheme 7.4). The synthetic pathway to **30** is once again based on the different chemical reactivities of the three chlorides of 2,4,6-trichloro-1,3,5-triazine upon nucleophilic aromatic substitution. One equivalent of 9-(methylaminomethyl)-anthracene is used substitute the last chloride of **28** in the presence of one equivalent of DIPEA

in THF. The reaction is performed under reflux temperature overnight. The pure, desired product **30** is obtained after purification by column chromatography with a yield of 79%.

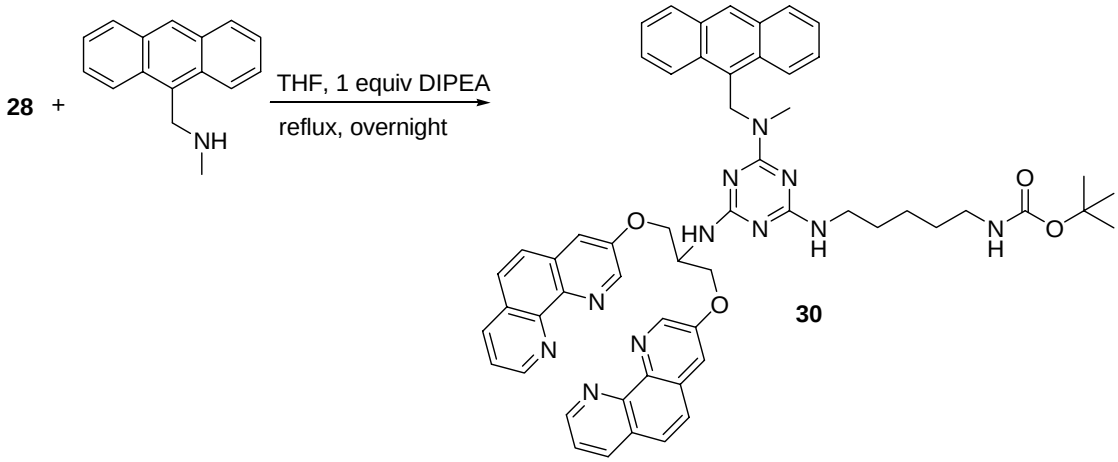

Scheme 7.4 Synthesis scheme of the ligand **30**.

Prior to the coordination experiments, the amine group of ligands **28**, **29** and **30** is deprotected (Scheme 7.5). The Boc group is removed with TFA at 0 °C, leading to the free amine within 30 minutes. The excess of TFA is evaporated under reduced pressure. The amine group of the deprotected ligands **28**, **29** and **30** is subsequently platinated with $\{(P(C_6H_6)_4\}[Pt(NH_3)Cl_3]$ (**31**)[38] in DMF at 100 °C overnight. This reaction of the three ligands with the platinum source has been followed in time by ^{195}Pt NMR. They all proceed at 100 °C overnight. Figure 7.4 shows a representative example (**28**) as a function of time. After one night at 100 °C, one product is formed and the entire starting complex **31** is consumed.

The complexes **3CP-triz-Pt**, **3CP-triz-2Pt** and **3CP-triz-F-Pt** are obtained with one or two TFA molecules (protonating the 3-Clip-Phen moiety) by precipitation of the crude compound in diethyl ether. The precipitate is filtered and washed extensively with CH_2Cl_2 to remove the remaining starting materials, since compounds **28**-**31** are soluble in this solvent. The yields achieved are 80%, 69% and 59% for **3CP-triz-Pt**, **3CP-triz-2Pt** and **3CP-triz-F-Pt**, respectively. The target copper-platinum complexes are obtained by reaction of **3CP-triz-Pt**, **3CP-triz-2Pt** and **3CP-triz-F-Pt** in DMF with $CuCl_2$ at 50 °C overnight (Scheme 7.5). The desired multifunctional products **Cu3CP-triz-Pt**, **Cu3CP-triz-2Pt** and **Cu3CP-triz-F-Pt** are isolated by precipitation in diethyl ether and were characterized by UV-Vis, IR and EPR.

The EPR spectra of **Cu3CP-triz-Pt**, **Cu3CP-triz-2Pt** and **Cu3CP-triz-F-Pt** have shown that, similar to chapter 6, part of the copper has reacted with the solvent DMSO, to form the $Cu(DMSO)_x(H_2O)_{6-x}^{2+}$ complex. Nevertheless, part of the Cu(II) is to binding nitrogen ligands, indicating that the copper partly binds to the 3-Clip-Phen moiety. **Cu3CP-triz-2Pt** shows in contrast to **Cu3CP-triz-Pt** and **Cu3CP-triz-F-Pt** primarily the $Cu(DMSO)_x(H_2O)_{6-x}^{2+}$ spectrum.

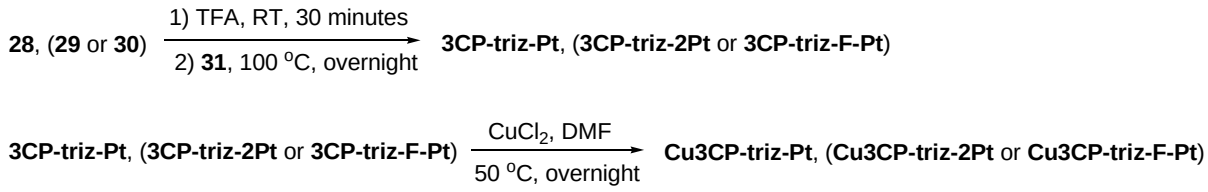

Scheme 7.5 Preparation of the complexes **3CP-triz-Pt**, **3CP-triz-2Pt**, **3CP-triz-F-Pt**, **Cu3CP-triz-Pt**, **Cu3CP-triz-2Pt** and **Cu3CP-triz-F-Pt**.

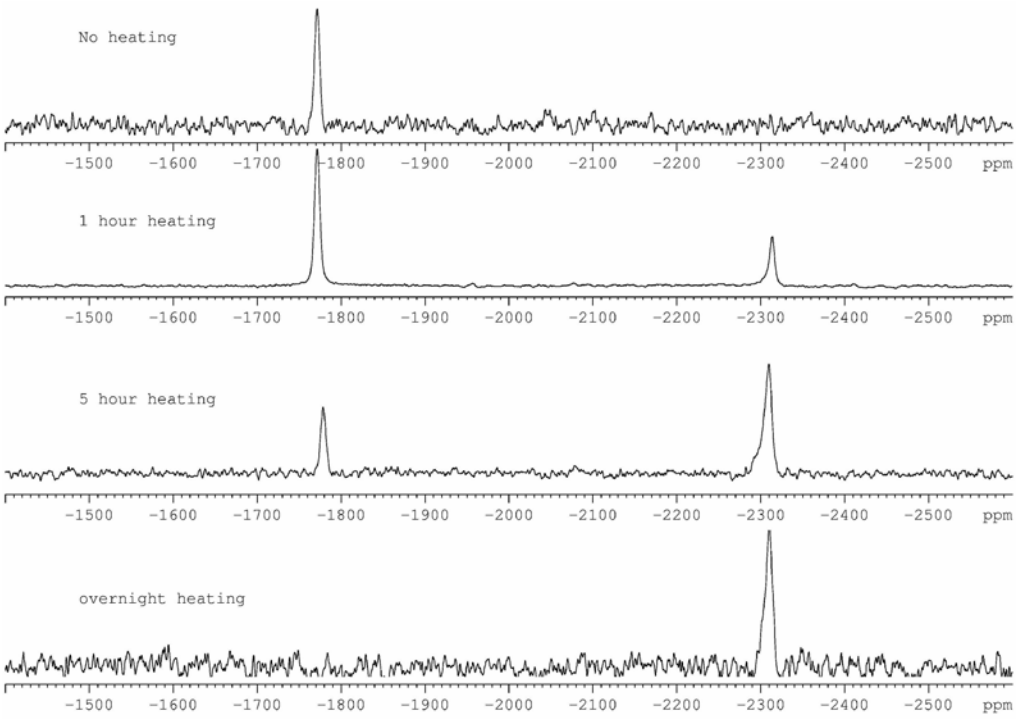

Figure 7.4 Reaction of **28** (Boc group has been removed) with **31** as followed by ^{195}Pt NMR. The peak in the top spectrum corresponds to the anion $[Pt(NH_3)Cl_3]$. The second spectrum is obtained after a reaction time of 1 hour in DMF at 100 °C. The third spectrum is recorded after 5 hours and the fourth spectrum after and overnight reaction in DMF (100 °C).

The conversion of supercoiled circular ΦX174 DNA (form I) into the relaxed (form II) and the linear (form III) conformations has been monitored to compare the aerobic cleavage abilities of complexes **Cu3CP-6-Pt**, **Cu3CP-triz-Pt**, **Cu3CP-triz-2Pt** and **Cu3CP-triz-F-Pt** in the presence of a reducing agent (Figure 7.5). The complexes are incubated for 20 h in order to allow the formation of platinum-DNA adducts. The nuclease activity is subsequently initiated by the addition of 5 mM mercaptopropionic acid (MPA) in air. The nuclease activity of **Cu3CP-triz-Pt** was found comparable to **Cu3CP-6-Pt**, the complex reported in chapter 3. Both complexes show a clear DNA cleavage at a complex concentration of 500 nM (compare lanes 3 and 7 for **Cu3CP-6-Pt** and **Cu3CP-triz-Pt** respectively). The majority of the supercoiled DNA has reacted to circular (Form II) and linear DNA (Form III). Thus, the triazine unit in the complex **Cu3CP-triz-Pt** is not influencing the cleaving activity nor its ability to perform direct

double strand cuts, since supercoiled and linear DNA are visible at the same time. **Cu3CP-triz-2Pt** appears to be not able to cleave DNA under these experimental conditions. From the frozen solution EPR spectra recorded in a DMSO/H_2O solution (1/9) it is seen that a large part of the copper is extracted to coordinate to the DMSO solvent molecules in place of the 3-Clip-Phen ligand. However, the EPR complex solutions contain 10% DMSO, required to obtain a good glass, whereas the complex solutions used for the cleavage studies only contain a maximum of 0.01% DMSO. So, it assumed that here part of the Cu(II) is still coordinated to the 3-Clip-Phen unit. The poor solubility of **Cu3CP-triz-2Pt** in water may also explain its lack of cleaving activity. **Cu3CP-triz-F-Pt** is found markedly less active than **Cu3CP-6-Pt** or **Cu3CP-triz-Pt** (compare lanes 4, 8 and 16 for **Cu3CP-6-Pt**, **Cu3CP-triz-Pt** and **Cu3CP-triz-F-Pt**, respectively). The supercoiled DNA has partially reacted to circular and linear DNA, which indeed suggests that the complex **Cu3CP-triz-F-Pt** is able to perform direct double strand cuts.

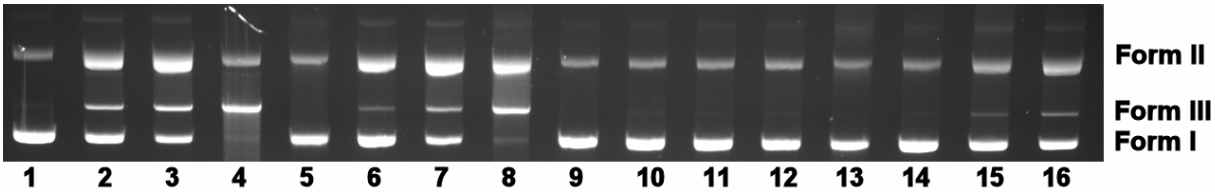

Figure 7.5 Comparison of the oxidative cleavage of ΦX174 plasmid DNA mediated by **Cu3CP-6-Pt**, **Cu3CP-triz-Pt**, **Cu3CP-triz-2Pt** and **Cu3CP-triz-F-Pt** in the presence of 5 mM MPA. Lane 1: control DNA. Lane 2: 250 nM **Cu3CP-6-Pt**. Lane 3: 500 nM **Cu3CP-6-Pt**. Lane 4: 1 μM **Cu3CP-6-Pt**. Lane 5: 1 μM **Cu3CP-triz-Pt** without MPA. Lane 6: 250 nM **Cu3CP-triz-Pt**. Lane 7: 500 nM **Cu3CP-triz-Pt**. Lane 8: 1 μM **Cu3CP-triz-Pt**. Lane 9: 1 μM **Cu3CP-triz-2Pt** without MPA. Lane 10: 250 nM **Cu3CP-triz-2Pt**. Lane 11: 500 nM **Cu3CP-triz-2Pt**. Lane 12: 1 μM **Cu3CP-triz-2Pt**. Lane 13: 1 μM **Cu3CP-triz-F-Pt** without MPA. Lane 14: 250 nM **Cu3CP-triz-F-Pt**. Lane 15: 500 nM **Cu3CP-triz-F-Pt**. Lane 16: 1 μM **Cu3CP-triz-F-Pt**.

Anthracene derivatives are known to exhibit fluorescent properties.[37] To follow the pathway of the complex inside living cells, an anthracene unit has been linked to the triazine core, yielding the trifunctional compound **Cu3CP-triz-F-Pt**. Indeed, this complex is expected to form inert coordination bonds with DNA and to cleave the DNA strands. In addition, its fluorescent group should allow its monitoring inside the cells. The cellular processing studies were performed with U2-OS human osteosarcoma cells. The cells have been incubated with 5 μM **3CP-triz-F-Pt** and **Cu3CP-triz-F-Pt** at various incubation times. Higher complex concentrations (for instance 10 μM) lead to cell stress (causing their death) within 1 hour; therefore, the distribution of the complexes inside the cells has been followed at a lower concentration of 5 μM. The phase contrast and fluorescence images of U2-OS cells are displayed in Figure 7.6. Green fluorescence is observed for these complexes. The accumulation of the drug inside the cells is observed after an incubation time of 15 minutes, as deduced from an increase of the fluorescence intensity is detected in the cytosol of the cells. Interestingly, the fluorescence is not located at the nucleus

(see Figure 7.6, fluorescence images). After 24 hours, the fluorescence is still only observed outside the nuclei. Both complexes show similar results. These preliminary and promising results should be supported by more elaborate studies to explore the exact cellular processing of these multifunctional drugs, which is beyond the scope of this thesis.

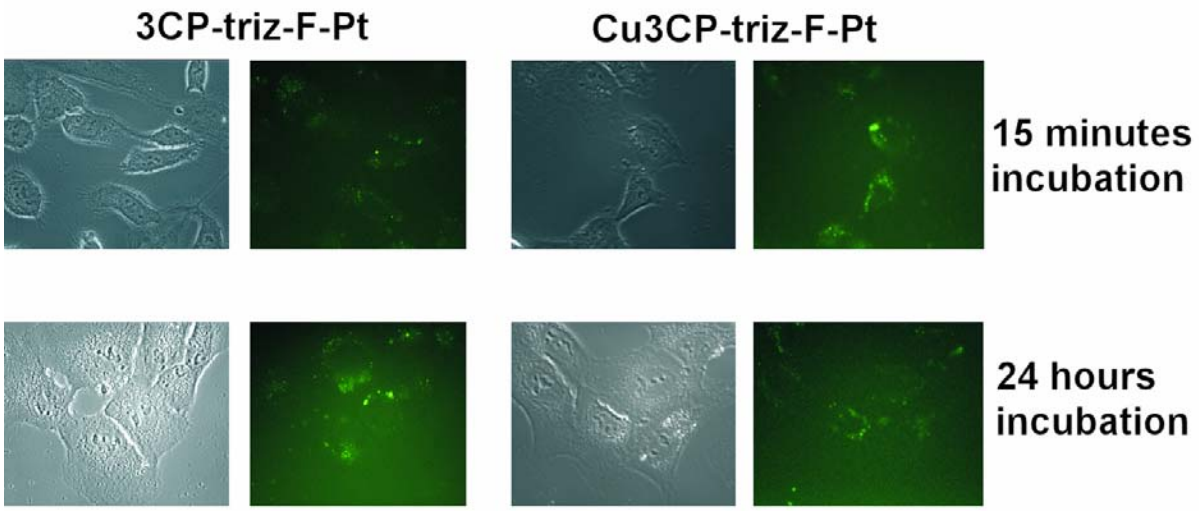

Figure 7.6 Cellular processing of **3CP-triz-F-Pt** and **Cu3CP-triz-F-Pt** in U2-OS human osteosarcoma cells followed by fluorescence microscopy. The fluorescence images taken after an incubation time of 15 minutes are presented in the top row, and their appearance after 24 hours are shown in the bottom row. Phase contrast images of the cells for each complex at these time points are presented on the left; the corresponding fluorescence images are shown on the right.

7.3 Conclusions

A new synthetic approach to design multifunctional anti-tumor drugs is reported. 2,4,6-Trichloro-1,3,5-triazine has been employed to design and prepare three different bi- or trifunctional complexes. **Cu3CP-triz-Pt** possesses a platinum unit that can coordinate and anchor to DNA and a Cu(3-Clip-Phen) moiety capable of cleaving the DNA strands. **Cu3CP-triz-2Pt** has two such platinum units and one Cu(3-Clip-Phen) moiety, and **Cu3CP-triz-F-Pt** has a third function added, a fluorescent substituent. Similar to **Cu3CP-6-Pt**, **Cu3CP-triz-Pt** and **Cu3CP-triz-F-Pt** are able to cleave DNA in a double strand fashion. However, the activity of **Cu3CP-triz-F-Pt** is lower compared to the former two complexes. **Cu3CP-triz-2Pt** does not cleave DNA, most likely as a result of its precipitation in water, or because the majority of the copper has dissociated from the ligand due to the presence of the DMSO solvent. **Cu3CP-triz-F-Pt** appears to be able to rapidly accumulate inside the cancer cells and to kill them at a complex concentration of 10 μM. It appears that this complex cannot enter the cellular nucleus, but more detailed biological studies will be required to confirm this observation. In summary, the triazine building unit has proven to be an excellent synthon for the

rational design and the synthesis of anti-tumor drugs bearing up to three distinct, specific functional groups.

7.4 Experimental

General procedures and materials: All NMR measurements were performed with a 300 MHz Bruker DPX300 spectrometer holding a 5 mm multi-nuclei probe. The temperature was kept constant at 298 K with a variable temperature unit for temperature regulation. Chemical shifts are reported in δ (parts per million) relative to the solvent peak or tetramethylsilane (TMS) as reported for each compound. MS spectra were acquired using a ThermoFinnegan AQA ESI-MS. Sample solutions (methanol or water) were introduced in the ESI source by using a Dionex ASI-100 automated sampler injector and an eluent running at 0.2 mL/minute. Reagents were purchased from Aldrich or Acros, unless otherwise stated. Solvents were obtained from Applied Biosystems Inc. C, H and N analyses were carried out on an automatic Perkin-Elmer 2400 series II CHNS/O micro analyzer. X-band powder EPR spectra were obtained on a Bruker-EMX*plus* electron spin resonance spectrometer (Field calibrated with DPPH (g = 2.0036)).

***Tert*-butyl-5-aminopentylcarbamate (27).** A solution of di-*tert*-butyl dicarbonate (Boc_2O) (2g, 9.15 mmol) in 25 mL THF was added dropwise over a period of 1 h to a solution of 1,5-diaminopentane (5 mL, 42.5 mmol) in 15 mL THF. The mixture was allowed to stir for 22 h. The solvent was removed under reduced pressure and 50 mL of water was added to the resulting residue. The insoluble bi-substituted product was collected by filtration. The filtrate was extracted with dichloromethane (3 × 50 mL) and the dichloromethane extract was backwashed with water (3 × 50 mL) to remove the excess of 1,5-diaminopentane. Subsequently, the solvent was removed under reduced pressure, yielding a pale yellow oil (82% yield). The oil gradually solidified over a period of two weeks to yield a white solid. Data for compound (**27**): ^{1}H NMR ($CDCl_3$, 300 MHz) δ 4.52 (s, 1H), 3.09 (br, 2H), 2.70 (t, 2H, J = 6.71 Hz), 1.44 (s, 9H), 1.54-1.32 (m, 8H) ppm. ^{13}C-NMR ($CDCl_3$, 300 MHz) δ 156.2, 79.1, 41.6, 40.5, 32.3, 29.9, 28.6, 24.1 ppm. Low Resolution MS (ESI>0) m/z 203.10 [$(M+H)^+$; calcd for $C_{10}H_{23}N_2O_2^+$: 202.29]

2-{1,3-bis-(1,10-phenanthroline-3-yloxy)-propan-2-ylamino}-4-{*tert*-butyl-5-(1-ylamino)-pentylcarbamate}-6-chloro-1,3,5-triazine (28). 2,4,6-Trichloro-1,3,5-triazine (264 mg, 1.43 mmol) was dissolved in 30 mL of CH_2Cl_2. Two equivalents of diisopropylethylamine (DIPEA) (0.49 mL, 2.86 mmol) were added and the two-necked round bottom flask was cooled to 0 °C. A solution of **2** (640 mg, 1.43 mmol) in 60 mL of CH_2Cl_2 was added at 0 °C, and the resulting mixture was stirred overnight, allowing its slow warming to RT. Subsequently, the reaction was heated to 30 °C, followed by the addition of a solution of **27** (289 mg, 1.43 mmol) in the minimum amount of CH_2Cl_2. The ensuing mixture was stirred overnight. The solvent was removed under reduced pressure and the crude was purified by column chromatography (SiO_2, DCM:MeOH:NH_4OH, 95:5:0.5). Data for compound **28**: light brown powder (Yield: 74 %). ^{1}H-NMR ($CDCl_3$, 300 MHz) δ 9.11 (m, 2H), 8.91 (s, 2H), 8.15 (m, 2H), 7.72 (m, 2H), 7.64 (m, 2H), 7.53 (m, 4H), 6.49 (br, 0.37H), 6.43 (d, 0.37H, J = 8.26 Hz), 6.31 (d, 0.26H, J = 8.00 Hz), 5.95 (Br, 0.3H), 5.88 (Br, 0.3H), 5.55 (br, 0.4H), 4.99 (br, 1H), 4.52 (m, 5H), 3.34 (m, 2H), 3.08 (m, 2H), 1.53 (m, 4H), 1.39 (s, 9H), 1.22 (m, 2H) ppm. ^{13}C-NMR ($CDCl_3$, 300 MHz) δ 168.4, 165.4, 160.9, 155.7, 153.3, 150.1, 145.8, 142.2, 140.4, 135.6, 129.1, 127.1, 127.0, 125.7, 121.9, 114.9, 78.8, 65.8, 48.8, 40.6, 39.9, 29.4, 28.8, 28.1, 23.4 ppm. Low Resolution MS (ESI>0) m/z 761.12 [$(M+H)^+$; calcd for $C_{40}H_{42}ClN_{10}0_4^+$

762.28]. Anal. Calcd for $C_{40}H_{41}ClN_{10}0_4 \cdot 0.4\ CH_2Cl_2$: C 61.02, H 5.30, N 17.61; found: C 60.96, H 5.13, N 17.82.

2-{1,3-bis-(1,10-phenanthrolin-3-yloxy)-propan-2-ylamino}-4,6-bis-{*tert*-butyl-5-(1-ylamino)-pentylcarbamate}-1,3,5-triazine (29). 2,4,6-Trichloro-1,3,5-triazine (206.5 mg, 1.12 mmol) was dissolved in 90 mL of THF. Three equivalents of DIPEA (0.57 mL, 3.36 mmol) and 1 equivalent of **2** (500 mg, 1.12 mmol) were added to this solution. The reaction mixture was cooled to 0 °C and stirred for 1 h. The reaction was allowed to warm to RT before the addition of a solution of **27** (497 mg, 2.46 mmol) in 40 mL of THF. This mixture was refluxed for 40 h. The solvent was removed and the crude compound was purified by column chromatography (SiO_2, DCM:MeOH:NH_4OH, 85:15:1.5). Data for compound **29**: light brown powder (Yield: 34 %). ^{1}H-NMR ($CDCl_3$, 300 MHz) δ 9.11 (d, 2H, J = 2.81 Hz), 8.93 (s, 2H, J = 2.00 Hz), 8.15 (d, 2H, J = 7.25 Hz), 7.73 (m, 4H), 7.63 (m, 2H), 7.55 (m, 2H), 5.00 (br, 4H), 4.46 (br, 1H), 3.57 (br, 4H), 3.09 (br, 4H), 1.56 (br, 8H), 1.42 (s, 18H), 1.25 (m, 4H) ppm. ^{13}C-NMR ($CDCl_3$, 300 MHz) δ 164.2, 159.4, 156.8, 154.6, 151.2, 147.0, 143.4, 141.5, 136.7, 131.5, 130.2, 128.1, 126.9, 122.9, 116.1, 79.8, 67.3, 49.4, 47.3, 41.2, 30.5, 30.2, 29.2, 24.8 ppm. Low Resolution MS (ESI>0) m/z 927.21 [$(M+H)^+$; calcd for $C_{50}H_{63}N_{12}0_6^+$ 928.11]. Anal. Calcd for $C_{50}H_{62}N_{12}0_6 \cdot 0.8\ CH_2Cl_2$: C 61.32, H 6.44, N 16.89; found: C 61.23, H 6.74, N 16.82.

2-{1,3-bis-(1,10-phenanthrolin-3-yloxy)-propan-2-ylamino}-4-{*tert*-butyl-5-(1-ylamino)-pentylcarbamate}-6-{9-(methylaminomethyl)-anthracene}-1,3,5-triazine (30). A solution of **28** (100 mg, 0.13 mmol) and DIPEA (23 µL, 0.13 mmol) in 5 mL of THF was added to a solution of 9-(methylaminomethyl)-anthracene (29.07 mg, 0.13 mmol) dissolved in 2 mL of THF. The reaction mixture was refluxed under argon for 24 h. The solvent was removed under reduced pressure and the crude compound was purified by column chromatography (SiO_2, DCM:MeOH:NH_4OH, 95:5:0.5). Data for compound **30**: light brown powder (Yield: 79 %). The peaks of the ^{1}H-NMR spectrum are broad. ^{1}H-NMR analysis was performed at different temperatures. The spectra obtained reveal significant changes which indicate that intramolecular interactions occur in solution. ^{1}H-NMR ($CDCl_3$, 300 MHz) δ 9.08 (br, 2H), 8.93 (br, 2H), 8.38 (br, 2H), 8.23 (br, 1H), 8.1 (br, 2H), 7.94 (br, 2H), 7.48 (br, 13H), 5.72 (br, 2H), 5.21 (br, 2H), 4.48 (br, 5H), 3.42 (br, 2H), 3.03 (br, 3H), 2.63 (br, 4H), 1.35 (br, 15H). ^{13}C-MNR ($CDCl_3$, 300 MHz) δ 166.74, 166.51, 166.32, 155.85, 153.68, 150.17, 145.95, 142.48, 140.37, 135.73, 133.92, 131.22, 129.24, 129.03, 127.86, 127.23, 127.12, 127.03, 126.13, 125.89, 124.80, 124.29, 121.97, 115.04, 78.84, 66.48, 48.56, 42.36,.26, 31.41, 29.65, 28.8, 28.26, 23.98 ppm. HRMS: m/z (with z = 2) 473.72896 [$(M + 2H)^{2+}$; calc for $C_{56}H_{57}N_{11}O_4^{2+}$: 473.72920] Anal. Calcd for $C_{56}H_{55}N_{11}O_4 \cdot 1.9\ CDCl_3$: C 59.19, H 4.72, N 13.11; Found: C 59.26, H 5.15, N 13.31.

[Pt(2-{1,3-bis-(1,10-phenanthroline-3-yloxy)-propan-2-ylamino}-4-{5-amino-(1-ylamino)-pentyl}-6-chloro-1,3,5-triazine]-platinum)Cl_2], (3CP-triz-Pt) [Pt_2(2-{1,3-bis-(1,10-phenanthroline-3-yloxy)-propan-2-ylamino}-4,6-bis-{5-amino-(1-ylamino)-pentyl}-1,3,5-triazine)Cl_4], (3CP-triz-2Pt) and [Pt(2-{1,3-bis-(1,10-phenanthroline-3-yloxy)-propan-2-ylamino}-4-{5-amino-(1-ylamino)-pentyl}-6-{9-(methylaminomethyl)-anthracyl}-1,3,5-triazine)Cl_2], (3CP-triz-F-Pt). The preparation of {$(P(C_6H_6)_4$}[$Pt(NH_3)Cl_3$] (**31**) was carried out as previously described.[38] Compounds **28**, **29** or **30** (0.13 mmol) were dissolved in 2 mL of TFA. The mixture was stirred at RT for 30 minutes prior to the removal of the excess of TFA. The resulting solid was dissolved in 10 mL of DMF and **31** (94.9 mg, 0.15 mmol) was added. The reaction was heated at 100 °C overnight. Most of the DMF was evaporated under

reduced pressure and the remaining solution was added to 75 mL of diethyl ether containing 0.1 mL of DIPEA. The precipitate obtained was filtered and washed with CH_2Cl_2 (3 × 10 mL). Data for **3CP-triz-Pt**: off-white powder (Yield: 80 %). ^{1}H-NMR ($CDCl_3$, 300 MHz) δ 9.02 (br, 4H), 8.41-7.95 (m, 10H), 4.56 (br, 5H), 1.47-1.29 (m, 6H). ^{195}Pt NMR (DMF-d^6, 300 MHz): δ -2313 ppm. Low Resolution MS (ESI>0) m/z 908.69 [(M – Cl)$^+$; calcd $C_{35}H_{36}Cl_2N_{11}O_2Pt^+$ 908.72], 926.65 [(M – Cl + H_2O) calcd $C_{35}H_{38}Cl_2N_{11}O_3Pt^+$ 926.73]. IR (neat, cm^{-1}): 3058, 2938, 1684, 1590, 1506, 1436, 1362, 1239, 1200, 1175, 1041, 880, 834, 798, 730, 707. UV-Vis (DMSO/H_2O 10/90) λ_{max}/nm (ε/dm^3 mol^{-1} cm^{-1}): 331 (6986), 277 (26223). Anal. Calcd for $C_{38}H_{43}Cl_3N_{12}O_3Pt{\cdot}CH_2Cl_2{\cdot}1TFA$: C 40.49, H 3.81, N 13.82. Found: C 40.38, H 3.80, N 13.42. Data for **3CP-triz-2Pt**: light brown powder (Yield: 69 %). ^{1}H-NMR ($CDCl_3$, 300 MHz) δ 9.43-8.66 (br, 6H), 7.98-7.72 (m, 8H), 5.24 (br, 1H), 4.56 (br, 4H), 2.72 (m, 2H), 1.54-1.49 (m, 6H). ^{195}Pt NMR (DMF-d^6, 300 MHz): δ -2311 ppm. Low Resolution MS (ESI>0) m/z (with z = 2) 629.75 [(M – 2Cl)$^{2+}$; calcd $C_{40}H_{56}Cl_2N_{14}O_4Pt_2^+$ 629.01] IR (neat, cm^{-1}): 3048, 3931, 1684, 1575, 1506, 1436, 1362, 1255, 1201, 1175, 1043, 880, 835, 780, 722, 706. UV-Vis (DMSO/H_2O 10/90) λ_{max}/nm (ε/dm^3 mol^{-1} cm^{-1}): 329 (10603), 285 (24435). Anal. Calcd for $C_{46}H_{66}Cl_4N_{16}O_4Pt_2{\cdot}3.2CH_2Cl_2{\cdot}2TFA$: C 32.95, H 3.87, N 11.56. Found: C 32.84, H 3.83, N 11.47. Data for **3CP-triz-F-Pt**: brown powder (Yield: 59 %). ^{1}H-NMR ($CDCl_3$, 300 MHz) δ 9.70-8.62 (br, 6H), 8.62-7.79 (br, 8H), 4.55 (br, 5H), 1.41-1.17 (m, 6H). ^{195}Pt NMR (DMF-d^6, 300 MHz): δ -2315 ppm. IR (neat, cm^{-1}): 3342, 1668, 175, 1506, 1436, 1362, 1254, 1174, 1042, 880, 834, 812, 731, 707. UV-Vis (DMSO/H_2O 10/90) λ_{max}/nm (ε/dm^3 mol^{-1} cm^{-1}): 277 (29982).

[PtCu(2-{1,3-bis-(1,10-phenanthroline-3-yloxy)-propan-2-ylamino}-4-{5-amino-(1-ylamino)-pentyl}-6-chloro-1,3,5-triazine]-platinum)Cl_4], (Cu3CP-triz-Pt) [Pt_2Cu(2-{1,3-bis-(1,10-phenanthroline-3-yloxy)-propan-2-ylamino}-4,6-bis-{5-amino-(1-ylamino)-pentyl}-1,3,5-triazine)Cl_4], (Cu3CP-triz-2Pt) and [PtCu(2-{1,3-bis-(1,10-phenanthroline-3-yloxy)-propan-2-ylamino}-4-{5-amino-(1-ylamino)-pentyl}-6-{9-(methylaminomethyl)-anthracyl}-1,3,5-triazine)Cl_2], (Cu3CP-triz-F-Pt). To a suspension of **3CP-triz-Pt**, **3CP-triz-2Pt** or **3CP-triz-F-Pt** (24.7 μmol) in 12 mL of DMF was added $CuCl_2$ (4.64 mg, 27.2 μmol). This mixture was heated at 50 °C overnight. The volume of the green solution was reduced to 5 mL and 25 mL of diethyl ether were added to precipitate the complex formed. The green precipitate was filtered off and washed with diethyl ether (3 × 20 mL). Data for **Cu3CP-triz-Pt,** green powder (Yield: 92 %). X-Band EPR (frozen DMSO/H_2O (1/9) solution): $Cu(DMSO)_x(H2O)_{6-x}^{2+}$ $g_\perp$ = 2.08, $g_{//}$ = 2.41, $A_{//}$ = 10.5 mT; Second species $g_\perp$ = 2.07, $g_{//}$ = 2.33, $A_{//}$ = 12.5 mT (comparable to chapter 6, the copper cation is coordinating partially to the DMSO solvent) IR (neat, cm^{-1}): 3058, 2937, 1622, 1506, 1432, 1362, 1253, 1175, 1110, 1085, 1042, 888, 837, 785, 719, 707. UV-Vis (DMSO/H_2O 10/90) λ_{max}/nm (ε/dm^3 mol^{-1} cm^{-1}): 384 (1620), 322 (11952), 283 (28268). Data for **Cu3CP-triz-2Pt,** green powder (Yield: 89 %). IR (neat, cm^{-1}): 3058, 2932, 1652, 1544, 1436, 1361, 1253, 1175, 1111, 1085, 1042, 883, 834, 780, 706. UV-Vis (DMSO/H_2O 10/90) λ_{max}/nm (ε/dm^3 mol^{-1} cm^{-1}): 387 (2618), 326 (12005), 285 (25196). X-Band EPR (frozen solution): $g_\perp$ = 2.08, $g_{//}$ = 2.41, $A_{//}$ = 10.5 mT (the majority of the copper is coordinating to the DMSO solvent). Data for **Cu3CP-triz-F-Pt,** green powder (Yield: 91 %). IR (neat, cm^{-1}): 3316, 1576, 1436, 1362, 1253, 1174, 1112, 1085, 1042, 888, 837, 810, 779, 708. UV-Vis (DMSO/H_2O 10/90) λ_{max}/nm (ε/dm^3 mol^{-1} cm^{-1}): 388 (2531), 324 (14285), 283 (32427). X-Band EPR (frozen DMSO/H_2O (1/9) solution): $Cu(DMSO)_x(H2O)_{6-x}^{2+}$ $g_\perp$ = 2.08, $g_{//}$ = 2.41, $A_{//}$ = 10.5 mT; Second species $g_\perp$ = 2.08, $g_{//}$ = 2.28, $A_{//}$ = 14.2 mT (comparable to chapter 6, the copper cation is coordinating partially to the DMSO solvent).

Cleavage studies. Complexes were prepared as 1 mM solutions in DMSO, and diluted to

respectively 1, 2 and 4 μM with water purchased from Eppendorf. 5 μL of complex solution were added to 10 μL of supercoiled ΦX174 DNA ((Invitrogen)7 nM, 40 μM base pairs) in 6 mM NaCl, 20 mM sodium phosphate buffer (pH 7.2), and incubated for 20 h at 37 °C. To initiate the cleavage, 5 μL of a 20 mM mercaptopropionic acid solution in water were added, and the resulting reaction mixture was incubated at 37 °C for 1 h. The reaction was quenched at 4 °C, followed by the addition of 4 μL of loading buffer (bromophenol blue) prior to its loading on a 0.8 % agarose gel containing 1 μg mL^{-1} of ethidium bromide. The gels were run at a constant voltage of 70 V for 90 minutes in TBE buffer containing 1 μg mL^{-1} of ethidium bromide. The gels were visualized under a UV transilluminator, and the bands were quantified using a BioRad Gel Doc 1000 apparatus interfaced with a computer.

Digital fluorescence microscopy studies. Preliminary fluorescence Microscopy experiments were performed on a Axiovert 135 TV (Zeiss,Jena, Germany) inverted microscope equipped with a 100 W mercury arc lamp for fluorescence excitation and bright field illumination for phase contrast images. The filter set to detect **3CP-triz-F-Pt** or **Cu3CP-triz-F-Pt** fluorescence consisted of an hq 480/40 nm band-pass excitation filter, an hq 535/50 band-pass emitter filter, and a Q505 long-pass beam splitter. The temperature of the culture medium was controlled between 36 and 37 °C by a BIOPTECHS (Butler, PA) objective heater and a heated ring surrounding the culture chamber. Digital images were taken with cooled CCD camera (Photometrix PLX, Tucson, AZ) using SCILL Image software (Multihouse, The Netherlands).

Incubation of the compounds with cells: The U2-OS human osteosarcoma cells were grown to about 30-50% confluence in Dulbecco's modified minimal essential medium without phenol red (Life Technologies) supplemented with 10% fetal calf serum and antibiotics (Gibco) in 35 mm culture dishes with glass cover slip incorporated in the bottom, which is directly in contact with the heated 40x; N.A. 1.30 oil-immersion objective during observations. The compounds were added to the cells at a final concentration of 5 μM in serum-free medium and incubated for 30 minutes at 37 ºC in a 5% CO_2 containing incubator. Next, the cells were washed twice with PBS and fresh medium supplemented with 10% fetal calf serum and antibiotics was added. The phase contrast and the corresponding fluorescence images were taken after the incubation at different time points including 24 hours after the incubation.

7.5 References

[1] S. van Zutphen, J. Reedijk, *Coord. Chem. Rev.* **2005**, *249*, 2845.

[2] K. Greish, *J. Drug Target.* **2007**, *15*, 457.

[3] E. Gianasi, M. Wasil, E. G. Evagorou, A. Keddle, G. Wilson, R. Duncan, *Eur. J. Cancer* **1999**, *35*, 994.

[4] X. Lin, Q. Zhang, J. R. Rice, D. R. Stewart, D. P. Nowotnik, S. B. Howell, *Eur. J. Cancer* **2004**, *40*, 291.

[5] G. V. Kalayda, B. A. J. Jansen, C. Molenaar, P. Wielaard, H. J. Tanke, J. Reedijk, *J. Biol. Inorg. Chem.* **2004**, *9*, 414.

[6] G. V. Kalayda, B. A. J. Jansen, P. Wielaard, H. J. Tanke, J. Reedijk, *J. Biol. Inorg. Chem.* **2005**, *10*, 305.

[7] E. T. Martins, H. Baruah, J. Kramarczyk, G. Saluta, C. S. Day, G. L. Kucera, U. Bierbach, *J. Med. Chem.* **2001**, *44*, 4492.

[8] V. Murray, H. Motyka, P. R. England, G. Wickham, H. H. Lee, W. A. Denny, W. D. McFadyen, *J. Biol. Chem.* **1992**, *267*, 18805.

[9] P. de Hoog, C. Boldron, P. Gamez, K. Sliedregt-Bol, I. Roland, M. Pitié, R. Kiss, B. Meunier, J. Reedijk, *J. Med. Chem.* **2007**, *50*, 3148.

[10] H. Kostrhunova, V. Brabec, *Biochemistry* **2000**, *39*, 12639.

[11] M. Lee, J. E. Simpson, A. J. Burns, S. Kupchinsky, N. Brooks, J. A. Hartley, L. R. Kelland, *Med. Chem. Res.* **1996**, *6*, 365.

[12] H. Loskotova, V. Brabec, *Eur. J. Biochem.* **1999**, *266*, 392.

[13] S. Ronchi, D. Prosperi, F. Compostella, L. Panza, *Synlett* **2004**, 1007.

[14] J. M. Oliva, E. Azenha, H. D. Burrows, R. Coimbra, J. S. S. de Melo, M. L. Canle, M. I. Fernandez, J. A. Santaballa, L. Serrano-Andres, *ChemPhysChem* **2005**, *6*, 306.

[15] X. P. Hu, H. L. Chen, Z. Zheng, *Adv. Synth. Catal.* **2005**, *347*, 541.

[16] L. M. Pedroso, M. Castro, P. Simoes, A. Portugal, *Polymer* **2005**, *46*, 1766.

[17] P. de Hoog, P. Gamez, W. L. Driessen, J. Reedijk, *Tetrahedron Lett.* **2002**, *43*, 6783.

[18] P. de Hoog, P. Gamez, H. Mutikainen, U. Turpeinen, J. Reedijk, *Angew. Chem.-Int. Edit.* **2004**, *43*, 5815.

[19] P. Gamez, J. Reedijk, *Eur. J. Inorg. Chem.* **2006**, 29.

[20] Z. L. Lu, P. Gamez, I. Mutikainen, U. Turpeinen, J. Reedijk, *Cryst. Growth Des.* **2007**, *7*, 1669.

[21] T. J. Mooibroek, P. Gamez, *Inorg. Chim. Acta* **2007**, *360*, 381.

[22] B. K. Saha, R. K. R. Jetti, L. S. Reddy, S. Aitipamula, A. Nangia, *Cryst. Growth Des.* **2005**, *5*, 887.

[23] M. Arduini, M. Crego-Calama, P. Timmerman, D. N. Reinhoudt, *J. Org. Chem.* **2003**, *68*, 1097.

[24] T. Hayashi, A. Fujimoto, T. Kajiki, S. Kondo, Y. Yano, *Chem. Lett.* **2000**, 1018.

[25] J. L. Silen, A. T. Lu, D. W. Solas, M. A. Gore, D. Maclean, N. H. Shah, J. M. Coffin, N. S. Bhinderwala, Y. W. Wang, K. T. Tsutsui, G. C. Look, D. A. Campbell, R. L. Hale, M. Navre, C. R. DeLuca-Flaherty, *Antimicrob. Agents Chemother.* **1998**, *42*, 1447.

[26] L. H. Hurley, *Nat. Rev. Cancer* **2002**, *2*, 188.

[27] J. Y. Chen, J. Stubbe, *Nat. Rev. Cancer* **2005**, *5*, 102.

[28] E. R. Jamieson, S. J. Lippard, *Chem. Rev.* **1999**, *99*, 2467.

[29] B. Rosenberg, L. van Camp, T. Krigas, *Nature* **1965**, *205*, 698.

[30] J. Reedijk, *Proc. Natl. Acad. Sci. U. S. A.* **2003**, *100*, 3611.

[31] P. M. Takahara, A. C. Rosenzweig, C. A. Frederick, S. J. Lippard, *Nature* **1995**, *377*, 649.

[32] H. Umezawa, K. Maeda, T. Takeuchi, Y. Okami, *J. Antibiot.* **1966**, *19*, 200.

[33] R. M. Burger, *Chem. Rev.* **1998**, *98*, 1153.

[34] M. Pitié, B. Sudres, B. Meunier, *Chem. Commun.* **1998**, 2597.

[35] M. Pitié, C. J. Burrows, B. Meunier, *Nucleic Acids Res.* **2000**, *28*, 4856.

[36] M. Pitié, J. D. Van Horn, D. Brion, C. J. Burrows, B. Meunier, *Bioconjugate Chem.* **2000**, *11*, 892.

[37] M. E. Huston, K. W. Haider, A. W. Czarnik, *J. Am. Chem. Soc.* **1988**, *110*, 4460.

[38] F. P. Intini, A. Boccarelli, V. C. Francia, C. Pacifico, M. F. Sivo, G. Natile, D. Giordano, P. De Rinaldis, M. Coluccia, *J. Biol. Inorg. Chem.* **2004**, *9*, 768.

* Parts of this chapter will be submitted for publication (Paul de Hoog, Stefanie van der Steen, Karlijn van der Schilden, Patrick Gamez, and Jan Reedijk)

8.1 Introduction

DNA can be modified irreversibly by: (1) oxidation of the deoxyribose moieties or the nucleobases; (2) hydrolysis of the phosphate backbone.[1-6] Compounds able to perform such DNA modifications have potential applications as biological tools to elucidate the mechanisms of the natural enzymes involved in DNA scission, repair, and signal transduction,[7-10] or as anti-tumor drugs.[11, 12]

Bleomycin, a natural product, was the first compound reported to be able to cleave DNA.[11-14] The Fe, Cu or Co complexes of bleomycin, in the presence of a reductant, are capable of abstracting the H4' proton from the deoxyribose unit of DNA. Nowadays, this ligand is clinically used against lymphomas, head and neck cancers, and germ-cell tumors.[12] This discovery has led to the search for complexes that mimic its efficient cleavage activity. The group of Sigman *et al.* reported the nuclease activity of the first synthetic examples, i.e. $[Cu^{I/II}(phen)_2]$.[15] It has been found that $[Cu^{I/II}(phen)_2]$ oxidizes the deoxyribose unit in the minor groove of DNA. $[Cu^{I/II}(phen)_2]$ mainly abstracts the H1' proton and to a lesser extent the protons H4' and H5'. The dissociation of one of the phenanthroline ligands limits the applicability of this complex. This problem has been overcome by making a connection of the two phenanthroline ligands with a serinol bridge.[16, 17] The nuclease activities of the resulting Cu(Clip-Phen) complexes is increased by up to 40 times. Other examples of effective artificial nuclease active agents are $[Fe^{II}(edta)]$,[18, 19] Cu(kanamycin)[20] or (tri)Cu_3 (Chapter 1, Figure 1.22).[21]

In order to improve the sequence selectivity and/or the nuclease activity of such compounds, the cleavage center can be associated with a DNA targeting agent. For example, Cu(Clip-Phen) has been attached to distamycin or to an intercalating agent.[22-24] Sequence-selective DNA cleavage at AT tracts, which is the preferred binding site for distamycin, has been observed for the Clip-Phen conjugate with distamycin.[24] The attachment of Cu(3-Clip-Phen) to an intercalator significantly increases the nuclease activity of the Cu(3-Clip-Phen) component of this bifunctional molecule.[22]

Metallointercallators have a very high affinity for DNA.[25, 26] In general, the ligands of these complexes are aromatic and planar, which can insert and stack between the base pairs of double-helical DNA. Moreover, the cationic nature of the metallointercalators strengthens their electrostatic interaction with DNA as well. These intercalating complexes have potential anti-tumor properties and are capable of targeting specific DNA sites. The group of Barton has developed a number of intercalating complexes.[27] The ligand has been varied, as well as the

metal ion.[25] For example, a ruthenium complex with dipyrido[3,2-*a*:2¢,3¢-*c*]phenazine (DPPZ) exhibits a DNA binding constant > 10^6 M^{-1}.[28] The properties of these ruthenium complexes make them particularly interesting for the preparation of DNA targeting bifunctional compounds. For instance, the $[Rh(chrysenequinonediimine)(bipy)_2]^{3+}$ unit linked to a cisplatin moiety directs the platinum to a DNA mismatch and not to the preferred site of interaction of cisplatin.[29]

Van der Schilden *et al.* designed heteronuclear ruthenium-platinum complexes to investigate their anti-tumor properties.[30, 31] A variety of ruthenium metallointercalators have now been synthesized that are linked by a flexible bridge to a terpyridine (terpy) unit. In the present chapter, the *in situ* preparation and the nuclease activity of heteronuclear bifunctional complexes are reported (Figure 8.1). The synergistic effect between the ruthenium targeting agent and the copper-terpy moiety is investigated. The ruthenium moiety is designed to direct the copper unit to the DNA, so that the copper can subsequently cleave the DNA. The Cu(terpy) complex is known to be able to cleave RNA,[32] but in this chapter, its ability to cleave DNA is reported for the first time. Both the nuclease activity and the mechanism of cleavage of these bifunctional complexes are explored in detail.

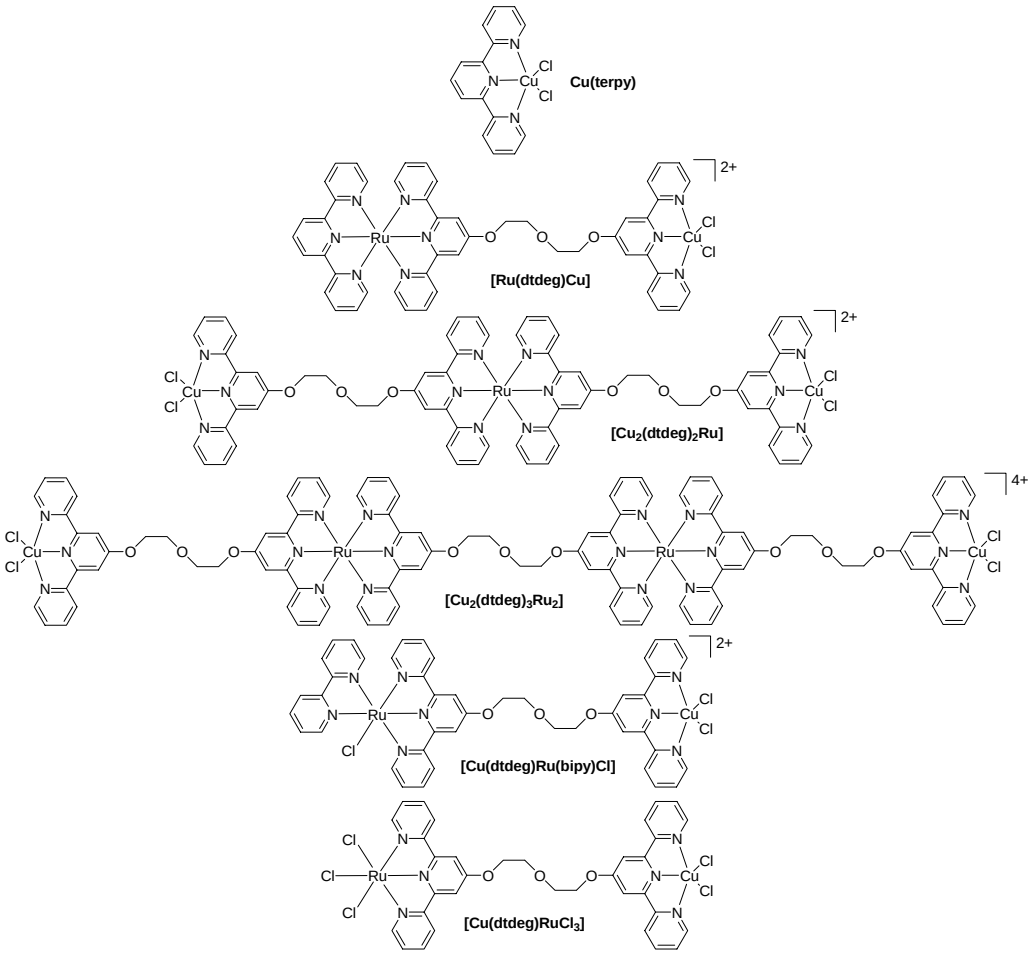

Figure 8.1 Schematic representations of the heteronuclear complexes **Cu(terpy)**, **[Ru(dtdeg)Cu]**, **[Cu_2(dtdeg)$_2$Ru]**, **[Cu_2(dtdeg)$_3$$Ru_2$]**, **[Cu(dtdeg)Ru(bipy)Cl]** and **[Cu(dtdeg)$RuCl_3$]**.

8.2 Results and discussion

8.2.1 Coordination studies

UV-Vis studies have been carried out to investigate the ability of the terpy ligand to bind copper (Figure 8.2). The spectra obtained are comparable to previously published spectra collected for both copper and platinum terpy complexes.[33] The initial spectrum of terpy changes drastically upon addition of $CuCl_2$. The differences in the spectra of 0.5 equivalents of copper and 1 equivalents of copper are distinct. For example, a strong increase in absorption is observed at 220 nm with increasing copper concentration. Moreover, the sharp peak at 280 nm is observed only for 1 or more equivalents of copper, and not for 0.5 equivalents of copper per terpy ligand. The spectrum does not change so drastically upon addition of more than one equivalent of $CuCl_2$ to the terpy ligand, although marked differences are observed at 260 and 220 nm. Nevertheless, the complexes **Cu(terpy)**, **[Ru(dtdeg)Cu]**, **[Cu_2(dtdeg)$_2$Ru]**, **[Cu_2(dtdeg)$_3$$Ru_2$]**, **[Cu(dtdeg)Ru(bipy)Cl]** and **[Cu(dtdeg)$RuCl_3$]** have been prepared *in situ* with one equivalent of copper per terpy ligand throughout the whole study presented in this chapter, since no differences in cleaving activity have been observed with one, or one and a half equivalents of copper per terpy unit.

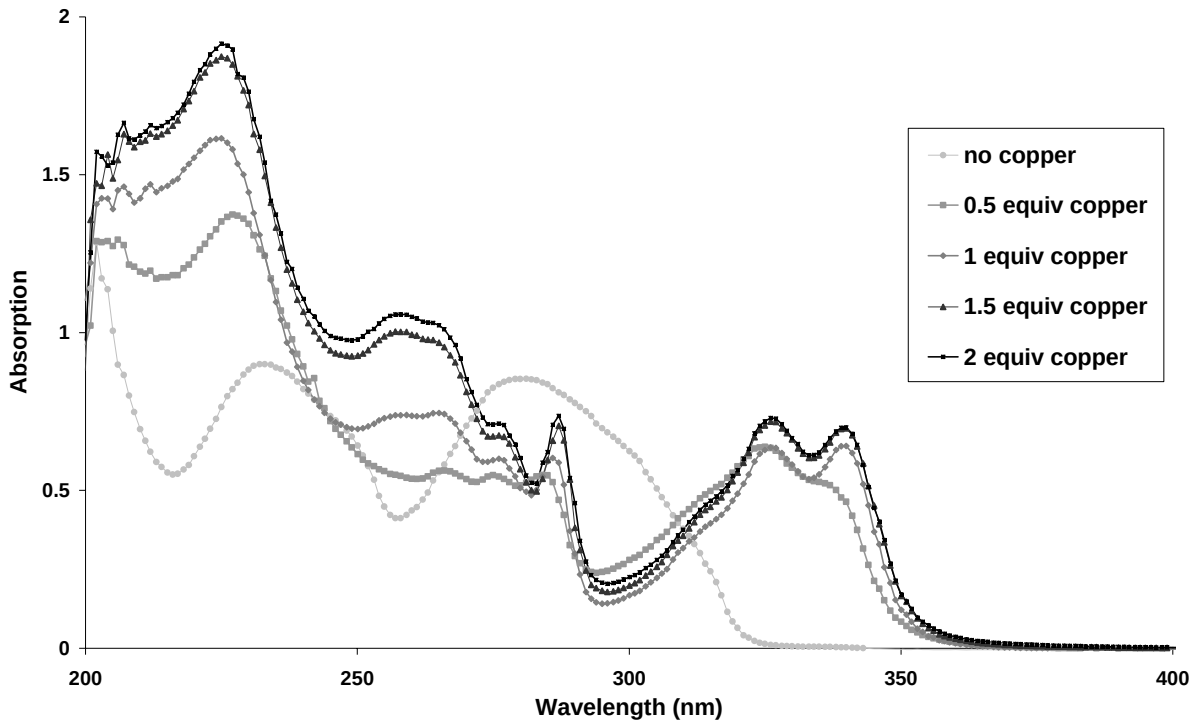

Figure 8.2 Titration of $CuCl_2$ to the ligand terpy (50 μM) followed by UV-Vis spectroscopy. Four different quantities of copper have been used: 0.5, 1, 1.5 and 2 equivalents per 1 equivalent of terpy ligand.

Frozen EPR spectra have been recorded of the complexes **Cu(terpy)**, **[Ru(dtdeg)Cu]**, **[Cu_2(dtdeg)$_2$Ru]**, **[Cu_2(dtdeg)$_3$$Ru_2$]**, **[Cu(dtdeg)Ru(bipy)Cl]** and **[Cu(dtdeg)$RuCl_3$]** in H_2O. It is shown that a part of the Cu(II) of the **Cu(terpy)** and **[Cu(dtdeg)$RuCl_3$]** has dissociated from the ligand to the form the $Cu(H_2O)_6^{2+}$ complex. Nevertheless, unique peaks are observed that correspond with Cu(II) binding to nitrogen ligands. The recorded EPR signals of the other complexes are too broad, because the freezing of H_2O solution of the complexes did not lead to a good glass. It is assumed that the other complex solutions have similar behavior, since the binding unit for the copper is the same.

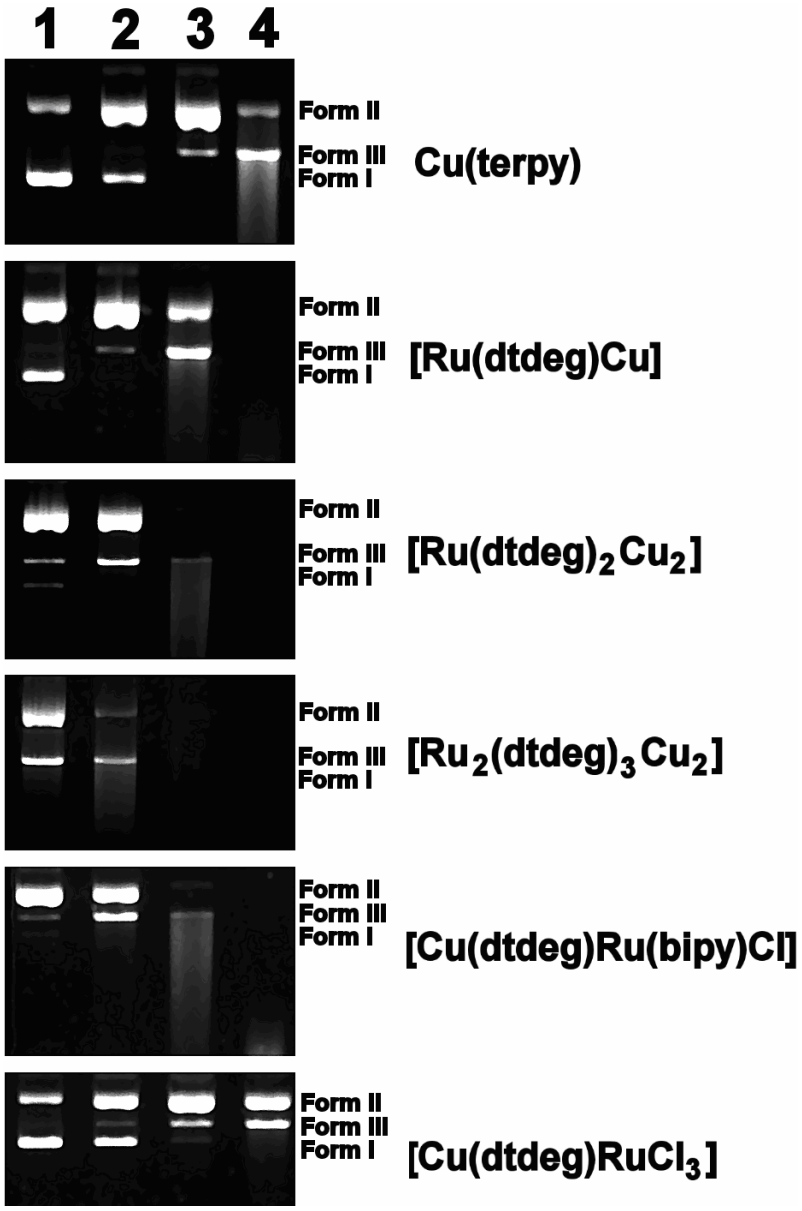

Figure 8.3 DNA cleavage activity of **Cu(terpy)**, **[Ru(dtdeg)Cu]**, **[Cu_2(dtdeg)$_2$Ru]**, **[Cu_2(dtdeg)$_3$$Ru_2$]**, **[Cu(dtdeg)Ru(bipy)Cl]** and **[Cu(dtdeg)$RuCl_3$]** (see scheme 1 for complex details). Lane 1 : complex concentration of 1 μM. Lane 2 : complex concentration of 2 μM. Lane 3 : complex concentration of 5 μM. Lane 4: complex concentration of 10 μM.

8.2.2 Cleavage of supercoiled DNA

The relaxation of supercoiled circular ΦX174 DNA (form I) into the relaxed (form II) and the linear (form III) conformations mediated by the complexes **Cu(terpy)**, **[Ru(dtdeg)Cu]**, **[Cu_2(dtdeg)$_2$Ru]**, **[Cu_2(dtdeg)$_3$$Ru_2$]**, **[Cu(dtdeg)Ru(bipy)Cl]** and **[Cu(dtdeg)$RuCl_3$]** has been investigated and compared. The concentrations shown in this chapter are of the complexes, therefore **[Cu_2(dtdeg)$_2$Ru]** and **[Cu_2(dtdeg)$_3$$Ru_2$]** have a two times higher copper concentration compared to the other complexes. The ruthenium compounds in combination with other metal ions, like Fe, Ni, Co and Mn do not show any nuclease activity. DNA is reacted for 1 hour with the complexes and mercaptopropionic acid (MPA) prior to loading the samples on agarose gel. The optimal cleavage conditions are obtained with phosphate buffer (pH 7.2) and MPA, because significantly lower cleavage activities are observed in HEPES buffer (pH 7.2) and with ascorbate acid as reductant. All the experiments have been performed reproducibly with phosphate buffer and MPA as added reductant.

The activity of each complex has been tested at four different concentrations (1, 2, 5 and 10 μM; Figure 8.3). The complexes do not show any nuclease activity in the absence of copper or MPA. With copper and MPA activity is observed, and the following cleavage activity sequence has been found: **[Cu_2(dtdeg)$_3$$Ru_2$]** > **[$Cu_2$(dtdeg)$_2$Ru]** ≈ **[Cu(dtdeg)Ru(bipy)Cl]** > **[Ru(dtdeg)Cu]** >> **Cu(terpy)** ≥ **[Cu(dtdeg)$RuCl_3$]**. It should be noted that **[Cu_2(dtdeg)$_3$$Ru_2$]** and **[$Cu_2$(dtdeg)$_2$Ru]** have two active copper units compared to the other complexes. The nuclease activity of **Cu(terpy)** is low at 2 μM, because only a small fraction of supercoiled DNA is converted to circular DNA. At higher complex concentrations, linear DNA is also formed and a smear appears at a concentration of 10 μM. Compared to **Cu(terpy)**, the complex **[Ru(dtdeg)Cu]**, including one ruthenium moiety and one copper unit, is substantially more active per copper ion. At a complex concentration of 2 μM, the entire supercoiled DNA is transformed to circular and linear DNA. At 10 μM, all DNA is cut into relatively small fragments that cannot be visualized by their treatment with ethidium bromide. Logically, the complex that contains two copper units and one ruthenium moiety shows an increased nuclease activity compared to **[Ru(dtdeg)Cu]** and **Cu(terpy)**. A smear (multi-fragmented DNA) already appears at a **[Cu_2(dtdeg)$_2$Ru]** concentration of 5 μM. At a concentration of 1 μM, the supercoiled DNA is totally converted to mainly circular DNA and, to a lesser extent, to linear DNA. The most active cleaving agent **[Cu_2(dtdeg)$_3$$Ru_2$]** has two ruthenium units and two copper centers. A large fraction of linear DNA (Form III) is observed at a complex concentration of 1 μM. A smear starts to appear at a concentration of 2 μM and the three forms of DNA are not detectable at a

complex concentration of 5 μM. The complex **[Cu(dtdeg)Ru(bipy)Cl]** exhibits a different ruthenium unit, consisting of a ruthenium(III) ion coordinated by one terpy and one bipy ligands and a chloride anion. Interestingly, this complex shows a nuclease activity (at similar complex concentrations) comparable to the one of **[Cu_2(dtdeg)$_2$Ru]** at similar complex concentrations even though it holds only one copper unit. Probably, the interaction of the ruthenium unit of **[Cu(dtdeg)Ru(bipy)Cl]** with DNA is stronger than the one of the Ru moiety of **[Cu_2(dtdeg)$_2$Ru]**. The neutral complex **[Cu(dtdeg)$RuCl_3$]** is less active than **Cu(terpy)**. This difference in reactivity is clearly observed at 10 μM, where the action of **[Cu(dtdeg)$RuCl_3$]** produces a smear, while **Cu(terpy)** does not. The ruthenium unit of **[Cu(dtdeg)$RuCl_3$]** is not charged and therefore its interaction with DNA is less favored compared to the charged complexes **[Ru(dtdeg)Cu]**, **[Cu_2(dtdeg)$_2$Ru]** and **[Cu_2(dtdeg)$_3$$Ru_2$]**, **[Cu(dtdeg)Ru(bipy)Cl]**.

Time-course studies of DNA cleavage mediated by the complexes **Cu(terpy)**, **[Ru(dtdeg)Cu]**, **[Cu_2(dtdeg)$_2$Ru]**, **[Cu_2(dtdeg)$_3$$Ru_2$]**, **[Cu(dtdeg)Ru(bipy)Cl]** and **[Cu(dtdeg)$RuCl_3$]** have been carried out to further investigate their cleaving ability (Figure 8.4). The major difference is the use of larger volumes of reactant solutions (see experimental section) for the kinetic studies (compared to the typical experiments), which may result in small discrepancies regarding the cleavage activities. These experiments confirm the sequence of cleavage ability determined earlier. It has to be noticed that **[Cu_2(dtdeg)$_2$Ru]** and **[Cu(dtdeg)Ru(bipy)Cl]** show lower cleaving activities at the same complex concentrations, using these experimental conditions compared to the results shown in Figure 8.3. All plots illustrate a decrease of Form I with concomitant increase of Form II. Form III is not formed, or only in a slight amount at a later stage of the cleavage reaction, and only after all Form I is converted. In all cases, less than 10 % of Form III is formed, at the end of the cleavage reactions. All the complexes display the typical behavior of single-strand cleaving agents. Indeed, the action of double strand cleaving agents is characterized by the production of Form III directly from the beginning of the cleavage reaction (see for example the mechanism of action of the complexes reported in chapters 3 and 4).[34]

The nature of the active species responsible for the cleavage of DNA can be investigated by the addition of inhibitors. So, NaN_3, superoxide dismutase, DMSO or ethanol have been added to the reaction mixture containing the complexes **Cu(terpy)**, **[Ru(dtdeg)Cu]**, **[Cu_2(dtdeg)$_2$Ru]**, **[Cu_2(dtdeg)$_3$$Ru_2$]**, **[Cu(dtdeg)Ru(bipy)Cl]**, or **[Cu(dtdeg)$RuCl_3$]** to uncover the active species of the cleavage reaction. Cleavage reactions have also been performed under argon, pure dioxygen and in the dark. NaN_3 is able to quench singlet oxygen, superoxide dismutase is able to scavenge superoxide radicals, and DMSO and ethanol are known to neutralize hydroxyl radicals. The reaction under argon reveals an active role of dioxygen in the reaction medium. The reactions carried out in the dark reveal the potential of the complexes to perform photocleavage of DNA. If dioxygen is involved in the cleavage process and its binding

to the complex is the rate-determining step, then the amount of DNA cuts would be expected to increase under an atmosphere of dioxygen.

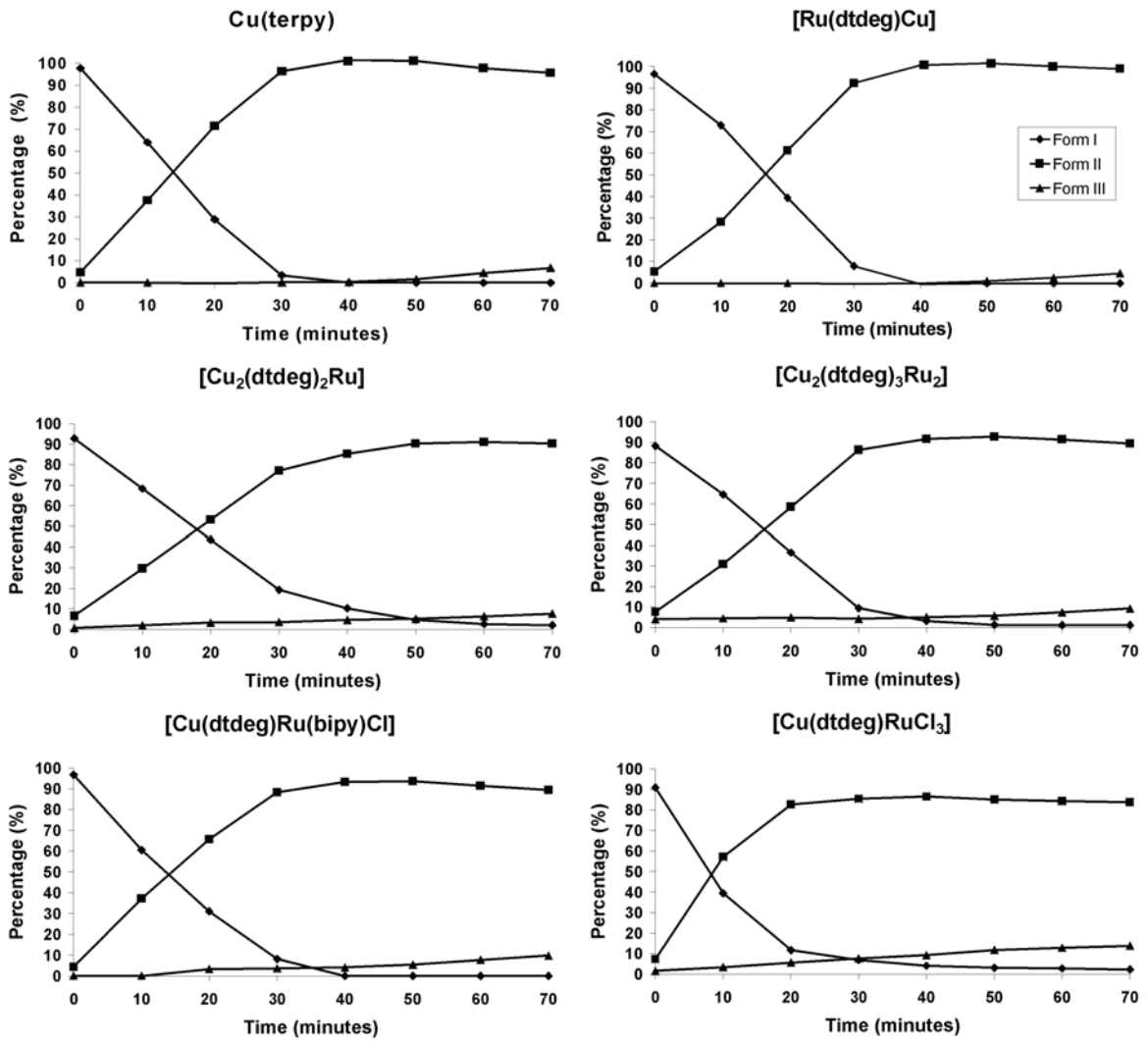

Figure 8.4 Time-course experiments of DNA cleavage (20 μM base pairs) over a period of 70 minutes in the presence of 5 mM MPA and air. The different plots have been obtained using, respectively, 5 μM **Cu(terpy)**, 2 μM **[Ru(dtdeg)Cu]**, 2 μM **[Cu_2(dtdeg)$_2$Ru]**, 1 μM **[Cu_2(dtdeg)$_3$$Ru_2$]**, 3 μM **[Cu(dtdeg)Ru(bipy)Cl]** and 8 μM **[Cu(dtdeg)$RuCl_3$]**.

Cleavage reactions in the presence of scavengers have been investigated for all complexes. However, only the results obtained with **[Ru(dtdeg)Cu]** are depicted in Figure 8.5, because all the compounds give comparable results suggesting very similar mechanisms. In Figure 8.5, lane 1 illustrates the aerobic cleavage reaction mediated by **[Ru(dtdeg)Cu]** in the presence of MPA (normal cleavage conditions). The reactions of **[Ru(dtdeg)Cu]** with DNA in the presence of NaN_3, superoxide dismutase, DMSO, ethanol, under dioxygen, or in the dark are similar to the one performed under normal cleavage conditions. In contrast, the reaction under argon is almost completely inhibited, which indicates that dioxygen is involved in the cleavage reaction. The

active species generated from **Cu(terpy)**, **[Ru(dtdeg)Cu]**, **[Cu_2(dtdeg)$_2$Ru]**, **[Cu_2(dtdeg)$_3$$Ru_2$]**, **[Cu(dtdeg)Ru(bipy)Cl]** and **[Cu(dtdeg)$RuCl_3$]** is therefore most likely a copper bound oxidant, which is not affected by the presence of any of the used scavengers.

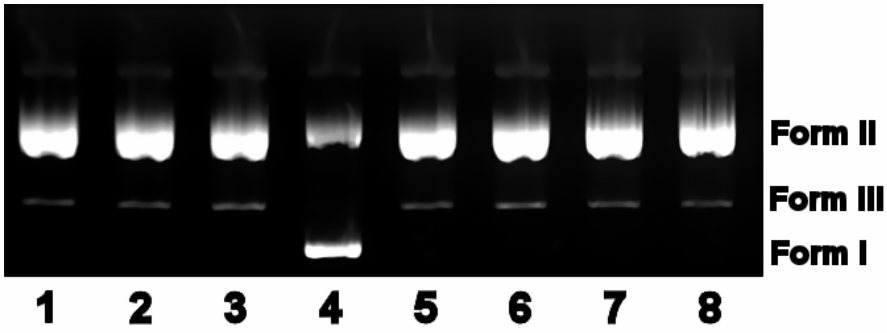

Figure 8.5 Cleavage reactions mediated by **[Ru(dtdeg)Cu]** in the presence of various scavengers performed in air (except lane 4). All experiments were performed with a complex concentration of 5 μM. Lane 1: no extra additives. Lane 2: 100 μM NaN_3. Lane 3: 0.5 units superoxide dismutase. Lane 4: under argon. Lane 5: in the dark. Lane 6: under dioxygen. Lane 7: 20 μM DMSO. Lane 8: 20 μM ethanol.

The ruthenium units are probably able to interact with DNA by electrostatic interaction and partial intercalation. An increase of the ionic strength of the reaction medium is expected to reduce the affinity of such compounds for DNA. Therefore, experiments have been performed with increasing concentrations of NaCl. Only the cleavage products obtained with **Cu(terpy)** and **[Ru(dtdeg)Cu]** are shown in Figure 8.6, because the use of complexes **[Cu_2(dtdeg)$_2$Ru]**, **[Cu_2(dtdeg)$_3$$Ru_2$]**, **[Cu(dtdeg)Ru(bipy)Cl]** and **[Cu(dtdeg)$RuCl_3$]** gives analogous results compared to **[Ru(dtdeg)Cu]**. The cleaving activities of all complexes start to decrease from a NaCl concentration of 50 mM and above (Lanes 4 and 12, Figure 8.6). At 300 mM NaCl, no cleaving activity is observed for **[Ru(dtdeg)Cu]**, **[Cu_2(dtdeg)$_2$Ru]**, **[Cu_2(dtdeg)$_3$$Ru_2$]**, **[Cu(dtdeg)Ru(bipy)Cl]** and **[Cu(dtdeg)$RuCl_3$]**. The cleaving activity of **Cu(terpy)** is diminished at a NaCl concentration of 300 mM, but the nuclease activity is not quenched. This result indicates that **Cu(terpy)** interacts in a different manner with DNA, compared with the complexes that include a ruthenium moiety. Its interaction with DNA is apparently dominated by partial intercalation of the terpy ligand, which is not perturbed by an enhancement of the ionic strength of the solution.

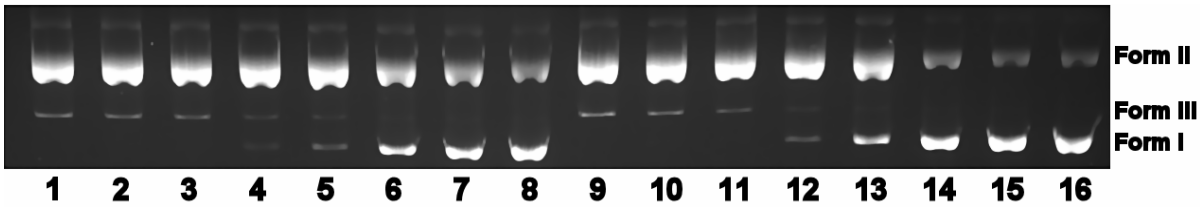

Figure 8.6 Influence of the ionic strength on the cleavage abilities of **Cu(terpy)** and**[Ru(dtdeg)Cu]**. Lanes 1-8: **Cu(terpy)** (5 μM). Lanes 9-16: **[Ru(dtdeg)Cu]** (2 μM). Lanes 1

and 9: no NaCl. Lanes 2 and 10: 10 mM NaCl. Lanes 3 and 11: 20 mM NaCl. Lanes 4 and 12: 50 mM NaCl. Lanes 5 and 13: 100 mM NaCl. Lanes 6 and 14: 300 mM NaCl. Lanes 7 and 15: 500 mM NaCl. Lanes 8 and 16: 625 mM NaCl.

The ruthenium unit in **[Cu(dtdeg)Ru(bipy)Cl]** and **[Cu(dtdeg)RuCl$_3$]** has the possibility to coordinate to DNA, because the complexes have respectively one and three chloride ligands. As mentioned in previous chapters, the complexes have been pre-incubated with DNA for 24 hours before the initiation of the cleavage reaction. However, no difference in nuclease activity between the experiments with and without pre-incubation time is observed. In the following experiment, the DNA was precipitated after the pre-incubation time, prior to the cleavage reaction, to remove any unreacted complex. Interestingly, the complexes do not show any DNA cleavage under these experimental conditions. To increase their reactivity towards DNA, **[Cu(dtdeg)Ru(bipy)Cl]** and **[Cu(dtdeg)RuCl$_3$]** have been treated with, respectively, one and three equivalents of $AgNO_3$ to remove the chloride ligands. This method is commonly used for replacing a chloride by a water ligand in order to enhance the reactivity of a platinum center towards nucleophiles. After a pre-incubation time of 24 hours and precipitation of DNA or not, the DNA cleavage reaction is initiated (Figure 8.7). Both complexes are less efficient cleaving agents after treatment with $AgNO_3$ and pre-incubation time of 24 hours. It is expected that the complexes would have a stronger DNA interaction after removal of the chlorides and thus higher nuclease activity. However, the nuclease activity is lower after $AgNO_3$ treatment. The explanation for these surprising results is not yet available. Without precipitation step, **[Cu(dtdeg)Ru(bipy)Cl]** (lanes 1 and 2, Figure 8.7) and **[Cu(dtdeg)RuCl$_3$]** (lanes 5 and 6, Figure 8.7) display cleavage activities. With a precipitation step no cleavage is observed for both complexes (Lanes 3, 4, 7, and 8, Figure 8.7). These results indicate that the two complexes, despite preactivation, do not coordinate to supercoiled DNA under these experimental conditions.

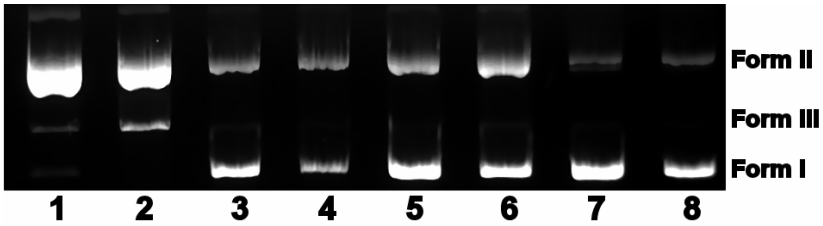

Figure 8.7 DNA Cleavage experiments of **[Cu(dtdeg)Ru(bipy)Cl]** and **[Cu(dtdeg)RuCl$_3$]** after reaction with $AgNO_3$ and a pre-incubation time of 24 hours. Lane 1: 5 μM **[Cu(dtdeg)Ru(bipy)Cl]**, no precipitation step. Lane 2: 10 μM **[Cu(dtdeg)Ru(bipy)Cl]**, no precipitation step. Lane 3: 5 μM **[Cu(dtdeg)Ru(bipy)Cl]**, with precipitation step. Lane 4: 10 μM **[Cu(dtdeg)Ru(bipy)Cl]**, with precipitation step. Lane 5: 5 μM **[Cu(dtdeg)RuCl$_3$]**, no precipitation step. Lane 6: 10 μM **[Cu(dtdeg)RuCl$_3$]**, no precipitation step. Lane 7: 5 μM **[Cu(dtdeg)RuCl$_3$]**, with precipitation step. Lane 8: 10 μM **[Cu(dtdeg)RuCl$_3$]**, with precipitation step.

8.2.3 Cleavage of the ODN I strand of the ODN I/ODN II duplex

High-resolution analyses of the cleavage of **Cu(terpy)**, **[Ru(dtdeg)Cu]**, **[Cu_2(dtdeg)$_2$Ru]**, **[Cu_2(dtdeg)$_3$$Ru_2$]**, **[Cu(dtdeg)Ru(bipy)Cl]** and **[Cu(dtdeg)$RuCl_3$]** have been performed with the aim to investigate the sequence selective cleavage and the target for the oxidation. The cleavage of a 36 base-pair sequence has been investigated by PAGE (Figure 8.8). The target is labeled at the 5'-end of ODN I. The reaction of each complex with the ODN duplex is carried out for 1 hour in the presence of MPA. The concentration of complexes **Cu(terpy)** and **[Cu(dtdeg)$RuCl_3$]** is taken two times higher compared to the other complexes, because no cleavage is observed at 5 μM. After the cleavage reaction, the complexes are removed by precipitation. For some of these experiments, additional treatments have been performed: i.e. (i) treatment with piperidine to reveal the oxidation of nucleobases (Figure 8.9) and (ii) treatment with HEPES at pH 8.0 to cleave the metastable products resulting from the oxidation of deoxyribose (Figure 8.10).

```
                                    ↓
5'-AACTTAATAGTATACATTGGACACAACAACAACAAC-3' ODN I
3'-TTGAATTATCATATGTAACCTGTGTTGTTGTTGTTG-5' ODN II
```

Figure 8.8 Nucleobase sequences of the ODN I and ODN II fragments used for the PAGE cleavage experiments. The arrow shows the cleavage position in the ODN I fragment, which is not generated by the complexes, because it is present in the blank experiments as well.

The strong signal at the adenine base, indicated by an arrow in Figures 8.8 and 8.9, is not attributable to sequence selective cleavage of the complexes. The experiments without cleavage events also show a strong signal at this site (lanes 3, 6, 9, 12, 15 and 18, Figure 8.9). The complexes in the presence of MPA cleave the DNA without any sequence selectivity (Lanes 1, 4, 7, 10, 13, 16, Figure 8.9 and 8.10), since cleavage sites are observed at all the nucleobases.

Nucleobase oxidation does not result in direct strand cleavage; consequently, a second treatment is needed. In general, the products resulting from nucleobase oxidation are cleaved by a heating step in piperidine.[4] The metastable adducts resulting from deoxyribose oxidation are also cleaved by the treatment with piperidine. The piperidine treatment of the reactions with the complexes results in stronger cleavages (compare lanes 1 and 2, 4 and 5, 7 and 8, 10 and 11, 13 and 14, 16 and 17, Figure 8.9). For **[Cu_2(dtdeg)$_2$Ru]** (lanes 7 and 8), **[Cu_2(dtdeg)$_3$$Ru_2$]** (lanes 10 and 11), **[Cu(dtdeg)Ru(bipy)Cl]** (lane 13 and 14) and **[Cu(dtdeg)$RuCl_3$]** (lanes 16 and 17), the higher activities are clearly evidenced. In addition, the resolution of the different cleavage patterns is higher compared to those achieved with the use of MPA only. These results indicate that the nucleobases are also oxidized by the complexes.[4] The direct cleavage of the DNA strand is observed as well, which suggests that deoxyribose oxidation is also occurring. HEPES

treatments at pH 8 have been performed to investigate whether the deoxyribose oxidation is the unique pathway of the cleavage. The abasic sites resulting from the oxidation of nucleobases are not cleaved during treatment with HEPES, which is in contrast to the metastable products resulting from the oxidation of deoxyribose. A second precipitation step is performed for these experiments; therefore, part of the labeled ODN I fragment is lost, resulting in a weaker signal, as is evidenced in Figure 8.10 (for instance, compare lanes 7 and 8). The cleavage activities of all complexes are not improved, thus indicating that only small amounts of metastable sites are produced during the cleavage reactions. Hence, the cleavage induced by the piperidine treatment originates from the oxidation of nucleobases and not from the cleavage of metastable products developed from deoxyribose oxidation.

[Cu(dtdeg)Ru(bipy)Cl] and **[Cu(dtdeg)RuCl$_3$]** have been incubated for 24 hours with the ODN duplex in order to investigate their ability to bind to DNA (see also chapters 3, 4 and 5 for the platinum-Cu(3-Clip-Phen) complexes). Complexes able to coordinate to DNA are expected to retard the migration of the complexed-DNA during denaturing PAGE, as a result of the increase in molecular weight and the change of the overall charge. In fact, the results (Figure 8.9 and 8.10, lanes 13-18) confirm that **[Cu(dtdeg)Ru(bipy)Cl]** and **[Cu(dtdeg)RuCl$_3$]** are not capable of coordinating to the ODN duplex, since no change in "free" ODN I is observed.

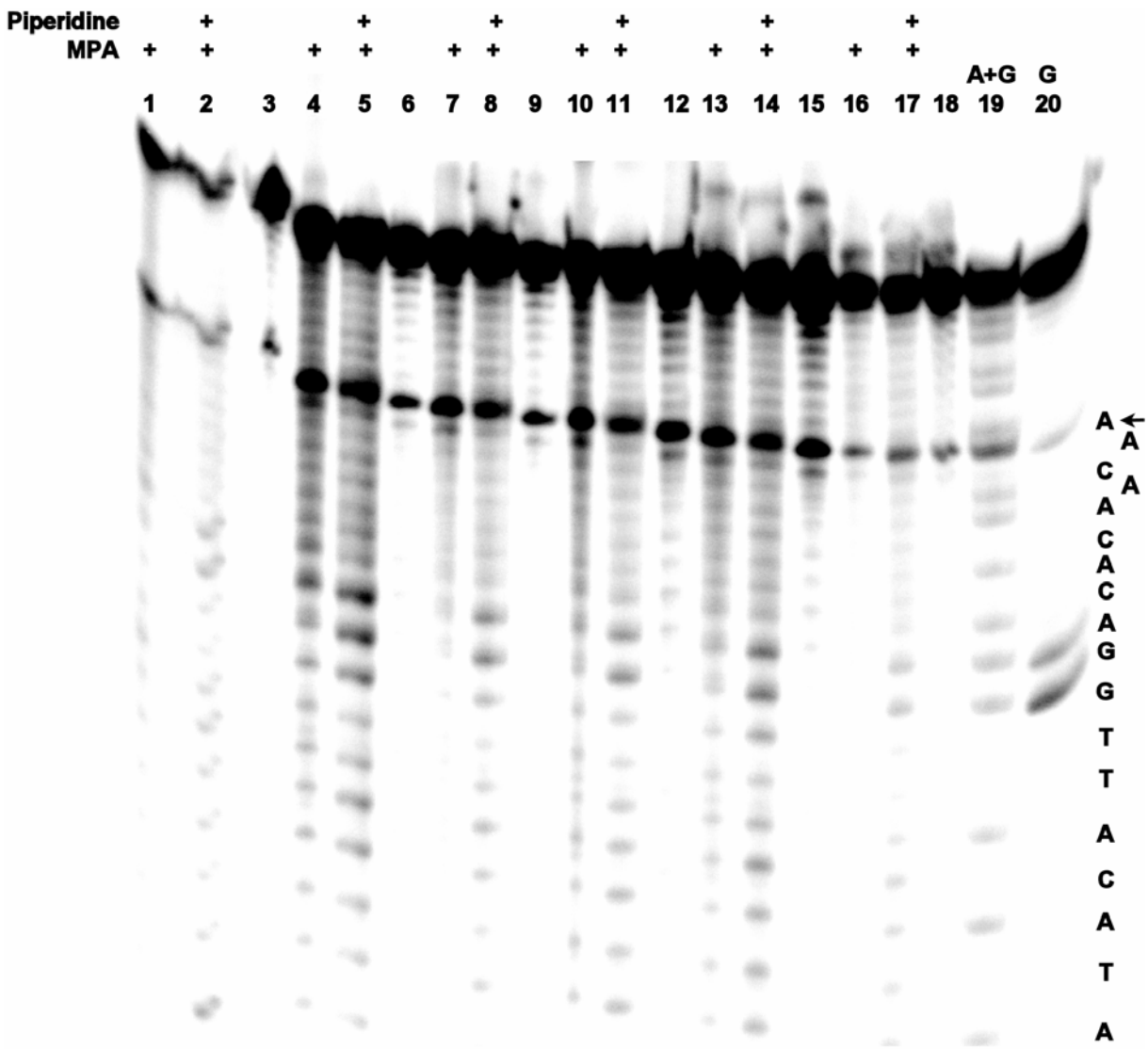

Figure 8.9 PAGE analysis of the cleavage of the ODN I fragment of the ODN I-ODN II duplex (1 μM) mediated by **Cu(terpy)** (10 μM), **[Ru(dtdeg)Cu]** (5 μM), **[Cu_2(dtdeg)$_2$Ru]** (5 μM), **[Cu_2(dtdeg)$_3$$Ru_2$]** (5 μM), **[Cu(dtdeg)Ru(bipy)Cl]** (5 μM) and **[Cu(dtdeg)$RuCl_3$]** (10 μM). The cleavage reactions are initiated with MPA (5 mM) under aerobic conditions (Lanes 1, 4, 7, 10, 13 and 16) or by heating 30 min at 90 °C in aqueous piperidine 0.2 M (Lanes 2, 5, 8, 11, 14 and 17). The Maxam-Gilbert sequencing reactions A + G (lane 19) and G (lane 20) allow determining the cleavage sites. The additives used in the experiments are indicated on top of the gel (details are given in the experimental part). Lanes 1-3: **Cu(terpy)**. Lanes 4-6: **[Ru(dtdeg)Cu]**. Lanes 7-9: **[Cu_2(dtdeg)$_2$Ru]**. Lanes 10-12: **[Cu_2(dtdeg)$_3$$Ru_2$]**. Lanes 13-15: **[Cu(dtdeg)Ru(bipy)Cl]**. Lanes 16-18: **[Cu(dtdeg)$RuCl_3$]**. The arrow shows the cleavage position in the ODN I fragment, which is not generated by the complexes, because it occurs in the blank experiments as well.

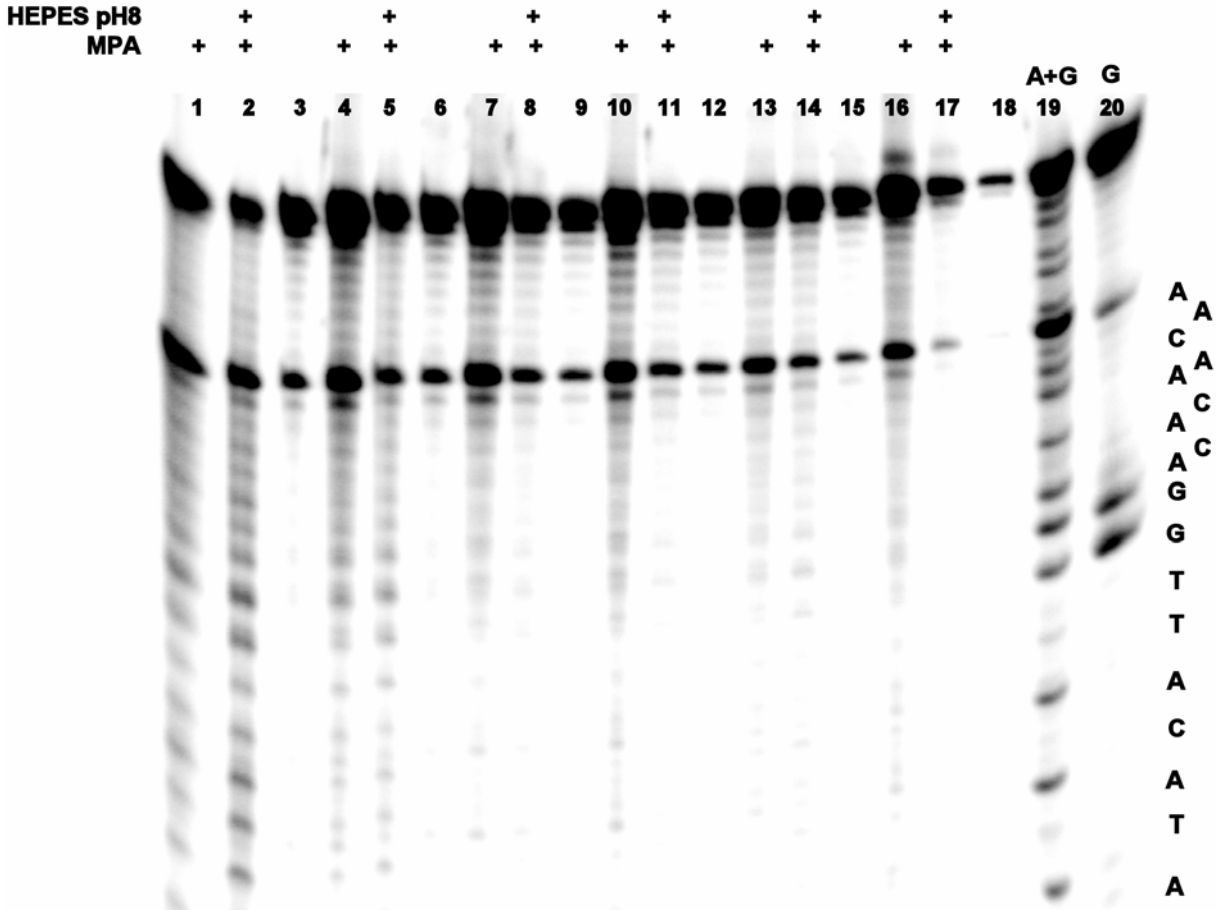

Figure 8.10 PAGE analysis of the cleavage of the ODN I fragment of the ODN I-ODN II duplex (1 μM) mediated by **Cu(terpy)** (10 μM), **[Ru(dtdeg)Cu]** (5 μM), **[Cu_2(dtdeg)$_2$Ru]** (5 μM), **[Cu_2(dtdeg)$_3$$Ru_2$]** (5 μM), **[Cu(dtdeg)Ru(bipy)Cl]** (5 μM) and **[Cu(dtdeg)$RuCl_3$]** (10 μM). The cleavage reactions are initiated by the addition of MPA (5 mM) under aerobic conditions (Lanes 1, 4, 7, 10, 13 and 16), or by a heating step at ΔpH 8 for 30 min at 90 °C in HEPES/NaOH buffer (0.1 M, pH 8.0) (Lanes 2, 5, 8, 11, 14 and 17). The Maxam-Gilbert sequencing reactions A + G (lane 19) and G (lane 20) are performed to determine the cleavage sites. The additives used in the experiments are indicated on top of the gel (details are given in the experimental part). Lanes 1-3: **Cu(terpy)**. Lanes 4-6: **[Ru(dtdeg)Cu]**. Lanes 7-9: **[Cu_2(dtdeg)$_2$Ru]**. Lanes 10-12: **[Cu_2(dtdeg)$_3$$Ru_2$]**. Lanes 13-15: **[Cu(dtdeg)Ru(bipy)Cl]**. Lanes 16-18: **[Cu(dtdeg)$RuCl_3$]**.

8.3 Conclusions

The complexes **Cu(terpy)**, **[Ru(dtdeg)Cu]**, **[Cu_2(dtdeg)$_2$Ru]**, **[Cu_2(dtdeg)$_3$$Ru_2$]**, **[Cu(dtdeg)Ru(bipy)Cl]** and **[Cu(dtdeg)$RuCl_3$]** all exhibit good nuclease activities. The order of nuclease efficiency as measured per complex concentration **[Cu_2(dtdeg)$_3$$Ru_2$]** > **[$Cu_2$(dtdeg)$_2$Ru]** ≈ **[Cu(dtdeg)Ru(bipy)Cl]** > **[Ru(dtdeg)Cu]** >> **Cu(terpy)** ≥ **[Cu(dtdeg)$RuCl_3$]** illustrates the importance of the charged ruthenium unit that probably targets the copper component of the heteronuclear complex to DNA. The cleavage activities of the complexes bearing a ruthenium unit are substantially higher than the one of **Cu(terpy)**, except for **[Cu(dtdeg)$RuCl_3$]**. This latter complex is not charged; therefore, its interaction with DNA is

less favored. Dioxygen, a reductant and copper appear to be essential factors for the cleavage efficacy of these complexes. The copper(II) compounds are first reduced by MPA *in situ*. The subsequent reaction with dioxygen generates as yet unknown copper-bound oxygen species, which are able to cleave DNA. All the complexes are single-strand cleaving agents that cut DNA without any apparent sequence selectivity. Most likely, the complexes oxidize both the nucleobases and the deoxyribose units. The oxidation of the nucleobases is evidenced by the increase of the cleavage upon treatment with piperidine, while HEPES does not lead to such enhancement of the nuclease efficiency. In addition, direct DNA strand breaks are observed, which cannot be achieved through the oxidation of only the nucleobases. The products resulting from nucleobase and deoxyribose oxidation should be investigated in detail to confirm these results.

8.4 Experimental

In situ preparation of the metal complexes: The ruthenium complexes were synthesized by Van der Schilden and have been used as such in the present studies.[30, 31] The ruthenium complexes were reacted with one equivalent of copper per terpy ligand. Typically, 500 μL of a ruthenium complex (2 μM) solution in MilliQ H_2O was added to a 500 μL solution of (2 μM or 4 μM depending on the terpy units) $CuCl_2$ in MilliQ H_2O. Further dilutions have been made with MilliQ H_2O to obtain the appropriate complex concentrations for the cleavage studies. These solutions were stored in the fridge. X-band powder EPR spectra were obtained on a Bruker-EMX*plus* electron spin resonance spectrometer (Field calibrated with DPPH (g = 2.0036)). X-Band EPR (frozen solution): **Cu(terpy)**, first species: $g_\perp$ = 2.05, $g_{//}$ = 2.30, $A_{//}$ = 12.6 mT; second species: $g_\perp$ = 2.05, $g_{//}$ = 2.25, $A_{//}$ = 13.1 mT; **[Ru(dtdeg)Cu]**, g = 2.09 (signal broad); **[Cu_2(dtdeg)$_2$Ru]**, g = 2.12 (signal broad); **[Cu_2(dtdeg)$_3$$Ru_2$]**, $g_\perp$ = 2.07, $g_{//}$ = 2.25, $A_{//}$ = 14.7 mT (signal broad); **[Cu(dtdeg)Ru(bipy)Cl]**, $g_\perp$ = 2.07, $g_{//}$ = 2.27, $A_{//}$ = 16.7 mT (signal broad); **[Cu(dtdeg)$RuCl_3$]**, the absorbance of g = 2.02 is attributed to one of the signals of the Ru(III) unit.[35] The other Ru^{III} signals are hidden underneath the Cu $g_\perp$ signals. The $g_\perp$ = 2.07, $g_{//}$ = 2.37, $A_{//}$ = 11.4 mT (first species), and $g_\perp$ = 2.07, $g_{//}$ = 2.26, $A_{//}$ = 13.8 mT (second species) are assigned to the copper moiety.

Nuclease activity on supercoiled DNA: 1 mM MilliQ H_2O solutions of the complexes investigated were diluted to respectively 4, 8, 20 and 40 μM with MilliQ water. 5 μL of the complex solution were added to 10 μL of supercoiled ΦX174 DNA (Invitrogen, 7 nM, 40 μM base pairs) in 6 mM NaCl, and 20 mM sodium phosphate buffer (pH 7.2). To initiate the cleavage, 5 μL of a 20 mM mercaptopropionic acid solution in water were added, and the resulting reaction mixture was incubated at 37 °C for 1 h. The reaction was quenched at 4 °C by ice, followed by the addition of 4 μL of loading buffer (glycerol with bromophenol blue) prior to its loading on a 0.8% agarose gel containing 1 μg mL^{-1} of ethidium bromide. The gels were run at a constant voltage of 70 V for 90 min in TBE buffer containing 1 μg mL^{-1} of ethidium bromide. The gels were visualized under a UV trans-illuminator, and the bands were quantified using a BioRad Gel Doc 1000 apparatus interfaced with a computer.

Time-course experiments of DNA cleavage: 50 μL of complex solution were added to 100 μL of supercoiled ΦX174 DNA (Invitrogen, 7 nM, 40 μM base pairs) in 6 mM NaCl, and 20 mM sodium phosphate buffer (pH 7.2), and the resulting reaction mixture was incubated for 20 h at 37 °C. To initiate the cleavage, 50 μL of 20 mM mercaptopropionic acid were added, and a sample was taken out every 10 min. 4 μL of loading buffer (glycerol with bromophenol blue) were added, and the sample was directly frozen in liquid nitrogen. When all samples were collected, they were loaded on a 0.8% agarose gel containing 1 μg mL^{-1} of ethidium bromide.

Cleavage of [Cu(dtdeg)Ru(bipy)Cl] and **[Cu(dtdeg)RuCl$_3$] after treatment with AgNO$_3$:** 0.5 mL of **[(dtdeg)Ru(bipy)Cl]** or **[(dtdeg)RuCl$_3$]** in MilliQ water (1 mM, no copper) were added to a 0.5 mL $AgNO_3$ solution in MilliQ water (1 mM for **[(dtdeg)Ru(bipy)Cl]** and 3 mM for **[(dtdeg)RuCl$_3$]**). This mixture was stirred overnight at 50 °C in the dark. The eppendorff tube containing the reaction mixture was centrifuged for 15 minutes and 800 μL were transferred in a new vial. 200 μL of a $CuCl_2$ (2 mM) solution in MilliQ were added. 0.4 mM MilliQ H_2O solutions of the complexes investigated were diluted to respectively 20 and 40 μM with MilliQ water. 5 μL of the complex solution were added to 10 μL of supercoiled ΦX174 DNA (Invitrogen, 7 nM, 40 μM in base pairs) in 6 mM NaCl, and 20 mM sodium phosphate buffer (pH 7.2). The complexes were incubated for 24 hours prior to the precipitation of the DNA with NaOAc (3 M) and cold ethanol. The samples were dissolved in 15 μL MilliQ H_2O. To initiate the cleavage, 5 μL of a 20 mM mercaptopropionic acid solution in water was added, and the resulting reaction mixture was incubated at 37 °C for 1 h. The reaction was quenched at 4 °C, followed by the addition of 4 μL of loading buffer (glycerol with bromophenol blue) prior to its loading on a 0.8% agarose gel containing 1 μg mL^{-1} of ethidium bromide. The gels were run at a constant voltage of 70 V for 90 min in TBE buffer containing 1 μg mL^{-1} of ethidium bromide. The gels were visualized under a UV trans-illuminator, and the bands were quantified using a BioRad Gel Doc 1000 apparatus interfaced with a computer.

Analyses with 5'-^{32}P-end-labeled DNA: The ODNs I and II fragments (Figure 8.8) were purchased from Invitrogen. The concentrations of single-stranded ODNs were determined by UV titration at 260 nm.[36] The ODNs were end-labeled with ^{32}P using standard procedures with T_4 polynucleotide kinase (New England BioLabs) and [γ-^{32}P]ATP for the 5'-end, before being purified on a MicroSpin G25 column (Pharmacia).[37, 38]

Comparison of the cleavage patterns of ODN I-ODN II induced by the copper complexes: The 5'-end labeled 36mer target ODN I (2 μM) was annealed to 1 equiv of its complementary strand ODN II in 1100 μL of Tris-HCl (20 mM, pH 7.2) by heating to 90 °C for 5 min, followed by slow cooling to room temperature. To 10 μL of this solution were added 5 μL of **Cu(terpy)** (40 μM), **[Ru(dtdeg)Cu]** (20 μM), **[Cu$_2$(dtdeg)$_2$Ru]** (20 μM), **[Cu$_2$(dtdeg)$_3$Ru$_2$]** (20 μM), **[Cu(dtdeg)Ru(bipy)Cl]** (20 μM), or **[Cu(dtdeg)RuCl$_3$]** (40 μM) solutions and 5 μL MPA (5 μL of water were added to the controls). The samples were incubated at 37 °C for 1 h, followed by precipitation in 20 μL of sodium acetate buffer (3 M, pH 5.2) containing 1 μg of calf-thymus testes DNA and 180 μL of cold ethanol. Pellets were rinsed with ethanol and lyophilized. In order to study the DNA-cleavage mechanism, additional treatments were performed on some samples: (i) heating at 90 °C in 50 μL of HEPES-NaOH buffer (0.1 M, pH 8.0) for 30 min, followed by ethanol precipitation; (ii) heating at 90 °C in 50 μL of piperidine (0.2 M in water) for 30 min, followed by lyophilization. The samples were analyzed

by denaturing 20% polyacrylamide gel electrophoresis and subsequent phosphorimagery. The Maxam and Gilbert sequencing scale was used to analyze the DNA fragments.[39]

8.5 References

[1] C. H. B. Chen, L. Milne, R. Landgraf, D. M. Perrin, D. S. Sigman, *Chembiochem* **2001**, *2*, 735.

[2] M. Pitié, C. Boldron, G. Pratviel, *Advances In Inorganic Chemistry, Vol. 58*, Elsevier Academic Press Inc, San Diego, **2006**.

[3] G. Pratviel, J. Bernadou, B. Meunier, *Angew. Chem.-Int. Edit. Engl.* **1995**, *34*, 746.

[4] C. J. Burrows, J. G. Muller, *Chem. Rev.* **1998**, *98*, 1109.

[5] J. A. Cowan, *Curr. Opin. Chem. Biol.* **2001**, *5*, 634.

[6] E. L. Hegg, J. N. Burstyn, *Coord. Chem. Rev.* **1998**, *173*, 133.

[7] T. W. Bruice, J. G. Wise, D. S. E. Rosser, D. S. Sigman, *J. Am. Chem. Soc.* **1991**, *113*, 5446.

[8] C. Q. Pan, R. C. Johnson, D. S. Sigman, *Biochemistry* **1996**, *35*, 4326.

[9] P. S. Pendergrast, Y. W. Ebright, R. H. Ebright, *Science* **1994**, *265*, 959.

[10] J. Pfau, D. N. Arvidson, P. Youderian, L. L. Pearson, D. S. Sigman, *Biochemistry* **1994**, *33*, 11391.

[11] R. M. Burger, *Chem. Rev.* **1998**, *98*, 1153.

[12] J. Y. Chen, J. Stubbe, *Nat. Rev. Cancer* **2005**, *5*, 102.

[13] U. Galm, M. H. Hager, S. G. Van Lanen, J. H. Ju, J. S. Thorson, B. Shen, *Chem. Rev.* **2005**, *105*, 739.

[14] H. Umezawa, K. Maeda, T. Takeuchi, Y. Okami, *J. Antibiot.* **1966**, *19*, 200.

[15] D. S. Sigman, D. R. Graham, V. Daurora, A. M. Stern, *J. Biol. Chem.* **1979**, *254*, 2269.

[16] M. Pitié, B. Donnadieu, B. Meunier, *Inorg. Chem.* **1998**, *37*, 3486.

[17] M. Pitié, B. Sudres, B. Meunier, *Chem. Commun.* **1998**, 2597.

[18] R. P. Hertzberg, P. B. Dervan, *J. Am. Chem. Soc.* **1982**, *104*, 313.

[19] M. W. van Dyke, R. P. Hertzberg, P. B. Dervan, *Proc. Natl. Acad. Sci. U. S. A.* **1982**, *79*, 5470.

[20] A. Sreedhara, J. A. Cowan, *Chem. Commun.* **1998**, 1737.

[21] K. J. Humphreys, K. D. Karlin, S. E. Rokita, *J. Am. Chem. Soc.* **2001**, *123*, 5588.

[22] C. Boldron, S. A. Ross, M. Pitié, B. Meunier, *Bioconjugate Chem.* **2002**, *13*, 1013.

[23] M. Pitié, C. J. Burrows, B. Meunier, *Nucleic Acids Res.* **2000**, *28*, 4856.

[24] M. Pitié, J. D. Van Horn, D. Brion, C. J. Burrows, B. Meunier, *Bioconjugate Chem.* **2000**, *11*, 892.

[25] K. E. Erkkila, D. T. Odom, J. K. Barton, *Chem. Rev.* **1999**, *99*, 2777.

[26] N. J. Wheate, C. R. Brodie, J. G. Collins, S. Kemp, J. R. Aldrich-Wright, *Mini-Rev. Med. Chem.* **2007**, *7*, 627.

[27] S. Delaney, M. Pascaly, P. K. Bhattacharya, K. Han, J. K. Barton, *Inorg. Chem.* **2002**, *41*, 1966.

[28] A. E. Friedman, J. C. Chambron, J. P. Sauvage, N. J. Turro, J. K. Barton, *J. Am. Chem. Soc.* **1990**, *112*, 4960.

[29] A. Petitjean, J. K. Barton, *J. Am. Chem. Soc.* **2004**, *126*, 14728.

[30] K. van der Schilden, PhD thesis, Leiden University (Leiden), **2006**.

[31] K. van der Schilden, F. Garcia, H. Kooijman, A. L. Spek, J. G. Haasnoot, J. Reedijk, *Angew. Chem.-Int. Edit.* **2004**, *43*, 5668.

[32] S. H. Liu, A. D. Hamilton, *Chem. Commun.* **1999**, 587.

[33] K. Ohr, B. P. Gilmartin, M. E. Williams, *Inorg. Chem.* **2005**, *44*, 7876.

[34] P. de Hoog, C. Boldron, P. Gamez, K. Sliedregt-Bol, I. Roland, M. Pitié, R. Kiss, B. Meunier, J. Reedijk, *J. Med. Chem.* **2007**, *50*, 3148.

[35] S. Ghumaan, B. Sarkar, M. P. Patil, J. Fiedler, R. B. Sunoj, W. Kaim, G. K. Lahiri, *Polyhedron* **2007**, *26*, 3409.

[36] G. Fasman, *Handbook of biochemistry and molecular biology: nucleic acids, Vol. 3rd edn.*, Boca Raton, p175, **1975**.

[37] J. Sambrook, E. F. Fritsch, T. Maniatis, *Molecular Cloning: A Laboratory Manuel, Vol. 2nd Edn.*, Cold Spring Harbor Laboratory Press, Cold Spring Harbor, NY, **1989**.

[38] H. Baruah, U. Bierbach, *Nucleic Acids Res.* **2003**, *31*, 4138.

[39] A. M. Maxam, W. Gilbert, *Proc. Natl. Acad. Sci. U. S. A.* **1977**, *74*, 560.

Chapter 9

Summary, general discussions and perspectives

9.1 Introduction

Cancer is a disease that has a high mortality rate worldwide.[1] Several approaches are employed to treat cancer, such as surgery, chemotherapy, radiation therapy, monoclonal antibody therapy or combinations of these therapies. The choice of the appropriate treatment depends on the nature of the tumor, the stage of the disease and the general state of the patient. The curing rate of chemotherapy has improved over the last decades, since new anti-cancer agents have been discovered, and significant advances in the different treatment protocols have been achieved.[2] Nowadays, cancer is almost always treated by a combination of several drugs (and/or applying different types of therapy). The treatment of testicular cancer, which has a curing rate approaching 100%, is a prime example that characterizes the progress accomplished.[3] This cancer is treated with a combination of cisplatin, bleomycin and etoposide. For example, Lance Armstrong, a famous cyclist, survived an advanced testicular cancer, thanks to this chemotherapeutic treatment. Moreover, he won seven consecutive times the Tour de France after his victory over cancer. Nevertheless, chemotherapy is still acquainted with severe side effects and intrinsic or acquired resistance to the drug(s).

This thesis deals with the design and synthesis of novel antitumor drugs with two distinct functions, namely a DNA-interacting component and a DNA-cleaving unit. These bifunctional molecules have been designed to possibly exhibit synergism between both active moieties, resulting in the improvement of both the cleavage and the cytotoxic activities. The compounds described in chapters 2-7 are based on the linkage of a DNA binding unit (derived from cisplatin chemistry) to the complex Cu(3-Clip-Phen),[4] which is a very efficient DNA cleaving agent. In chapter 8, a novel DNA cleaving unit is reported which is covalently linked to a ruthenium unit having high a DNA affinity.

9.2 Summary and general discussions

Chapter 1 outlines the basis of this thesis and gives an overview of the relevant literature. The discovery of a leading antitumor drug, namely cisplatin is first stated and its mechanism of action is described. Other anticancer platinum-based drugs in clinical use, and novel alternative platinum complexes are reported as well. The second part of chapter 1 focuses on the field of DNA cleavage. The discovery of the nuclease activity of bleomycin, $[Cu^{I/II}(phen)_2]$ and Cu(3-Clip-Phen) is described in detail together with their mechanism of action. Other copper-based chemical nucleases are presented as well.

Chapter 2 primarily deals with DFT calculations that have been carried out to investigate the molecular geometry and the electronic properties of a variety of Cu(Clip-Phen) complexes in the gas phase. The computational results have been correlated with the experimental findings of

Pitié et al.[5] The length of the bridge linking the two phenanthroline units strongly affects the magnitude of the changes in coordination geometries between the Cu(I) and the Cu(II) oxidation states of the corresponding Cu(Clip-Phen) complexes. The geometries of the Cu(I) and Cu(II) oxidation states of complexes bearing a short bridge (i.e. a bridge with 2 or 3 methylene groups) show only small differences, in contrast to those of complexes with 4 or 5 carbon atoms in the bridge. Moreover, these theoretical data correlates with the cleaving abilities of the compounds. The complexes with a short bridge are more efficient cleaving agents than the complexes containing 4 or 5 carbons in the bridges.

Potential cytotoxic heterodinuclear platinum-copper complexes are described in chapters 3 and 4. This new class of bifunctional complexes has been designed to form kinetically inert bonds with DNA followed by its cleavage in the close proximity of the Pt-DNA adducts. The two DNA-targeting units (Cu(3-Clip-Phen) and platinum) have been linked by a long flexible, or a short rigid bridge. The DNA-cleavage experiments have shown that the complexes are capable of inducing direct double-strand cuts, most likely as a result of repetitive single-strand cuts in the close proximity of the platinum-DNA adducts. It has been demonstrated that the platinum parts of the complexes indeed can bind to a 36-mer DNA duplex at two neighboring guanine bases. The sequence selective cleavage has been investigated in more detail for the complexes with rigid bridges and the results are described in chapter 4. This study shows that this complex indeed cleaves the DNA strands in the close proximity of the platinum adducts. In addition, treatment with piperidine gives rise to an activation of the complexes, which is a phenomenon observed for the first time. The complexes reported in chapter 3 show moderate cytotoxicities toward several cancer cell lines. The complex described in chapter 4 shows only very weak cytotoxic activities toward two cell lines. Nevertheless, a clear difference in cytotoxicities between the complexes with copper or without copper is observed, suggesting a different cellular distribution.

The synthesis and the biological activity of rigid platinum-copper complexes are described in chapter 5. These complexes contain a (a)symmetric, DNA-binding platinum moiety with different configurations (*cis* or *trans*), and one or two Cu(3-Clip-Phen) groups that can cleave the DNA strands. Due to the rigidity of the complexes, either the platinum moiety or the Cu(3-Clip-Phen) part will not interact with its ideal site of interaction, thereby changing its intrinsic mechanism of action. The platinum moieties of the asymmetric (both the *cis* and *trans* compounds) complexes are able to coordinate to DNA. The complexes mediate direct double strand cuts with activities comparable to those achieved with the complexes described in chapters 3 and 4. Interestingly, the trinuclear complex which contains a Pt ion coordinated by two *trans*-Cu(3-Clip-Phen) units cannot bind to DNA; actually, this complex rather acts as two single Cu(3-Clip-Phen) moieties. Nevertheless, it is the most efficient cleaving agent reported in this thesis. In addition, the cytotoxic properties of this complex are better than the ones of the other complexes mentioned in the present thesis, including cisplatin. In fact, the other compounds

reported in this chapter only show moderate or do not show any activity at all toward several cell lines.

The complexes described in chapter 6 possess amine-functionalized bridges linking the platinum and the Cu(3-Clip-Phen) entities. These complexes have been designed to favor a possible triple interaction with DNA, namely with the major groove (platinum unit), with the minor groove (copper unit) and with the phosphate backbone (amine function). The linker distance between the NH group and the platinum unit was varied between 6 and 10 methylene groups. Unfortunately, the incorporation of an NH function does not improve the cleavage activity, since both complexes are less efficient nuclease active agents compared to the amine-free complex reported in chapter 3. Nonetheless, both complexes can cleave the DNA in a direct double-stranded fashion.

A wide variety of sophisticated compounds can be easily prepared from the low-cost cyanuric chloride.[6] The three chlorides of cyanuric chloride can be easily substituted by nucleophiles at different temperatures. The possibility to selectively substitute these chlorides has been exploited to prepare potential bi- and trifunctional antitumor drugs, derived from Cu(3-Clip-Phen) and a platinum coordination moiety. The trifunctional compound prepared includes a Cu(3-Clip-Phen) group, a platinum moiety and a fluorophore covalently attached to a triazine core. Chapter 7 copes with the synthesis, the nuclease activity and fluorescence microscopy studies of these *s*-triazine-based multi-functional complexes. The DNA-cleaving abilities of the three complexes prepared are drastically distinct. Indeed, the complex with one Cu(3-Clip-Phen) and platinum unit is highly active, the complex including a Cu(3-Clip-Phen) group, a platinum moiety and a fluorophore only shows a moderate activity and the complex bearing two platinum moieties and one Cu(3-Clip-Phen) unit appears to be inactive. The cellular processing of the trifunctional triazine-based complex has been followed by fluorescence microscopy, revealing that the derivative accumulates within 15 minutes in the cytosol. Furthermore, cell death is observed at relatively low complex concentrations.

In chapter 8, the nuclease activities of five novel ruthenium-copper complexes are described. The precursor ruthenium complexes have been earlier prepared in our group.[7] Such, cationic metallointercalators are known for their high DNA affinity.[8] The ruthenium compounds used in this study are characterized by the presence of one or two free terpyridine ligands, which have been coordinated to copper. The ruthenium unit is expected to direct the copper moieties near the DNA strands, thus favoring the cleavage of the duplex. These heteropolynuclear complexes are active in nuclease activity in the presence of air and a reductant. Interestingly, the complexes with a ruthenium unit show markedly higher DNA-cleavage activities compared to the corresponding compound lacking this moiety. All the complexes appear to act as single-strand

cleaving agents, most likely through the oxidation of both the nucleobases and the deoxyribose units of DNA.

9.3 Future perspectives

Chemotherapy has improved over the last decades, but clinical treatments are always associated with considerable side effects and acquired resistance to the drugs. Therefore, the search for new, more active and less toxic anti-tumor drugs is of vital importance in the field of chemotherapy. This thesis deals with the design and synthesis of novel bifunctional anti-tumor drugs that can bind to DNA and cleave it in the close proximity of the complex-DNA adducts. This novel strategy has led to the preparation of three bifunctional complexes, i.e. **Cu3CP-6-Pt**, **Asym-*cis*** and **Cu(sym-*trans*)** (Scheme 3.1 and Figure 5.1), that show moderate to good cytotoxicities toward six cancer cell lines. More cancer cell lines should be tested to appraise the efficiency of three compounds on a broader range of tumor cells, since well over 100 different types of cancer are known. Moreover, toxicity studies have to be carried out to investigate if these complexes can be used on animal models.

The complexes presented in this thesis have been conceived with the objective to explore a possible different mechanism of action of platinum based anti-tumor drugs. Therefore, the mechanism of action of these bifunctional complexes in cancer cells have to be investigated in detail and compared to those of cisplatin and Cu(3-Clip-Phen). The cellular distribution, the identification of the cellular target, the initiation of cell death, and the damage repair processes are of great importance to fully comprehend the specific activities of these complexes against cancer cells. These studies may allow answering the question whether the eradication of the cancer cells is due to the action of the platinum moiety or the Cu(3-Clip-Phen) unit, or whether the heteronuclear complexes initiate a unique cascade of cellular responses. Moreover, the data collected will help to rationally design new bifunctional anti-tumor complexes.

DNA has been assumed to be the main target for the complexes described in this thesis. The platinum and Cu(3-Clip-Phen) moieties display specific DNA interactions; the platinum unit forms kinetically inert coordinating bonds in the major groove of DNA, and Cu(3-Clip-Phen) is believed to interact from the minor groove of DNA by partial intercalation and electrostatic interactions. The bridge between the platinum unit and the Cu(3-Clip-Phen) moiety of the complexes described chapter 3 and 6 should be long enough to cross the phosphate backbone of DNA and to allow a minor-major groove interaction. The complexes reported in chapters 3, 4, 5 and 7 have short bridges; therefore, only one of the two metal-containing moieties can interact with its preferred target site. However, NMR studies of the DNA-complex adducts are required to confirm whether or not such presumed minor-major groove interactions are present. These studies in combination with molecular modeling investigations should give information on the

DNA distortion induced by the complexes. In particular, NMR studies involving the complexes described in chapter 6 would be of great interest to appraise the influence (beneficial or not) of the (bridge) amino group on their interaction with DNA.

Cisplatin-DNA adducts are recognized by proteins in the cells. This recognition can have a beneficial effect, like in the case of HMG proteins,[9] or a negative effect, like in the case of the NER repair system.[10] The bifunctional complexes herein presented may form similar platinum-DNA adducts and cleave the DNA strands in the close proximity of them. It would therefore be appealing to investigate the recognition of the bifunctional complex-DNA adducts by the NER system and the HMG proteins and to study the effect of the DNA lesions on the repair proteins.

Upon binding of cisplatin to DNA, the duplex is bended towards the major groove and the minor groove is opened. The bifunctional platinum complexes with a *cis*-configuration probably induce similar DNA damages upon binding. As a result, the Cu(3-Clip-Phen) moiety of the complexes with bridges long enough to cross the phosphate backbone will interact with an altered minor groove. Moreover, the Cu(3-Clip-Phen) moiety of the complexes that cannot cross the phosphate backbone will inevitably interact and cleave the DNA from the major groove. Such feature can be demonstrated by the analyses of the cleavage products resulting from an oxidative cleavage of DNA. The protons from the deoxyribose unit, normally abstracted by Cu(3-Clip-Phen), are either pointing toward the minor or the major groove of DNA. The abstraction of each of the seven protons from the deoxyribose unit results in a unique product which can be clearly identified and attributed to a specific proton. Therefore, the investigation of these characteristic products will determine the location of the Cu(3-Clip-Phen) unit of the bifunctional complexes in DNA.

The incorporation of a targeting group to platinum drugs can be a very successful approach to increase the therapeutic efficacy or to decrease the side effects of chemotherapy.[11] The triazine core of the ligands described in chapter 7 can be used to covalently link a targeting moiety. A possible efficient complex to be synthesized in this way may include a Cu(3-Clip-Phen) unit, a platinum moiety, and the third chloride can be substituted by any targeting molecule.

The strategy presented in chapters 3-7 of this thesis can be extended to other bifunctional molecules, such as the ones described in chapter 8. The high DNA affinity of the ruthenium unit clearly improves the cleaving ability of the Cu(terpy) moiety. Therefore, the linkage of other DNA binding units to other cleaving agents can lead to very efficient nuclease active agents and novel anti-tumor drugs.

9.4 References

[1] www.who.int, *World Health Organization*, **2005**.

[2] B. A. Chabner, T. G. Roberts, *Nat. Rev. Cancer* **2005**, *5*, 65.

[3] L. H. Einhorn, *Proc. Natl. Acad. Sci. U. S. A.* **2002**, *99*, 4592.

[4] M. Pitié, B. Sudres, B. Meunier, *Chem. Commun.* **1998**, 2597.

[5] M. Pitié, C. Boldron, H. Gornitzka, C. Hemmert, B. Donnadieu, B. Meunier, *Eur. J. Inorg. Chem.* **2003**, 528.

[6] P. Gamez, J. Reedijk, *Eur. J. Inorg. Chem.* **2006**, 29.

[7] K. van der Schilden, PhD thesis, Leiden University (Leiden), **2006**.

[8] K. E. Erkkila, D. T. Odom, J. K. Barton, *Chem. Rev.* **1999**, *99*, 2777.

[9] P. M. Pil, S. J. Lippard, *Science* **1992**, *256*, 234.

[10] V. M. Gonzalez, M. A. Fuertes, C. Alonso, J. M. Perez, *Mol. Pharmacol.* **2001**, *59*, 657.

[11] S. van Zutphen, J. Reedijk, *Coord. Chem. Rev.* **2005**, *249*, 2845.

Samenvatting

Kanker behoort tot een groep van ziekten die wereldwijd een hoog overlijdingspercentage hebben. Deze ziekte kan op verschillende manieren behandeld worden, door middel van chirurgie, bestraling, chemotherapie, therapie via een monoklonaal antilichaam, of combinaties van deze behandelingen. De keuze van de behandeling hangt af van de tumorsoort, het stadium van de ziekte en de toestand van de patiënt. De overlevingskans is verbeterd tijdens de laatste decennia, omdat nieuwe medicijnen zijn uitgevonden en doordat vooruitgang is geboekt in de behandelingen. Tegenwoordig worden sommige kankersoorten vrijwel altijd behandeld door middel van een combinatie van antikanker-medicijnen. Een uitstekend voorbeeld van deze vooruitgang is de behandeling van teelbalkanker, waarbij de overlevingskans nu bijna 100% is. Deze kanker soort wordt behandeld met een combinatie van cisplatina, bleomycin en etopside. Lance Armstrong, een beroemde wielrenner, had teelbalkanker met metastase, maar is door deze behandeling volledig genezen en heeft daarna nog zeven opeenvolgende keren de Tour de France gewonnen. Niettemin, de behandeling van kanker veroorzaakt nog steeds diverse storende bijeffecten en de kankercellen kunnen resistentie hebben of ontwikkelen tegen de medicijnen.

Dit proefschrift beschrijft het ontwerp en de synthese van nieuwe antikanker-geneesmiddelen met twee verschillende functies, namelijk een eenheid die interactie heeft met DNA en een eenheid die DNA kan knippen. Deze bifunctionele moleculen kunnen synergie bewerkstelligen tussen beide actieve eenheden. Dit kan resulteren in de verbetering van de antikankeractiviteit. De moleculen beschreven in hoofdstuk 2-7 zijn gebaseerd op cisplatina en Cu(3-Clip-Phen), dat een heel effectieve DNA-schaar is. In hoofdstuk 8 is een nieuwe DNA-knipper beschreven, die verbonden is met een rutheniumdeel met sterke affiniteit voor DNA.

Hoofdstuk 1 geeft een overzicht van de relevante literatuur waarop het onderzoek van dit proefschrift is gebaseerd. Ten eerste wordt de ontdekking van een veel gebruikt antikanker-geneesmiddel, cisplatina, en de mechanismen achter de werking van dit medicijn beschreven. Tevens worden andere op platina gebaseerde geneesmiddelen, die momenteel in ziekenhuizen gebruikt worden en nieuwe alternatieve complexen beschreven. Het tweede gedeelte van hoofdstuk 1 is gericht op het onderzoeksgebied van het DNA knippen. De knipactiviteit van bleomycine, $[Cu^{I/II}(phen)_2]$ en Cu(3-Clip-Phen) worden in detail beschreven samen met hun knip-mechanisme. Andere op koper gebaseerde complexen die DNA kunnen knippen, worden daar ook beschreven.

In hoofdstuk 2 worden DFT-berekeningen beschreven die zijn uitgevoerd om de geometrie en de elektronische eigenschappen te onderzoeken van een serie Cu(Clip-Phen)-complexen in de gasfase. Deze resultaten zijn vergeleken met de experimentele experimenten van Pitié et al. De lengte van de koolstofketen die de twee fenantroline-groepen met elkaar verbindt,

heeft een sterke invloed op de grootte van de veranderingen in de coördinatiegeometrieën tussen de Cu(I)- en de Cu(II)-oxidatietoestanden van de overeenkomstige complexen. De verschillen in de geometrieën van de Cu(I)- en de Cu(II)-oxidatietoestanden van de complexen met een korte brug (2 of 3 koolstofatomen) zijn klein in tegenstelling tot die van de complexen met 4 of 5 koolstofatomen in de brug. Tevens correleert de theoretische data met de knipactiviteit van de complexen, want de complexen met een korte brug zijn efficiëntere DNA-knippers vergeleken met de complexen met een brug van 4 of 5 koolstofatomen.

Dinucleaire platinum-koper-complexen die potentiële antikankeractiviteit hebben, worden beschreven in hoofdstuk 3 en 4. Deze nieuwe categorie van bifunctionele complexen is ontworpen om kinetisch inerte verbindingen te vormen met DNA en om in de nabijheid van deze platina-DNA-verbinding het DNA te knippen. De twee actieve componenten zijn verbonden door middel van een lange en flexibele brug, of door een korte inflexibele brug. De DNA-knipexperimenten hebben uitgewezen, dat de complexen beide strengen tegelijk kunnen knippen, waarschijnlijk doordat de complexen beide strengen apart meerdere malen knippen in de nabijheid van de platina-DNA-produkten. Het platinagedeelte van de bifunctionele complexen kan inderdaad binden aan twee naast elkaar gelegen guanine-basenparen van een uit 36 basenparen bestaande DNA-duplex. In hoofdstuk 4 is de sequentieselectiviteit van het knippen van het complex met een inflexibele brug onderzocht in meer detail. Deze studie bewijst, dat het complex inderdaad knipt in de nabijheid van de platina-DNA-producten. Voor het eerst is het waargenomen dat de behandeling met piperidine leidt tot activering van dit type complexen. De gerapporteerde complexen van hoofdstuk 3 tonen matige antitumoractiviteit voor verscheidene cellijnen. De complexen van hoofdstuk 4 hebben een lage antitumoractiviteit. Niettemin, zijn verschillen in de antikankeractiviteit tussen de complexen met of zonder koper geobserveerd, wat een indicatie is voor een andere distributie van de complexen in de kankercellen.

De synthese en de biologische activiteit van inflexibele platina-koper-complexen worden beschreven in hoofdstuk 5. Deze complexen hebben een (a)symmetrische platinagroep met verschillende configuraties (cis of trans) en een of twee Cu(3-Clip-Phen)-groepen, die DNA kunnen knippen. De platina- of Cu(3-Clip-Phen)-groep kan geen interactie hebben met de ideale bindingslocatie in DNA vanwege de inflexibiliteit van deze complexen. Daardoor zal het werkingsmechanisme van een van de twee actieve eenheden veranderen. De platinagroepen van beide asymmetrische complexen kunnen coördineren aan DNA. Vergelijkbaar met de resultaten beschreven in hoofdstuk 3 en 4, kunnen deze complexen beide ketens van DNA direct knippen. In tegenstelling tot de asymmetrische complexen kan het complex met twee Cu(3-Clip-Phen)-eenheden niet coördineren aan DNA. Dit complex gedraagt zich als of het twee aparte Cu(3-Clip-Phen)-groepen heeft. Niettemin heeft dit complex van alle in dit proefschrift beschreven complexen de hoogste knipactiviteit en ook de beste antikankeractiviteit. De andere complexen gerapporteerd in dit hoofdstuk vertonen geen of matige antikankeractiviteit in de meeste kankercellijnen.

The complexen beschreven in hoofdstuk 6 hebben een aminegroep in de brug tussen de platina- en Cu(3-Clip-Phen)-eenheden. Deze complexen zijn ontworpen om een drievoudige interactie te hebben met DNA. Ze kunnen namelijk binden in de wijde groef van DNA door middel van de platinagroep, in de smalle groef van DNA met de Cu(3-Clip-Phen)-eenheid en kunnen elektrostatische interactie hebben met de fosfaatruggengraat van DNA via de aminegroep. De afstand van de platinagroep naar de aminegroep is variabel, namelijk 6 of 10 koolstofatomen. Helaas levert de incorporatie van de aminegroep in brug geen voordeel op voor de knipactiviteit van DNA, vergeleken met het complex zonder deze aminegroep. Niettemin kunnen beide complexen beide ketens van DNA direct knippen.

Een grote verscheidenheid aan asymmetrische moleculen kunnen worden bereid door gebruik te maken van het goedkope cyanuurchloride. De drie chlooratomen van cyanuurchloride kunnen reageren met nucleofiele reagentia op verschillende temperaturen. De mogelijkheid om selectief de drie chloriden te substitueren is gebruikt om antikankermedicijnen met twee of drie functies te maken. De triazine complexen bestaan uit een platina-eenheid, een Cu(3-Clip-Phen)-groep, al of niet uitgebreid met een fluorescerende eenheid. Hoofdstuk 7 beschrijft de synthese, de knipactiviteit en de fluorescentiemicroscopische studies van deze op triazine gebaseerde multifunctionele complexen. De knipactiviteit van de drie gerapporteerde complexen zijn erg verschillend. Het complex met een platina- en een Cu(3-Clip-Phen)-groep is heel actief, het complex met de drie functies is matig actief en het complex met twee platinagroepen en een Cu(3-Clip-Phen)-eenheid is niet actief. Het complex met drie functies is in de cel gevolgd door middel van fluorescentiemicroscopische studies. Dit complex accumuleert binnen 15 minuten in de cel en kan de cel doden met relatief lage complexconcentraties.

In hoofdstuk 8 is de knipactiviteit van vijf nieuwe ruthenium-koper-complexen beschreven. De rutheniumcomplexen waren al eerder gesynthetiseerd in deze groep. Dit type complexen is bekend om de hoge DNA-affiniteit. De gebruikte rutheniumcomplexen hebben nog een of twee vrije terpy-liganden, die in deze studie gecoördineerd zijn aan koper. De ruthenium-eenheid zou de kopergroepen naar het DNA moeten brengen en daarbij de knipactiviteit verhogen. In de aanwezigheid van zuurstof en een reducerend agens kunnen deze complexen DNA knippen. Grote verschillen in knipactiviteit zijn geobserveerd tussen de complexen met of zonder een ruthenium-eenheid. Deze complexen knippen het DNA per keten waarschijnlijk door middel van de oxidatie van de suikergroep en oxidatie van de nucleobasen. Verdere ontwikkeling van deze strategie en onderzoek naar de distributie van dit type complexen in kanker cellen zou kunnen leiden tot nieuwe geneesmiddelen.

Curriculum vitae

Paul de Hoog was born on April 10, 1979 in Sliedrecht (The Netherlands). From 1991 until 1997, he attended secondary school in Papendrecht. In 1997 he commenced with his bachelor studies in chemistry at the Hogeschool Rotterdam & Omstreken (Delft, The Netherlands). During his final year, a research project titled: "Oxidative phenol coupling and the controlled synthesis of macromolecules" was carried out with Prof. dr. Jan Reedijk. He continued his study at Leiden University and obtained a M.Sc. degree in Chemistry in May 2004. He performed a research project in the field of catalysis under the supervision of dr. Ronald Hage at Unilever (Vlaardingen, The Netherlands).

In the last year of his M.Sc degree he started his PhD project in the group of Prof. dr. Jan Reedijk. During the next four years, he carried out research concerning bifunctional platinum-copper complexes for anticancer applications. He collaborated intensively with the group of Prof. dr. Bernard Meunier and Prof. dr. Robert Kiss. From January 2006 to April 2006, a part of his work was performed at the LCC of the CNRS in Toulouse (France).

Parts of the research described in this thesis has been presented at several national and international meetings, including the NCCC V meeting in Noordwijkerhout, The Netherlands (2004), the ICBIC-12 in Ann Harbor, USA (2005), the 1st European Chemistry Congress in Budapest, Hungary (2006), the NWO meeting: Ontwerp en Synthese, Structuur en Reactviteit Biomoleculaire Chemie in Lunteren, The Netherlands (2006), the ESF-COST meeting in Athens, Greece (2006), and the ICBIC-13 in Vienna, Austria (2007).

List of publications

[1] P. Gamez, P. de Hoog, O. Roubeau, M. Lutz, W. L. Driessen, A. L. Spek and J. Reedijk, *Chem. Commun.* **2002**, 1488-1489.

[2] P. de Hoog, P. Gamez, W. L. Driessen and J. Reedijk, *Tetrahedron Lett.* **2002**, 43, 6783-6786.

[3] P. de Hoog, P. Gamez, O. Roubeau, M. Lutz, W. L. Driessen, A. L. Spek and J. Reedijk, *New J. Chem.* **2003**, 27, 18-21.

[4] P. Gamez, P. de Hoog, M. Lutz, W. L. Driessen, A. L. Spek and J. Reedijk, *Polyhedron* **2003**, 22, 205-210.

[5] P. Gamez, P. de Hoog, M. Lutz, A. L. Spek and J. Reedijk, *Inorg. Chim. Acta* **2003**, 351, 319-325.

[6] P. de Hoog, P. Gamez, M. Luken, O. Roubeau, B. Krebs and J. Reedijk, *Inorg. Chim. Acta* **2004**, 357, 213-218.

[7] P. de Hoog, L. D. Pachon, P. Gamez, M. Lutz, A. L. Spek and J. Reedijk, *Dalton Trans.* **2004**, 2614-2615.

[8] P. de Hoog, P. Gamez, H. Mutikainen, U. Turpeinen and J. Reedijk, *Angew. Chem.-Int. Edit.* **2004**, 43, 5815-5817.

[9] P. U. Maheswari, P. de Hoog, R. Hage, P. Gamez and J. Reedijk, *Adv. Synth. Catal.* **2005**, 347, 1759-1764.

[10] M. Quesada, P. de Hoog, P. Gamez, O. Roubeau, G. Aromi, B. Donnadieu, C. Massera, M. Lutz, A. L. Spek and J. Reedijk, *Eur. J. Inorg. Chem.* **2006**, 1353-1361.

[11] P. U. Maheswari, S. Barends, S. Ozalp-Yaman, P. de Hoog, H. Casellas, S. J. Teat, C. Massera, M. Lutz, A. L. Spek, G. P. van Wezel, P. Gamez and J. Reedijk, *Chem.-Eur. J.* **2007**, 13, 5213-5222.

[12] P. de Hoog, C. Boldron, P. Gamez, K. Sliedregt-Bol, I. Roland, M. Pitie, R. Kiss, B. Meunier and J. Reedijk, *J. Med. Chem.* **2007**, 50, 3148-3152.

[13] A. Robertazzi, A. Magistrato, P. de Hoog, P. Carloni and J. Reedijk, *Inorg. Chem.* **2007**, 46, 5873-5881.

[14] A. Robertazzi, A. Magistrato, P. de Hoog, J. Reedijk and P. Carloni, *Drug Future* **2007**, 32, 139-140.

[15] P. de Hoog, M. Louwerse, P. Gamez, M. Pitié, E. J. Baerends, B. Meunier and J. Reedijk, *Eur. J. Inorg. Chem.* in press

[16] P. J. Kitson, Y-F. Song, P. Gamez, P. de Hoog, D-L. Long, A. D. C. Parenty, J. Reedijk and L. Cronin, *Inorg. Chem.* in press.

[17] P. de Hoog, M. Pitié, G. Amadei, P. Gamez, B. Meunier, R. Kiss and J. Reedijk, *submitted.*

[18] S. Özalp-Yaman, P. de Hoog, G. Amadei, M. Pitié, P. Gamez, I. Roland, B. Meunier, R. Kiss and J. Reedijk, *submitted.*

[19] S. van der Steen, P. de Hoog, K. van der Schilden, P. Gamez and J. Reedijk, *manuscript in preparation.*

[20] T. Estruch Millet, A. Garcia Ramos, P. de Hoog, P. Marqués Callego, G. V. Kalayda, M. Pitié, P. Gamez, B. Meunier and J. Reedijk, *manuscript in preparation.*

[21] A. Vanossi, L. Bouquerel, P. de Hoog, M. Pitié, P. Gamez, B. Meunier and J. Reedijk, *manuscript in preparation.*

Acknowledgements

De laatste pagina's van dit proefschrift zou ik willen wijden aan familie, vrienden en collega's, die hebben bijgedragen aan de totstandkoming van dit werk. Als eerste zou ik mijn ouders, mijn zus en zwager willen noemen. Zij steunen mij altijd onvoorwaardelijk door dik en dun, wat de grondslag is voor een gelukkig en succesvol leven.

Ik ben blij dat mijn schoonouders altijd klaar staan voor ons en ze af en toe ons een nachtje rust te gunnen, door op Jesse op te passen.

Part of the results described in this thesis have been performed by bachelor or master students, who spend up to nine months with me and have become friends. I have enjoyed working with you and I also learned a lot from you. Liselotte and Andrea have performed the synthesis of the complexes described in chapter 6. I have been fortunate to work with (proud) students from Valencia, namely Angel and Teresa. They have synthesized the compounds shown chapter 7. Jorge has not been my student, but it is impossible to separate him from Teresa. Thank you guys, for the nice time and all the nice things from Valencia. Stefanie heeft mij erg weten te verbazen door haar ongelooflijke efficiëntie. De resultaten gerapporteerd in hoofdstuk 8 zijn mede door haar werk, verkregen in maar drie maanden. I want to say to my students: sorry for all the columns!

Tijdens mijn onderzoek heb ik met meerdere mensen/groepen samengewerkt en daardoor heel veel geleerd. Christophe gave me a jump start in the first half year of my thesis. No doubt, without him this thesis would contain less results. He and his wife Jordane are also thanked for their hospitality, provided to me when I stayed in Toulouse. I have enjoyed my stay in Toulouse in the group of Bernard Meunier and the discussions with Marguerite Pitié. I also would like to mention Céline, Luc and Vanessa for taking care of me in the lab. I have appreciated the fruitful collaboration with Arturo, Alessandra and Paolo Carloni from Trieste, which yielded a very nice publication. Hoofdstuk 2 zou niet tot stand zijn gekomen zonder de fantastische hulp van Manuel Louwerse en Evert-Jan Baerends. Zij hebben mij geïntroduceerd in de wereld van het onderzoek doen met de computer. I am grateful to Isabelle Roland, Janique Dewelle and Robert Kiss for their efforts, to perform the cytotoxicity tests, reported in this thesis. Şeniz Özalp-Yaman worked with me in the lab for one year. I have learned a lot in this period and I have enjoyed this period tremendously. Zonder de prachtige rutheniumcomplexen van Karlijn had hoofdstuk 8 niet geschreven kunnen worden.

De groep wordt administratief altijd prima ondersteund door Yvonne Snellenberg en Ingrid Bekooy. Voor de vele metingen die ik nodig heb gehad om mijn complexen te karakteriseren, heb ik gelukkig veel hulp gehad van erg kundige mensen. Ik ben dankbaar voor de geduldige hulp van Fons Lefeber en Kees Erkelens voor de NMR-metingen, Jopie Erkelens, John van Dijk, Hans van Elst en Karen Sliedregt-Bol voor de massa spectrometrische metingen en Gé van Albada voor de EPR. Later hoop ik net zo vrolijk en levendig in het leven te staan als Jos van Brussel. De "enorme" discussies over Poetin en over buffer 4 zal ik zonder twijfel missen. In vrijwel elk hoofdstuk van dit proefschrift zijn DNA-knipexperimenten beschreven. Dit had niet gekund zonder de hulp en gastvrijheid van Tineke de Ruijter, Riekje Brandsma en Jaap Brouwer.

Uiteraard heb ik ook veel geleerd van de andere platinabikkels. Elena, Steven, Seiji and Ann started a couple of years before me and shared their experience and showed me the tricks to obtain pure platinum complexes. Ann and Patricia are the light in darkness on cellular level, and hopefully we will have a nice joint publication. I would like mention Uma and Sudeshna as well. Uiteraard hebben mijn collega's Manu, Ira, Graham, Tiddo, Jimmy, Joris, Meenal, Guillem, Yufei, Ariadna, Kristian, Erasmus students en alle andere collega's van de CBAC-groep fantastisch bijgedragen aan de goede sfeer in het lab. In het bijzonder zou ik Peter willen noemen, bij wie ik startte met mijn onderzoek. I am very grateful that José will be one of my paranymphs and I will miss his dry sense of humor.

Uiteraard zijn er een aantal mensen, namelijk Marcel, Mirjam, Ben, Fatima, Erik, Edwin en Ilse, waar ik buiten het lab ook veel plezier mee beleef. Hopelijk kan ik jullie binnenkort weer een keertje ouderwets afschieten tijdens een potje Call of Duty. Ik zal ook nooit vergeten, dat Edwin nooit verzaakte om een potje te klaverjassen op de dinsdag of woensdag, wat op zich al een prestatie is, gezien mijn onuitstaanbare fanatisme.

Tijdens mijn promotietijd zijn er ook veel dingen in mijn leven buiten de universiteit heel positief veranderd. Ik ben tijdens dit onderzoek getrouwd met Debbie en we hebben samen onze zoon Jesse gekregen. Ik ben dankbaar, dat dit alles onze hechte band extra heeft versterkt en ik heb goede hoop dat de toekomst ons drietjes nog heel veel moois gaat brengen!

Paul